Electro-oxidation of 1,2-dihydroxybenzene in Presence of Alanine, Phenylalanine and Leucine at Different pH Media

by

Palash Kumar Dhar

A thesis submitted in partial fulfillment of the requirements for the degree of
Master of Science in Chemistry

Khulna University of Engineering & Technology
Khulna 9203, Bangladesh

August 2016

Dedicated

To My Parents

Kalipada Dhar and Chandana Rani Dhar

Declaration

This is to certify that the thesis work entitled “Electro-oxidation of 1, 2-dihydroxybenzene in Presence of Alanine, Phenylalanine and Leucine at Different pH Media” has been carried out by Palash Kumar Dhar in the Department of Chemistry, Khulna University of Engineering & Technology, Khulna, Bangladesh. The above thesis work has not been submitted anywhere for the award of any degree or diploma.

Signature of Supervisor

Signature of Candidate

Acknowledgements

All praises are due to the omnipotent Almighty God, the great creator and supreme authority of the universe, whose blessing enables me to pursue higher education and also to complete this research work in time and for preparation of this thesis for the M.Sc. degree in Chemistry successfully.

I would like to express my heart-felt sense of gratitude, indebtedness and sincere appreciation to my Honorable Supervisor **Dr. Md. Abdul Motin**, Professor and Head, Department of Chemistry, Khulna University of Engineering & Technology, Khulna for his distinguishable scholastic guidance, congenial co-operation, kind supervision, constant inspiration, valuable suggestions, perceptive comments, sincere advice and timely instruction throughout the entire period of research work.

I am happy to thank **Md. Abdul Hafiz Mia**, Lecturer, Department of Chemistry, Khulna University of Engineering & Technology, Khulna for his helpful advice, cordial co-operation and authentic information during the period of study.

I wish to convey my hearty thanks to all my friends especially **Md. Nazim Uddin** for his help and support in many respects.

I am grateful to my **Parents** for their inspiration, blessing, supports and encouragement throughout the period of study.

Palash Kumar Dhar

Abstract

The electro-oxidation of 1,2-dihydroxybenzene generates *o*-benzoquinone (Michael acceptor) and its reaction in presence of different concentration of L-Alanine, L-Phenylalanine and L-Leucine (nucleophiles) has been investigated. The overall study has been carried out in buffer solution of different pH (5, 7, 9 and 11) by using Cyclic Voltammetry (CV), Controlled Potential Coulometry (CPC) and Differential Pulse Voltammetry (DPV) techniques at different electrodes (GC, Pt and Au) and scan rates (0.05-0.5 V/s). Cyclic voltammogram of electro-active 1,2-dihydroxybenzene in pure buffer solution (5-11) shows one anodic and corresponding cathodic peak within a quasi-reversible process. Pure L-Alanine, L-Phenylalanine and L-Leucine are electro-inactive having no peak in the potential range of investigation (-0.6 to 0.9V).

Addition of different composition of L-Alanine (10-150 mM), L-Phenylalanine (2-100 mM) and L-Leucine (30-200 mM) in fixed 2 mM of 1,2-dihydroxybenzene solution, in the second scan of potential a new anodic peak (A_0) arises at the more negative potential with respect to the pure 1,2-dihydroxybenzene. The anodic (A_1) and cathodic peak (C_1) current intensity of 1,2-dihydroxybenzene also decreases significantly. This indicates the participation of 1,4-Michael addition reaction of *o*-benzoquinone with L-Alanine, L-Phenylalanine and L-Leucine to produce 2-((3,4-dihy droxyphenyl)amino)propanoic acid, 2-((3,4-dihydroxyphenyl)amino)-3-phenylpropanoic acid and 2-((3,4-dihydroxyphenyl) amino)-4-methyl-pentanoic acid adducts. The 1,4-Michael addition reaction of 1,2-dihydroxybenzene is strongly influenced by the concentration of nucleophiles. The electro-oxidation of 2 mM 1,2-dihydroxybenzene is mostly favorable in 50 mM of L-Alaline, 20 mM of L-Phenylalanine and 100 mM of L-Leucine respectively.

The effect of pH on 1,2-dihydroxybenzene in presence of different nucleophiles has been studied by varying pH ranging from 5 to 11. In acidic pH media (pH <7), no new anodic peak arises after repetitive cycling due to protonation of amine group. But in the neutral (pH=7) and basic media (pH >7), *o*-benzoquinone undergoes nucleophilic attack by the amine part of amino acids and the maximum peak current is observed at pH 7. The slope value of 1,2-dihydroxybenzene-Alanine, 1,2-dihydroxybenzene-Phenylalanine and 1,2-

dihydroxybenzene-Leucine adducts have been calculated (70.5 mV/pH for first anodic peak A_1), (59 mV/pH for first anodic peak A_1) and (68.5 mV/pH for first anodic peak A_1) at 0.1 V/s respectively. These values indicate that the nucleophilic substitution reactions are preceded via $1e^-/1H^+$ process. It is also suggested that during the course of reaction, electron and proton are released simultaneously from the 1,2-dihydroxybenzene-Amino acid adducts. The nature of voltammogram, peak position and current intensity for the studied systems are different for different electrodes and the voltammetric response of GC electrode is better than Au and Pt electrodes.

The effect scan rates on cyclic voltammogram of 1,2-dihydroxybenzene in presence of L-Alanine, L-Phenylalanine and L-Leucine have also been studied. The peak current of both the anodic and the corresponding cathodic peaks increases with the increase of scan rate. The nearly proportionality of the anodic and corresponding cathodic peak suggests that the peak current of the reactant at each redox reaction is controlled by diffusion process with some chemical complications. The current function, $I_p/v^{1/2}$ vs scan rates (v) of 1,2-dihydroxybenzene-Amino acid adducts are found to be decreased exponentially with increasing scan rate which suggests that the behavior of reaction mechanism is Electron transfer-Chemical reaction-Electron transfer (ECE) type for all the studied system. The products obtained by bulk electrolysis have also been analyzed by FTIR spectra.

Contents

CHAPTER IV Results and Discussion

LIST OF TABLES

LIST OF FIGURES

CHAPTER I

Introduction

1.1 General

1,2-dihydroxybenzene is well known in biological systems often as a reactive center of electron transfer in the structure of many natural compounds [1,2] and biologically reactive molecules capable of exhibiting both anti- and pro-oxidant behavior. [3] Because electrochemical oxidation very often parallels the oxidation of 1,2-dihydroxybenzene in the mammalian central nervous system and this process occurs in the human body [4]. It was interesting to study the electro-oxidation of 1,2-dihydroxybenzene in the presence of nucleophiles such as L-Alanine, L-Phenylalanine and L-Leucine. The most well-known characteristic of the 1,2-dihydroxybenzene is that they can be easily oxidized mainly due to their antioxidant activity and low oxidation potentials [5]. The *o*-benzoquinones (Michael acceptor) formed are quite reactive and can be easily attacked by various nucleophiles such as: Methanol, Diethylamine, Dimethylamine, Sulfanilic acid, Paracetamol, L-Glycine, L-Aspartic acid, L-Glutamic acid, Imidazole, L-Serine, L-Arginine, 4-hydroxycoumarin, 4-hydroxy-6-methyl-2-pyrone, 6-methyl-1,2,4-triazine-3-thion-5-one [6-8] and so on. There are many reports on electro-oxidation of 1,2-dihydroxybenzenes to produce *o*-quinone as reactive intermediates that is susceptible for nucleophilic substitution in many useful homogeneous reactions which has drawn our attention for this research. On the other hand, amino acids are electrically inactive. Because of the pharmacological, physiological and industrial importance of amino acids, 1,2-dihydroxybenzene and 1,2-dihydroxybenzene-amino acid adducts; the electro-oxidation of 1,2-dihydroxybenzene in presence of L-Alanine, L-Phenylalanine and L-Leucine have been extensively investigated by means of Voltammetric techniques.

Electrochemical techniques are inevitable tools in almost every chemical, biochemical and Pharmaceutical research laboratory. In addition to their application in fundamental studies of oxidation and reduction processes to unravel reaction mechanisms, these techniques are also used in studying the kinetics and thermodynamics of electron and ion transfer

processes. Moreover, electrochemical techniques have also proven to be useful tools for the study of adsorption and crystallization phenomena at electrode surfaces [9]. Among the electrochemical techniques applied in food analysis, the principal ones are polarographic and voltammetric techniques. It provides powerful and versatile tools for food analysis: powerful with regard to detecting very low concentrations, while providing a wide linear relationship between the measured signal (current intensity) and concentration; versatile as a consequence of the possibility of simultaneous analysis, extended to a large number of organic and inorganic compounds that can be found in food. One of the main advantages of electrochemical techniques is usually considered to be the possibility of direct analysis of the sample without tedious and long preparative steps and subsequent separation.

Voltammetry is an electroanalytical technique that measures current as a function of potential. The common characteristic of all voltammetric techniques is that they involve the application of a potential (E) to an electrode and the monitoring of the resulting current (i) flowing through the electrochemical cell. In many cases the applied potential is varied or the current is monitored over a period of time (t). Thus, all voltammetric techniques can be described as some function of E, i, and t. voltammetric techniques present irreplaceable tools due to their robustness and ability to provide a vast amount of important thermodynamics and kinetics information. These techniques used to characterize electro-catalyst surfaces and kinetics of some of the electro-catalytic reactions being most important in ever-growing fields of fuel cells, electrolysis and battery technologies, such as hydrogen oxidation/evolution reaction, oxygen reduction reaction, as well as the oxidation of carbon-monoxide and low-molecular weight alcohols. The analytical advantages of these techniques include excellent sensitivity with a very large useful linear concentration range for both inorganic and organic species (10^{-12} to 10^{-1} M), a large number of useful solvents and electrolytes. The term voltammetry encompasses a broad area of electroanalytical chemistry that includes polarography, linear scan voltammetry (LSV), Cyclic Voltammetry (CV), Pulsed voltammetry (PV), and Stripping Voltammetry. Stripping voltammetry is now a significant trace analytical method, particularly for the determination of metals in the environment. Differential pulse polarography and rapid scan voltammetry are important for the determination of species of pharmaceutical interest. In controlled-current coulometry, we completely oxidize or reduce the analyte by passing a fixed current through the analytical solution.

Cyclic voltammetry is one of the most exploited techniques in electrochemical studies. Its primary advantage comes from the fact that it gives insight into both the half-reactions taking place at the working electrode, providing at the same time information about the chemical or physical phenomena coupled to the studied electrochemical reaction. Hence cyclic voltammetry is often considered as electrochemical spectroscopy. Controlled-potential (potentiostatic) techniques deal with the study of charge transfer processes at the electrode–solution interface, and are based on dynamic (non-zero-current) situations. The advantages of controlled-potential techniques include high sensitivity, and selectivity toward electroactive species, a wide linear range, portable and low-cost instrumentation, speciation capability, and a wide range of electrodes that allow assays of unusual environments [10-12].

By taking the advantages of voltammetric techniques especially cyclic voltammetry (CV), Differential pulse voltammetry (DPV) and Controlled Potential Coulometry (CPC) it has been possible to investigate the electro-oxidation nature of 1,2-dihydroxybenzene in presence of electrochemically inactive nucleophiles (alanine, phenylalanine and leucine). The nucleophilic attacks that lead to the formation of 1,2-dihydroxybenzene derivatives with more or less positive oxidation potentials are followed by more E steps and C steps depends on the structure of intermediates by EC reaction. Amino acids are very essential for human health any precursor for drug synthesis. Due to weak alkaline nature of amino acids in neutral media it may act as a nucleophile and presence of one lone pair electron on nitrogen enables it to take participation in 1, 4-Michael addition reaction with *o*-benzoquinone. The purpose of the recent study is thus a basic work to have better insight of the possible redox interactions of 1,2-dihydroxybenzene with Alanine, Phenylalanine and Leucine compounds. These compounds go through redox reaction on the electrode surface within the potential range. The electro activeness of such compounds depends upon the pH of the medium, nature of the electrode and active moiety (electrophore) present in their structures.

1.2.1 1,2-dihydroxybenzene

1,2-dihydrooxybenzene is also known as catechol or pyrocatechol having molecular formula $C_6H_4(OH)_2$ shown in Figure 1.1. It is a colorless crystal with a phenolic odor and soluble in water and most of organic solvents. It is easily sublimes and can react with oxidizing materials. 1,2-dihydroxybenzene occurs as feathery white crystals that are very rapidly soluble in water. The 1,2-dihydroxybenzene skeleton also occurs in a variety of natural products specially the antioxidant. The most well-known characteristic of the 1,2-dihydroxybenzene is that they can be easily oxidized mainly due to their antioxidant activity and low oxidation potentials. The products of oxidation are the corresponding reactive and electron-deficient o-quinones. One of the most successful in situ generations of reactive o-quinones species is the electrochemical oxidation [13].

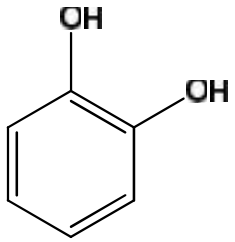

Figure 1.1: Structure of 1,2-dihydroxybenzene

1.2.2 Natural occurrence of 1,2-dihydroxybenzene

1,2-dihydroxybenzene is a natural polyphenolic compound that widely exists in higher plants such as tea, vegetables, fruits, tobacco and in crude beet sugar coal and some traditional Chinese medicines along with the enzyme polyphenol oxidase. It is also found in the leaves and branches of oak and willow trees. It is one of the main natural phenols in argan oil. 1,2-dihydroxybenzene is also found in *Agaricus bisporus*. It is also a component of castoreum, a substance from castors, used in perfumery [13].

1.2.3 Use of 1,2-dihydroxybenzene

1,2-dihydroxybenzene is one of the important building blocks in organic synthesis and it is produced in industrial scales as the precursor of pesticides, perfumes and pharmaceuticals.

1,2-dihydroxybenzene is mainly used as an intermediate for the synthesis of pharmaceuticals, agrochemicals and in formulation. Approximately 50% of the synthetic 1,2-dihydroxybenzene is consumed in the production of pesticides, the remainder being used as a precursor to fine chemicals such as perfumes and pharmaceuticals [12]. Several industrially significant flavors and fragrances such as vanillin or eugenol (synthetic "vanilla" aroma and flavor), piperonal (a flowery scent), guaiacol are prepared starting from 1,2-dihydroxybenzene that are used in food industry, perfumery, home and personal care products [13]. The Cate route of vanillin synthesis is far more environmentally friendly than the o-nitrochlorobenzene route. Cate also used as a black-and-white photographic developer.

1.3.1 L-Alanine

L-Alanine (abbreviated as Ala) is an α-amino acid that is used in the biosynthesis of proteins. It contains an α-amino group (which is in the protonated $-NH_3^+$ form under biological conditions), an α-carboxylic acid group (which is in the deprotonated $-COO^-$ form under biological conditions), and a side chain methyl group, classifying it as a nonpolar (at physiological pH), aliphatic amino acid. It is non-essential in humans, meaning the body can synthesize it [14].

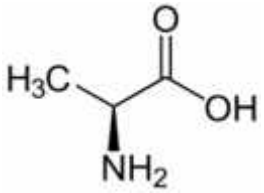

Figure 1.2: Structure of L-Alanine

1.3.2 Natural occurrence of L-Alanine

Good sources of alanine include meat, seafood, caseinate, dairy products, eggs, fish, gelatin, lactalbumin whereas vegetarian sources are beans, nuts, seeds, soy, whey, brewer's yeast, brown rice, bran, corn, legumes, whole grains [14].

1.3.3 Physiological function and uses of L-Alanine

L-Alanine plays a key role in glucose–alanine cycle between tissues and liver. In muscle and other tissues that degrade amino acids for fuel, amino groups are collected in the form of glutamate by transamination. Glutamate can then transfer its amino group through the action of alanine aminotransferase to pyruvate, a product of muscle glycolysis, forming alanine and α-ketoglutarate. Alpha-alanine is used for low blood sugar (hypoglycemia), diarrhea-related dehydration, liver disease, enlarged prostate (benign prostatic hypertrophy, BPH), fatigue, stress, and certain inherited disorders including glycogen storage disease and urea cycle disorders [14].

1.4.1 L-Phenylalanine

L-Phenylalanine is an α-amino acid with the formula $C_9H_{11}NO_2$. It can be viewed as a benzyl group substituted for the methyl group of alanine, or a phenyl group in place of a terminal hydrogen of L-Alanine. This essential amino acid is classified as neutral, and nonpolar because of the inert and hydrophobic nature of the benzyl side chain [15].

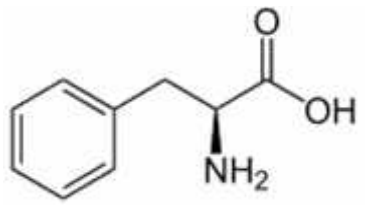

Figure 1.3: Structure of L-Phenylalanine

1.4.2 Natural occurrence of L-Phenylalanine

Good sources of L-Phenylalanine are eggs, chicken, liver, beef, milk, and soybeans. Other sources include spinach and leafy greens, tofu, amaranth leaves, and lupin seeds [15].

1.4.3 Physiological functions and uses of L-Phenylalanine

L-Phenylalanine is biologically converted into L-tyrosine, another one of the DNA-encoded amino acids. L-tyrosine in turn is converted into L-DOPA, which is further converted into dopamine, norepinephrine (noradrenaline), and epinephrine (adrenaline). The latter three are known as the 1,2-dihydroxybenzene-amines. L-Phenylalanine uses the same active transport channel as tryptophan to cross the blood–brain barrier. It is used in the manufacture of food and drink products and sold as a nutritional supplement for its reputed analgesic and antidepressant effects. It is a direct precursor to the neuromodulator L-Phenethylamine, a commonly used dietary supplement [15].

1.5.1 L-Leucine

L-Leucine (abbreviated as Leu or L) is an α-amino acid used in the biosynthesis of proteins. It contains an α-amino group (which is in the protonated $-NH_3^+$ form under biological conditions), an α-carboxylic acid group (which is in the deprotonated $-COO-$ form under biological conditions), and an isobutyl side chain, classifying it as a nonpolar (at physiological pH) amino acid. It is essential in humans-meaning the body cannot synthesize it and thus must obtain from the diet [16].

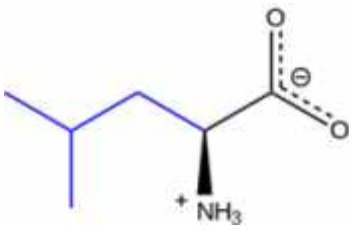

Figure 1.4: Structure of L-Leucine

1.5.2 Uses of L-Leucine

L-Leucine is a major component of the subunits in ferritin, astacin, and other "buffer" proteins. Leucine is used in the liver, adipose tissue, and muscle tissue. Adipose and muscle tissue use leucine in the formation of sterols. It has the ability to stimulate protein

synthesis, to help turn on the body's switch to build muscle and spare muscle when dieting. Consumption of it before, during or after training supports muscle protein synthesis, decrease protein catabolism and are very important to the use and production of glucose for energy. It enhances insulin's anabolic response and it is also used as a food additive and as a flavor enhancer [16].

1.6 Electrochemical properties of 1,2-dihydroxybenzene derivatives

Investigation of the electrochemical behavior of 1,2-dihydroxybenzene in presence of some other nucleophiles such as Imidazole, L-Serine, L-Arginine, L-Aspartic acid, L-Glutamic acid, L-Glycine, Benzenesulfinic acid, Barbituric acid, Indole, some Azacrown Ethers and Transition Metal Ions in Acetonitrile, Benzoyl acetonitrile, Dibuthylamine, Diethylamine, Thiourea, Methanol, 4-hydroxycoumarin, Ethanol, 2-thiobarbituric acid, β-diketones, 4-hydroxy-6-methyl-2-pyrone, 2-thiouracil, Dimedone, 4,7-dihydroxycoumarin, 4,5,7-trihydroxycoumarin, 4-hydroxy-6-bromocoumarin, 3-hydroxycoumarin, 4-hydroxy-6-methyl-a-pyrone, 4-hydroxy-6-methyl-2-pyridone, 4-hydroxycarbostyrile, sulfonic acid, Dopamine and 4-amino-3-thio-1,2,4-triazole were studied [6-8, 17-32].

Few works have been done on electrochemical oxidation of 1,2-dihydroxybenzene with amino acid [6,7]. However, aminoquinones are biologically important compounds in this direction, therefore, it demands detail electrochemical studies of 1,2-dihydroxybenzene in the presence of amines. In this research work, we have studied the electro-catalytic effect of 1,2-dihydroxybenzene in presence of L-Alanine, L-Phenylalanine and L-Leucine for three different electrodes (Au, GC and Pt) and various concentration (L-Alanine (10-150 mM), L-Phenylalanine (2-100 mM) and L-Leucine (30-200 mM)) and different pH (5-11)) at different scan rate. The primary aim of the present study is thus a fundamental realization to have better insight of the possible redox interactions of 1,2-dihydroxybenzene with L-Alanine, L-Phenylalanine and L-Leucine compounds. To the best of our knowledge, comparison of electrochemical study of 1,2-dihydroxybenzene with mentioned nucleophiles at different conditions has not been reported before this work.

1.7 Objectives of this Thesis

Attempt will be made in the present research work is systematic study of biologically important 1,2-dihydroxybenzene-amino acid adducts which may help to understand the role of amino drugs and them adducts in biological process.

The specific aims of this study are:

i) to diagnose the mechanism of the redox processes of the reaction
ii) to study the effect of pH, scan rate, concentration on the reaction
iii) to know the redox interaction of the species by CV, DPV and CPC techniques
iv) to recognize the most favorable condition for the reaction
v) to determine of the electron, transfer numbers of electro-synthesizing species with single step and/or multi-step electron transfer reaction
vi) to characterize the new features of the species by electrochemical and spectral analysis.

CHAPTER II

Theoretical Background

Electrochemistry can be broadly defined as the study of charge-transfer phenomena. The field of electroanalytical chemistry is the field of electrochemistry that utilizes the relationship between chemical phenomena which involve charge transfer (e.g. redox reactions, ion separation, etc.) and the electrical properties that accompany these phenomena for various analytical determination. Electrochemical techniques have been used since many years ago to study the thermodynamics and kinetics of heterogeneous reactions involving organic compounds. These techniques are concerned with the interplay between electricity and chemistry, namely, the measurements of electrical quantities, such as current, potential, or charge and their relationship to chemical parameters. Such use of electrical measurements for analytical purposes has found a vast range of applications, including environmental monitoring, pharmaceutical, industrial quality control, or biomedical analysis.

Amongst the variety of electrochemical methods and techniques available for drug analysis, voltammetry (current is measured as a function of applied potential) has become the most important and widespread. Sweep voltammetry in unstirred solution, based on continuously varying the potential that is applied across the electrode–solution interface and measuring the resulting current, where the predominant mode of mass transport is diffusion, is one of the most important and useful techniques for the study of electrochemical reactions and their mechanisms. The form of the current–potential curves at stationary electrodes, in unstirred solution, depends on the rate of change of applied potential. Analyzing these curves can give information about the kinetics and mechanism of reactions associated with electron transfer at the electrode.

Voltammetry (abbreviation of volt-amper-metry) is a branch of electrochemistry that was developed by the discovery of polarography in 1922 by Jaroslav Heyrovsky (Nobel Prize in 1959). voltammetric techniques present irreplaceable tools due to their robustness and

ability to provide a vast amount of important thermodynamics and kinetics information. This technique is used to characterize electro catalyst surfaces and kinetics of some of the electro catalytic reactions being most important in ever-growing fields of fuel cells, electrolysis and battery technologies, such as hydrogen oxidation/evolution reaction, oxygen reduction reaction, as well as the oxidation of carbon-monoxide and low-molecular weight alcohols. Voltammetry applies a constant and/or varying potential at an electrode's surface and measures the resulting current with a three electrode system. This method in practical terms is nondestructive since only a very small amount of the analyte is consumed at the two-dimensional surface of the working and auxiliary electrodes. The electrode can act as a source (for reduction) or a sink (for oxidation) of electrons transferred to or from the species in solution:

$$O + ne \rightarrow R$$

Where, O and R are the oxidized and reduced species. In order for the electron transfer to occur, there must be a correspondence between the energies of the electron orbitals where transfer takes place in the donor and acceptor. In the electrode this level is the highest filled orbital, which in a metal is Fermi energy level. In the soluble species it is the orbital of the valence electron to be given or received. For reduction, there is a minimum energy that the transferable electrons from the electrode must have before the transfer can occur, which corresponds to a sufficiently negative potential. For an oxidation, there is a maximum energy that the lowest unoccupied level in the electrode can have in order to receive electrons from the species in solution, corresponding to a sufficiently positive potential. In order to study electrode reactions, reproducible experimental conditions must be created which enable minimization of all unwanted factors that can contribute to the measurements and diminish their accuracy. That means to suppress migration effects, confine the interfacial region as close as possible to the electrode, and minimize solution resistance. These objectives are achieved by the addition of large amount (around 1 mol dm^{-3}) of inert electrolyte, the electroactive species being at a concentration of 5 mM or less [35]. Since an electrode predominantly attracts positively and negatively charged species, which may or may not undergo reaction at the surface, it should be remembered that the species may adsorb at the electrode surface. This makes it clear that in the description of any electrode process we have to consider the transport of species to the electrode surface as well as the electrode reaction itself. This transport can occur by diffusion, convection or migration.

2.1 Mass transfer process in voltammetry

The movement of the electro-active substance through solution is referred as mass transfer at the electrode surface. In electrochemical systems, there are different types of mass transfer system by which a substance may be transferred to the electrode surface from bulk solution. Depended on the experimental conditions, any of these or more than one might be operating in a given experiment system.

A reacting species may be brought to an electrode surface by three types of mass transfer processes:

- Migration
- Diffusion
- Convection

2.1.1 Migration

Migration refers to movement of a charge particle in a potential field. It occurs by the movement of ions through a solution as a result of electrostatic attraction between the ions and the electrodes. In general, most electrochemical experiment it is unwanted but can be eliminated by the addition of a large excess of supporting electrolytes. In the electrolysis solution, ions will move towards the charged electrode that means cations to the cathode and anions to the anode. This motion of charged particle through solution, induced by the charges on the electrodes is called migration [36]. This charge movement constitutes a current. This current is called migration current. The fraction of the current carried by a given cation and anion is known as its transport number. The larger the number of different kinds of ions in a given solution, the smaller is the fraction of the total charge that is carried by a particular species. Electrolysis is carried out with a large excess of inert electrolyte in the solution so the current of electrons through the external circuit can be balanced by the passage of ions through the solution between the electrodes, and a minimal amount of the electroactive species will be transported by migration. Migration is the movement of charged species due to a potential gradient. In voltammetric experiments, migration is undesirable but can be eliminated by the addition of a large excess of supporting electrolytes in the electrolysis solution. The effect of migration is applied zero by a factor of fifty to hundred ions excess of an inert supporting electrolyte. Electrolysis is

carried out with a large excess of inert electrolyte in the solution so the current of electrons through the external circuit can be balanced by the passage of ions through the solution between the electrodes, and a minimal amount of the electroactive species will be transported by migration. Migration is the movement of charged species due to a potential gradient.

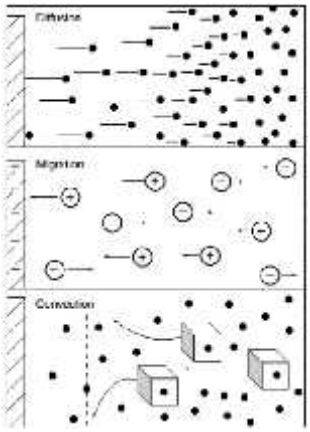

Figure 2.1: Three modes of mass transfer

In voltammetric experiments, migration is undesirable but can be eliminated by the addition of a large excess of supporting electrolytes in the electrolysis solution. The effect of migration is applied zero by a factor of fifty to hundred ions excess of an inert supporting electrolyte.

2.1.2 Diffusion

The movement of a substance through solution by random thermal motion is known as diffusion. Whereas a concentration gradient exists in a solution, that is the concentration of a substance, is not uniform throughout the solution. There is a driving force for diffusion of the substance from regions of high concentration to regions of lower concentration. In any experiment in which the electrode potential is such that the electron transfer rate is very high, the region adjacent to the electrode surface will become depleted of the electro-active species, setting up a concentration in which this species will constantly be arriving at the electrode surface by the diffusion from points further away [37]. The one kind of mode of mass transfer is diffusion to an electrode surface in an electrochemical cell. The

rate of diffusion is directly proportional to the concentration difference. When the potential is applied, the cations are reduced at the electrode surface and the concentration is decreased at the surface film. Hence a concentration gradient is produced. Finally, the result is that the rates of diffusion current become larger.

2.1.3 Convection

By mechanical way reactants can also be transferred to or from an electrode. Thus forced convection is the movement of a substance through solution by stirring or agitation. This will tend to decrease the thickness of the diffuse layer at an electrode surface and thus decrease concentration polarization. Natural convection resulting from temperature or density differences also contributes to the transport of species to and from the electrode [38]. At the same time a type of current is produced. This current is called convection current. Removing the stirring and heating can eliminate this current. Convection is a far more efficient means of mass transport than diffusion.

Electrochemical cell

An electrochemical cell is a device capable of either generating electrical energy from chemical reactions or facilitating chemical reactions through the introduction of electrical energy [39]. This electrochemical cell may be either two or three electrode system. The electrochemical reaction of interest takes place at the working electrode and the electrical current at this electrode due to electron transfer is termed as faradic current.

Fig: The three electrode system consisting of a working electrode, a reference electrode and a counter electrode.

Electrodes

(1) **Working electrode:** Working electrode is a glassy carbon electrode (GCE) with 3 mm diameter. The working electrode is an electrode where the redox reaction takes place. We measure the potential of the working electrode.

(2) **References electrode:** Ag/AgCl electrode used as references electrode. We measure the potential of working electrode with respect the reference electrode.

(3) **Counter electrode:** Pt wire is used as a working electrode. The counter electrode in the three-electrode system is made of an inert metal. The counter electrode used to complete the cell and reduce the resistances of the solution.

2.3 Cyclic voltammetry (CV)

There are several well established electrochemical techniques for the study of electrochemical reactions. We chose the CV technique to study and analyze the redox reactions occurring at the polarizable electrode surface. This technique helps us to understand the mechanism of electron transfer reaction of the compounds as well as the nature of adsorption of reactants or products on the electrode surface. Cyclic voltammetry is a very versatile electrochemical technique which allows proving the mechanics of redox and transport properties of a system in solution. This is accomplished with a three electrode arrangement whereby the potential relative to some reference electrode is scanned at a working electrode while the resulting current flowing through a counter (or auxiliary) electrode is monitored in a quiescent solution. More precisely, the controlling electronic is designed such that the potential between the reference and the working electrodes can be adjusted but the big impedance between these two components effectively forces any resulting current to flow through the auxiliary electrode. Usually the potential is scanned back and forth linearly with time between two extreme values – the switching potentials using triangular potential waveform (see Figure 2.1). When the potential of the working electrode is more positive than that of a redox couple present in the solution, the corresponding species may be oxidized (i.e. electrons going from the solution to the electrode) and produce an anodic current. Similarly, on the return scan, as the working electrode potential becomes more negative than the reduction potential of a redox couple, reduction (i.e. electrons flowing away from the electrode) may occur to

cause a cathodic current. By IUPAC convention, anodic currents are positive and cathodic currents negative.

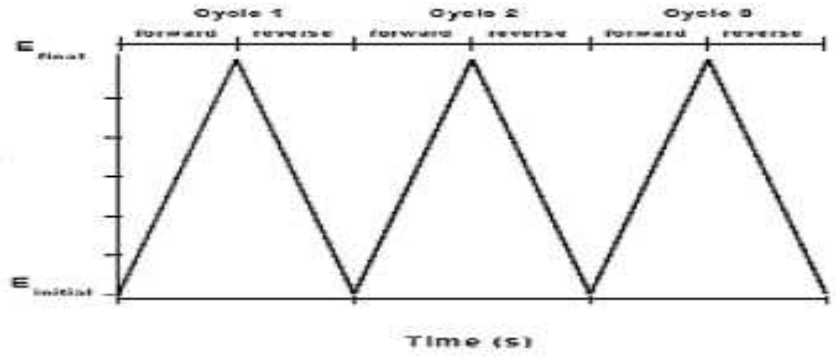

Figure 2.1: A cyclic voltammetry potential waveform with switching potentials

The magnitude of the observed faradaic current can provide information on the overall rate of the many processes occurring at the working electrode surface. As is the case for any multi–step process, the overall rate is determined by the slowest step. For an redox reaction induced at a working electrode, the rate determining step may be any one of the following individual step depending on the system: rate of mass transport of the electro-active species, rate of adsorption or de-sorption at the electrode surface, rate of the electron transfer between the electro-active species and the electrode, or rates of the individual chemical reactions which are part of the overall reaction scheme.

For the oxidation reaction involving *n* electrons

$$\text{Red} \rightleftarrows \text{Ox} + ne^-$$

the *Nernst Equation* gives the relationship between the potential and the concentrations of the oxidized and reduced form of the redox couple at equilibrium (at 298 K):

$$E = E^{0'} + \frac{0.059}{n} \log_{10} \frac{[\text{Ox}]}{[\text{Red}]}$$

where E is the applied potential and $E^{0'}$ the formal potential; [OX] and [Red] represent surface concentrations at the electrode/solution interface, *not* bulk solution concentrations. Note that the Nernst equation may or may not be obeyed depending on the system or on the experimental conditions.

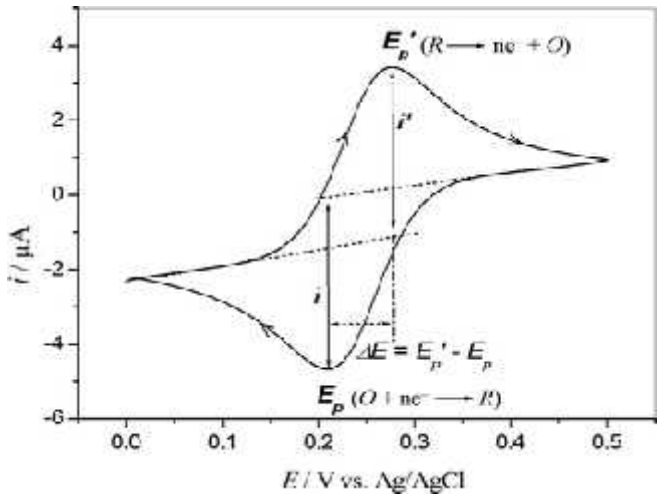

Figure 2.2: The expected response of a reversible redox couple during a single potential cycle

A typical voltammogram is shown in Figure 2.2. The current is first observed to peak at E_{pa} (with value i_{pa}) indicating that an oxidation is taking place and then drops due to depletion of the reducing species from the diffusion layer. During the return scan the processes are reversed (reduction is now occurring) and a peak current is observed at E_{pc} (corresponding value, i_{pc}). Providing that the charge–transfer reaction is reversible, that there is no surface interaction between the electrode and the reagents, and that the redox products are stable (at least in the time frame of the experiment), the ratio of the reverse and the forward current $i_{pr}/i_{pf} = 1.0$ (in Figure 2.2 $i_{pa} = i_{pf}$ and $i_{pc} = i_{pr}$). In addition, for such a system it can be shown that:

- the corresponding peak potentials E_{pa} and E_{pc} are independent of scan rate and concentration
- the formal potential for a reversible couple $E^{0'}$ is centered between E_{pa} and E_{pc}: $E^{0'} = (E_{pa} + E_{pc})/2$
- the separation between peaks is given by $\Delta E_p = E_{pa} - E_{pc} = 59/n$ mV (for a n electron transfer reaction) at all scan rates (however, the measured value for a reversible process is generally higher due to uncompensated solution resistance and non-linear diffusion. Larger values of ΔE_p, which increase with increasing scan rate, are characteristic of slow electron transfer kinetics).

It is possible to relate the half-peak potential ($E_{p/2}$, where the current is half of the peak current) to the polarographic half-wave potential, $E_{1/2}$: $E_{p/2} = E_{1/2} \pm 29mV/n$ (The sign is positive for a reduction process.) Simply stated, in the forward scan, the reaction is $O + e^- \rightarrow R$, R is electrochemically generated as indicated by the cathodic current. In the reverse scan, $R \rightarrow O + e^-$, R is oxidized back to O as indicated by the anodic current. The CV is capable of rapidly generating a new species during the forward scan and then probing its fate on the reverse scan [40]. This is a very important aspect of the technique.

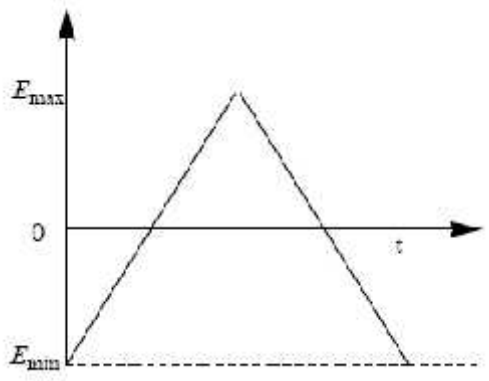

Figure 2.3: Variation of potential with time in cyclic voltammetry

A characteristic feature is the occurrence of peaks, identified by the peak potential E_p, which corresponds to electron transfer reactions. The repetitive triangular potential excitation signal for CV causes the potential of the working electrode to sweep backward and forward between two designate values (the switching potentials). In cyclic voltammetry of reversible system, the product of the initial oxidation or reduction is then reduced or oxidized, respectively, on reversing the scan direction. Adsorbed species lead to changes in the shape of the cyclic voltammogram, since they do not have to diffuse from the electrode surface. In particular, if only adsorbed species are oxidized or reduced, in the case of fast kinetics the cyclic voltammogram is symmetrical, with coincident oxidation and reduction peak potentials [41].

Cyclic voltammetry is one of the most versatile techniques for the study of electroactive species, as it has a provision for mathematical analysis of an electron transfer process at the electrode [42-45]. It is an electroanalytical tool for monitoring and recognition of

many electrochemical processes taking place at the surface of electrode and can be used to study redox processes in biochemistry and macromolecular chemistry [46].

2.3.1 Single electron transfer process

Based upon the values of electrochemical parameters, i.e., peak potential E_p, half peak potential ($E_{p/2}$), half wave potential ($E_{1/2}$), peak current (I_p), anodic peak potential E_{pa}, cathodic peak potential E_{pc} etc, it can be ascertained whether a reaction is reversible, irreversible or quasi-reversible. The electrochemical parameters can be graphically obtained from the voltammogram as shown in the Figure 2.3.

Three types of single electron transfer process can be studied.

a. Reversible process. b. Irreversible process and c. Quasi-reversible.

2.3.1(a) Reversible processes

The peak current for a reversible couple (at 25°C), is given by the Randles-Sevcik equation: $\boldsymbol{i}_p = (2.69 \times 10^5)\, n^{3/2} A C D^{1/2} v^{1/2}$

where n is the number of electrons, A the electrode area (in cm^2), C the concentration (in mol/cm^3), D the diffusion coefficient (in cm^2/s), and v the scan rate (in V/s). Accordingly, the current is directly proportional to concentration and increases with the square root of the scan rate. The ratio of the reverse-to-forward peak currents, $\boldsymbol{i}_{pr}/\boldsymbol{i}_{pf}$, is unity for a simple reversible couple. The current peaks are commonly measured by extrapolating the preceding baseline current. The position of the peaks on the potential axis (E_p) is related to the formal potential of the redox process. The formal potential for a reversible couple is centered between E_{pa} and E_{pc}:

$$E^\circ = (E_{pa} + E_{pc})/2$$

The separation between the peak potentials (for a reversible couple) is given by:

$$\Delta E_p = E_{pa} - E_{pc} = 59mV/n$$

Thus, the peak separation can be used to determine the number of electrons transferred, and as a criterion for a Nernstian behavior. Accordingly, a fast one-electron process exhibits a ΔE_p of about 59 mV. Both the cathodic and anodic peak potentials are

independent of the scan rate. It is possible to relate the half-peak potential ($E_{p/2}$, where the current is half of the peak current) to the polarographic half-wave potential, $E_{1/2}$

$$E_{p/2} = E_{1/2} \pm 29mV/n$$

(The sign is positive for a reduction process.) For multi electron-transfer (reversible) processes, the cyclic voltammogram consists of several distinct peaks, if the E^o values for the individual steps are successively higher and are well separated. An example of such mechanism is the six-step reduction of the fullerenes C_{60} and C_{70} to yield the hexaanion products C_{60}^{6-} and C_{70}^{6-} where six successive reduction peaks can be observed. The situation is very different when the redox reaction is slow or coupled with a chemical reaction. Indeed, it is these "nonideal" processes that are usually of greatest chemical interest and for which the diagnostic power of cyclic voltammetry is most useful. Such information is usually obtained by comparing the experimental voltammograms with those derived from theoretical (simulated) ones.

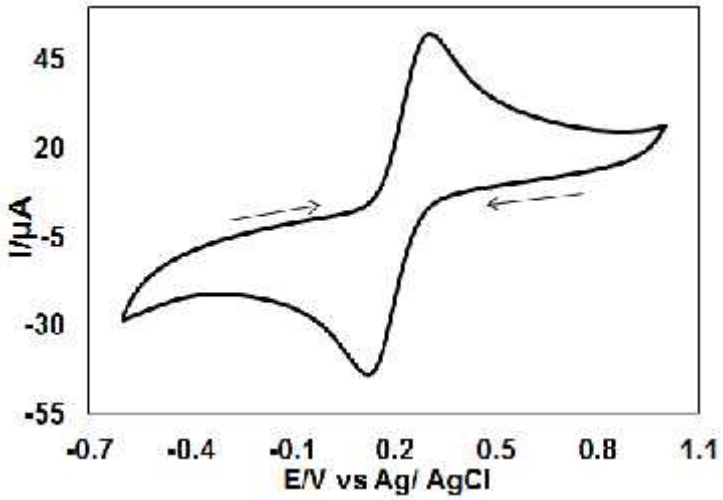

Figure 2.4: Reversible cyclic voltammogram of redox process

2.3.1(b) Irreversible processes

For irreversible processes (those with sluggish electron exchange), the individual peaks are reduced in size and widely separated. Totally irreversible systems are characterized by a shift of the peak potential with the scan rate:

$$E_p = E° - (RT/\alpha n_a F)[0.78 - \ln(k^o/(D)^{1/2}) + \ln (\alpha n_a F\nu/RT)^{1/2}]$$

Where, α is the transfer coefficient and n_a is the number of electrons involved in the charge-transfer step. Thus, E_p occurs at potentials higher than E°, with the overpotential related to k° and a. Independent of the value k°, such peak displacement can be compensated by an appropriate change of the scan rate. The peak potential and the half-peak potential (at 25°C) will differ by $48/\alpha n$ mV. Hence, the voltammogram becomes more drawn-out as $\alpha\mathbf{n}$ decreases.

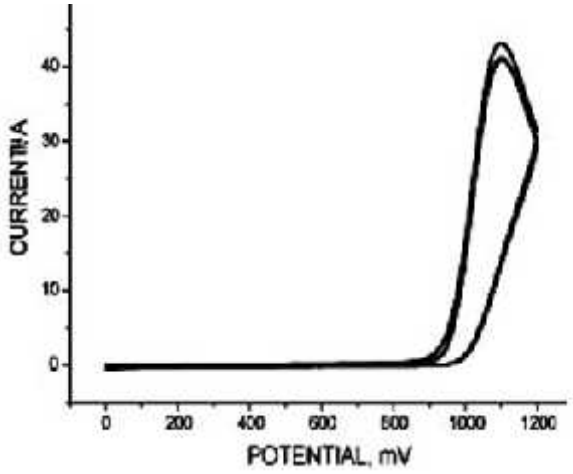

Figure 2.5: Cyclic voltammogram of irreversible redox process

2.3.1(c) Quasi-reversible process

Quasi-reversible process is termed as a process, which shows intermediate behavior between reversible and irreversible processes. In such a process the current is controlled by both the charge transfer and mass transfer.

Cyclic voltammogram for quasi-reversible process is shown in Figure 2.6 [47].

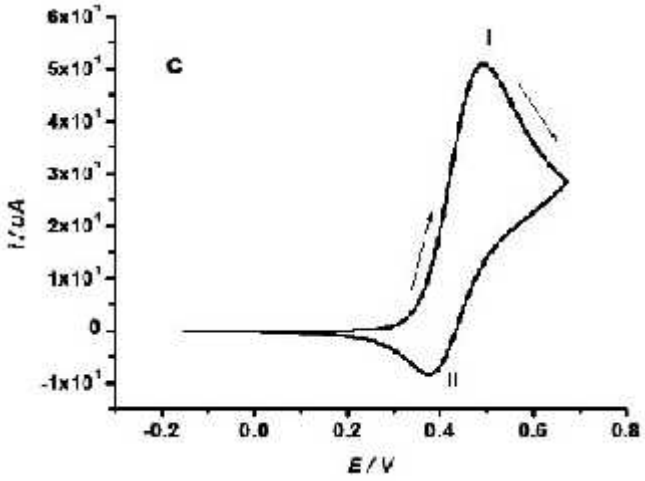

Figure 2.6: Cyclic voltammogram of quasi-reversible redox process

For quasi-reversible process the value of standard heterogeneous electron transfer rate constant, k_{sh}^{o} lies in the range of 10^{-1} to 10^{-5} cm sec^{-1} [48]. An expression relating the current to potential dependent charge transfer rate was first provided by Matsuda and Ayabe [49].

$$I(t) = C_{o(0,t)} k_{sh}^{o} Exp\left[-\frac{\alpha nF}{RT}\left\{E(t) - E^{o}\right\}\right] - C_{R(0,t)} k_{sh}^{o} Exp\left[-\frac{nF}{RT}\left\{E(t) - E^{o}\right\}\right] \text{….2.1}$$

where k_{sh}^{o} is the heterogeneous electron transfer rate constant at standard potential E^{0} of redox system. α is the transfer coefficient and β = 1- α. In this case, the shape of the peak and the various peak parameters are functions of α and the dimensionless parameter, Λ, defined as [50]

$$\Lambda = \frac{k_{s,h}}{D^{1/2}(nF/RT)^{1/2}\nu^{1/2}} \text{ ………………………….....2.2}$$

when $D_{o} = D_{R} = D$

D_{o} and D_{R} are the diffusion coefficients of oxidized and reduced species respectively.

For quasi-reversible process current value is expressed as a function of $\psi(E)$ [53].

$$I = nFAC_{o}^{*}\frac{k_{sh}^{o}}{\Lambda}\psi(E) \text{ ………………………………..2.3}$$

where $\psi(E)$ is expressed as

$$\psi(E) = \frac{I}{nFAC_{o}^{*}D_{o}^{1/2}(nF/RT)^{1/2}\nu^{1/2}} \text{ ………………..2.4}$$

It is observed that when $\Lambda \geq 10$, the behavior approaches that of a reversible system [51]. For three types of electrode processes, Matsuda and Ayabe [49] suggested following zone boundaries.

- Reversible (Nernstian)

  $k_{sh}^{o} \geq 0.3\nu^{1/2}$ cm s^{-1}

- Quasi-reversible

  $0.3\nu^{1/2} \geq k_{sh}^{o} \geq 2\times10^{-5}\nu^{1/2}$ cm s^{-1}

- Totally irreversible

$$k_{sh}^{o} \leq 2 \times 10^{-5} 3^{1/2} \text{ cm s}^{-1}$$

2.3.2 Multi electron transfer processes

Multi-electron transfer process usually takes place in different steps. A two-step mechanism each characterized by its own electrochemical parameters is called an "EE mechanism".

A two-step reversible "EE mechanism" is represented as;

$$O + n_1 e \leftrightarrow R_1 \qquad (E_1^o) \ldots\ldots\ldots\ldots\ldots\ldots\ldots 2.5$$

$$R + n_1 e \leftrightarrow R_2 \qquad (E_2^o) \ldots\ldots\ldots\ldots\ldots\ldots.. 2.6$$

Each heterogeneous electron transfer step is associated with its own electrochemical parameters i.e., k_{sh}^{o} and α_i, where i = 1, 2 for the 1st and 2nd electron transfer respectively. The value of k_{sh}^{o} for first reversible electron transfer limiting case can be calculated as [52]:

$$k_{sh} = k_{sh}^{o} \exp\left[- \sim 1 F \Delta E^{o} / 2RT\right] \ldots\ldots\ldots\ldots\ldots\ldots\ldots\ldots\ldots 2.7$$

where

$$\Delta E^{o} = E_2^{o} - E_1^{o}$$

For ΔE^0 greater than 180 mV, shape of wave does not dependent on the relative values of E^0, otherwise shapes of peak and peak currents depend upon ΔE^0 [53]. Based on the value of ΔE^0, we come across different types of cases as shown in the Figure 2.6.

Types of two electron transfer reactions

Case 1**:** $\Delta E^0 \geq 150$ mV peaks separation

When $\Delta E^0 \geq 150$ mV the EE mechanism is termed as "disproportionate mechanism [54]. Cyclic voltammogram consists of two typical one-electron reduction waves. The heterogeneous electron transfer reaction may simultaneously be accompanied by homogenous electron transfer reaction, which in multi-electron system leads to disproportionation which can be described as:

$$R_1 \rightarrow O + n_1 e \ldots\ldots\ldots\ldots\ldots\ldots\ldots\ldots\ldots\ldots\ldots\ldots\ldots\ldots.. 2.8a$$

$$R_1 + n_2 e \rightarrow R_2 \quad \text{.....2.8b}$$

$$2R_1 \leftrightarrow O + R_2 \quad \text{.....2.8c}$$

$$k_{disp} = \frac{[O][R_2]}{[R_1]^2} \quad \text{.....2.9}$$

$$\ln k_{disp} = \left[\frac{nF}{RT}\right](E_2^o - E_1^o) \quad \text{.....2.10}$$

***Case 2*:** ΔE^0 < 100 mV ----- Peaks overlapped

In this case, the individual waves merge into one broad distorted wave whose peak height and shape are no longer characteristics of a reversible wave. The wave is broadened similar to an irreversible wave, but can be distinguished from the irreversible voltammogram, in that the distorted wave does not shift on the potential axis as a function of the scan rate.

***Case 3*:** ΔE^0 = 0 mV ----- Single peak

In this case, in cyclic voltammogram, only a single wave would appear with peak current intermediate between those of a single step one electron and two electron transfer reactions and E_p-E_p/2 = 56 mV.

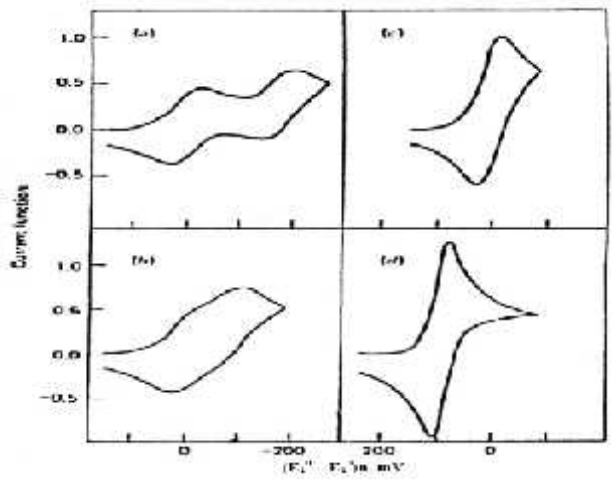

Figure 2.7 Cyclic voltammograms for a reversible two-step system (a) ΔE^0**= - 180 mV, (b)** ΔE^0 **= -90 mV, (c)** ΔE^0 **= 0 mV, (d)** ΔE^0 **= 180 mV.** (Taken from ref. [58])

Contrary to the convention the direction of the current in these voltammograms has been shown cathodic above the base line and anodic below the base line.

Case 4: $E^0_1 < E^0_2$ ----2nd Reduction is easy than 1st one

If the energy required for the second electron transfer is less than that for the first, one wave is observed, having peak height equal to $2^{3/2}$ times that of a single electron transfer process. In this case, E_p-$E_p/2$ = 29 mV. The effective E^0 for the composite two electron wave is given by $\frac{(E_1^o + E_2^o)}{2}$ as reported in literature [55].

2.4 Pulse techniques

The basis of all pulse techniques is the difference in the rate of decay of the charging and the faradaic currents following a potential step (or pulse). The charging current decays considerably faster than the faradaic current. A step in the applied potential or current represents an instantaneous alteration of the electrochemical system. Analysis of the evolution of the system after perturbation permits deductions about electrode reactions and their rates to be made. The potential step is the base of pulse voltammetry. After applying a pulse of potential, the capacitive current dies away faster than the faradic one and the current is measured at the end of the pulse. This type of sampling has the advantage of increased sensitivity and better characteristics for analytical applications. At solid electrodes there is an additional advantage of discrimination against blocking of the electrode reaction by adsorption [41].

2.4.1 Differential pulse voltammetry (DPV)

Differential pulse voltammetry (DPV) is often used to make electrochemical measurements. It can be considered as a derivative of linear sweep voltammetry, with a series of regular voltage pulses superimposed on the potential linear sweep. The current is measured immediately before each potential change, and the current difference is plotted as a function of potential. By sampling the current just before the potential is changed, the effect of the charging current can be decreased [56]. The potential wave form for differential pulse voltammetry (DPV) is shown in Figure 2.8. The potential wave form consists of small pulses (of constant amplitude) superimposed upon a staircase wave form. Unlike Normal pulse voltammetry (NPV),

the current is sampled twice in each Pulse Period (once before the pulse, and at the end of the pulse), and the difference between these two current values is recorded and displayed.

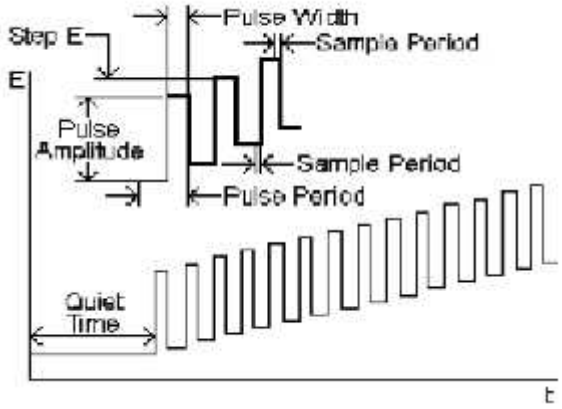

Figure 2.8: Scheme of application of potential

The important parameters for pulse techniques are as follows:

- Pulse amplitude is the height of the potential pulse. This may or may not be constant depending upon the technique.
- Pulse width is the duration of the potential pulse.
- Sample period is the time at the end of the pulse during which the current is measured.
- For some pulse techniques, the pulse period or drop time must also be specified. This parameter defines the time required for one potential cycle, and is particularly significant for polarography (i.e., pulse experiments using a mercury drop electrode), where this time corresponds to the lifetime of each drop (i.e., a new drop is dispensed at the start of the drop time, and is knocked off once the current has been measured at the end of the drop time - note that the end of the drop time coincides with the end of the pulse width).

CHAPTER III

Experimental

Electro-oxidation of 1,2-Dihydroxybenzene in presence of L-Alanine, L-Phenylalanine and L-Leucine at different pH has been examined by using Cyclic voltammetry (CV), Differential pulse voltammetry (DPV) and Controlled potential coulometry at Glassy carbon (GC), Gold (Au) and Platinum (Pt) electrode. Details of the instrumentation are given in the following sections. The source of different chemicals, the instruments and brief description of the methods are given below.

3.1 Chemicals

All chemicals and solvents used in the electrochemical synthesis and analytical work were of analytical grade. Chemicals were used in this investigation are listed below-

Sl. No.	Chemicals	Molecular formula	Molar mass	Reported purity	Producer
1.	Catechol	$C_6H_4(OH)_2$	110.11	99%	Fisher Scientific UK Ltd.
2.	L-Alanine	$C_3H_7NO_2$	89.09	99%	E-Merck, Germany
3.	L-Phenylalanine	$C_9H_{11}NO_2$	165.19	99%	Merk Specialities Pvt. Ltd., India
4.	L-Leucine	$C_6H_{13}NO_2$	131.17	99.5%	E-Merck, Germany
4.	Glacial Acetic Acid	CH_3COOH	60.05	99.5%	Loba Chemie Pvt. Ltd., India
5.	Sodium Acetate	$CH_3COONa.3H_2O$	136.08	99%	Merk Specialities Pvt. Ltd., India
6.	Potasium Chloride	KCl	74.60	99.5%	E-Merck, Germany

Sl. No.	Chemicals	Molecular formula	Molar mass	Reported purity	Producer
7.	Sodium Di-hydrogen Orthophosphate	$NaH_2PO_4.2H_2O$	156.01	98-100%	Loba Chemie Pvt. Ltd., India
8.	Di-sodium Hydrogen Orthophosphate	$Na_2HPO_4.2H_2O$	177.99	97-100%	Thermo Fisher Scientific India Pvt. Ltd.
9.	Sodium Hydroxide	NaOH	40.0	97%	E-Merck, Germany
10.	Sodium Bicarbonate	$NaHCO_3$	84.0	99%	E-Merck, Germany

3.2 Equipments

During this research work the following instruments were used-

- The electrochemical studies (CV, DPV) were performed with a computer controlled potentiostats/ galvanostats (µstat 400, Drop Sens, Spain)
- A Pyrex glass micro cell with teflon cap
- Glassy carbon (GC)/ Gold (Au)/ Platinum (Pt) as working electrode (BASi, USA)
- Three carbon rods (Local market Dhaka, Bangladesh)
- Ag/ AgCl as reference electrode (BASi, USA)
- Liquid micro size (0.05um) polishing alumina (BAS Inc. Japan)
- Pt wire as counter electrode (Local market, Dhaka, Bangladesh)
- A HR 200 electronic balance with an accuracy of ± 0.0001g was used for weighting and
- A pH meter (pH Meter, Hanna Instruments, Italy) was employed for maintaining the pH of the solutions.

3.3 Cyclic voltammetry (CV)

Cyclic voltammetry is one of the most exploited techniques in electrochemical studies. Its primary advantage comes from the fact that it gives insight into both the half-reactions taking place at the working electrode, providing at the same time information about the chemical or physical phenomena coupled to the studied electrochemical reaction. In

several well established electrochemical techniques for the study of electrochemical reactions, we have chosen the CV technique to study and analyze the redox reactions occurring at the polarizable electrode surface. This technique helps us to understand the mechanism of electron transfer reaction of the compounds as well as the nature of adsorption of reactants or products on the electrode surface. CV is often the first experiment performed in an electrochemical study. CV consists of imposing an excitation potential nature on an electrode immersed in an unstirred solution and measuring the current and its potential ranges varies from a few millivolts to hundreds of millivolts per second in a cycle. This variation of anodic and cathodic current with imposed potential is termed as voltammogram [38]. The technique involves under the diffusion controlled mass transfer condition at a stationary electrode utilizing symmetrical triangular scan rate ranging from 1 mVs^{-1} to hundreds millivolts per second. In CV the current function can be measured as a function of scan rate. The potential of the working electrode is controlled vs a reference electrode such as Ag/AgCl electrode. The electrode potential is ramped linearly to a more negative potential and then ramped is reversed back to the starting voltage. The forward scan produces a current peak for any analyte that can be reduced through the range of potential scan. The current will increase as the current reaches to the reduction potential of the analyte [65].

The current at the working electrode is monitored as a triangular excitation potential is applied to the electrode. The resulting voltammogram can be analyzed for fundamental information regarding the redox reaction. The potential at the working electrode is controlled vs a reference electrode, Ag/AgCl (standard NaCl) electrode. The excitation signal varies linearly with time. First scan positively and then the potential is scanned in reverse, causing a negative scan back to the original potential to complete the cycle. Signal on multiple cycles can be used on the scan surface. A cyclic voltammogram is plot of response current at working electrode to the applied excitation potential.

3.4 Important features of CV

An electrochemical system containing species ‘O’ capable of being reversibly reduced to ‘R’ at the electrode is given by,

$$O + ne^- = R \quad \ldots\ldots\ldots\ldots\ldots\ldots\ldots\ldots 3.1$$

Nernst equation for the system is

$$E = E^0 - \frac{0.059}{n}\log\frac{C_0^s}{C_R^s} \quad \text{.....3.2}$$

Where,

E = Potential applied to the electrode

E^0 = Standard reduction potential of the couple versus reference electrode

n = Number of electrons in Equation (3.1)

C_0^s = Surface concentration of species 'O'

C_R^s = Surface concentration of species 'R'

A redox couple that changes electrons rapidly with the working electrode is termed as electrochemically reverse couple. The relation gives the peak current i_{pc}

$$i_{pc} = 0.4463\ nFA\ (D\Im)^{1/2}C \quad \text{.....3.3}$$

$$\sim = \frac{nFv}{RT} = \frac{nv}{0.026}$$

Where,

i_{pc} = peak current in amperes

F= Faraday`s constant (approximately 96500)

A = Area of the working electrode in cm^2

v= Scan rate in volt/ sec

C= Concentration of the bulk species in mol/L

D= Diffusion coefficient in cm^2 /sec

In terms of adjustable parameters, the peak current is given by the Randless-Sevcik equation,

$$i_{pc} = 2.69 \times 10^5 \times n^{3/2} A D^{1/2} C v^{1/2} \quad \text{.....3.4}$$

The peak potential E_p for reversible process is related to the half wave potential $E_{1/2}$, by the expression,

$$E_{pc} = E_{1/2} - 1.11\frac{RT}{nF} \quad , \quad \text{at } 25^0\text{C} \text{.....3.5}$$

$$E_{pc} = E_{1/2} - \frac{0.0285RT}{n} \quad \text{.....} \quad 3.6$$

The relation relates the half wave potential to the standard electrode potential

$$E_{1/2} = E^0 - \frac{RT}{nF}\ln\frac{f_{red}}{f_{ox}}\left(\frac{D_{ox}}{D_{ox}}\right)^{1/2}$$

$$E_{1/2} = E^0 - \frac{RT}{nF}\ln\left(\frac{D_{ox}}{D_{red}}\right)^{1/2} \quad \text{.....3.7}$$

Assuming that the activity coefficient f_{ox} and f_{red} are equal for the oxidized and reduced species involved in the electrochemical reaction.

From Equation (3.6), we have,

$$E_{pa} - E_{pc} = 2.22\frac{RT}{nF} \quad \text{at } 25^0\text{C} \text{..... 3.8}$$

$$\text{or } E_{pa} - E_{pc} = \frac{0.059}{n} \quad \text{at } 25^0\text{C} \text{.....3.9}$$

This is a good criterion for the reversibility of electrode process. The value of i_{pa} should be close for a simple reversible couple,

$$i_{pa}/i_{pc} = 1 \text{.....3.10}$$

And such a system $E_{1/2}$ can be given by,

$$E_{1/2} = \frac{E_{pa} + E_{pc}}{2} \text{.....3.11}$$

For irreversible processes (those with sluggish electron exchange), the individual peaks are reduced in size and widely separated, totally irreversible systems are characterized by a shift of the peak potential with the scan rate [66];

$$E_p = E^0 - (RT/\Im n_a F)[0.78 - \ln(k^0/(D)^{1/2}) + \ln(\Im n_a F\Im/RT)^{1/2}] \text{.....3.12}$$

Where $\Im$ is the transfer coefficient and n_a is the number of electrons involved in the charge transfer step. Thus E_p occurs at potentials higher than E^0, with the over potential related to k^0 (standard rate constant) and $\Im$. Independent of the value k^0, such peak displacement can be compensated by an appropriate change of the scan rate. The peak potential and the half-peak potential (at 25^0 C) will differ by 48/ $\Im$n mV. Hence, the voltammogram becomes more drawn-out as $\Im$n decreases.

The peak current, given by

$$i_p = (2.99 \times 10^5) n(\Im n_a)^{1/2} A C D^{1/2} v^{1/2} \text{.....3.13}$$

is still proportional to the bulk concentration , but will be lower in height (depending upon the value of $\Im$) . Assuming $\Im$ = 0.5, the ratio of the reversible–to–irreversible current peaks is 1.27 (i.e. the peak current for the irreversible process is about 80% of the peak for

a reversible one). For quasi- reversible systems (with $10^{-1} > k^0 > 10^{-5}$ cm/s) the current is controlled by both the charge transfer and mass transport [70]. The shape of the cyclic voltammogram is a function of the ratio k^0 ($\Leftrightarrow$nFD/RT) $^{1/2}$. As the ratio increases, the process approaches the reversible case. For small values of it, the system exhibits an irreversible behavior. Overall, the voltammograms of a quasi-reversible system are more drawn out and exhibit a larger separation in peak potential compared to a reversible system. Unlike the reversible process in which the current is purely mass transport controlled, currents due to quasi-reversible process are controlled by a mixture of mass transport and charge transfer kinetics [67, 68]. The process occurs when the relative rate of electron transfer with respect to that of mass transport is insufficient to maintain Nernst equilibrium at the electrode surface.

3.5 Differential pulse voltammetry (DPV)

Differential pulse voltammetry (DPV) is a technique that is designed to minimize background charging currents. The waveform in DPV is a sequence of pulses, where a baseline potential is held for a specified period of time prior to the application of a potential pulse. Current is sampled just prior to the application of the potential pulse. The potential is then stepped by a small amount (typically < 100 mV) and current is sampled again at the end of the pulse. The potential of the working electrode is then stepped back by a lesser value than during the forward pulse such that baseline potential of each pulse is incremented throughout the sequence. By contrast, in normal pulse voltammetry the current resulting from a series of ever larger potential pulse is compared with the current at a constant 'baseline' voltage. Another type of pulse voltammetry is square wave voltammetry, which can be considered a special type of differential pulse voltammetry in which equal time is spent at the potential of the ramped baseline and potential of the superimposed pulse. The potential wave form consists of small pulses (of constant amplitude) superimposed upon a staircase wave form [56]. Unlike NPV, the current is sampled twice in each pulse Period (once before the pulse, and at the end of the pulse), and the difference between these two current values is recorded and displayed.

3.6 Important features of DPV

Differential pulse voltammetry has these prominences:

i) Current is sampled just prior to the application of the potential pulse.

ii) Reversible reactions show symmetrical peaks and irreversible reaction show asymmetrical peaks.

iii) The peak potential is equal to $E_{1/2}^{r}$-ζE in reversible reactions, and the peak current is proportional to the concentration.

3.7 Computer controlled potentiostats (for CV, DPV and CA experiment)

The main instrument for voltammetry is the Potentiostats/ Galvanostats (μStat 400, DropSens, Spain), which will be applied to the desired potential to the electrochemical cell (i.e. between a working electrode and a reference electrode), and a current-to-voltage converter, which measures the resulting current, and the data acquisition system produces the resulting voltammogram.

3.8 Electrochemical cell

This research work was performed by a three electrode electrochemical cell. The voltammetric cell also contains a Teflon cap. The electrochemical reaction of interest takes place at the working electrode and the electrical current at this electrode due to electron transfer is termed as faradic current. The counter electrode is driven by the potentiostatic circuit to balance the faradic process at the working electrode with an electron transfer of opposite direction.

3.9 Electrodes

Three types of electrodes are used in this research:

i) Working electrodes are Glassy carbon (GC) electrode with 3.0 mm diameter disc, Gold (Au) & Platinum (Pt) electrode with 1.6 mm diameter disc and three carbon rods (diameter 6.0 mm)

ii) Ag/AgCl (standard NaCl) electrode used as reference electrode from BASi, USA

iii) Counter electrode is a Pt wire

The working electrode is an electrode on which the reaction of interest is occurring. The reference electrode is a half-cell having a known electrode potential and it keeps the potential between itself and the working electrode. The counter electrode is employed to allow for accurate measurements to be made between the working and reference electrodes.

3.10 Preparation of electrodes

In this study, Glassy carbon (GC), Gold (Au) and Platinum (Pt) electrodes purchase from the BASi, USA are used as working electrode. Electrode preparation includes polishing and conditioning of the electrode. The electrode was polished with 0.05µm alumina powder on a wet polishing cloth. For doing so a part of the cloth was made wet with deionized water and alumina powder was sprinkled over it. Then the electrode was polished by softly pressing the electrode against the polishing surface at least 10 minutes. The electrode surface would look like a shiny mirror after thoroughly washed with deionized water.

3.11 Removing dissolved Oxygen from solution

Dissolved oxygen can interfere with observed current response so it is needed to remove it. Experimental solution was indolent by purging for at least 5-10 minutes with 99.99% pure and dry nitrogen gas (BOC, Bangladesh). By this way, traces of dissolved oxygen were removed from the solution.

3.12 Electrode polishing

Materials may be adsorbed to the surface of a working electrode after each experiment. Then the current response will degrade and the electrode surface needs to clean. In this case, the cleaning required is light polishing with 0.05µm alumina powder. A few drops of polish are placed on a polishing pad and the electrode is held vertically and the polish

rubbed on in a figure-eight pattern for a period of 30 seconds to a few minutes depending upon the condition of the electrode surface. After polishing the electrode surface is rinsed thoroughly with deionized water.

3.13 Experimental procedure

The electrochemical cell filled with solution 50mL of the experimental solution and the Teflon cap was placed on the cell. The working electrode together with reference electrode and counter electrode was inserted through the holes. The electrodes were sufficiently immersed. The solution system is deoxygenated by purging the nitrogen gas for about 10 minutes. The solution has been kept quiet for 10 seconds. After determination the potential window the voltammogram is taken at various scan rates, pH and concentrations from the Drop View Software.

3.14 Preparation of buffer solutions

Acetate Buffer Solution: To prepare acetate buffer (pH 3.0-5.0) solution definite amount of sodium acetate was dissolved in 0.1M acetic acid in a volumetric flask and the pH was measured. The pH of the buffer solution was adjusted by further addition of acetic acid and / or sodium acetate.

Phosphate Buffer Solution: Phosphate buffer solution (pH 6.0-8.0) was prepared by mixing a solution of 0.1M sodium dihydrogen ortho-phosphate ($NaH_2PO_4.2H_2O$) with a solution of 0.1M disodium hydrogen ortho-phosphate ($Na_2HPO_4.2H_2O$). The pH of the prepared solution was measured with pH meter.

Bicarbonate Buffer Solution: To prepare hydroxide buffer (pH 9.0-11.0) solution definite amount of sodium hydroxide was dissolved in 0.1M sodium bicarbonate in a volumetric flask. The pH of the prepared solution was measured with pH meter.

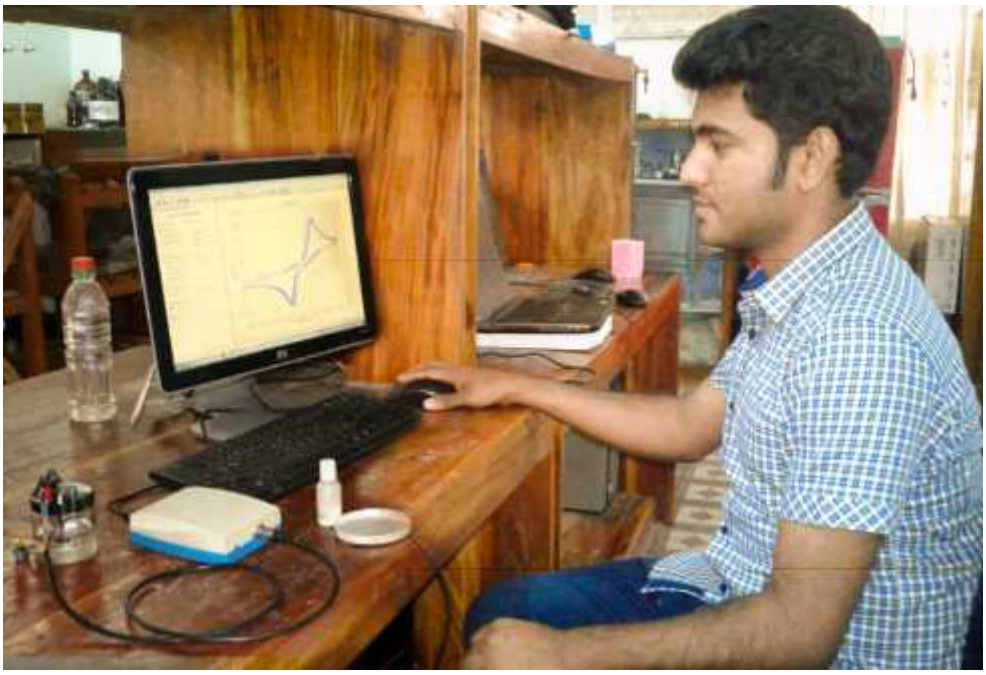

Figure 3.1: Experimental setup (Software controlled Potentiostats (µstat 400))

CHAPTER IV

Results and Discussion

This section describes all graphical and experimental data elaborately. The reaction of electrochemically produced *o*-benzoquinone from oxidation of 1,2-dihydroxybenzene as Michael acceptor with alanine, L-Phenylalanine and L-Leucine as nucleophiles has been studied in details in aqueous solution with various pH values (5-11), different electrodes (GC, Pt and Au) and different concentration of nucleophiles using Cyclic Voltammetry (CV), Controlled Potential Coulometry (CPC) and Differential Pulse Voltammetry (DPV). The participation of reaction of *o*-benzoquinone with different concentration of nucleophiles in the second scan of potential has been observed. The adducts were isolated for FTIR spectral analysis. By conducting this investigation, we have extracted some important information regarding redox behavior, number of electron transfer and nucleophilic substitution reaction of electroactive 1,2-dihydroxybenzene in presence of L-Alanine, L-Phenylalanine and L-Leucine.

4.1.1 Electrochemical behavior of 1,2-dihydroxybenzene

Fig. 4.1 represents the cyclic voltammogram of the first 15^{th} cycles of 2 mM 1,2-dihydroxybenzene of GC (3 mm) electrode in buffer solution of pH 7. The voltammogram at the $0.1Vs^{-1}$ scan rate has one anodic peak at 0.38 V and corresponding cathodic peak at 0.03 V versus Ag|AgCl. In the subsequent potential cycles no new anodic peak appeared. This can be attributed that 1,2-dihydroxybenzene showed one anodic peak related to its transformation to *o*-quinone and corresponding cathodic peak related to its transformation to 1,2-dihydroxybenzene from *o*-benzoquinone (Scheme 1) within a quasi-reversible two-electron transfer process (Table 4.1).

4.1.2 Electrochemical behavior of 1,2-dihydroxybenzene in presence of L-Alanine

Cyclic voltammogram of only 1,2-dihydroxybenzene (Green line), only L-Alanine (Blue line) and 1,2-dihydroxybenzene with L-Alanine (Red line) at Gc (3mm) electrode in buffer

solution of pH 7 and scan rate 0.1V/s in Fig. 4.2. According to this cyclic voltammogram it can be observed that 1,2-dihydroxybenzene shows one redox pair at A_1 (0.26V)/C_1 (0.05V) related to its transformation to *o*-benzoquinone and vice versa. As pure L-Alanine is an electrochemically inactive amino acid hence shows no redox peak in the potential range of investigation (Fig. 4.2, blue line). Cyclic voltammogram of 1,2-dihydroxybenzene in the presence of L-Alanine in neutral media (pH=7) shows one anodic peak in the first cycle of potential and on the reverse scan the corresponding cathodic peak slowly decreases and new peak C_0 is observed at less positive potential -0.35V. In the second cycle of potential a new anodic peak A_0 is also observed at less positive potential at 0.02V. This phenomenon can be explained by the fact of nucleophilic attack of L-Alanine to *o*-benzoquinone as well as the current intensity of 1,2-dihydroxybenzene reduces. Because of the conduction of nucleophilic substitution reaction of L-Alanine with 1,2-dihydroxybenzene, the *o*-benzoquinone concentration in reaction layer decreases, consequently the A_1 and C_1 peaks reduce. Whereas in the same time 1,2-dihydroxybenzene-Alanine adducts produces and consequently the new peak A_0 appears. The peak current ratio for the peaks A_1 and C_1 (I_{Pa1}/I_{pc1}) decreased noticeably, which indicated the chemical reaction of L-Alanine (2) with the o-quinone (1a) takes place at the surface of electrode. These observations may ascribe the formation of 2-((3,4-dihydroxyphenyl)amino)propanoic acid (Scheme 1: 2nd step) through nucleophilic substitution reaction.

If the constituent is such that the potential for the oxidation of product is lower, then further oxidation of the product is lower, the further oxidation and further addition may occur [70]. According to this concept it can be said that, the oxidation of 1,2-dihydroxybenzene-Alanine is easier than the oxidation of parent 1,2-dihydroxybenzene in the presence of excess amount of nucleophile and this substituted product can be further attacked by L-Alanine. The 1,2-dihydroxybenzene-amino acid adduct produced that can also react with *o*-benzoquinone to give peak at lower potential. In the absence of other nucleophiles, water or hydroxide ion often adds to the *o*-benzoquinone [79].

This cyclic voltammogram in Fig. 4.3 represents the comparison of only 2 mM 1,2-dihydroxybenzene (green line), pure L-Alanine (blue line) and 1,2-dihydroxybenzene (2 mM) with L-Alanine (50 mM) (Red line) in the second scan of potential at the same condition. After the addition of 50 mM L-Alanine to the solution at first scan of potential a new reduction peak (C_0) appears at -0.28 V. The peak current decreases significantly with

respect to the only 1,2-dihydroxybenzene. In the second scan of potential 1,2-dihydroxybenzene with L-Alanine shows two anodic peaks at -0.02 V and 0.3 V and the corresponding two cathodic peaks at -0.28 V and 0.05 V, respectively. Upon addition of L-Alanine to 1,2-dihydroxybenzene solution, the cathodic peak C_1 decreases and a new cathodic peak C_0 appears. Also, in the second scan of potential a new anodic peak A_o appears and anodic peak A_1 decreases similar to GC electrode. This observation can be stated by considering nucleophilic attack of L-Alanine to *o*-benzoquinone. The nucleophilic attack of L-Alanine to *o*-benzoquinone reduces the *o*-benzoquinone concentration in reaction layer. Accordingly, the A_1 and C_1 peaks reduce, whereas in the same time produces 1,2-dihydroxybenzene-Alanine adduct and consequently the peak A_0 and C_0 appears (Scheme 1).

A similar behavior is observed when we used a Gold (Au) electrode for the investigation of same solution in the same condition. Fig. 4.4 shows the CV of 1,2-dihydroxybenzene (2 mM) in the presence of L-Alanine (50 mM) at Au electrode in the second scan of potential. Upon addition of L-Alanine to 1,2-dihydroxybenzene solution at the Gold (Au) electrode it shows three anodic and three cathodic peaks for the second scan of potential. The newly appearance of A_0 and C_0 peak, and decrease of A_1 and C_1 peak, and also shifting of the positions of peaks A_1 and C_1 also indicates that it is due to follow up reaction of 1,2-dihydroxybenzene with L-Alanine (Scheme 1) at Au electrode. In case of GC and Pt electrodes, it shows two anodic and two cathodic peaks. The third peak of Au electrodes is due to the oxidation of Au in buffer solution. This unlike behavior has been discussed in the effect of electrode materials section.

4.1.3 Effect of scan rate on 1,2-dihydroxybenzene with L-Alanine

Fig. 4.5 represents different scan rates comparison graph of 2 mm 1,2-dihydroxybenzene with 50 mM L-Alanine at pH 7 and all required data has been tabulated in table 4.2. According to this voltammogram it can be seen that the peak current intensity of newly appeared peak gradually increases with the increase of scan rates and the cathodic peak for reduction of o-benzoquinone is almost disappeared in the scan rate of 0.05 V/s. The cathodic peaks shift towards left whereas the anodic peaks move to the right direction with increase of scan rate. Fig. 4.6 shows plot of the anodic and cathodic net peak currents for second cycle against the square-root of the scan rates where the net current means the

second peak subtracted from the first one by the scan-stopped method in the same condition [70]. The proportional ratio in between redox pair indicates that the peak current of the reactant at each redox reaction is controlled by diffusion process with some chemical complications. The corresponding peak current ratio (I_{pa1}/I_{pc1}) vs scan rate (v) for a mixture of 1,2-dihydroxybenzene and L-Alanine decreases with increasing scan rate firstly and then after 0.25 V/s, it remains almost unchanged (Fig 4.7). The anodic peak current ratio (I_{pa0}/I_{pa1}) vs scan rate for a mixture of 1,2-dihydroxybenzene and L-Alanine firstly increases and then after 0.3 V/s scan rate the peak current remains constant in (Fig. 4.7). On the other hand, the value of current function ($Ip/v^{1/2}$) is found to be decreased with increasing scan rate (Fig. 4.8). The exponential nature of the current function versus the scan rate plot indicates the ECE mechanism for electrode process [80]. This also indicates the reactivity of *o*-benzoquinone (1a) towards L-Alanine (2) firstly increases at slow scan rate and then at higher scan rate it decreases. The existence of a subsequent chemical reaction between *o*-benzoquinone **1a** and L-Alanine **2** is supported by the following evidence.

(i) In the presence of L-Alanine both I_{pc1} and I_{pa1} decreases during second cycle (fig. 4.5), this could be indicative of the fact that electrochemically generated *o*-benzoquinone **1a** is removed partially by chemical reaction with L-Alanine (**2**).

(ii) Corresponding peak current ratio (I_{pa1}/I_{pc1}) varies with potential sweep rate. In this case, a well-defined cathodic peak C_1 is observed at highest sweep rate. For lower sweep rates, the peak current ratio (I_{pa1}/I_{pc1}) is less than one and increases with increasing sweep rate. This is indicative of departure from intermediate and arrival to diffusion region with increasing sweep rate [70].

(iii) Increase in the scan rate causes a decrease in the progress of the chemical reaction of 1a with 2 during the period of recording the cyclic voltammogram and therefore, decease in peak current ratio (I_{pa0}/I_{pa1}) at higher scan rate.

(iv) The current function, $I_p/v^{1/2}$ for A_1 was found to be decreased exponentially with increasing scan rate. This indicates the reaction mechanism of the system was of ECE type (Scheme 1).

According to the results, it is assumed that L-Alanine (2) undergoes the 1,4-Michael addition reaction with *o*-benzoquinone (1a) leads to product 3. The oxidation of this

compound (3) is easier than the oxidation of parent molecule (1) by virtue of the presence of electron donating amine group. Product 3 can further react with another molecules of o-benzoquinone to produce byproducts at lower potential than 1,2-dihydroxybenzene (Scheme 1).

Reaction Scheme-1

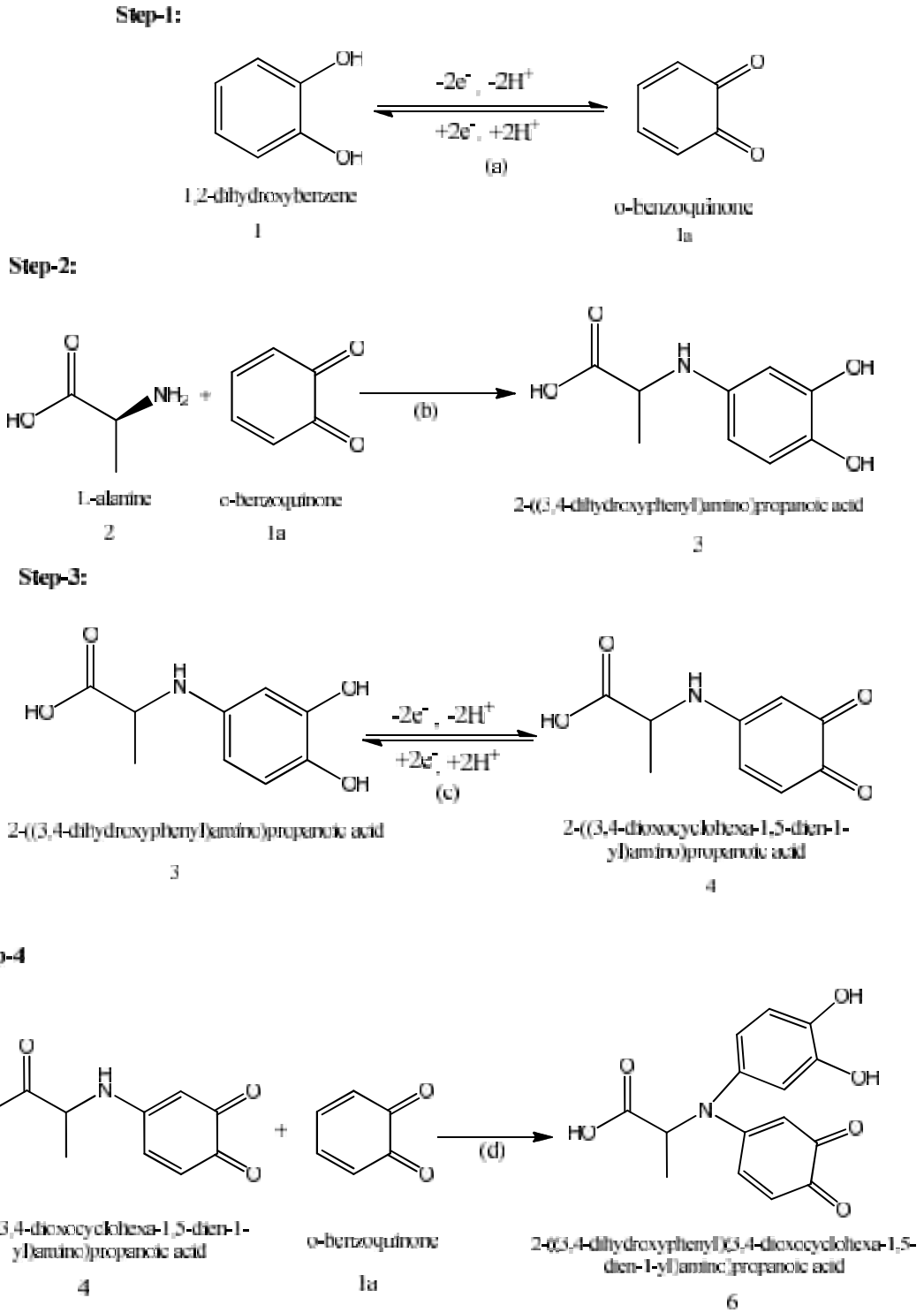

The CV of second scan of potential at Pt electrode of 2 mM 1,2-dihydroxybenzene with 50 mM L-Alanine at pH 7 and different scan rate shows in fig. 4.9. The peak current of both the anodic and cathodic peaks increases with the increase of scan rate. By the increase of scan rates the anodic peaks shift towards right direction and the cathodic peaks move toward left. Fig. 4.10 shows plots of the anodic and cathodic peak currents for second scan of potential as a function of square-root of the scan rates. The proportionality of the anodic and the cathodic peaks ascribed that the peak current of the reactant at each redox reaction is controlled by diffusion process. The anodic and cathodic peak currents, peak potentials, corresponding peak potential differences and peak current ratio are tabulated in Tables 4.3.

Fig. 4.11 indicates the variation of peak current ratio of corresponding peak (I_{pa1}/I_{pc1}) and anodic peak (I_{pa0}/I_{pa1}) vs scan rate (v) of 2 mM 1,2-dihydroxybenzene with 50 mM L-Alanine in the same condition. The corresponding peak current ratio (I_{pa1}/I_{pc1}) vs scan rate for a mixture of 1,2-dihydroxybenzene and L-Alanine decreases with increasing scan rate firstly and then after 0.3V/s, it starts to be increased. The anodic peak current ratio (I_{pa0}/I_{pa1}) vs scan rate for a mixture of 1,2-dihydroxybenzene and L-Alanine firstly increases and then after 0.1V/s scan rate the peak current starts to be decreased (Fig. 4.11). Beside this, the value of current function ($Ip/v^{1/2}$) is found to be decreased with increasing scan rate (Fig. 4.12). The exponential nature of the current function versus the scan rate plot indicates the ECE mechanism for the electrode process.

The voltammetric behavior of the above systems has been investigated at Au electrode. Fig. 4.12 shows the CV of 1,2-dihydroxybenzene with 50 mM L-Alanine for second cycle of potential at different scan rate in pH 7. This voltammogram is consistent with Fig. 4.5 and Fig. 4.9. According to Fig. 4.14 and tabulated data in 4.4 it can be seen that the anodic and cathodic net peak currents against the square-root of the scan rates is nearly proportional which suggests that the peak current of the reactant at each redox reaction is controlled by diffusion process. Fig. 4.15 shows variation of peak current ratio of corresponding peak (I_{pa1}/I_{pc1}) and anodic peak (I_{pa0}/I_{pa1}) vs scan rate (v) in the same condition. The (I_{pa1}/I_{pc1}) peak current ratio decreases up to 0.3V/s and then it remains almost constant whereas the anodic peak current ratio observed maximum at 0.15V/s and after that it degreases slowly with increasing scan rates. The exponentially decreasing nature indicates that the reaction is taken place by ECE mechanism (Fig. 4.16). The effect

of different scan rates on 1,2-dihydroxybenzene in presence of L-Alanine is maximum favorable at slow scan rates which is controlled by diffusion process.

4.1.4 Influence of pH on 1,2-dihydroxybenzene with L-Alanine

The effect of buffer solution of different pH (5, 7, 9 and 11) on 2 mM 1,2-dihydroxy benzene with 50 mM L-Alanine has been studied by means cyclic voltammogram at Gc (3mm) electrode (Fig. 4.17). The voltammetric behavior of 1,2-dihydroxybenzene at pH 5, 9 and 11 in the presence of 50 mM L-Alanine show no new anodic peak after repetitive cycling hence the reaction between *o*-benzoquinone and L-Alanine has not occurred. This can be attributed to the fact that at pH 5 or lowers the nucleophilic property of amine groups is diminished through protonation and forms form zwitterion. Whereas, in the higher pH range (e.g., pH 9-11), the cyclic voltammogram of 1,2-dihydroxybenzene show irreversible behavior. It is thus suggested that the oxidation of 1,2-dihydroxybenzene followed by an irreversible chemical reaction with hydroxyl ion, especially in alkaline solutions [81]. However, amines in this condition can also act as nucleophiles. The peak position of the redox couple is found to be dependent upon pH. The anodic peak potential of 1,2-dihydroxybenzene shifts toward left with the increase of pH. Fig. 4.19 shows the plot of oxidation peak (A_0) current, I_p against pH of solution. At the pH 7, the difference between the peak current ratio (I_{pC0}/I_{pA0}) in the presence of L-Alanine is observed maximum (Table 4.5). Consequently, pH 7 has been selected as optimum condition for electrochemical study of 1,2-dihydroxybenzene, at which the electro-oxidation is facilitated by neutral media and hence the rate of electron transfer is faster.

CV of 1,2-dihydroxybenzene in presence of 50 mM L-Alanine at Platinum (Pt) (1.6 mm) electrode in the second scan of potential has been studied from pH 5 to 11 (Fig. 4.20). The voltammetric response of 2 mM 1,2-dihydroxybenzene at pH 5 in the presence of 50 mM L-Alanine shows one anodic peak and corresponding cathodic peak after repetitive cycling that indicates the reaction between *o*-quinone and L-Alanine has not occurred. This can be assigned to the fact that at acidic media, the nucleophilic property of amine groups is diminished through protonation. In the pH 7-11 the *o*-quinone undergoes nucleophilic attack by the L-Alanine through a Michael addition reaction. The peak position of the redox couple is found to be depended upon pH. Fig. 4.21 shows the plot of oxidation peak

current, I_p against pH solution and the maximum peak current is obtained at pH 7 (Table 4.6). Fig. 4.22 represents the plot of peak potential, E_p vs pH. The slope value of the plot is obtained 69.5mV/pH which is nearer to the value of one electron, one proton transfer process.

The effect of pH on the cyclic voltammogram of 2 mM 1,2-dihydroxybenzene in presence of 50 mM L-Alanine at Au (1.6 mm) electrode in the second scan of potential was studied at pH from 5 to 11 (Fig. 4.23). The influence of pH for Au electrode in the same systems, the voltammetric properties are slightly different from GC electrode. The voltammetric behavior of 1,2-dihydroxybenzene at pH 5 in the presence of L-Alanine shows no new peak in the second scan of potential. This can be indicated to the fact that in lower pH, the nucleophilic property of amine groups is diminished through protonation. In the pH 7-9, the o-benzoquinone undergoes L-Alanine attack by the amine through Michael addition reaction reflected that voltammetric new anodic peak A_0 appears after repetitive cycling. In the higher pH (e.g., pH 11), no new anodic peak appeared in the second scan of potential. However, the peak position of the redox species is found to be dependent upon pH. Fig. 4.24 shows the plots of oxidation peak current, I_p against pH of solution. It is seen that the maximum peak current is observed at pH 7 (Table 4.7) attributed that nucleophilic addition reaction is most favorable in neutral media. Fig. 4.25 shows the plot of the peak potential, E_p against pH at second cycle in the same condition. The slope of the plot was calculated (48.5 mV/pH for anodic peak A_1) which is close to theoretical value for two step one electron, one proton transfer process.

4.1.5 Concentration effect of L-Alanine

The influence of concentration of L-Alanine (10-150 mM) with fixed composition of 1,2-dihydroxybenzene (2 mM) has been illustrated by means of cyclic voltammetry of Gc electrode at pH 7 and scan rate 0.1V/s (Fig. 4.26). Upon addition of L-Alanine the anodic peaks shifts positively and a new peak appears at ~ 0.04V which suggests that the nucleophilic attack takes place and consequently 1,2-dihydroxybenzene-Alanine adduct deposits on the electrode surface. The peak current intensity of the newly appeared anodic and cathodic peak increases with the increase of L-Alanine concentration up to 50 mM and after that the redox peak current is started to be decreased (Fig. 4.27). The nucleophilic substitution reaction of 1,2-dihydroxybenzene in presence of L-Alanine was maximum

favorable up to 50 mM of L-Alanine at pH 7 (Table 4.8). The corresponding peak current ratio (I_{pc1}/I_{pa1}) changes with the concentration of L-Alanine. This was related to the increase of the homogenous reaction rate of following chemical reaction between *o*-benzoquinone 1a and L-Alanine 2 with increasing concentration of L-Alanine up to 50 mM. At higher concentration of L-Alanine (>50 mM), the excess electro-inactive L-Alanine may be deposited on the electrode surface and consequently the peak current decreased.

After addition of various composition of L-Alanine (10, 30, 50, 100 and 150 mM) into fixed concentration of 1,2-dihydroxybenzene (2 mM) at Gold (Au) and Platinum (Pt) electrodes has been also examined in the same conditions (Fig. 4.28 - 4.31). In the first scan of potential a new cathodic peak (C_0) is appeared at -0.3 V and -0.18 V at Pt and Au electrodes respectively. Upon addition of L-Alanine in the second scan of potential, the anodic peaks shifted and a new anodic peak appeared at -0.02 V and -0.1 V at Pt and Au electrodes respectively which suggests the formation of 1,2-dihydroxybenzene-Alanine adduct. The net current intensity of the newly appeared anodic and cathodic peak increases with the increase of composition up to 10 to 50 mM of L-Alanine. After further addition of L-Alanine (>50 mM), the anodic and cathodic peak current gradually decreases. At higher concentration of L-Alanine (>50 mM), the excess electro-inactive L-Alanine may be accumulated on the electrode surface and the peak current decreased. Therefore, the concentration effects of L-Alanine into the fixed concentration of 1,2-dihydroxybenzene (2 mM) for Au and Pt electrodes are few different from GC electrode.

4.1.6 Effect of electrode materials

Influence of different electrode materials on electrochemical properties 2 mM of 1,2-dihydroxybenzene (fixed) in absence and presence of 50 mM L-Alanine has been examined with the help of both CV and DPV by using different electrodes like Gc, Au and Pt at different pH at scan rate 0.1V/s has shown in Fig. 4.32 and Fig. 4.33. The nature of voltammogram, the peak position and current intensity for the studied systems are different for different electrodes although the diameter of Gc electrode (3mm) was higher than Au and Pt (1.6mm). The CV of GC electrode is significantly different from those of the Au and Pt electrodes based on peak current consideration. All electrodes show two anodic and corresponding cathodic peaks in the potential range of investigation. Among them the peak

current intensity of GC electrode is much higher than Au and Pt electrodes in Figures 4.32-4.33. Voltammetric measurements performed at an Au electrode in only buffer solution of without 1,2-dihydroxybenzene and L-Alanine at pH 7, showed a peak at 1.1 V to the formation of Au (III) hydroxide. Consequently, the third peak (1.08 V) of Au electrode in presence of 1,2-dihydroxybenzene and L-Alanine at pH 7 is due to the oxidation of Au in buffer solution. Similar behavior of oxidation of Au electrode in different pH has been reported [82]. In the case of GC and Pt electrodes for the second cycle of potential a new oxidation and reduction peak appear at lower oxidation potential which can be attributed to the oxidation of adduct formed between the *o*-benzoquinone and L-Alanine. Electrochemical properties of 1,2-dihydroxybenzene with L-Alanine for example change of pH, concentration, scan rate etc. have been studied in detail using Pt and Au electrodes. But among the electrodes, the voltammetric response of GC electrode is better than Pt and Au electrodes in the studied systems.

DPV technique has also been applied to support the above argument. According to DPV electrode comparison graph (Fig. 4.33) it can be seen that Gc electrode shows better voltammetric response having three anodic peak at -0.32V, -0.02V and 0.255V. We considered the 1,2-dihydroxybenzene-adduct peak at -0.02V and another very small peak at lower potential -0.32 could be due to side reaction like polymerization, further oxidation of 1,2-dihydroxybenzene adducts or nucleophilic attack by hydroxyl ion. Among Gc, Pt and Au electrode the peak current and voltammetric response of Gc electrode was found much better than Pt electrode under this investigation. Therefore, Gc electrode is selected as electrode material for this investigation.

4.1.7 Subsequent cycles of CV of 1,2-dihydroxybenzene with L-Alanine

Subsequent 15 cycles of CV of 2 mM 1,2-dihydroxybenzene with 50 mM L-Alanine has been showed in Fig. 4.34-4.36 at different electrodes (GC, Pt and Au) electrode in buffer solution of pH 7 for the potential range between -0.6 V to 0.9 V. The voltammogram at the scan rate 0.1 V/s has one anodic peak at 0.27 V and two cathodic peaks at -0.32 V and 0.05 V when considered the first scan of potential (red line). In the subsequent potential cycles a new anodic peak appeared at ~ 0.04V and intensity of the first anodic peak current increased progressively on cycling but the second anodic peak current decreases and shifted positively on cycling. This can be attributed to produce of the 1,2-

dihydroxybenzene-Alanine adduct through nucleophilic substitution reaction in the surface of electrode (Scheme 1). The successive decrease in the height of the 1,2-dihydroxybenzene oxidation and reduction peaks with cycling can be ascribed to the fact that the concentrations of 1,2-dihydroxybenzene-Alanine adduct formation increased by cycling leading to the decrease of concentration of 1,2-dihydroxybenzene or quinone at the electrode surface. The positive shift of the second anodic peak in the presence of L-Alanine is probably due to the formation of a thin film of product at the surface of the electrode, inhibiting to a certain extent the performance of electrode process. Along with the increase in the number of potential cycles the first anodic peak current increased up to 10 cycles and then the peak current almost unchanged with subsequent cycle (Fig. 4.34). This may be due to the block of electrode surface by the newly formed species after more cycling.

In Fig. 4.36 at Au electrode there are two anodic peaks at 0.25V and 1.1 V and three cathodic peaks at -0.23 V, 0.11 V and 0.46 V respectively in the first scan of potential (red line). In the subsequent scan of potential Au electrode shows a new anodic peak at -0.07 V with another three anodic peaks (blue line). But in Pt electrode there is one anodic peaks at 0.27 V and two cathodic peaks at -0.3 V and 0.04 V in the first scan of potential (red line) (Fig. 4.35). In the subsequent potential cycles a new anodic peak appeared at -0.03 V and the first anodic peak current increased progressively on cycling but the second anodic peak current decreases and shifted positively on cycling. This can be suggested to produce the 1,2-dihydroxybenzene-Alanine adduct through nucleophilic substitution reaction in the surface of electrode (Scheme 1).

4.1.8 Controlled-potential coulometry of 1,2-dihydroxybenzene with L-Alanine

To provide more evidence about the nucleophilic substitution reaction of L-Alanine (nucleophile) with 1,2-dihydroxybenzene (substrate), Controlled-potential coulometry technique has been performed with the help of CV and DPV in aqueous solution containing 1 mM of 1,2-dihydroxybenzene and 25 mM of L-Alanine at 0.45V in pH 7 (Figures 4.37-4.38). This voltammogram informs that, during the course of coulometry the peaks A_0 appears and the height of the A_0 peak increases to the advancement of coulometry, parallel to the decrease in height of anodic peak A_1. After some couples of

hour both redox couple of appeared peak does not increase with the successive decrease of concentration of 1,2-dihydroxybenzene which has been showed by both CV and DPV in (Fig. 4.38). This observation could lead us to draw a concept that the capacitive current was increased or side reactions were taken place.

These observations allow us to propose the pathway in Scheme 1 for the electro-oxidation of 1,2-dihydroxybenzene **(1)** in the presence of L-Alanine **(2)**. According to our results, it seems that the 1,4 addition reaction of **(2)** to *o*-benzoquinone **(1a)** is faster than other secondary reactions, leading to the intermediate **3**. The oxidation of this compound **(3)** is easier than the oxidation of parent starting molecule **(1)** by virtue of the presence of electron-donating group. Like *o*-quinone **1a**, adduct **4** can also be attacked from the C-5 position by L-Alanine **(2)**. Product 4 can also react with another molecule of **1a** to produce adduct **(5)**.

4.1.9 pH effect on DPV of 1,2-dihydroxybenzene with L-Alanine

To understand the nucleophilic substitution reaction of 50 mM of L-Alanine on 2 mM 1,2-dihydroxybenzene more clearly DPV has taken in second scan in buffer solution of different pH (5, 7, 9 and 11) at (GC, Pt and Au) electrode has shown in Fig. 4.39. In the buffer solution of pH 7, 1,2-dihydroxybenzene with L-Alanine gives two well-developed wave at 0.01V and 0.3V respectively (Fig. 4.39). But in pH 5, 9 and 11 no significant new peak appears. As can be seen two completely separated anodic peaks with high current intensity are observed in pH 7, which can be attributed to the oxidations of *o*-benzo quinone-Alanine (new compound) and 1,2-dihydroxybenzene respectively.

Fig. 4.40 represents differential pulse voltammogram of 2 mM 1,2-dihydroxybenzene in the presence of 50 mM L-Alanine in first and second scan of potential at different pH (5-11) in (Epulse 0.02 V, tpulse 20 ms and scan rate 0.1 V/s). It is noticed that the peak positions of the DPV of 1,2-dihydroxybenzene with L-Alanine shifts negatively this indicates that the nucleophilic reaction is easier at pH 7. But, in pH 5 no new peak appears in the second scan of potential and in pH 9-11, the species are totally electro-inactive. High current intensity is observed at pH 7, which can be attributed to the formation of 1,2-dihydroxybenzene-Alanine adduct.

Gold (Au) electrode is also used for the investigation in the similar condition (Fig. 4.41). In Buffer solution of pH 7-9, new anodic peak A_0 appears which may be attributed to the formation of 1,2-dihydroxybenzene-Alanine adduct. But, in lower and higher pH media no new anodic peak appeared. In the buffer solution of pH 7, the voltammogram shows two well-developed peak ascribed the formation of adduct similar to GC electrode. The DPV of Au and Pt electrodes are consistent with the GC electrode in the studied systems at the same condition.

4.1.10 Effect of deposition time change of DPV of 1,2-dihydroxybenzene with L-Alanine

DPV of deposition time change (0, 10, 30, 60, 90, 120 and 180s) of 2 mM 1,2-dihydroxybenzene 50 mM L-Alanine of pH 7 has been showed in fig. 4.42. According to this figure it can be seen, increasing of deposition time leads to develop two new peaks at -0.31V and -0.02 V. When the deposition time increases 30s, more and more nucleophilic attack occurs and consequently more 1,2-dihydroxybenzene-Alanine adduct is formed which leads to decreasing in the concentration of *o*-benzoquinone and increasing in the concentration of 1,2-dihydroxybenzene-Alanine adduct at the surface of electrode. Maximum peak intensity is obtained up to 30s. For further increase of deposition time from 60s to 180s, both first and second anodic peak current decreases. This confirmed that with the increase of time decreases the concentration of *o*-benzoquinone due to follow up the reaction.

4.1.11 Effect of concentration of DPV of 1,2-dihydroxybenzene with L-Alanine

The effect of different composition of L-Alanine on 1,2-dihydroxybenzene has been studied by using the differential pulse voltammetry. DPV of 2 mM 1,2-dihydroxybenzene with 10 to 150 mM L-Alanine at pH 7 has been shown in fig. 4.43. There we observed again three separated anodic peaks appeared after addition of different concentration of L-Alanine into 1,2-dihydroxybenzene. In this case, the gradual increasing of the concentration of L-Alanine up to 50 mM leads to increasing of first anodic peak current. For further increase of concentration from 60 to 150 mM, all anodic peak decreases gradually. In lower concentration of L-Alanine (<50 mM), the nucleophilic substitution reaction take place in comparable degree, whereas increasing the concentration of L-

Alanine (>50mM) make favorable nucleophilic attack of L-Alanine toward *o*-benzoquinone generated at the surface of electrode. For further addition of L-Alanine (>50mM) into 1,2-dihydroxybenzene solution, the excess electro-inactive L-Alanine deposited on the electrode surface and hence the peak current decreases.

The effect of L-Alanine concentration on the DPV of 1,2-dihydroxybenzene has also been studied by using Platinum (Pt) (1.6 mm) electrode in the same condition (Fig. 4.44). As reported in Fig. 4.43, in the second scan there are two completely separated anodic peaks appear after addition of L-Alanine into 1,2-dihydroxybenzene. In lower concentration of L-Alanine (<50 mM), the nucleophilic substitution reaction take place in comparable degree, whereas increasing the concentration of L-Alanine (50 mM) make susceptible for nucleophilic attack of L-Alanine towards o-benzoquinone generated at the surface of electrode. For more addition of L-Alanine (>50 mM) into 1,2-dihydroxybenzene solution, the excess electro-inactive L-Alanine accumulated on the electrode surface and hence the peak current decreases.

Gold (Au) electrode was also employed for the investigation on the DPV of fixed 2 mM 1,2-dihydroxybenzene with different concentration (10-150 mM) of L-Alanine in buffer solution pH 7 at 0.1 Vs^{-1}. Fig. 4.45 shows the second scan of potential of the studied systems at different concentration, respectively. In second scan of potential an appeared peak, A_0 was obtained which may be attributed the formation of 1,2-dihydroxybenzene-Alanine adduct. In this investigation different concentration 10-150 mM of L-Alanine has been used to determine the favorable condition for the nucleophilic substitution reaction on 1,2-dihydroxybenzene. As the reaction was occurred at moderately high concentration of nucleophiles, consequently the voltammetric peaks (CV and DPV) for adduct appeared noticeably. In contrast, comparatively low concentration of L-Alanine is not favorable for the study of electrochemical oxidation of 1,2-dihydroxybenzene because the appearing peak is not so prominent.

From the experimental study it is noticeable that L-Alanine acts properly as a nucleophile at pH 7. When the pH is below 7 that are at acidic media, the nucleophilic activity of L-Alanine reduces due to the protonation of amine. Whereas at basic condition, other nucleophiles such as –OH produce in solution, therefore, the activity of amines decreases and the oxidation of 1,2-dihydroxybenzene followed by an irreversible chemical reaction

with hydroxyl ion [83]. Therefore, from the above discussion it is clear that the nucleophilic substitution reaction of 1,2-dihydroxybenzene in presence of L-Alanine is maximum favorable at 50 mM of L-Alanine and at pH 7 which is consistent with both CV and DPV. All above observations could be attributed to the reaction between L-Alanine and *o*-benzoquinone species produced at the surface of electrode, with the new anodic peak being attributed to the oxidation of newly formed *o*-benzoquinone-Alanine adduct.

4.1.12 Spectral analysis of 1,2-dihydroxybenzene with L-Alanine

The FTIR spectrum of the vibrational modes of the 1,2-dihydroxybenzene-Alanine adduct, 1,2-dihydroxybenzene and L-Alanine has been shown in Figure 4.134. The 1,2-dihydroxybenzene reveals the O-H stretching band at 3454 cm^{-1} whereas L-Alanine shows the O-H stretching band at 3473 cm^{-1} and N-H stretching band at 2609 cm^{-1}. The absorption peaks due to the O-H broad stretching vibration is appeared at 3462 cm^{-1}, C=O stretching at 1639 cm^{-1} and absorption peaks due to the N-H stretching vibration is disappeared at the wave number for the 1,2-dihydroxybenzene-Alanine adduct. Also the finger print region is different for adduct from pure 1,2-dihydroxybenzene and pure L-Alanine.

4.2.1 Electrochemical nature of 1,2-dihydroxybenzene in presence of L-Phenylalanine

The electro-oxidation nature of 1,2-dihydroxybenzene in presence of L-Phenylalanine has been studied in details by using different buffer solution of pH (5-11), various composition of L-Phenylalanine (2-100 mM), different electrodes and scan rates (0.05-0.5V/s). Fig. 4.46 represents the cyclic voltammogram of only 1,2-dihydroxybenzene (Green line), only L-Phenylalanine (Blue line) and 1,2-dihydroxybenzene with L-Phenylalanine (Red line) at Gc (3mm) electrode in buffer solution of pH 7 and scan rate 0.1V/s. The cyclic voltammogram of 1,2-dihydroxybenzene shows one anodic peak at A_1 (0.44V) and corresponding cathodic peak at C_1 (0.12V) related to its transformation to *o*-quinone and vice versa. Pure L-Phenylalanine is electrochemically inactive amino acid hence shows no redox pair in the potential range investigated (Fig. 4.46, blue line).

Cyclic voltammogram of 1,2-dihydroxybenzene in the presence of L-Phenylalanine in buffer solution of pH 7 shows one anodic peak in the first cycle of potential and on the reverse scan the corresponding cathodic peak slowly decreases and new peak C_0 is

observed at less positive potential -0.33V. In the second cycle of potential a new anodic peak A_0 is also observed at less positive potential at 0.04V. Due to formation of new redox couple the current intensity of 1,2-dihydroxybenzene reduces. This phenomenon can be explained by the fact of nucleophilic attack of L-Phenylalanine towards *o*-benzoquinone reduces the concentration of *o*-benzoquinone, consequently the A_1 and C_1 peaks reduce. Whereas in the same time 1,2-dihydroxybenzene-Phenylalanine adducts produces and consequently the new peak A_0 appears. The peak current ratio for the peaks A_1 and C_1 (I_{Pa1}/I_{pc1}) decreased noticeably, which indicates the chemical reaction of L-Phenylalanine (2) with the o-quinone (1a) produced at the surface of electrode. These observations may ascribe the formation of 2-((3,4-dihydroxyphenyl)amino)-3-phenylpropanoic acid through nucleophilic substitution reaction (Scheme 1). If the constituent is such that the potential for the oxidation of product is lower, then further oxidation of the product is lower, the further oxidation and further addition may occur [70]. According to this concept it can be drawn that, the oxidation of 1,2-dihydroxybenzene-Phenylalanine is easier than the oxidation of parent 1,2-dihydroxybenzene in the presence of excess amount of nucleophile and this substituted product can be further attacked by L-Phenylalanine. However, it was not observed in cyclic voltammogram because of the low activity of o-quinone 4 toward 2. This behavior is in agreement with that reported by other research groups for similar electrochemically generated compounds such as 1,2-dihydroxybenzene and different nucleophiles [70-78]. In the absence of other nucleophiles, water or hydroxide ion often adds to the o-benzoquinone [79].

CV of second scan of potential of 2 mM 1,2-dihydroxybenzene with 20 mM L-Phenylalanine at Platinum (Pt) (1.6mm) electrode has been taken in the similar condition (Fig. 4.47). This cyclic voltammogram shows the comparison of only 2mM 1,2-dihydroxybenzene (green line), pure L-Phenylalanine (blue line) and 1,2-dihydroxybenzene (2 mM) with L-Phenylalanine (20 mM) (Red line) in the second scan of potential at the same condition. A new reduction peak (C_0) appears at -0.27 V after the addition of 20 mM L-Phenylalanine to the solution at first scan of potential. The peak current decreases significantly with respect to the only 1,2-dihydroxybenzene. In the second scan of potential 1,2-dihydroxybenzene with L-Phenylalanine shows two anodic peaks at -0.02 V and 0.29 V and the corresponding two cathodic peaks at -0.27 V and 0.05 V, respectively. Upon addition of L-Phenylalanine to 1,2-dihydroxybenzene solution, the

cathodic peak C_1 decreases and a new cathodic peak C_0 appears. Also, in the second scan of potential a new anodic peak A_0 appears and anodic peak A_1 decreases similar to GC electrode. This observation can be stated by considering nucleophilic attack of L-Phenylalanine to *o*-benzoquinone. The nucleophilic attack of L-Phenylalanine to *o*-benzoquinone reduces the *o*-benzoquinone concentration in reaction layer as well as the A_1 and C_1 peaks reduce and consequently the peak A_0 and C_0 appears (Scheme 2). A similar behavior has been observed in Gold (Au) electrode for the investigation of same solution in the same condition (Fig. 4.48). Upon addition of 20 mM of L-Phenylalanine to 2 mM 1,2-dihydroxybenzene solution at the Gold (Au) electrode it shows three anodic and three cathodic peaks for the second scan of potential. The newly appearance of A_0 and C_0 peak, and decrease of A_1 and C_1 peak, and also shifting of the positions of peaks A_1 and C_1 also indicates that it is due to follow up reaction of 1,2-dihydroxybenzene with L-Phenylalanine (Scheme 2) at Au electrode. In case of GC and Pt electrodes, it shows two anodic and two cathodic peaks. The third peak of Au electrodes is due to the oxidation of Au in buffer solution. This unlike behavior has been discussed in the effect of electrode materials section.

4.2.2 Effect of scan rate of 1,2-dihydroxybenzene with L-Phenylalanine

To monitor the effect of scan rates on the voltammogram of 2 mM of 1,2-dihydroxybenzene with 20 mM of L-Phenylalanine, CV has been taken at 0.05V, 0.1V, 0.2V, 0.3V, 0.4V and 0.5V (Fig. 4.49). According to this voltammogram it can be seen that the peak current intensity of newly appeared peak gradually increases with the increase of scan rates. The cathodic peaks shift towards left whereas the anodic peaks move to the right direction with increase of scan rate. Fig. 4.50 shows plot of the anodic and cathodic net peak currents for second cycle against the square-root of the scan rates where the net current means the second peak subtracted from the first one by the scan-stopped method in the same condition [70]. The nearly proportional ratio in between redox couple indicates that the peak current of the reactant at each redox reaction is controlled by diffusion process with some chemical complications. It can be seen in Fig. 4.49, the cathodic peak for reduction of o-benzoquinone is almost disappeared in the scan rate of 0.05 V/s. By increasing the scan rate, the cathodic peak for reduction of o-benzoquinone starts to appear and increasing.

The corresponding peak current ratio (I_{pa1}/I_{pc1}) vs scan rate for a mixture of 1,2-dihydroxybenzene and L-Phenylalanine decreases with increasing scan rate firstly and then after 0.25 V/s, it remains almost unchanged (Fig. 4.51). The anodic peak current ratio (I_{pa0}/I_{pa1}) vs scan rate for a mixture of 1,2-dihydroxybenzene and L-Phenylalanine firstly increases and then after 0.3V/s scan rate the peak current starts to be decreased in (Fig. 4.51 and Table 4.11). On the other hand, the value of current function ($Ip/v^{1/2}$) is found to be decreased with increasing scan rate (Fig. 4.52). The exponential nature of the current function versus the scan rate plot indicates the ECE mechanism for electrode process [80]. This confirms the reactivity of *o*-benzoquinone (1a) towards L-Phenylalanine (2) firstly increases at slow scan rate and then at higher scan rate it decreases. According to the results, it was assumed that L-Phenylalanine (2) undergoes the 1,4-Michael addition reaction with *o*-benzoquinone (1a) leads to product 3. The oxidation of this compound (3) is observed easier than the oxidation of parent molecule (1) by virtue of the presence of electron donating amine group.

Reaction schemes-2:

Step-1:

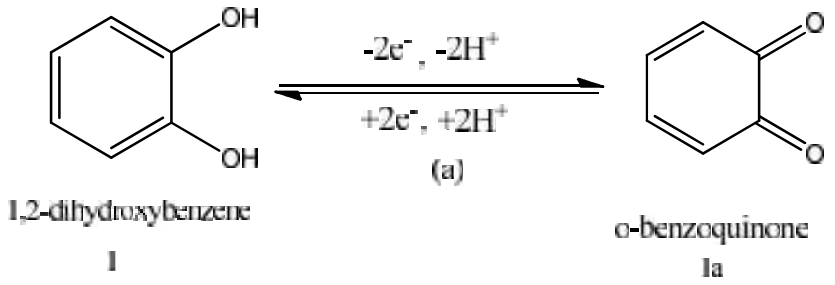

1,2-dihydroxybenzene
1

o-benzoquinone
1a

Step-2:

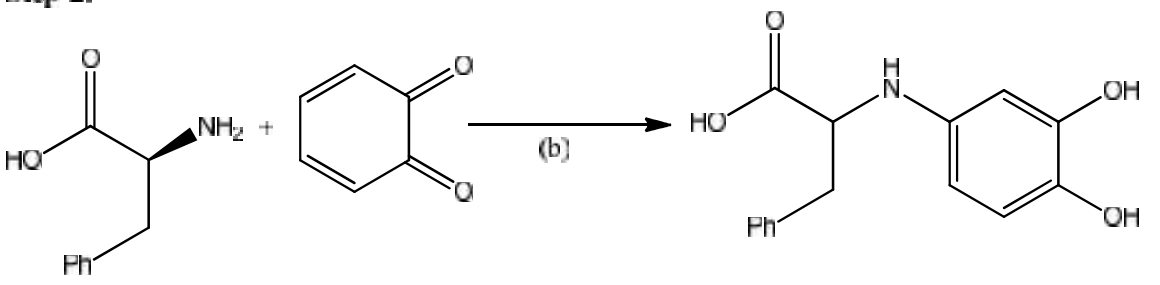

L-Phenylalanine
2

o-benzoquinone
1a

2-((3,4-dihydroxyphenyl)amino)-3-phenylpropanoic acid
3

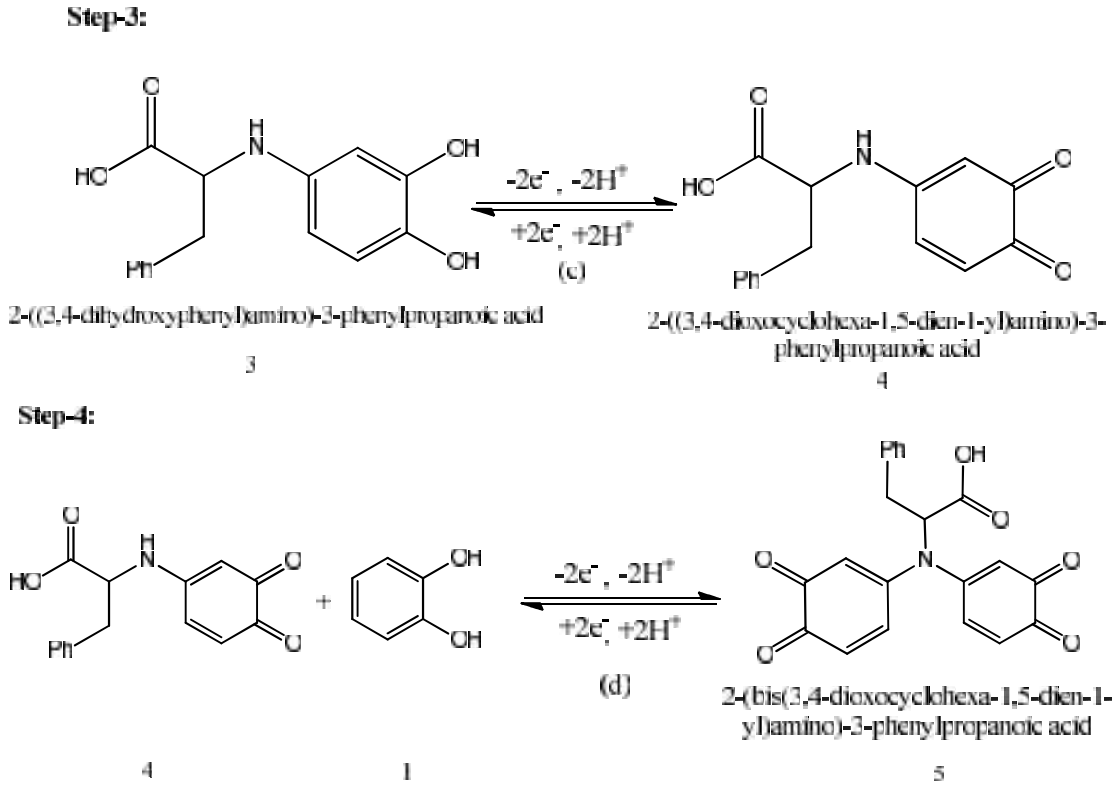

Fig. 4.53 shows the CV of second scan of potential at Pt electrode of 2 mM 1,2-dihydroxybenzene with 20 mM L-Phenylalanine at pH 7 and different scan rate. The peak current of both the anodic and cathodic peaks increases with the increase of scan rate. The anodic peaks are shifted towards right direction and the cathodic peaks are to the left with increase in the scan rate. Fig. 4.54 shows plots of the anodic and cathodic peak currents for second scan of potential as a function of square-root of the scan rates. The proportionality of the anodic and the cathodic peaks ascribed that the peak current of the reactant at each redox reaction is controlled by diffusion process. The anodic and cathodic peak currents, peak potentials, corresponding peak potential differences and peak current ratio are tabulated in Tables 4.12.

Fig. 4.55 shows variation of peak current ratio of corresponding peak (I_{pa1}/I_{pc1}) and anodic peak (I_{pa0}/I_{pa1}) vs scan rate (v) of 2 mM 1,2-dihydroxybenzene with 20 mM L-Phenylalanine in the same condition. The corresponding peak current ratio (I_{pa1}/I_{pc1}) vs scan rate for a mixture of 1,2-dihydroxybenzene and L-Phenylalanine decreases with increasing scan rate firstly and then after 0.1V/s, it started to be decreased (Fig 4.55). The anodic peak current ratio (I_{pa0}/I_{pa1}) vs scan rate for a mixture of 1,2-dihydroxybenzene and L-Phenylalanine firstly increases and then after 0.15V/s scan rate the peak current

suddenly starts to be decreased up to 0.3 V/s and then it remains constant (Fig. 4.55). Beside this, the value of current function ($Ip/v^{1/2}$) is found to be decreased with increasing scan rate (Fig. 4.56). The exponential nature of the current function versus the scan rate plot indicates the ECE mechanism for electrode process.

Similarly, the voltammetric behavior of the above systems has been investigated at Au electrode. Fig. 4.57 shows the CV of 1,2-dihydroxybenzene with 20 mM L-Phenylalanine for second cycle of potential at different scan rate in pH 7. This voltammogram is consistent with Fig. 4.49 and Fig. 4.53. According to Fig. 4.58 it can be seen that the anodic and cathodic net peak currents against the square-root of the scan rates is nearly proportional which suggests that the peak current of the reactant at each redox reaction is controlled by diffusion process. Fig. 4.59 shows variation of peak current ratio of corresponding peak (I_{pa1}/I_{pc1}) and anodic peak (I_{pa0}/I_{pa1}) vs scan rate (v) in the same condition. The (I_{pa1}/I_{pc1}) peak current ratio decreases up to 0.15 V/s and then it remains almost constant whereas the anodic peak current ratio observed maximum at 0.1 V/s and after that it degreases sharply and remains constant after 0.3 V/s with increasing scan rates. The exponentially decreasing nature with increasing scan rates in Fig. 4.60 indicates that the reaction is taken place by ECE mechanism. According to all system it can be said that, the nucleophilic substitution reaction of 1,2-dihydroxybenzene in presence of L-Phenylalanine is maximum favorable at slow scan rate by diffusion process.

4.2.3 Influence of pH on 1,2-dihydroxybenzene with L-Phenylalanine

Cyclic voltammogram of 1,2-dihydroxybenzene in presence of 20 mM L-Phenylalanine of Gc (3mm) electrode has been studied at different buffer solution of pH 5 to 11 (Fig. 4.61). The voltammetric behavior of 1,2-dihydroxybenzene at pH 5, 9 and 11 in the presence of 20 mM L-Phenylalanine show no new anodic peak after repetitive cycling indicating that the reaction between o-benzoquinone and L-Phenylalanine has not occurred. This can be attributed to the fact that at pH 5, the nucleophilic property of amine groups is diminished through protonation (Fig. 4.61). This can be explained by the fact that at pH 5 or lowers, the amino group undergoes protonation by excess proton and form zwitterion. But, in the higher pH 11 the cyclic voltammogram of 1,2-dihydroxybenzene show irreversible behavior. It is thus suggested that the oxidation of 1,2-dihydroxybenzene followed by an

irreversible chemical reaction with hydroxyl ion, especially in alkaline solutions. However, amines in this condition can also act as nucleophiles. The peak position of the redox couple is found to be dependent upon pH. The anodic peak potential of 1,2-dihydroxybenzene shifted towards left with the increase of pH. Fig. 4.62 shows the plot of peak potential, E_p vs pH. The slope value of the plot is obtained 56.5mV/pH for A_0 and 59 mV/pH which is nearer to the value of one electron, one proton transfer process (Table 4.14). Fig. 4.63 represents the plot of oxidation peak (A_0) current, I_p against pH of solution. From this figure the maximum peak current is obtained at pH 7 (Table 4.14) that has been selected as optimum condition for electrochemical study of 1,2-dihydroxybenzene, at which the electro oxidation is facilitated in neutral media and hence the rate of electron transfer is faster.

CV of 1,2-dihydroxybenzene in presence of 20 mM L-Phenylalanine at Platinum (Pt) (1.6 mm) electrode in the second scan of potential has been studied in pH 5 to 11 (Fig. 4.64). The voltammetric behavior of 2 mM 1,2-dihydroxybenzene at pH 5 in the presence of 20 mM L-Phenylalanine shows one anodic peak and corresponding cathodic peak after repetitive cycling expressing that the reaction between o-quinone and L-Phenylalanine has not occurred. This can be assigned to the fact that at acidic media, the nucleophilic property of amine groups is diminished through protonation. In the pH 7-11 the *o*-quinone undergoes L-Phenylalanine attack by the amine through a Michael addition reaction suggests that voltammetric new anodic peak A_0 appeared after repetitive cycling. However, amines in this condition can also act as nucleophiles. The peak position of the redox couple is found to be depended upon pH. Fig. 4.65 shows the plot of oxidation peak current, I_p against pH solution. It is seen that the maximum peak current is obtained at pH 7. Fig. 4.66 shows the plot of peak potential, E_p vs pH. The slope value of the plot is obtained 69 mV/pH which is nearer to the value of one electron, one proton transfer process (Table 4.15).

The effect of pH on the cyclic voltammogram of 2 mM 1,2-dihydroxybenzene in presence of 20 mM L-Phenylalanine at Au (1.6 mm) electrode in the second scan of potential has been studied at pH from 5 to 11 (Fig. 4.67). The influence of pH for Au electrode in the same systems, the voltammetric properties are slightly different from GC electrode. The voltammetric behavior of 1,2-dihydroxybenzene at pH 5 in the presence of L-

Phenylalanine shows no new peak in the second scan of potential. In the pH 7-9, the o-benzoquinone undergoes L-Phenylalanine attack by the amine through Michael addition reaction reflected that voltammetric new anodic peak A_0 appeared after repetitive cycling. In the higher pH (e.g., pH 11), no new anodic peak appears in the second scan of potential. However, the peak position of the redox species is found to be dependent upon pH. Fig. 4.68 shows the plots of oxidation peak current, I_p against pH of solution. It is seen that the maximum peak current is obtained at pH 7 attributed that nucleophilic addition reaction is most favorable in neutral media. Fig. 4.69 shows the plot of the peak potential, E_p against pH at second cycle in the same condition. The slope value of the plot is 55.5 mV/pH for anodic peak A_1 which is close to theoretical value for two step one electron, one proton transfer process (Table 4.16).

4.2.4 Concentration effect of L-Phenylalanine

Voltammogram obtained by the addition of different composition of L-Phenylalanine ranging from (2, 10, 20, 50 and 100 mM) with fixed composition of 1,2-dihydroxybenzene of Gc electrode at pH 7 and scan rate 0.1V/s has been shown in (Fig. 4.70). Upon addition of L-Phenylalanine the anodic peaks shifts positively and a new peak appears at ~ 0.04V which suggests that the nucleophilic attack takes place and consequently 1,2-dihydroxybenzene-Phenylalanine adduct deposits on the electrode surface. The peak current intensity of the newly appeared anodic and cathodic peak increases with the increase of L-Phenylalanine concentration up to 20 mM and after that the redox peak current is started to be decreased (Fig. 4.71). The nucleophilic substitution reaction of 1,2-dihydroxybenzene in presence of L-Phenylalanine is maximum favorable up to 20 mM of L-Phenylalanine at pH 7 (Table 4.17). The corresponding peak current ratio (I_{pc1}/I_{pa1}) changes with the concentration of L-Phenylalanine. This is related to the increase of the homogenous reaction rate of following chemical reaction between *o*-benzoquinone 1a and L-Phenylalanine 2 with increasing concentration of L-Phenylalanine up to 20 mM. At higher concentration of L-Phenylalanine (>20mM), the excess electro-inactive L-Phenylalanine may be deposited on the electrode surface and consequently the peak current decreased.

Influence of different concentration of L-Phenylalanine (2, 10, 20, 50 and 100 mM) into fixed concentration of 1,2-dihydroxybenzene (2 mM) at Gold (Au) and Platinum (Pt)

electrodes has been also examined in the same conditions (Fig. 4.72 and Fig. 4.74). In the first scan of potential a new cathodic peak (C_0) appears at -0.26 V and -0.29 V at Pt and Au electrodes respectively. In the second scan of potential, the anodic peaks shifted and a new anodic peak appeared at -0.02 V and -0.06 V at Pt and Au electrodes respectively which suggests the formation of 1,2-dihydroxybenzene-Phenylalanine adduct. The net current intensity of the newly appeared anodic and cathodic peak increases with the increase of composition up to 2 to 20 mM of L-Phenylalanine. After further addition of L-Phenylalanine (>20 mM), the anodic and cathodic peak current gradually decreases (Tables 4.18-4.19). At higher concentration of L-Phenylalanine (>20mM), the excess electro-inactive L-Phenylalanine may be accumulated on the electrode surface and the peak current decreased. Therefore, the concentration effects of L-Phenylalanine into the fixed concentration of 1,2-dihydroxybenzene (2 mM) for Au and Pt electrodes are few different from GC electrode.

4.2.5 Effect of electrode materials

The voltammetric response is also influenced by different electrode materials. Electrochemical properties of 1,2-dihydroxybenzene have been studied in absence and presence of 20 mM L-Phenylalanine with the fixed composition of 2 mM 1,2-dihydroxybenzene by means of both cyclic voltammetry (CV) and Differential pulse voltammetry (DPV) by using different electrodes like Gc, Au and Pt at different pH at scan rate 0.1V/s (Fig. 4.76 and Fig. 4.77). The nature of voltammogram, the peak position and current intensity for the studied systems are different for different electrodes although the diameter of Gc electrode (3mm) is higher than Au and Pt (1.6mm). The CV of GC electrode is significantly different from those of the Au and Pt electrodes based on peak current consideration. All electrodes show two anodic and corresponding cathodic peaks in the potential range of investigation. Among them the peak current intensity of GC electrode is much higher than Au and Pt electrodes in Fig. 4.76. In the case of GC and Pt electrodes for the second cycle of potential a new oxidation and reduction peak appear at lower oxidation potential which can be attributed to the oxidation of adduct formed between the *o*-benzoquinone and L-Phenylalanine. Electrochemical properties of 1,2-dihydroxybenzene with L-Phenylalanine for example change of pH, concentration, scan rate etc. were studied in detail using Pt and Au electrodes. But among the electrodes, the

voltammetric response of GC electrode was better than Pt and Au electrodes in the studied systems.

According to DPV electrode comparison graph (Fig. 4.77) it can be seen that Gc electrode shows better voltammetric response having three anodic peak at -0.295V, -0.01V and 0.295V. We considered the 1,2-dihydroxybenzene-adduct peak at -0.01V and another very small peak at lower potential -0.3 could be due to side reaction like polymerization, further oxidation of 1,2-dihydroxybenzene-adduct or nucleophilic attack of hydroxyl ion. Among Gc, Pt and Au electrode the peak current and voltammetric response of Gc electrode is much better than Pt electrode under this investigation. Therefore, Gc electrode has been chosen as electrode material for this investigation.

4.2.6 Subsequent cycles of CV of 1,2-dihydroxybenzene with L-Phenylalanine

Fig. 4.78 shows the cyclic voltammogram of the first 15 cycles of 2 mM 1,2-dihydroxybenzene with 20 mM L-Phenylalanine of GC (3 mm) electrode in buffer solution of pH 7 for the potential range between -0.6 V to 0.9 V. The voltammogram at the scan rate 0.1 Vs^{-1} has one anodic peak at 0.3 V and two cathodic peaks at -0.29 V and 0.04 V when considered the first scan of potential (red line). In the subsequent potential cycles a new anodic peak appeared at ~ 0.04V and intensity of the first anodic peak current increased progressively on cycling but the second anodic peak current decreases and shifted positively on cycling. This can be attributed to produce of the 1,2-dihydroxybenzene-Phenylalanine adduct through nucleophilic substitution reaction in the surface of electrode (Scheme 2). The successive decrease in the height of the 1,2-dihydroxybenzene oxidation and reduction peaks with cycling can be ascribed to the fact that the concentrations of 1,2-dihydroxybenzene-Phenylalanine adduct formation increased by cycling leading to the decrease of concentration of 1,2-dihydroxybenzene or *o*-quinone at the electrode surface. The positive shift of the second anodic peak in the presence of L-Phenylalanine is probably due to the formation of a thin film of product at the surface of the electrode, inhibiting to a certain extent the performance of electrode process. Along with the increase in the number of potential cycles the first anodic peak current increased up to 10 cycles and then the peak current almost unchanged with subsequent cycle (Fig. 4.78). This may be due to the block of electrode surface by the newly formed species after more cycling.

The effect of the cyclic voltammogram of the first 15 cycles of 2 mM 1,2-dihydroxybenzene with 20 mM L-Phenylalanine of Gold (Au) electrode and Platinum (Pt) electrode in buffer solution of pH 7 has been also studied in the same condition. In the first scan of potential (red line) at Au electrode there are two anodic peaks at 0.27V and 1.04 V and three cathodic peaks at -0.24 V, 0.11 V and 0.45 V respectively (Fig. 4.80). In the subsequent scan of potential Au electrode shows a new anodic peak at -0.05 V with another three anodic peaks (blue line). But at Pt electrode there is one anodic peaks at 0.29 V and two cathodic peaks at - 0.28 V and 0.04 V in the first scan of potential (red line) (Fig. 4.79). In the subsequent potential cycles a new anodic peak appeared at -0.02 V and the first anodic peak current increased progressively on cycling but the second anodic peak current decreases and shifted positively on cycling. This can be suggested to produce the 1,2-dihydroxybenzene-Phenylalanine adduct through nucleophilic substitution reaction in the surface of electrode (Scheme 2).

4.2.7 Controlled-potential coulometry of 1,2-dihydroxybenzene with L-Phenylalanine

Controlled-potential coulometry technique has been employed to investigate the electrolysis progress with the help of DPV and CV in aqueous solution containing 1 mM of 1,2-dihydroxybenzene and 10 mM of L-Phenylalanine at 0.4 V in pH 7 which has been showed in (Fig. 4.81). According to this voltammogram it can be seen that, during the course of coulometry the peaks A_0 appears and the height of the A_0 peak increases to the advancement of coulometry and as a result the anodic peak A_1 decreases. After some couples of hour both redox couple of appeared peak does not increase with the successive decrease of concentration of 1,2-dihydroxybenzene which has been showed by both CV and DPV in (Fig. 4.82). These observations allow us to propose the pathway in **Scheme 2** for the electro-oxidation of 1,2-dihydroxybenzene **(1)** in the presence of L-Phenylalanine **(2)**. According to our results, it seems that the 1,4 addition reaction of 2 to o-quinone **(1a)** (Step 2) is faster than other secondary reactions, leading to the intermediate 3. The oxidation of this compound (3) is easier than the oxidation of parent starting molecule **(1)** by virtue of the presence of electron-donating group. Like o-quinone **1a**, Compound **4** can also be attacked from the C-5 position by L-Phenylalanine **(2)**. However, no side reaction is observed during the voltammetric experiments because of the low activity of the *o*-

quinone **4** toward 1,4-(Michael) addition reaction with L-Phenylalanine (2). Product **(5)** can also be generated by the addition of **(4)** with **(1a)**.

4.2.8 pH effect on DPV of 1,2-dihydroxybenzene with L-Phenylalanine

Differential Pulse Voltammogram technique has been employed to monitor the 1,4-Michaael addition reaction of 2 mM 1,2-dihydroxybenzene in the presence of 20 mM L-Phenylalanine in second scan in different pH (5-11) at GC electrode has shown in Fig. 4.83. In the buffer solution of pH 7, 1,2-dihydroxybenzene shows two well-developed wave at -0.3V and 0.3V respectively in the presence of L-Phenylalanine. As can be seen two completely separated anodic peaks with high current intensity are observed in pH 7, which can be attributed to the oxidations of *o*-benzoquinone-Phenylalanine new compound and 1,2-dihydroxybenzene, respectively.

Gold (Au) and Pt electrodes are also used for the investigation of voltammogram of 2mM 1,2-dihydroxybenzene with 20 mM L-Phenylalanine in different buffer solution at 0.1 V/s. Figures 4.84-4.85 show the first and second scan of potential of 1,2-dihydroxybenzene with L-Phenylalanine solution at different pH, respectively. However, in pH 7-11 new peak A_0 appeared which may be attributed to the formation of 1,2-dihydroxybenzene-Phenylalanine adduct. But, in lower (pH <7) and higher pH media (pH >7) no new anodic peak appeared. In the buffer solution of pH 7, the voltammogram shows two well-developed peak ascribed the formation of adduct similar to GC electrode. High current intensity is observed at pH 7, which can be attributed to the formation of 1,2-dihydroxybenzene-Phenylalanine adduct. The DPV of Au and Pt electrodes are consistent with the GC electrode in the studied systems at the same condition.

4.2.9 Effect of deposition time change of DPV of 1,2-dihydroxybenzene with L-Phenylalanine

Fig. 4.86, indicates the DPV of deposition time change (0, 10, 30, 90, 120 and 150s) of 2 mM 1,2-dihydroxybenzene 20 mM L-Phenylalanine of pH 7. According to this figure it can be seen that, increasing of deposition time leads to develop two new peaks at -0.32V and 0.0 V. When the deposition time increases 30s, more nucleophilic attack occurs and

consequently more 1,2-dihydroxybenzene-Phenylalanine adduct form which leads to decreasing in the concentration of *o*-benzoquinone and increasing in the concentration of 1,2-dihydroxybenzene-Phenylalanine adduct at the surface of electrode. Maximum peak intensity is obtained up to 30s. For further increase of deposition time from 40s to 150s, both first and second anodic peak current decreases. This confirmed that with the increase of time decreases the concentration of o-benzoquinone due to follow up the reaction.

4.2.10 Effect of concentration of DPV of 1,2-dihydroxybenzene with L-Phenylalanine

The effect of different composition of L-Phenylalanine (2-100 mM) with 2 mM 1,2-dihydroxybenzene has been studied in details by using the differential pulse voltammetry (Fig. 4.87). There are three separated anodic peaks appears after the addition of different concentration of L-Phenylalanine into 1,2-dihydroxybenzene. In this case, the gradual increasing of the concentration of L-Phenylalanine up to 20 mM leads to increasing of first anodic peak current. For further increase of concentration from 30 to 100 mM, all anodic peak decreases gradually. In lower concentration of L-Phenylalanine (<20 mM), the nucleophilic substitution reaction take place in comparable degree, whereas increasing the concentration of L-Phenylalanine (>20 mM) make favorable nucleophilic attack of L-Phenylalanine toward *o*-benzoquinone generated at the surface of electrode. For further addition of L-Phenylalanine (>20 mM) into 1,2-dihydroxybenzene solution, the excess electro-inactive L-Phenylalanine deposits on the electrode surface and hence the peak current decreases.

The effect of L-Phenylalanine concentration on 1,2-dihydroxybenzene has been justified by employing DPV technique at Platinum (Pt) and Gold (Au) electrodes in the same condition. Figures 4.88-4.89 show the DPV for 2 mM of 1,2-dihydroxybenzene solution containing buffer (pH 7) in the presence of various concentration of L-Phenylalanine from 2 mM to 100 mM at the surface of Pt electrode for the first and second scan of potential. After addition of L-Phenylalanine into 1,2-dihydroxybenzene there are two separated anodic peaks appear in the second scan. In lower concentration of L-Phenylalanine (<20 mM), the nucleophilic substitution reaction take place in comparable degree, whereas increasing the concentration of L-Phenylalanine (20 mM) make susceptible for nucleophilic attack of L-Phenylalanine towards o-benzoquinone generated at the surface of electrode. For more addition of L-Phenylalanine (>20 mM) into 1,2-dihydroxybenzene

solution, the excess electro-inactive L-Phenylalanine accumulated on the electrode surface and hence the peak current decreases. Thus the effect of composition of L-Phenylalanine on 1,2-dihydroxybenzene is consistent with both CV and DPV.

In this investigation different concentrations (2-100 mM) of L-Phenylalanine have been used to determine the optimum condition for the nucleophilic substitution reaction on 1,2-dihydroxybenzene. As the reaction is occurred at low concentration of nucleophiles. In contrast, comparatively high concentration of L-Phenylalanine is not favorable for the current studied system and appearing peak is not so prominent. From the experimental study it is noticeable that L-Phenylalanine acts properly as a nucleophile at pH 7. When the pH is below 7 that are at acidic media, the nucleophilic activity of L-Phenylalanine reduces due to the protonation of amine. Whereas at basic condition, other nucleophiles such as –OH produce in solution, therefore, the activity of amines decreases and the oxidation of 1,2-dihydroxybenzene followed by an irreversible chemical reaction with hydroxyl ion [83].

Therefore, from the above discussion it is indicative that the nucleophilic substitution reaction of 1,2-dihydroxybenzene in presence of L-Phenylalanine is maximum favorable at 20 mM of L-Phenylalanine and at pH 7 which is consistent with both CV and DPV. All above observations could be attributed to the reaction between L-Phenylalanine and *o*-benzoquinone species produced at the surface of electrode, with the new anodic peak being attributed to the oxidation of newly formed *o*-benzoquinone-Phenylalanine adduct.

4.2.11 Spectral analysis of 1,2-dihydroxybenzene with L-Phenylalanine

The FTIR spectrum of the vibrational modes of the 1,2-dihydroxybenzene, L-Phenylalanine and 1,2-dihydroxybenzene-Phenylalanine adduct has been shown in Figure 4.135. Peak at 3450 cm^{-1} reveals the O-H stretching band in 1,2-dihydroxybenzene. A broad spectrum appeared in the range of 3600-1800 cm^{-1} indicates the overlap of O-H and N-H stretching vibration mode in L-Phenylalanine. The absorption peak due to the C=O stretching is appeared at 1850-1650 cm^{-1} in -COOH group. Also the finger print region for 1,2-dihydroxybenzene-Phenylalanine adduct is significantly different from pure 1,2-dihydroxybenzene and pure L-phenylalanine which indicates the formation of new adducts.

4.3.1 Electrochemical nature of 1,2-dihydroxybenzene in presence of L-Leucine

Cyclic voltammogram in Fig. 4.90 shows of only 1,2-dihydroxybenzene (Green line) only L-Leucine (Blue line) and 1,2-dihydroxybenzene with L-Leucine (Red line) at GC (3 mm) electrode in buffer solution of pH 7 and scan rate 0.1 V/s. The cyclic voltammogram of 1,2-dihydroxybenzene shows one anodic peak at A_1 (0.26 V) and corresponding cathodic peak at C_1 (0.05 V) related to its transformation to *o*-quinone and vice versa. Pure L-Leucine is electrochemically inactive amino acid hence no redox couple appears in the potential range of investigation. Cyclic voltammogram of 1,2-dihydroxybenzene in the presence of L-Leucine in buffer solution at pH 7 shows one anodic peak in the first cycle of potential and on the reverse scan the corresponding cathodic peak slowly decreases and new peak C_0 is observed at less positive potential -0.35 V.

In the second cycle of potential a new anodic peak A_0 is also observed at less positive potential at 0.05 V. Due to formation of new redox couple the current intensity of 1,2-dihydroxybenzene reduces. This phenomenon can be explained by the fact of nucleophilic attack of L-Leucine to *o*-benzoquinone. Due to the conduction of nucleophilic substitution reaction of L-Leucine with 1,2-dihydroxybenzene, the *o*-benzoquinone concentration in reaction layer reduces, consequently the A_1 and C_1 peaks reduce. Whereas in the same time 1,2-dihydroxybenzene-Leucine adducts produces and consequently the new peak A_0 appears. The peak current ratio for the peaks A_1 and C_1 (I_{Pa1}/I_{pc1}) decreased noticeably, which indicated the chemical reaction of L-Leucine (2) with the o-quinone (1a) produced at the surface of electrode. These observations may ascribe the formation of 2-((3,4-dihydroxyphenyl)amino)-4-methylpentanoic acid through nucleophilic substitution reaction (Scheme 3).

If the constituent is such that the potential for the oxidation of product is lower, then further oxidation of the product is lower, the further oxidation and further addition may occur [70]. According to this concept it can be said that, the oxidation of 1,2-dihydroxybenzene-Leucine is easier than the oxidation of parent 1,2-dihydroxybenzene in the presence of excess amount of nucleophile and this substituted product can be further attacked by L-Leucine. However, it was not observed in cyclic voltammogram because of the low activity of o-quinone 4 toward 2. This behavior is in agreement with that reported by other research groups for similar electrochemically generated compounds such as 1,2-

dihydroxybenzene and different nucleophiles [70-78]. In the absence of other nucleophiles, water or hydroxide ion often adds to the o-benzoquinone [79].

Fig. 4.91 represents the CV of second scan of potential of 2 mM 1,2-dihydroxybenzene with 100 mM L-Leucine at Platinum (Pt) (1.6 mm) electrode in pH 7 and at scan rate 0.1 V/s. This cyclic voltammogram shows the comparison of only 2 mM 1,2-dihydroxybenzene (green line), pure L-Leucine (blue line) and 1,2-dihydroxybenzene (2 mM) with L-Leucine (100 mM) (Red line) in the second scan of potential at the same condition. A new reduction peak (C_0) appears at -0.3 V after the addition of 100 mM L-Leucine to the solution at first scan of potential. The peak current decreases significantly with respect to the only 1,2-dihydroxybenzene. In the second scan of potential 1,2-dihydroxybenzene with L-Leucine shows two anodic peaks at -0.04 V and 0.29 V and the corresponding two cathodic peaks at -0.3 V and 0.06 V, respectively. Upon addition of L-Leucine to 1,2-dihydroxybenzene solution, the cathodic peak C_1 decreases and a new cathodic peak C_0 appears. Also, in the second scan of potential a new anodic peak A_0 appears and anodic peak A_1 decreases similar to GC electrode. This observation can be stated by considering nucleophilic attack of L-Leucine to *o*-benzoquinone. The nucleophilic attack of L-Leucine to *o*-benzoquinone reduces the *o*-benzoquinone concentration in reaction layer. Accordingly, the A_1 and C_1 peaks reduce, whereas in the same time produces 1,2-dihydroxybenzene- Leucine adduct and consequently the peak A_0 and C_0 appears (Scheme 3).

A similar behavior is also observed when we used a Gold (Au) electrode for the investigation of same solution in the same condition in fig. 4.92. Upon addition of 100 mM L-Leucine to 2 mM 1,2-dihydroxybenzene solution at the Gold (Au) electrode it shows three anodic and three cathodic peaks for the second scan of potential. The newly appearance of A_0 and C_0 peak, and decrease of A_1 and C_1 peak, and also shifting of the positions of peaks A_1 and C_1 also indicates that it is due to follow up reaction of 1,2-dihydroxybenzene with L-Leucine (Scheme 3) at Au electrode. In case of GC and Pt electrodes, it shows two anodic and two cathodic peaks. The third peak of Au electrodes is due to the oxidation of Au in buffer solution. This unlike behavior has been discussed in above two systems.

4.3.2 Effect of scan rate of 1,2-dihydroxybenzene with L-Leucine

To study the effect of different scan rates on 2 mM of 1,2-dihydroxybenzene with 100 mM of L-Leucine, CV technique has been employed in Fig. 4.93 at pH 7. According to this voltammogram it can be seen that the peak current intensity of newly appeared peak gradually increases with the increase of scan rates. The cathodic peaks shift towards left whereas the anodic peaks move to the right direction with increase of scan rate. Fig. 4.94 shows plot of the anodic and cathodic net peak currents for second cycle against the square-root of the scan rates where the net current means the second peak subtracted from the first one by the scan-stopped method in the same condition [70]. The nearly proportional ratio in between redox couple indicates that the peak current of the reactant at each redox reaction is controlled by diffusion process with some chemical complications. It can be seen in Fig. 4.93, the cathodic peak for reduction of *o*-benzoquinone is almost disappeared in the scan rate of 0.05 V/s. By increasing the scan rate, the cathodic peak for reduction of *o*-benzoquinone starts to appear and increasing. The corresponding peak current ratio (I_{pa1}/I_{pc1}) vs scan rate for a mixture of 1,2-dihydroxybenzene and L-Leucine decreases with increasing scan rate firstly and then after 0.1 V/s, it remains almost unchanged (Fig. 4.95, Table 4.20). The anodic peak current ratio (I_{pa0}/I_{pa1}) vs scan rate for a mixture of 1,2-dihydroxybenzene and L-Leucine firstly increases and then after 0.2 V/s scan rate the peak current remains constant. On the other hand, the value of current function ($Ip/v^{1/2}$) is found to be decreased with increasing scan rate (Fig. 4.96). The exponential nature of the current function versus the scan rate plot indicates the ECE mechanism for electrode process [75]. This confirms the reactivity of *o*-benzoquinone (1a) towards L-Leucine (2) firstly increases at slow scan rate and then at higher scan rate it decreases. According to the results, it can be mentioned that L-Leucine (2) undergoes the 1,4-Michael addition reaction with *o*-benzoquinone (1a) leads to product 3. The oxidation of this compound (3) is observed easier than the oxidation of parent molecule (1) by virtue of the presence of electron donating amine group. Similar behavior has been observed for the 1,2-dihydroxybenzene-Alanine and 1,2-dihydroxybenzene-Phenylalanine systems.

Reaction schemes-3:

Step-1:

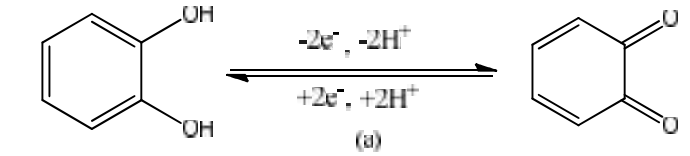

1,2-dihydroxybenzene
1

o-benzoquinone
1a

Step-2:

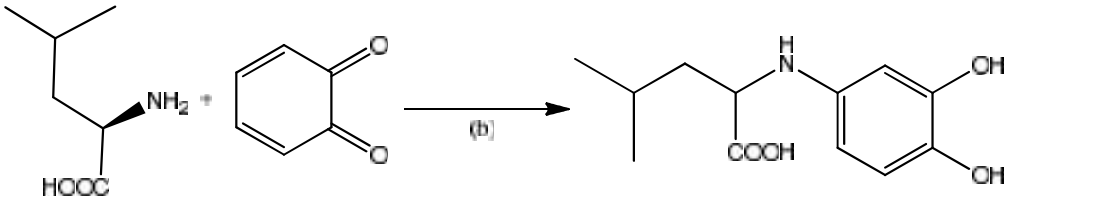

L-Leucine
2

o-benzoquinone
1a

2-((3,4-dihydroxyphenyl)amino)-4-methylpentanoic acid
3

Step-3:

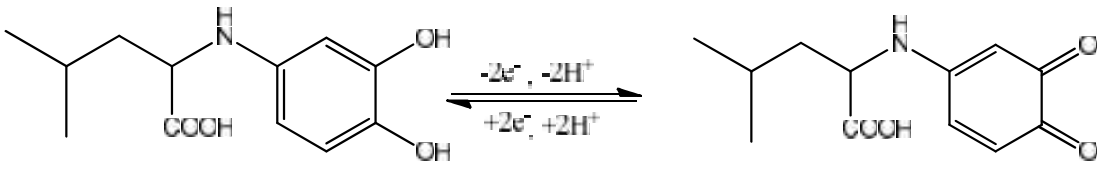

2-((3,4-dihydroxyphenyl)amino)-4-methylpentanoic acid
3

2-((3,4-dioxocyclohexa-1,5-dien-1-yl)amino)-4-methylpentanoic acid
4

Step-4:

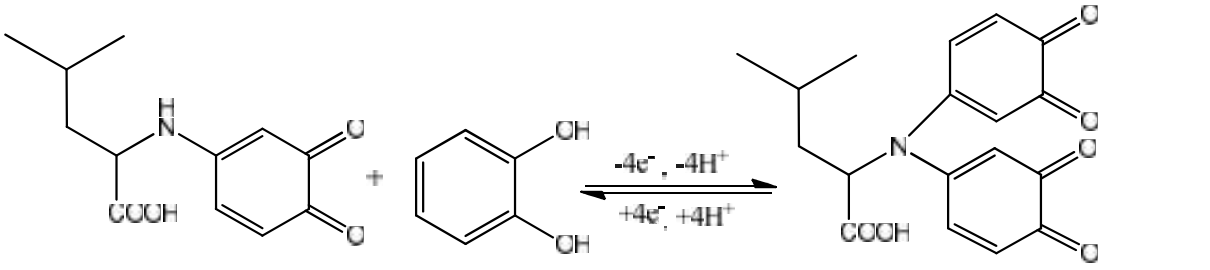

4

1

2-(bis(3,4-dioxocyclohexa-1,5-dien-1-yl)amino)-4-methylpentanoic acid
5

CV of second scan of potential at Pt electrode of 2 mM 1,2-dihydroxybenzene with 100 mM L-Leucine at pH 7 and different scan rate (Fig. 4.97- 4.100) The peak current of both the anodic and cathodic peaks increases with the increase of scan rate. The anodic peaks are shifted towards right direction and the cathodic peaks are to the left with increase in the scan rate. Fig. 4.98 shows plots of the anodic and cathodic peak currents for second scan of potential as a function of square-root of the scan rates. The proportionality of the anodic and the cathodic peaks ascribed that the peak current of the reactant at each redox reaction is controlled by diffusion process. The anodic and cathodic peak currents, peak potentials, corresponding peak potential differences and peak current ratio are tabulated in Tables 4.21. Fig. 4.99 shows variation of peak current ratio of corresponding peak (I_{pa1}/I_{pc1}) and anodic peak (I_{pa0}/I_{pa1}) vs scan rate (v) of 2 mM 1,2-dihydroxybenzene with 100 mM L-Leucine in the same condition. The corresponding peak current ratio (I_{pa1}/I_{pc1}) vs scan rate for a mixture of 1,2-dihydroxybenzene and L-Leucine decreases with increasing scan rate firstly and then after 0.2 V/s, it remains almost unchanged (Fig. 4.99). The anodic peak current ratio (I_{pa0}/I_{pa1}) vs scan rate for a mixture of 1,2-dihydroxybenzene and L-Leucine firstly increases and then after 0.15 V/s scan rate the peak current starts to be decreased (Fig. 4.99). Beside this, the value of current function ($Ip/v^{1/2}$) is found to be decreased with increasing scan rate (Fig. 4.100). The exponential nature of the current function versus the scan rate plot indicates the ECE mechanism for electrode process.

Similar behavior has been observed at Au electrode in the same condition (Fig. 4.101-4.104, Table 4.22). According to Fig. 4.102 it can be seen that the anodic and cathodic net peak currents against the square-root of the scan rates is nearly proportional which suggests that the peak current of the reactant at each redox reaction is controlled by diffusion process. Fig. 4.103 shows variation of peak current ratio of corresponding peak (I_{pa1}/I_{pc1}) and anodic peak (I_{pa0}/I_{pa1}) vs scan rate (v) in the same condition. The (I_{pa1}/I_{pc1}) peak current ratio gradually decreases with increasing scan rate whereas the anodic peak current ratio observed maximum at 0.2 V/s and after that it started to be decreased up to 0.4 V/s and then it remains constant with increasing scan rates. The exponentially decreasing nature with increasing scan rates in fig. 4.104 indicates that the reaction is taken place by ECE mechanism. According to all system it can be said that, the nucleophilic substitution reaction of 1,2-dihydroxybenzene in presence of L-Leucine is maximum favorable at slow scan rate by diffusion process.

4.3.3 Influence of pH on 1,2-dihydroxybenzene with L-Leucine

Electro-oxidation of 1,2-dihydroxybenzene in presence of 100 mM L-Leucine of GC (3 mm) electrode has been investigated at different pH media (5 to 11) and the voltammogram mentioned in Fig. 4.105. The voltammetric behavior of 1,2-dihydroxybenzene at pH 5, 9 and 11 in the presence of 100 mM L-Leucine show no new anodic peak appeared after repetitive cycling indicating that the reaction between *o*-benzoquinone and L-Leucine has not occurred. This can be attributed to the fact that at pH 5, the nucleophilic property of amine groups is diminished through protonation. This can be explained by the fact that at pH 5 or lowers, the amino group undergoes protonation by excess proton and forms zwitterion. Whereas, in the higher pH range (e.g., pH 9-11), the cyclic voltammogram of 1,2-dihydroxybenzene show irreversible behavior like 1,2-dihydroxybenzene-Alanine and 1,2-dihydroxybenzene-Phenylalanine system. The peak position of the redox couple is found to be dependent upon pH. The anodic peak potential of 1,2-dihydroxybenzene shifted towards left with the increase of pH. Fig. 4.106 shows the plot of the peak potential, E_p against pH at second cycle in the same condition. The slopes value is calculated (65 mV/pH for anodic peak A_1) which is close to theoretical value for two step one electron, one proton transfer process (Table 4.23). Fig. 4.107 shows the plot of oxidation peak (A_0) current, I_p against pH of solution. From this figure it can be seen that the maximum peak current is obtained at pH 7. At this pH, the difference between the peak current ratio (I_{pC0}/I_{pA0}) in the presence of L-Leucine is observed maximum. Consequently, pH 7 has been selected as optimum condition for electrochemical study of 1,2-dihydroxybenzene, at which the electro oxidation is facilitated in neutral media and hence the rate of electron transfer is faster.

CV of 1,2-dihydroxybenzene in presence of 100 mM L-Leucine at Platinum (Pt) (1.6 mm) electrode in the second scan of potential has also been studied in pH 5 to 11 (Fig. 4.108). The voltammetric behavior of 2 mM 1,2-dihydroxybenzene at pH 5 in the presence of 100 mM L-Leucine shows one anodic peak and corresponding cathodic peak after repetitive cycling expressing that the reaction between *o*-quinone and L-Leucine has not occurred. This can be assigned to the fact that at acidic media, the nucleophilic property of amine groups is diminished through protonation. In the pH 7-11, the o-quinone undergoes L-Leucine attack by the amine through a Michael addition reaction suggests that

voltammetric new anodic peak A_0 appeared after repetitive cycling. However, amines in this condition can also act as nucleophiles. The peak position of the redox couple is found to be dependent upon pH. Fig. 4.109 shows the plot of oxidation peak current, I_p against pH solution. It is seen that the maximum peak current is observed at pH 7 (Table 4.24). Fig. 4.110 shows the plot of peak potential, E_p vs pH. The slope value of the plot is obtained 51.0mV/pH which is nearer to the value of one electron, one proton transfer process.

The influence of pH for Au electrode in the same systems, the voltammetric properties are slightly different from GC electrode (Fig. 4.111). The voltammetric behavior of 1,2-dihydroxybenzene at pH 5 in the presence of L-Leucine shows no new peak in the second scan of potential. This can be indicated to the fact that in lower pH, the nucleophilic property of amine groups is diminished through protonation. In the pH 7-9, the *o*-benzoquinone undergoes L-Leucine attack by the amine through Michael addition reaction reflected that voltammetric new anodic peak A_0 appeared after repetitive cycling. In the higher pH (e.g., pH 11), no new anodic peak appears in the second scan of potential. However, the peak position of the redox species is found to be dependent upon pH. Fig. 4.112 shows the plots of oxidation peak current, I_p against pH of solution. It is seen that the maximum peak current is observed at pH 7 (Table 4.25) attributed that nucleophilic addition reaction is most favorable in neutral media. Fig. 4.113 shows the plot of the peak potential, E_p against pH at second cycle in the same condition. The slopes of the plot were (50.5 mV/pH for anodic peak A_1) which is close to theoretical value for two step one electron, one proton transfer process.

4.3.4 Concentration effect of L-Leucine

Composition of nucleophiles have strong influence on the nucleophilic substitution reaction and the effect of composition change of L-Leucine from 30 mM to 200 mM with fixed composition of 2 mM of 1,2-dihydroxybenzene has been carried out in different electrodes by means of cyclic voltammetry of GC electrode at pH 7 and scan rate 0.1 V/s (Fig. 4.114). Upon addition of L-Leucine the anodic peaks shift positively and a new peak appears at - 0.04 V which suggests that the nucleophilic attack takes place and consequently 1,2-dihydroxybenzene-L-Leucine adduct deposits on the electrode surface. The peak current intensity of the newly appeared anodic and cathodic peak increases with

the increase of L-Leucine concentration up to 100 mM and after that the redox peak current is started to be decreased (Fig. 4.115, Table 4.26). The nucleophilic substitution reaction of 1,2-dihydroxybenzene in presence of L-Leucine is maximum favorable up to 100 mM of L-Leucine at pH 7. The corresponding peak current ratio (I_{pc1}/I_{pa1}) changes with the concentration of L-Leucine. This is related to the increase of the homogenous reaction rate of following chemical reaction between *o*-benzoquinone 1a and L-Leucine 2 with increasing concentration of L-Leucine up to 100 mM. At higher concentration of L-Leucine (>100 mM), the excess electro-inactive L-Leucine may be deposited on the electrode surface and consequently the peak current decreases.

In addition of different concentration of L-Leucine (30, 50, 100, 150 and 200 mM) into fixed concentration of 1,2-dihydroxybenzene (2 mM) at Gold (Au) and Platinum (Pt) electrodes has been also examined in the same conditions (Fig. 4.118 and fig. 4.116). In the first scan of potential a new cathodic peak (C_0) is appeared at -0.3 V and -0.22 V at Pt and Au electrodes respectively. Upon addition of L-Leucine in the second scan of potential, the anodic peaks shifted and a new anodic peak appeared at -0.04 V and -0.1 V at Pt and Au electrodes respectively which suggests the formation of 1,2-dihydroxybenzene-Leucine adduct. The net current intensity of the newly appeared anodic and cathodic peak increases with the increase of composition up to 30 to 100 mM of L-Leucine (Tables 4.27-4.28). After further addition of L-Leucine (>100 mM), the anodic and cathodic peak current gradually decreases. At higher concentration of L-Leucine (>100 mM), the excess electro inactive L-Leucine may be accumulated on the electrode surface and the peak current decreased. Therefore, the concentration effects of L-Leucine into the fixed concentration of 1,2-dihydroxybenzene (2 mM) for Au and Pt electrodes are different from GC electrode.

4.3.5 Effect of electrode materials

Effect of different electrodes (GC, Au and Pt) materials on electrochemical properties of 1,2-dihydroxybenzene has been studied in absence and presence of 100 mM L-Leucine with the fixed composition of 2 mM 1,2-dihydroxybenzene by means of both Cyclic Voltammetry (CV) and Differential Pulse Voltammetry (DPV) at different pH at scan rate 0.1 V/s has shown in Fig. 4.120 and fig. 4.121. The CV of GC electrode is significantly different from those of the Au and Pt electrodes based on peak current consideration. All

electrodes show two anodic and corresponding cathodic peaks in the potential range of investigation. Among them the peak current intensity of GC electrode is much higher than Au and Pt electrodes in. In the case of second cycle of potential a new oxidation and reduction peak appear at lower oxidation potential which can be attributed to the oxidation of adduct formed between the o-benzoquinone and L-Leucine. Electrochemical properties of 1,2-dihydroxybenzene with L-Leucine for example change of pH, concentration, scan rate etc. were studied in detail using Pt and Au electrodes. But among the electrodes, the voltammetric response of GC electrode was better than Pt and Au electrodes in the studied systems.

According to DPV electrode comparison graph (Fig. 4.121) it can be seen that GC electrode shows better voltammetric response and having three anodic peak at -0.295 V, -0.01 V and 0.3 V. We considered the 1,2-dihydroxybenzene-Leucine adduct peak at -0.01 V and another peak at lower potential -0.295 could be due to side reaction like polymerization, further oxidation of adduct or nucleophilic attack of hydroxyl ion. Among GC, Pt and Au electrode the peak current and voltammetric response of GC electrode was found much better than Pt electrode under this investigation. Therefore, GC electrode has been chosen as electrode material for this investigation.

4.3.6 Subsequent cycles of CV of 1,2-dihydroxybenzene with L-Leucine

Fig. 4.122 represents the subsequent cycles of cyclic voltammogram of 2 mM 1,2-dihydroxybenzene with 100 mM L-Leucine of GC (3 mm) electrode in buffer solution of pH 7 for the potential range between -0.6 V to 0.9 V. The voltammogram at the scan rate 0.1 Vs^{-1} has one anodic peak at 0.29 V and two cathodic peaks at -0.3 V and 0.03 V when considered the first scan of potential (red line). In the subsequent potential cycles a new anodic peak appeared at ~ 0.04 V and intensity of the first anodic peak current increased progressively on cycling but the second anodic peak current decreases and shifted positively on cycling. This can be attributed to produce of the 1,2-dihydroxybenzene-Leucine adduct through nucleophilic substitution reaction in the surface of electrode (Scheme 3). The successive decrease in the height of the 1,2-dihydroxybenzene oxidation and reduction peaks with cycling can be ascribed to the fact that the concentrations of 1,2-dihydroxybenzene-Leucine adduct formation increased by cycling leading to the decrease of concentration of 1,2-dihydroxybenzene or quinone at the electrode surface. The positive

shift of the second anodic peak in the presence of L-Leucine is probably due to the formation of a thin film of product at the surface of the electrode, inhibiting to a certain extent the performance of electrode process. Along with the increase in the number of potential cycles the first anodic peak current increased up to 10 cycles and then the peak current almost unchanged with subsequent cycle (Fig. 4.122). This may be due to the block of electrode surface by the newly formed species after more cycling.

The effect of the cyclic voltammogram of the first 15 cycles of 2 mM 1,2-dihydroxybenzene with 100 mM L-Leucine of Gold (Au) electrode and Platinum (Pt) electrode in buffer solution of pH 7 have also been studied in the same condition. According to Fig. 4.124 at Au electrode there are two anodic peaks at 0.25 V and 1.06 V and three cathodic peaks at -0.25 V, 0.11 V and 0.44 V respectively in the first scan of potential (red line). In the subsequent scan of potential Au electrode shows a new anodic peak at -0.1 V with another three anodic peaks (blue line). But at Pt electrode there is one anodic peaks at 0.27 V and two cathodic peaks at -0.32 V and -0.03 V in the first scan of potential (red line) (Fig. 4.123). In the subsequent potential cycles a new anodic peak appeared at -0.05 V and the first anodic peak current increased progressively on cycling but the second anodic peak current decreases and shifted positively on cycling. This can be suggested to produce the 1,2-dihydroxybenzene-Leucine adduct through nucleophilic substitution reaction in the surface of electrode (Scheme 3).

4.3.7 Controlled-potential coulometry of 1,2-dihydroxybenzene with L-Leucine

Controlled-potential coulometry technique has been performed to monitor the electrolysis progress with the help of DPV and CV in aqueous solution containing 1 mM of 1,2-dihydroxybenzene and 50 mM of L-Leucine at 0.45 V in pH 7 which has been showed in (Fig. 4.125). This voltammogram indicates that, during the course of coulometry the peaks A_0 appears and the height of the A_0 peak increases to the advancement of coulometry, parallel to the decrease in height of anodic peak A_1. After some couples of hour both redox couple of appeared peak does not increase with the successive decrease of concentration of 1,2-dihydroxybenzene which has been showed by both CV and DPV in (Fig. 4.126). These observations allow us to propose the pathway in Scheme 1 for the electro-oxidation of 1,2-dihydroxybenzene (1) in the presence of L-Leucine (2). According to our results, it seems

that the 1,4 addition reaction of 2 to *o*-quinone (1a) (reaction (2) was faster than other secondary reactions, leading to the intermediate 3. The oxidation of this compound (3) is easier than the oxidation of parent starting molecule (1) by virtue of the presence of electron-donating group. Like *o*-quinone **1a**, *o*-quinone **4** can also be attacked from the C-5 position by L-Leucine (2). However, no over reaction was observed during the voltammetric experiments because of the low activity of the *o*-quinone **4** toward 1,4-(Michael) addition reaction with L-Leucine (2).

4.3.8 pH effect of DPV of 1,2-dihydroxybenzene with L-Leucine

To understand the effect of different pH media on the nucleophilic substitution reaction of 2 mM 1,2-dihydroxybenzene in the presence of 100 mM L-Leucine in second scan at GC electrode, DPV technique has been employed shown in Fig. 17. In the buffer solution of pH 7, 1,2-dihydroxybenzene shows three well-developed peaks at -0.3 V, 0.02 V and 0.25 V respectively in the presence of L-Leucine (Fig. 4.127). According to our observation the peak at -0.3 V could be due to the side reaction like polymerization or nucleophilic attack on newly appeared adduct which have been reported by a group of research worker [18]. It also can be seen that at pH 5 there are three oxidation peak observed at -0.18 V, 0.085 V and 0.38 V. As can be seen three completely separated anodic peaks with high current intensity are observed in pH 7, which can be attributed to the oxidations of *o*-benzoquinone-Leucine new compound and 1,2-dihydroxybenzene, respectively.

Gold (Au) electrode is also used for the investigation of DPV of 2 mM 1,2-dihydroxybenzene with 100 mM L-Leucine in different buffer solution at 0.1 Vs^{-1}. Fig. 4.129 shows the first and second scan of potential of 1,2-dihydroxybenzene with L-Leucine solution at different pH, respectively. However, in pH 7 new peak A_0 appeared which may be attributed to the formation of 1,2-dihydroxybenzene-Leucine adduct. But, in lower and higher pH media no new anodic peak appeared. In the buffer solution of pH 7, the voltammogram shows two well-developed peak ascribed the formation of adduct similar to GC electrode. The effect of pH on the DPV technique was also employed to make clearer for 1,2-dihydroxybenzene-Leucine addition reaction at Pt electrode in same condition. DPV of 2 mM 1,2-dihydroxybenzene in the presence of 100 mM L-Leucine in first and second scan of potential at different pH (5-11) were shown in Fig. 4.128 (Epulse 0.02 V, tpulse 20 ms and scan rate 0.1 V/s). It is noticed that the peak positions of the DPV

of 1,2-dihydroxybenzene with L-Leucine shifts negatively this indicates that the nucleophilic reaction is easier at pH 7. But, in pH 5, pH 9 and pH 11 no new peak appears in the second scan of potential. High current intensity is observed at pH 7, which can be attributed to the formation of 1,2-dihydroxybenzene-Leucine adduct. The DPV of Au and Pt electrodes are consistent with the GC electrode in the studied systems at the same condition.

4.3.9 Effect of deposition time change of DPV of 1,2-dihydroxybenzene with L-Leucine

Effect of deposition time change (0, 10, 30, 60, 90, 120 and 150s) of DPV of 2 mM 1,2-dihydroxybenzene 100 mM L-Leucine of pH 7 has been represented in Fig. 4.130. This voltammogram illustrates, increasing of deposition time leads to develop a new peak at 0.0 V. At 10s a new peak is observed and when the deposition time increases 30s, more nucleophilic attack occurred and consequently more 1,2-dihydroxybenzene-Leucine adduct was formed which leads to decreasing in the concentration of *o*-benzoquinone and increasing in the concentration of 1,2-dihydroxybenzene-Leucine adduct at the surface of electrode. Maximum peak intensity is obtained up to 30s and further increase of deposition time from 60s to 150s, both first and second anodic peak current decreases. This confirmed that with the increase of time decreases the concentration of *o*-benzoquinone due to follow up the reaction.

4.3.10 Effect of concentration of DPV of 1,2-dihydroxybenzene with L-Leucine

DPV obtained by the addition of different composition of L-Leucine (30, 50, 100, 150 and 200 mM) with 1,2-dihydroxybenzene at pH 7 has been shown in fig. 4.131. There are three separated anodic peaks appear after addition of different concentration of L-Leucine into 1,2-dihydroxybenzene. In this case, the gradual increasing of the concentration of L-Leucine up to 100 mM leads to increasing of first anodic peak current. For further increase of concentration from 150 to 200 mM, all anodic peak decreases gradually. In lower concentration of L-Leucine (<90 mM), the nucleophilic substitution reaction take place in comparable degree, whereas increasing the concentration of L-Leucine (>90 mM) make favorable nucleophilic attack of L-Leucine toward *o*-benzoquinone generated at the surface of electrode. For further addition of L-Leucine (>100 mM) into 1,2-dihydroxybenzene

solution, the excess electro inactive L-Leucine deposited on the electrode surface and hence the peak current decreases.

The effect of L-Leucine concentration on the DPV of 1,2-dihydroxybenzene has also been studied by using Pt (1.6 mm) electrode in the same condition. Fig. 4.132 shows DPV for 2 mM of 1,2-dihydroxybenzene solution containing buffer (pH 7) in the presence of various concentration of L-Leucine from 30 mM to 200 mM at the surface of Pt electrode for the first and second scan of potential. As reported in Fig. 4.131, in the second scan there are two separated anodic peaks appeared after addition of L-Leucine into 1,2-dihydroxybenzene. In lower concentration of L-Leucine (<100 mM), the nucleophilic substitution reaction take place in comparable degree, whereas increasing the concentration of L-Leucine (100 mM) make susceptible for nucleophilic attack of L-Leucine towards *o*-benzoquinone generated at the surface of electrode. For more addition of L-Leucine (>100 mM) into 1,2-dihydroxybenzene solution, the excess electro inactive L-Leucine accumulated on the electrode surface and hence the peak current decreases.

Gold (Au) electrode was also used for the investigation on the DPV of fixed 2 mM 1,2-dihydroxybenzene with different concentration (30-200 mM) of L-Leucine in buffer solution pH 7 at 0.1 Vs^{-1}. Fig. 4.133 shows the second scan of potential of the studied systems at different concentration, respectively. In second scan of potential an appeared peak, A_0 was obtained which may be attributed the formation of 1,2-dihydroxybenzene-Leucine adduct.

In this investigation different concentration 30-200 mM of L-Leucine was used to determine the optimum condition for the nucleophilic substitution reaction on 1,2-dihydroxybenzene. As the reaction was occurred at moderately high concentration of nucleophiles, consequently the voltammetric peaks (CV and DPV) for adduct appeared noticeably. In contrast, comparatively low concentration of L-Leucine was not favorable for the study of electrochemical oxidation of 1,2-dihydroxybenzene because the appearing peak was not so prominent. From the experimental study it is noticeable that L-Leucine acts properly as a nucleophile at pH 7. When the pH is below 7 that is acidic media, the nucleophilic activity of L-Leucine reduces due to the protonation of amine. Whereas at basic condition, other nucleophiles such as -OH produce in solution, therefore, the activity

of amines decreases and the oxidation of 1,2-dihydroxybenzene followed by an irreversible chemical reaction with hydroxyl ion [83]. Therefore, from the above discussion it is clear that the nucleophilic substitution reaction of 1,2-dihydroxybenzene in presence of L-Leucine is maximum favorable up to 100 mM at pH 7 which is consistent with both CV and DPV. All above observations could be attributed to the reaction between L-Leucine and *o*-benzoquinone species produced at the surface of electrode, with the new anodic peak being attributed to the oxidation of newly formed *o*-benzoquinone-Leucine adduct.

4.2.11 Spectral analysis of 1,2-dihydroxybenzene with L-Leucine

The FTIR spectrum of the vibrational modes of the 1,2-dihydroxybenzene-Leucine adduct, 1,2-dihydroxybenzene and L-Leucine has been shown in Figure 4.136. The 1,2-dihydroxybenzene reveals the O-H stretching band at 3450 cm^{-1} whereas L-Leucine shows a broad spectrum ranging from 3600-2600 cm^{-1} due to overlap of O-H and N-H stretching band. Peak at 1647 cm^{-1} indicates C=O stretching of –COOH group in L-Leucine. But in case of FTIR spectrum of 1,2-dihydroxybenzene-Leucine adduct, there is a significant change in finger print region (1400-667 cm^{-1}). This indicates formation of new 1,2-dihydroxybenzene-amino acid adduct.

Table 4.1: Peak potential (E_p), corresponding peak potential difference (ΔE), peak separation ($\Delta E_{1/2}$), peak current (I_p), corresponding peak current ratio (I_{pa}/I_{pc}) of 2 mM 1,2-dihydroxybenzene in aqueous buffer solution (pH 7) of GC electrode at different scan rate.

v/Vs^{-1}	E_{pa1} /V	E_{pc1} /V	$\Delta E = E_{pc1} \sim E_{pa1}$	I_{pa1} /μA	I_{pc1} /μA	I_{pa1}/ I_{pc1}
0.05	0.37	0.04	0.33	5.23	-5.22	1.01
0.10	0.38	0.03	0.34	5.89	-5.75	1.03
0.15	0.38	0.04	0.34	3.78	-8.23	0.46
0.20	0.40	0.04	0.36	3.99	-7.46	0.53
0.25	0.42	0.03	0.39	5.27	-7.59	0.69
0.30	0.43	0.03	0.40	3.53	-7.64	0.46
0.35	0.50	0.01	0.49	3.64	-7.27	0.69
0.40	0.51	-0.03	0.54	3.52	-8.21	0.43
0.45	0.52	-0.04	0.56	4.61	-9.99	0.46

Table 4.2: Peak current (I_p), corresponding peak current ratio (I_{pa}/I_{pc}) of 2 mM 1,2-dihydroxybenzene with 50 mM L-Alanine in buffer solution (pH 7) of GC electrode at different scan rate (2nd cycle).

v/Vs^{-1}	I_{pa0} /μA	I_{pa1} /μA	I_{pc0}/μA	I_{pc1}/μA	I_{pa0}/I_{pa1}	I_{pa1}/I_{pc1}
0.05	2.21	20.3	-6.62	-2.46	0.060463	-7.003
0.10	2.65	32.12	-7.41	-13.75	0.152973	-7.52033
0.15	3.09	46.93	-8.2	-25.05	0.092154	-2.336
0.20	3.45	54.34	-8.91	-30.35	0.065843	-1.87345
0.25	3.81	61.75	-9.62	-35.65	0.063489	-1.79044
0.30	4.05	66.96	-8.62	-41.71	0.0617	-1.73212
0.35	4.29	72.17	-7.63	-47.78	0.060484	-1.60537
0.40	4.66	76.9	-7.15	-54.665	0.059443	-1.51046
0.45	5.03	81.63	-6.68	-61.55	0.060598	-1.40675
0.50	2.21	20.3	-6.62	-2.46	0.06162	-1.32624

Table 4.3: Peak current (I_p), corresponding peak current ratio (I_{pa}/I_{pc}) of 2 mM 1,2-dihydroxybenzene with 50 mM L-Alanine in buffer solution (pH 7) of Pt electrode at different scan rate (2nd cycle).

v/Vs^{-1}	I_{pa0} /μA	I_{pa1} /μA	I_{pc0}/μA	I_{pc1}/μA	I_{pa0}/I_{pa1}	I_{pa1}/I_{pc1}
0.05	1.36	9.19	-2.21	-5.15	0.147987	1.784466
0.10	2.1	13.36	-2.88	-10.38	0.157186	1.287091
0.15	2.35	15.47	-2.63	-13.04	0.151907	1.18635
0.20	1.69	18.15	-2.86	-16.17	0.093113	1.122449
0.25	1.78	19.68	-2.72	-19.75	0.090447	0.996456
0.30	2.13	20.98	-2.61	-24.21	0.101525	0.866584
0.35	1.67	22.65	-2.14	-27.78	0.073731	0.815335
0.40	1.1	25.49	-1.83	-30.43	0.043154	0.83766
0.45	1.07	26.99	-1.69	-30.77	0.039644	0.877153
0.50	1.01	28.21	-1.5	-31.14	0.035803	0.905909

Table 4.4: Peak current (I_p), corresponding peak current ratio (I_{pa}/I_{pc}) of 2 mM 1,2-dihydroxybenzene with 50 mM L-Alanine in buffer solution (pH 7) of Au electrode at different scan rate (2nd cycle).

ν/Vs^{-1}	I_{pa0} /μA	I_{pa1} /μA	I_{pc0}/μA	I_{pc1}/μA	I_{pa0}/I_{pa1}	I_{pa1}/I_{pc1}
0.05	2.03	13.21	-4.29	-6.99	0.253671	1.889843
0.10	2.73	19.8	-5.43	-7.82	0.177879	2.531969
0.15	3.79	23.07	-4.67	-13.68	0.14	1.686404
0.20	3.87	28.02	-4.39	-19.65	0.138116	1.425954
0.25	3.9	27.98	-4.12	-22.28	0.1323	1.255835
0.30	3.93	32.94	-4.01	-25.05	0.119308	1.31497
0.35	3.44	34.56	-3.94	-29.74	0.099537	1.162071
0.40	3.34	37.07	-3.81	-34.58	0.0901	1.072007
0.45	3.17	38.09	-3.54	-35.33	0.083224	1.078121
0.50	3.05	39.61	-3.29	-36.56	0.077001	1.083425

Table 4.5: Peak Current I_p (μA), peak potential E_p (V) of 2 mM 1,2-dihydroxybenzene with 50 mM L-Alanine of GC electrode at scan rate 0.1V/s in different pH media (2nd cycle).

pH	Peak Current I_p (μA)	Peak potential E_p (V)
	Oxidation, A_0	Oxidation, A_1
5	0	0.43
7	3.45	0.4
9	2.67	0.22
11	0	0.02

Table 4.6: Peak Current I_p (μA), peak potential E_p (V) of 2 mM 1,2-dihydroxybenzene with 50 mM L-Alanine of Pt electrode at scan rate 0.1V/s in different pH media (2nd cycle).

pH	Peak Current I_p (μA)	Peak potential E_p (V)
	Oxidation, A_0	Oxidation, A_0
5	0	0.48
7	3.26	0.34
9	1.23	0.24
11	0.23	0.05

Table 4.7: Peak Current I_p (µA), peak potential E_p (V) of 2 mM 1,2-dihydroxybenzene with 50 mM L-Alanine of Au electrode at scan rate 0.1V/s in different pH media (2nd cycle).

pH	Peak Current I_p (µA)	Peak potential E_p (V)
	Oxidation, A_0	Oxidation, A_0
5	0	0.3
7	2.94	0.19
9	0.86	0.09
11	0.05	0.01

Table 4.8: Peak Current I_p (µA) of 2 mM 1,2-dihydroxybenzene with various concentration of L-Alanine of GC electrode at scan rate 0.1V/s in pH 7 (2nd cycle).

Concentration	Peak Current I_p (µA)
	Oxidation, A_0
10	1.01
30	2.88
50	3.45
70	3.01
100	2.23

Table 4.9: Peak Current I_p (µA) of 2 mM 1,2-dihydroxybenzene with various concentration of L-Alanine of Pt electrode at scan rate 0.1V/s in pH 7 (2nd cycle).

Concentration	Peak Current I_p (µA)
	Oxidation, A_0
10	0.27
30	1.1
50	2.11
70	1.77
100	1.82

Table 4.10: Peak Current I_p (µA) of 2 mM 1,2-dihydroxybenzene with various concentration of L-Alanine of Au electrode at scan rate 0.1V/s in pH 7 (2nd cycle).

Concentration	Peak Current I_p (µA)
	Oxidation, A_0
10	0.1
30	2.08
50	3.2
100	2.59
150	1.72

Table 4.11: Peak current (I_p), corresponding peak current ratio (I_{pa}/I_{pc}) of 2 mM 1,2-dihydroxybenzene with 20 mM L-Phenylalanine in buffer solution (pH 7) of GC electrode at different scan rate (2nd cycle).

ν/Vs^{-1}	I_{pa0} /μA	I_{pa1} /μA	I_{pc0}/μA	I_{pc1}/μA	I_{pa0}/I_{pa1}	I_{pa1}/I_{pc1}
0.05	3.28	19.7	-7.12	-6.19	0.166497	3.182553
0.10	5.13	27.78	-10.23	-10.24	0.184665	2.712891
0.15	6.736842	37.83158	-11.0144	-14.8278	0.178075	2.551404
0.20	7.67	44.1	-12.79	-20.75	0.173923	2.125301
0.25	8.93	47.63592	-14.3158	-27.9375	0.187464	1.705089
0.30	10.19	54.03	-14.41	-32.89	0.188599	1.642749
0.35	10.555	58.6599	-15.731	-37.0785	0.179936	1.582045
0.40	10.92	61.53	-16.58	-37.93	0.177474	1.622199
0.45	11.20707	64.02	-17.13	-41.3713	0.175056	1.54745
0.50	11.27	66.51	-17.68	-45.64	0.169448	1.457274

Table 4.12: Peak current (I_p), corresponding peak current ratio (I_{pa}/I_{pc}) of 2 mM 1,2-dihydroxybenzene with 20 mM L-Phenylalanine in buffer solution (pH 7) of Pt electrode at different scan rate (2nd cycle).

ν/Vs^{-1}	I_{pa0} /μA	I_{pa1} /μA	I_{pc0}/μA	I_{pc1}/μA	I_{pa0}/I_{pa1}	I_{pa1}/I_{pc1}
0.05	1.8038	6.94	-2.26	-3.23	0.259914	2.148607
0.10	1.977	8.53	-2.68	-6.18	0.23177	1.380259
0.15	2.984	10.49	-2.75	-8.41	0.284461	1.247325
0.20	2.014	12.63	-2.88	-8.65	0.159462	1.460116
0.25	2.098	14.825	-2.935	-11.67	0.141518	1.270351
0.30	2.174	17.02	-2.96	-14.89	0.127732	1.143049
0.35	2.172	17.59	-3.08	-17.52	0.123479	1.003995
0.40	2.182	18.17	-3.23	-19.52	0.120088	0.93084
0.45	2.229	18.53	-3.35	-20.89	0.120291	0.887027
0.50	2.28	19.09	-3.46	-22.25	0.119434	0.857978

Table 4.13: Peak current (I_p), corresponding peak current ratio (I_{pa}/I_{pc}) of 2 mM 1,2-dihydroxybenzene with 20 mM L-Phenylalanine in buffer solution (pH 7) of Au electrode at different scan rate (2nd cycle).

ν/Vs^{-1}	I_{pa0} /μA	I_{pa1} /μA	I_{pc0}/μA	I_{pc1}/μA	I_{pa0}/I_{pa1}	I_{pa1}/I_{pc1}
0.05	2.1489	8.53	-3.32	-4.82	0.251923	1.76971
0.10	3.53	10.53	-3.36	-6.1	0.335233	1.72623
0.15	3.66	12.25	3.55	-8.12	0.298776	1.508621
0.20	3.78	14.73	-3.78	-9.8	0.256619	1.503061
0.25	4.03	16.9	-3.98	-9.97	0.238462	1.695085
0.30	4.59	18.64	-4.12	-10.29	0.246245	1.811467
0.35	4.72	19.16	-3.54	-13.49	0.246347	1.420311
0.40	4.89	20.05	-4.76	-15.05	0.24389	1.332226
0.45	5	20.92	-4.87	-16.44	0.239006	1.272506
0.50	0.39	35.67	-1.29	-27.59	0.24313	1.216431

Table 4.14: Peak Current I_p (µA), peak potential E_p (V) of 2 mM 1,2-dihydroxybenzene with 20 mM L-Phenylalanine of GC electrode at scan rate 0.1V/s in different pH media (2^{nd} cycle).

pH	Peak Current I_p (µA)	Peak potential E_p (V)	
	Oxidation, A_0	Oxidation, A_0	Oxidation, A_1
5	1.77	0.1	0.43
7	7.65	0.04	0.35
9	5.96	-0.1	0.22
11	1.09	-0.23	0.08

Table 4.15: Peak Current I_p (µA), peak potential E_p (V) of 2mM 1,2-dihydroxybenzene with 20 mM L-Phenylalanine of Pt electrode at scan rate 0.1V/s in different pH media (2^{nd} cycle).

pH	Peak Current I_p (µA)	Peak potential E_p (V)
	Oxidation, A_0	Oxidation, A_0
5	0	0.44
7	2.18	0.3
9	1.47	0.09
11	0.23	0.05

Table 4.16: Peak Current I_p (µA), peak potential E_p (V) of 2 mM 1,2-dihydroxybenzene with 20 mM L-Phenylalanine of Au electrode at scan rate 0.1V/s in different pH media (2^{nd} cycle).

pH	Peak Current I_p (µA)	Peak potential E_p (V)
	Oxidation, A_0	Oxidation, A_0
5	0	0.34
7	2.18	0.2
9	0.98	0.08
11	0.45	0.01

Table 4.17: Peak Current I_p (µA) of 2 mM 1,2-dihydroxybenzene with various concentration of L-Phenylalanine of GC electrode at scan rate 0.1V/s in pH 7 (2^{nd} cycle).

Concentration	Peak Current I_p (µA)
	Oxidation, A_0
2	2.34
10	6.23
20	7.28
50	5.29
100	4.45

Table 4.18: Peak Current I_p (μA) of 2 mM 1,2-dihydroxybenzene with various concentration of L-Phenylalanine of Pt electrode at scan rate 0.1V/s in pH 7 (2^{nd} cycle).

Concentration	Peak Current I_p (μA)
	Oxidation, A_0
2	0.17
10	1.43
20	1.85
50	1.25
100	1.1

Table 4.19: Peak Current I_p (μA) of 2 mM 1,2-dihydroxybenzene with various concentration of L-Phenylalanine of Au electrode at scan rate 0.1V/s in pH 7 (2^{nd} cycle).

Concentration	Peak Current I_p (μA)
	Oxidation, A_0
2	1.01
10	2.2
20	2.31
50	1.57
100	1.49

Table 4.20: Peak current (I_p), corresponding peak current ratio (I_{pa}/I_{pc}) of 2 mM 1,2-dihydroxybenzene with 100 mM L-Leucine in buffer solution (pH 7) of GC electrode at different scan rate (2^{nd} cycle).

v/Vs^{-1}	I_{pa0} /μA	I_{pa1} /μA	I_{pc0}/μA	I_{pc1}/μA	I_{pa0}/I_{pa1}	I_{pa1}/I_{pc1}
0.05	2.45	19.93	-6.63	-1.67	0.12293	11.93413
0.10	3.99	24.26	-11.47	-3.36	0.164468	7.220238
0.15	5.74	27.12	-15.67	-7.13	0.211652	3.803647
0.20	7.5	30.78	-19.14	-13.14	0.243665	2.342466
0.25	8.29	36.89	-19.55	-17.87	0.224722	2.064354
0.30	9.08	41.23	-19.89	-22.56	0.220228	1.827571
0.35	10.95	48.68	-21.47	-25.54	0.224938	1.90603
0.40	12.81	53.55	-23.07	-30.61	0.239216	1.749428
0.45	12.9	59.55	-23.85	-34.98	0.216625	1.702401
0.50	13.42	63.07	-24.59	-38.45	0.212779	1.640312

Table 4.21: Peak current (I_p), corresponding peak current ratio (I_{pa}/I_{pc}) of 2 mM 1,2-dihydroxybenzene with 100 mM L-Leucine in buffer solution (pH 7) of Pt electrode at different scan rate (2nd cycle).

v/Vs^{-1}	I_{pa0} /μA	I_{pa1} /μA	I_{pc0}/μA	I_{pc1}/μA	I_{pa0}/I_{pa1}	I_{pa1}/I_{pc1}
0.05	1.14	4.19	-2.56	-2.78	0.272076	1.507194
0.10	2.35	5.99	-3.82	-4.87	0.392321	1.229979
0.15	2.7	6.56	-4.35	-7.84	0.411585	0.836735
0.20	3.06	7.83	-4.87	-9.66	0.390805	0.810559
0.25	2.89	8.98	-4.66	-11.34	0.321826	0.791887
0.30	2.78	10.3	-4.52	-12.76	0.269903	0.80721
0.35	2.57	11.34	-4.13	-12.83	0.226631	0.883866
0.40	2.45	12.23	-4.01	-13.23	0.200327	0.924414
0.45	2.21	13.45	-3.98	-13.45	0.164312	1
0.50	1.97	14.04	-3.89	-13.79	0.140313	1.018129

Table 4.22: Peak current (I_p), corresponding peak current ratio (I_{pa}/I_{pc}) of 2 mM 1,2-dihydroxybenzene with 100 mM L-Leucine in buffer solution (pH 7) of Au electrode at different scan rate (2nd cycle).

v/Vs^{-1}	I_{pa0} /μA	I_{pa1} /μA	I_{pc0}/μA	I_{pc1}/μA	I_{pa0}/I_{pa1}	I_{pa1}/I_{pc1}
0.05	2.91	7.74	-4.33	-4.25	0.375969	1.821176
0.10	3.2	9.81	-4.44	-7.5	0.326198	1.308
0.15	3.78	12.28	-4.52	-7.81	0.307818	1.572343
0.20	4.22	14.69	-4.67	-8.02	0.28727	1.831671
0.25	4.38	14.98	-5.03	-9.65	0.29239	1.552332
0.30	4.58	16.28	-5.68	-10.79	0.281327	1.508804
0.35	4.73	18.68	-5.89	-13.11	0.253212	1.424867
0.40	4.9	20.05	-6.79	-15.65	0.244389	1.28115
0.45	5.02	21.37	-6.84	-16.78	0.234909	1.27354
0.50	5.12	23.57	-6.98	-18.28	0.217225	1.289387

Table 4.23: Peak Current I_p (μA), peak potential E_p (V) of 2 mM 1,2-dihydroxybenzene with 100 mM L-Leucine of GC electrode at scan rate 0.1V/s in different pH media (2nd cycle).

pH	Peak Current I_p (μA)	Peak potential E_p (V)
	Oxidation, A_0	Oxidation, A_1
5	0	0.05
7	5.64	0.3
9	0	0.28
11	0	0.49

Table 4.24: Peak Current I_p (µA), peak potential E_p (V) of 2 mM 1,2-dihydroxybenzene with 100 mM L-Leucine of Pt electrode at scan rate 0.1V/s in different pH media (2nd cycle).

pH	Peak Current I_p (µA)	Peak potential E_p (V)
	Oxidation, A_0	Oxidation, A_0
5	0	0.46
7	2.89	0.3
9	2.32	0.21
11	2.21	0.15

Table 4.25: Peak Current I_p (µA), peak potential E_p (V) of 2 mM 1,2-dihydroxybenzene with 100 mM L-Leucine of Au electrode at scan rate 0.1V/s in different pH media (2nd cycle).

pH	Peak Current I_p (µA)	Peak potential E_p (V)
	Oxidation, A_0	Oxidation, A_0
5	0	0.38
7	3.2	0.2
9	2.77	0.13
11	2	0.03

Table 4.26: Peak Current I_p (µA) of 2 mM 1,2-dihydroxybenzene with various concentration of Leucine of GC electrode at scan rate 0.1V/s in pH 7 (2nd cycle).

Concentration	Peak Current I_p (µA)
	Oxidation, A_0
30	3.58
50	3.69
100	5.26
150	4.81
200	3.95

Table 4.27: Peak Current I_p (µA) of 2 mM 1,2-dihydroxybenzene with various concentration of L-Leucine of Pt electrode at scan rate 0.1V/s in pH 7 (2nd cycle).

Concentration	Peak Current I_p (µA)
	Oxidation, A_0
30	1.97
50	2.03
100	2.89
150	2.14
200	2.04

Table 4.28: Peak Current I_p (µA) of 2 mM 1,2-dihydroxybenzene with various concentration of L-Leucine of Au electrode at scan rate 0.1V/s in pH 7 (2^{nd} cycle).

Concentration	Peak Current I_p (µA)
	Oxidation, A_0
30	1.97
50	2.03
100	2.89
150	2.14
200	2.04

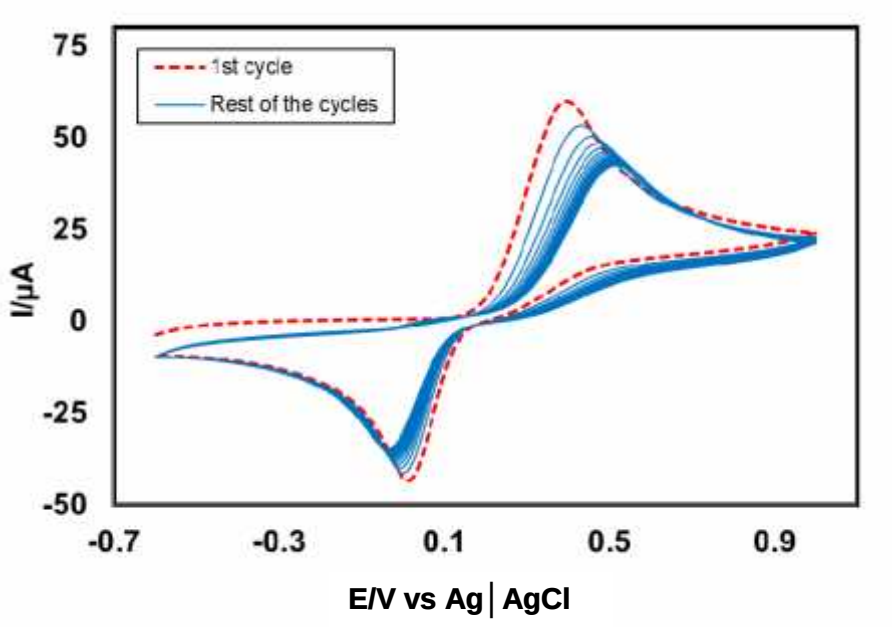

Fig. 4.1: Cyclic voltammogram (CV) of 15 cycles of 2 mM 1,2-dihydroxybenzene of GC electrode in buffer solution (pH 7) at scan rate 0.1 V/s.

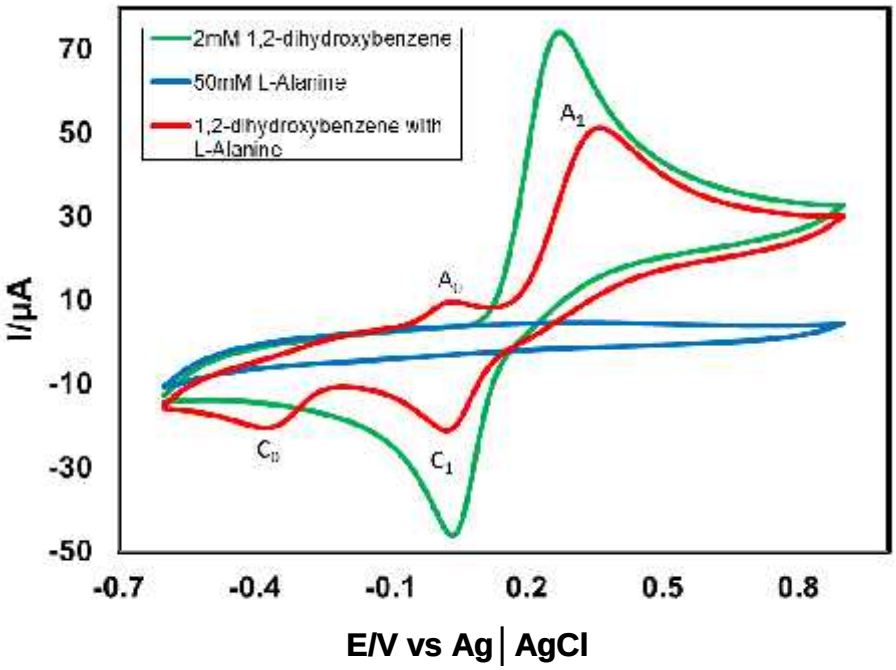

Fig. 4.2: Cyclic voltammogram of 2 mM 1,2-dihydroxybenzene (green line), 50 mM L-Alanine (blue line) and 2 mM 1,2-dihydroxybenzene with 50 mM L-Alanine (red line) of GC electrode in buffer solution (pH 7) at scan rate 0.1 V/s (2nd cycle). A_0 is appeared anodic peak and C_0 is corresponding cathodic peak.

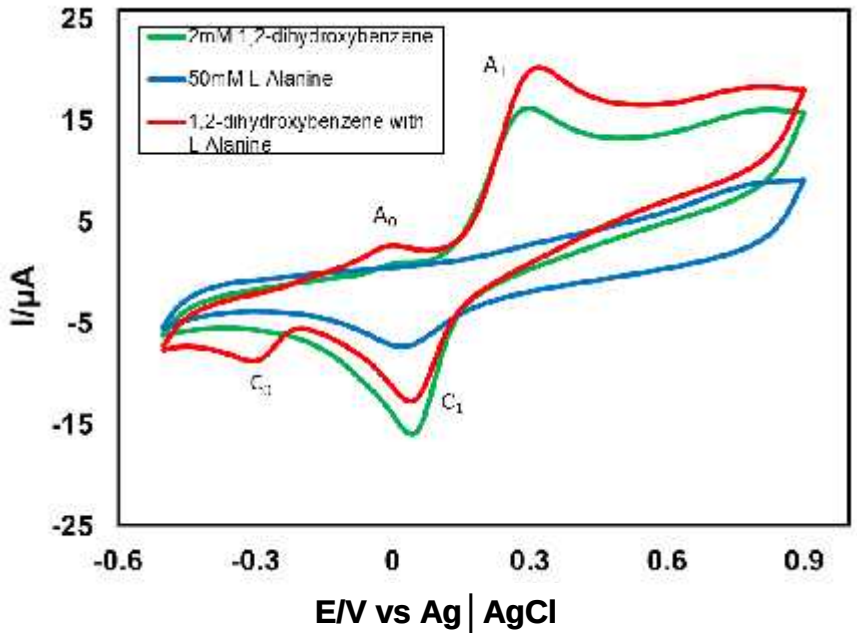

Fig. 4.3: Cyclic voltammogram of 2 mM 1,2-dihydroxybenzene (green line), 50 mM L-Alanine (blue line) and 2 mM 1,2-dihydroxybenzene with 50 mM L-Alanine (red line) of Pt electrode in buffer solution (pH 7) at scan rate 0.1 V/s (2nd cycle). A_0 is appeared anodic peak and C_0 is corresponding cathodic peak.

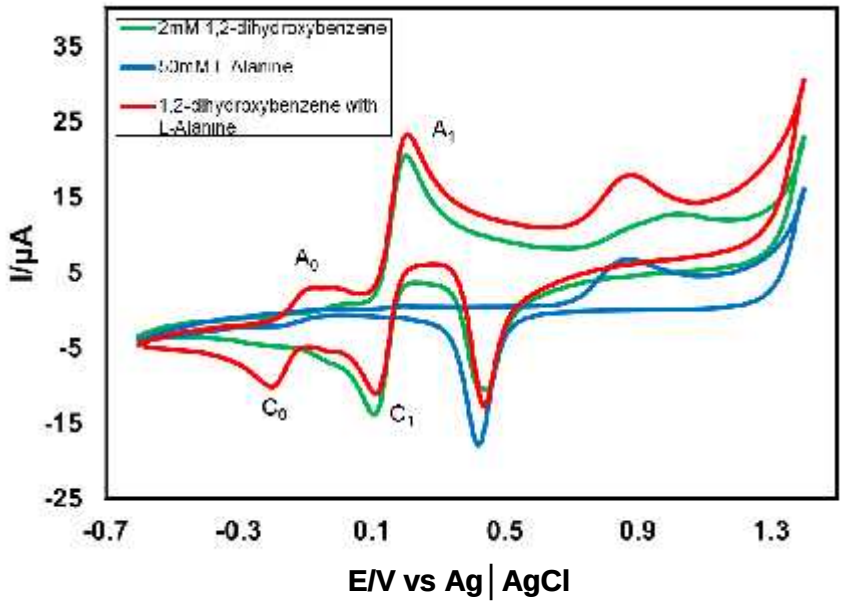

Fig. 4.4: Cyclic voltammogram of 2 mM 1,2-dihydroxybenzene (green line), 50 mM L-Alanine (blue line) and 2 mM 1,2-dihydroxybenzene with 50 mM L-Alanine (red line) of Au electrode in buffer solution (pH 7) at scan rate 0.1 V/s (2nd cycle). A_0 is appeared anodic peak and C_0 is corresponding cathodic peak.

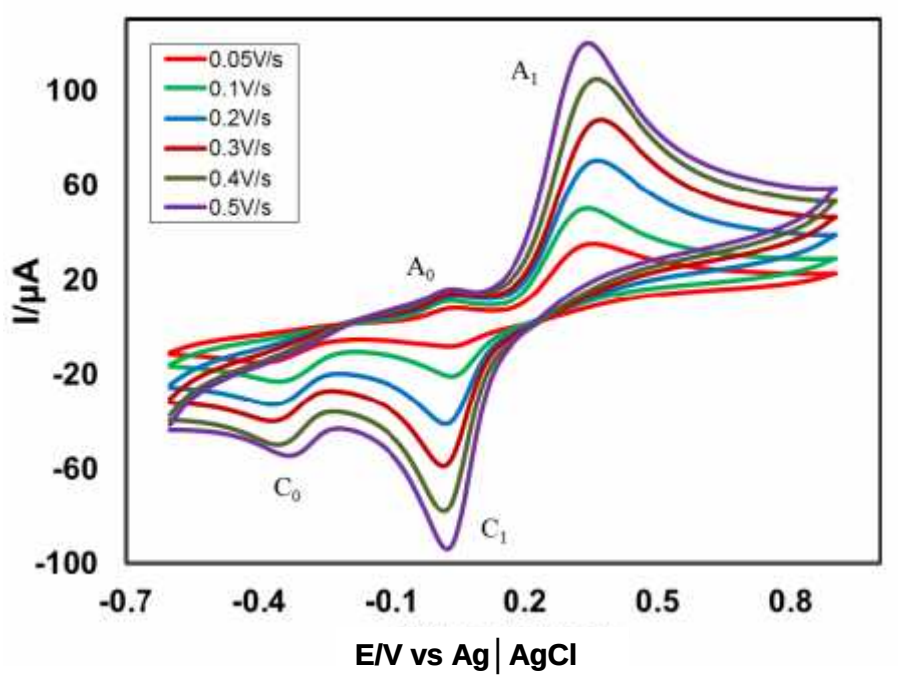

Fig. 4.5: Cyclic voltammogram of 2 mM 1,2-dihydroxybenzene with 50 mM L-Alanine in the second scan of potential at GC electrode in buffer solution (pH 7) at scan rate 0.05 V/s to 0.5 V/s.

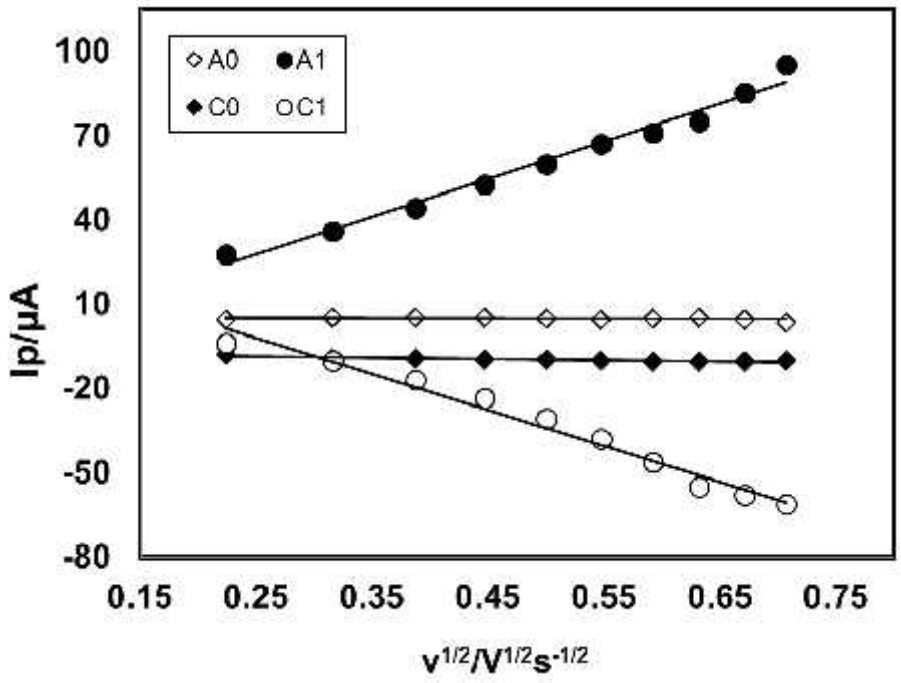

Fig. 4.6: Plots of peak current (I_p) versus square root of scan rate ($v^{1/2}$) of 2 mM 1,2-dihydroxybenzene with 50 mM L-Alanine of GC electrode in buffer solution (pH 7) (2^{nd} cycle).

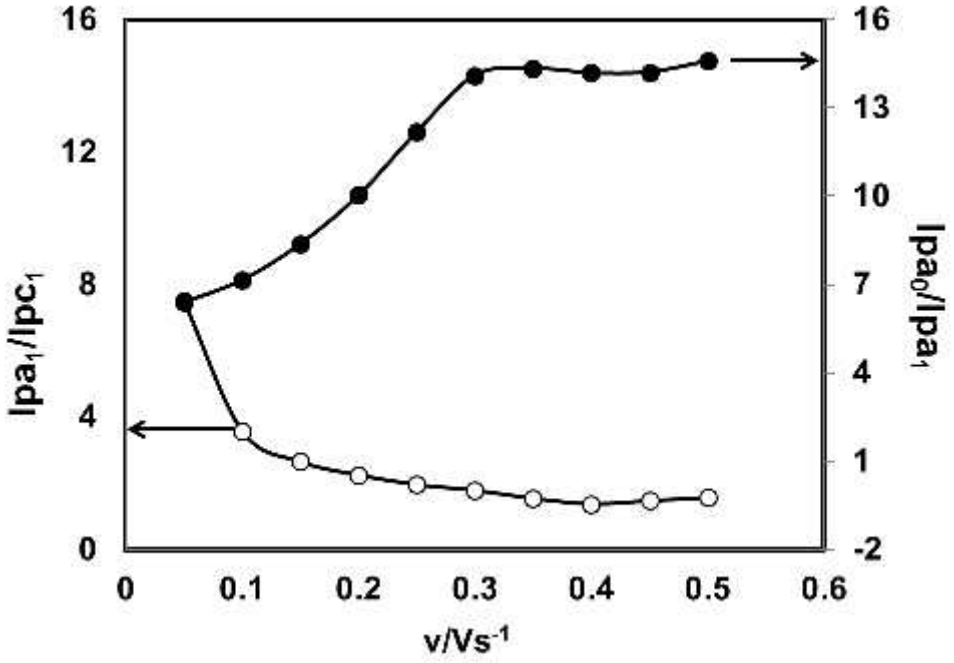

Fig. 4.7: Variation of peak current ratio of corresponding peak (I_{pa1}/I_{pc1}) and anodic peak (I_{pa0}/I_{pa1}) vs scan rate (v) of 2 mM 1,2-dihydroxybenzene with 50 mM L-Alanine of GC electrode in buffer solution (pH 7) at scan rate 0.1 V/s in the second scan of potential.

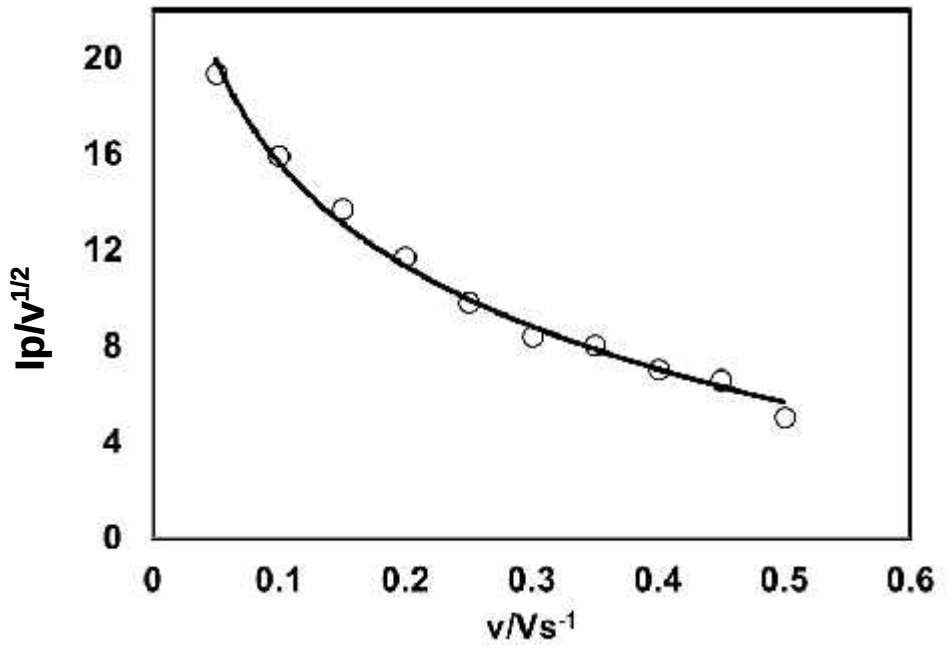

Fig. 4.8: Plot of current function ($I_p/v^{1/2}$) versus scan rate (v) of 2 mM 1,2-dihydroxybenzene with 50 mM L-Alanine of GC electrode in buffer solution (pH 7) of the Appeared anodic peak (A_0).

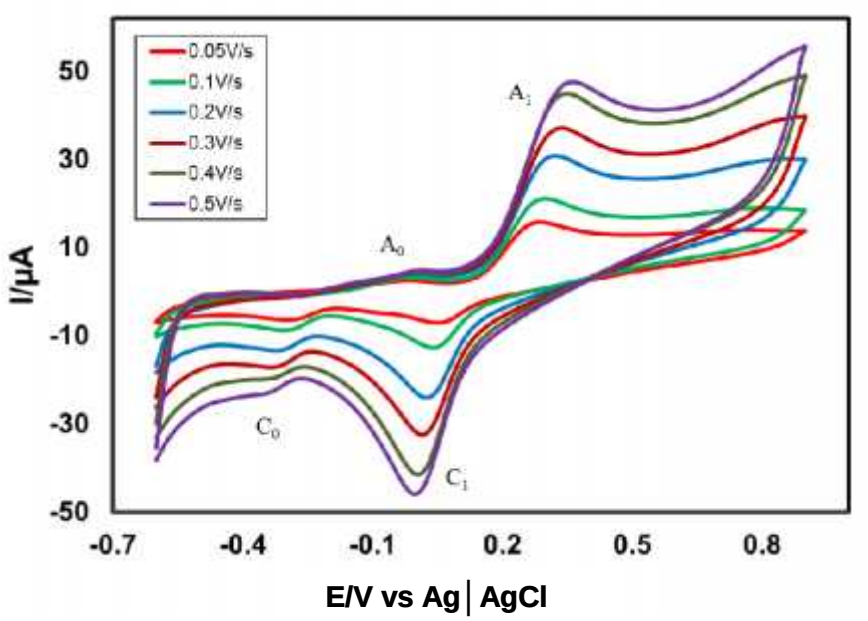

Fig. 4.9: Cyclic voltammogram of 2 mM 1,2-dihydroxybenzene with 50 mM L-Alanine in the second scan of potential at Pt electrode in buffer solution (pH 7) at scan rate 0.05 V/s to 0.5 V/s.

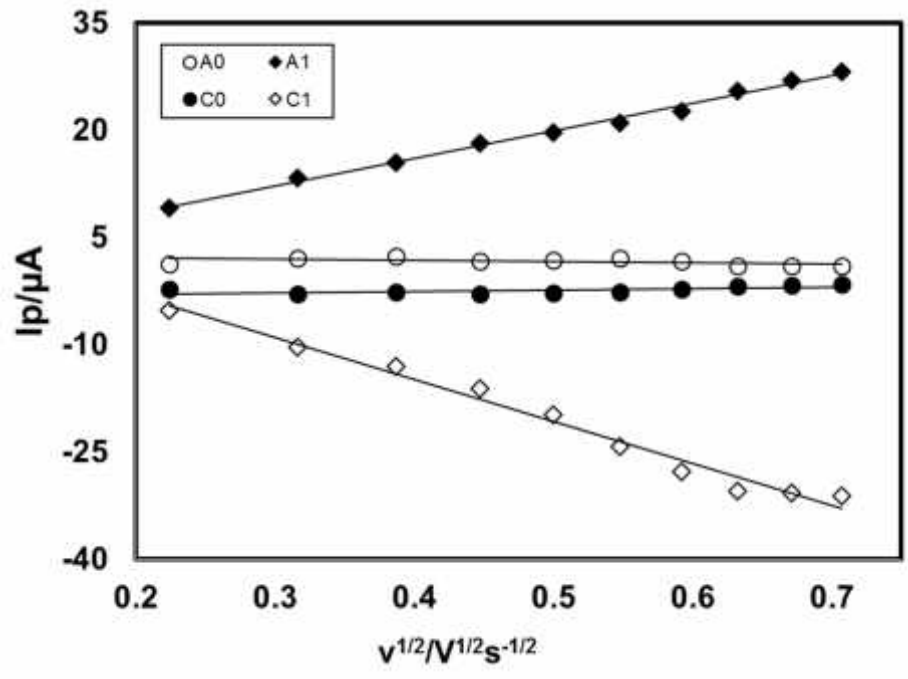

Fig. 4.10: Plots of peak current (I_p) versus square root of scan rate ($v^{1/2}$) of 2 mM 1,2-dihydroxybenzene with 50 mM L-Alanine of Pt electrode in buffer solution (pH 7) (2^{nd} cycle).

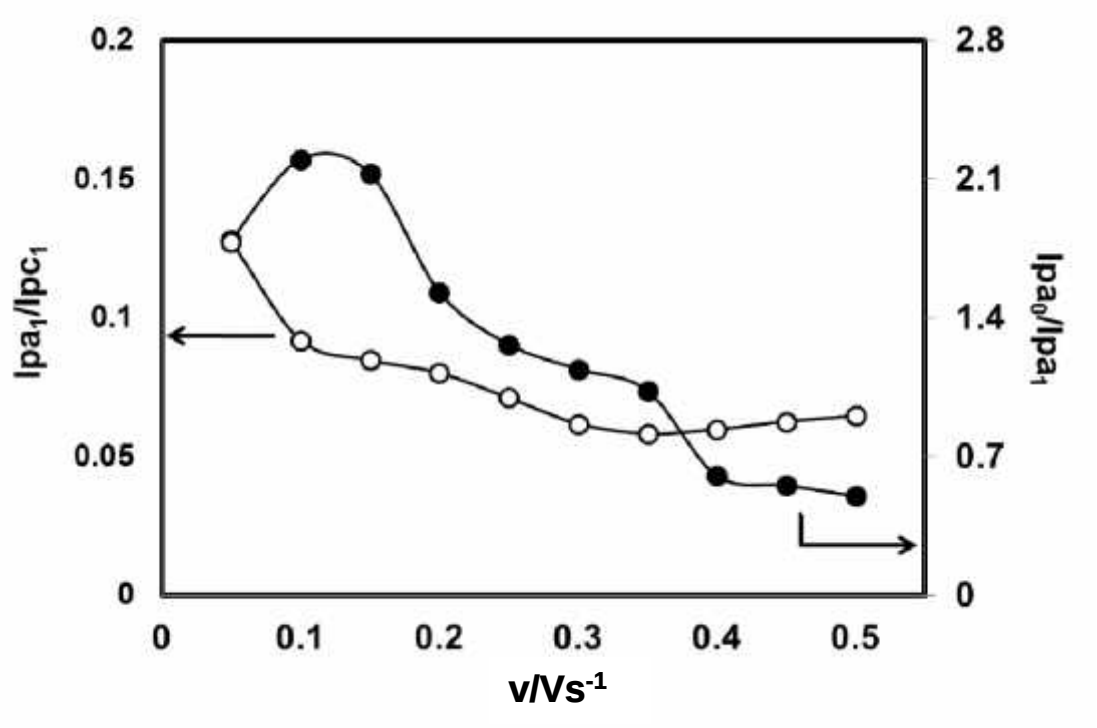

Fig. 4.11: Variation of peak current ratio of corresponding peak (I_{pa1}/I_{pc1}) and anodic peak (I_{pa0}/I_{pa1}) vs scan rate (v) of 2 mM 1,2-dihydroxybenzene with 50 mM L-Alanine of Pt electrode in buffer solution (pH 7) at scan rate 0.1 V/s in the second scan of potential.

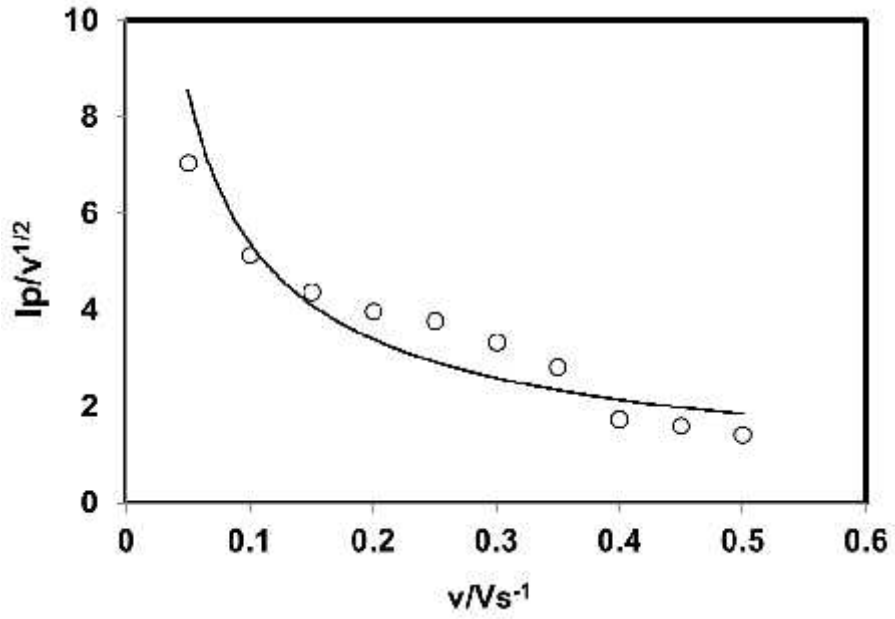

Fig. 4.12: Plots of current function ($I_p/v^{1/2}$) versus scan rate (v) of 2 mM 1,2-dihydroxybenzene with 50 mM L-Alanine of Pt electrode in buffer solution (pH 7) of the appeared anodic peak (A_0).

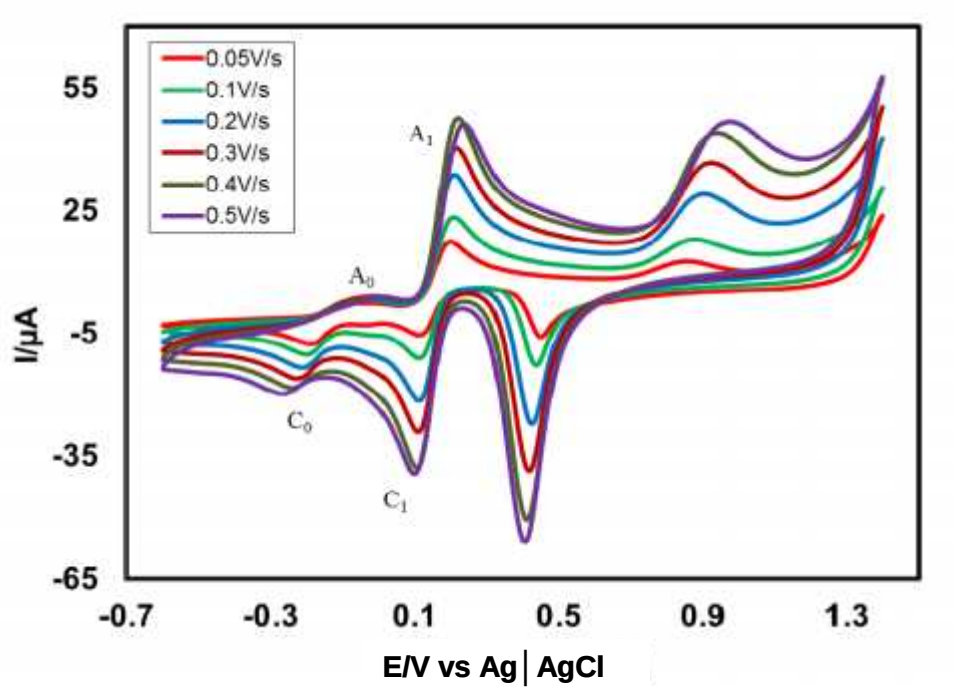

Fig. 4.13: Cyclic voltammogram of 2 mM 1,2-dihydroxybenzene with 50 mM L-Alanine in the second scan of potential at Au electrode in buffer solution (pH 7) at scan rate 0.05 V/s to 0.5 V/s.

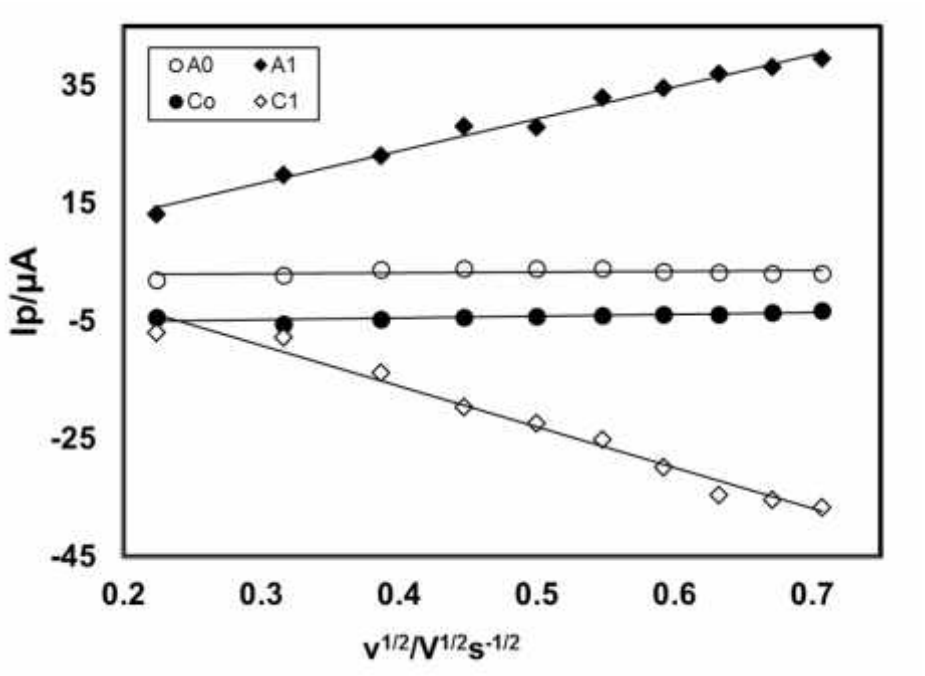

Fig. 4.14: Plots of peak current (I_p) versus square root of scan rate ($v^{1/2}$) of 2 mM 1,2-dihydroxybenzene with 50 mM L-Alanine of Au electrode in buffer solution (pH 7) (2^{nd} cycle).

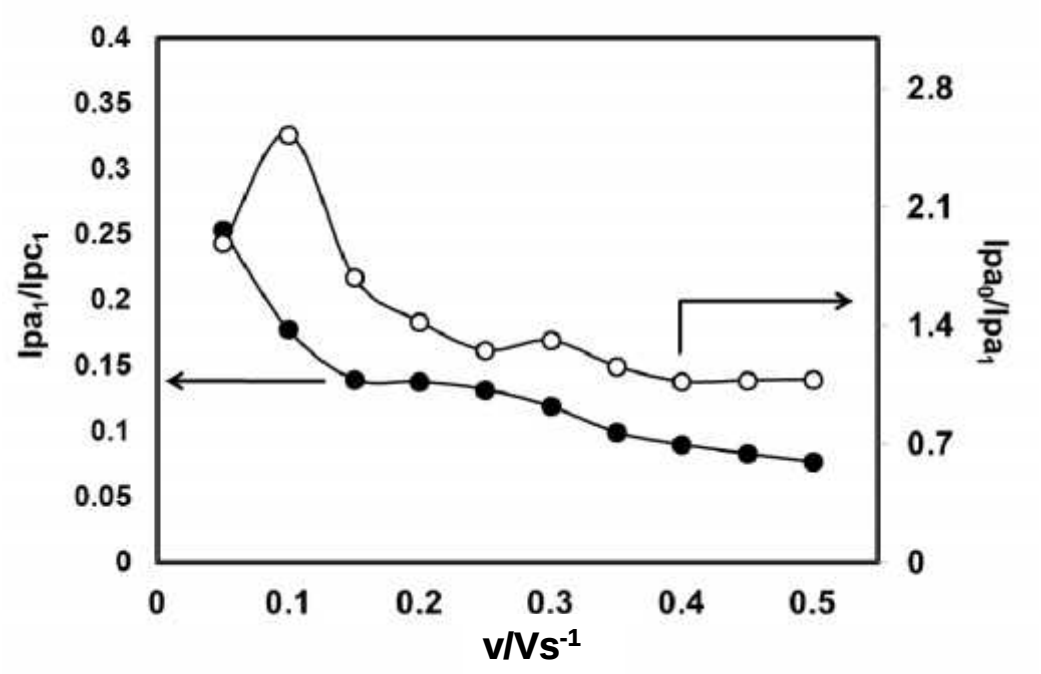

Fig. 4.15: Variation of peak current ratio of corresponding peak (I_{pa1}/I_{pc1}) and anodic peak (I_{pa0}/I_{pa1}) vs scan rate (v) of 2 mM 1,2-dihydroxybenzene with 50 mM L-Alanine of Au electrode in buffer solution (pH 7) at scan rate 0.1 V/s in the second scan of potential.

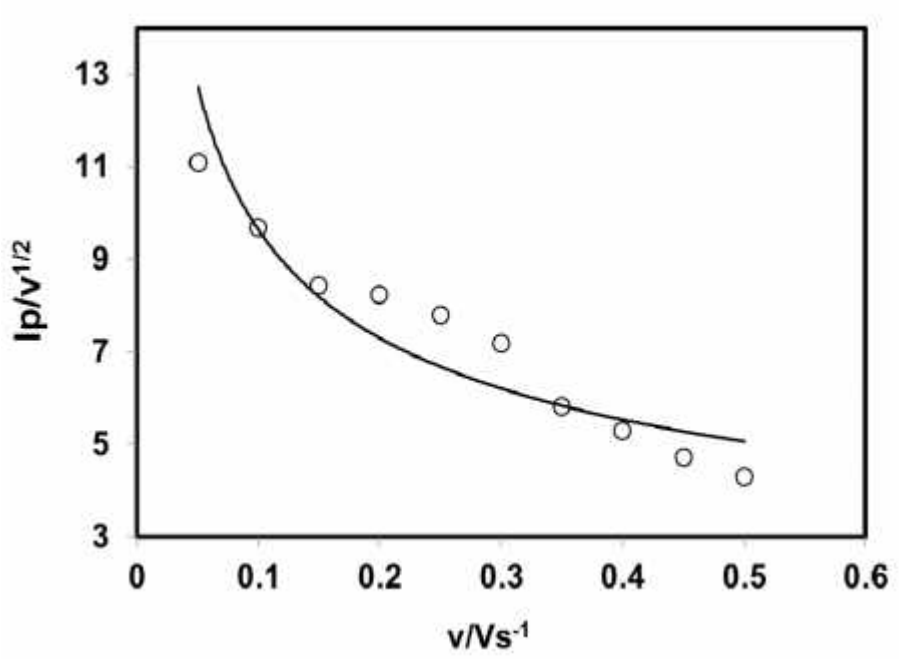

Fig. 4.16: Plots of current function ($I_p/v^{1/2}$) versus scan rate (v) of 2 mM 1,2-dihydroxybenzene with 50 mM L-Alanine of Au electrode in buffer solution (pH 7) of the Appeared anodic peak (A_0).

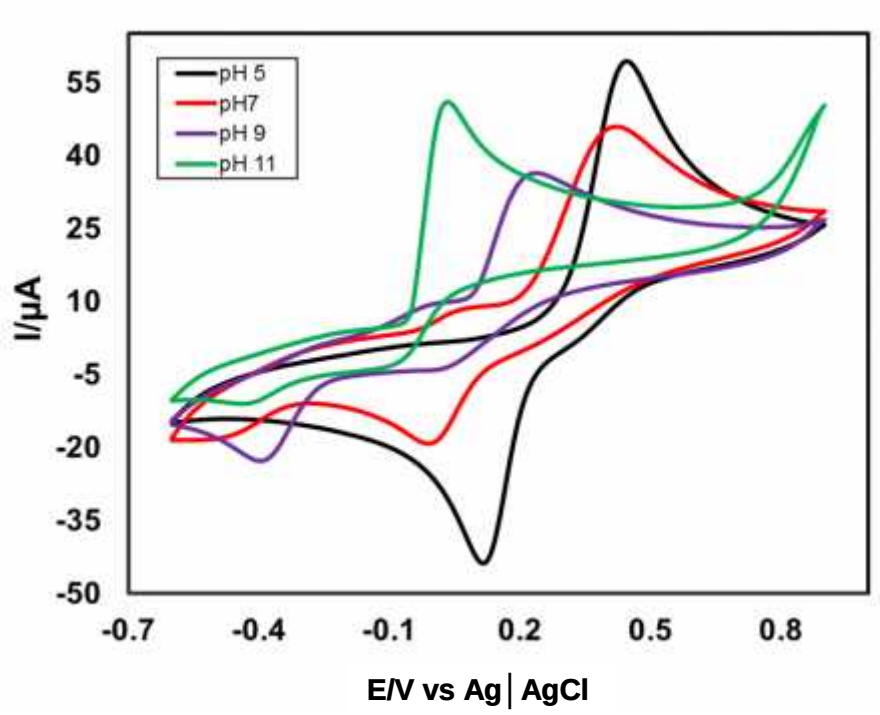

Fig. 4.17: Cyclic voltammogram of 2 mM 1,2-dihydroxybenzene with 50 mM L-Alanine of GC (3mm) electrode in different pH (5, 7, 9 and 11) at scan rate 0.1 V/s.

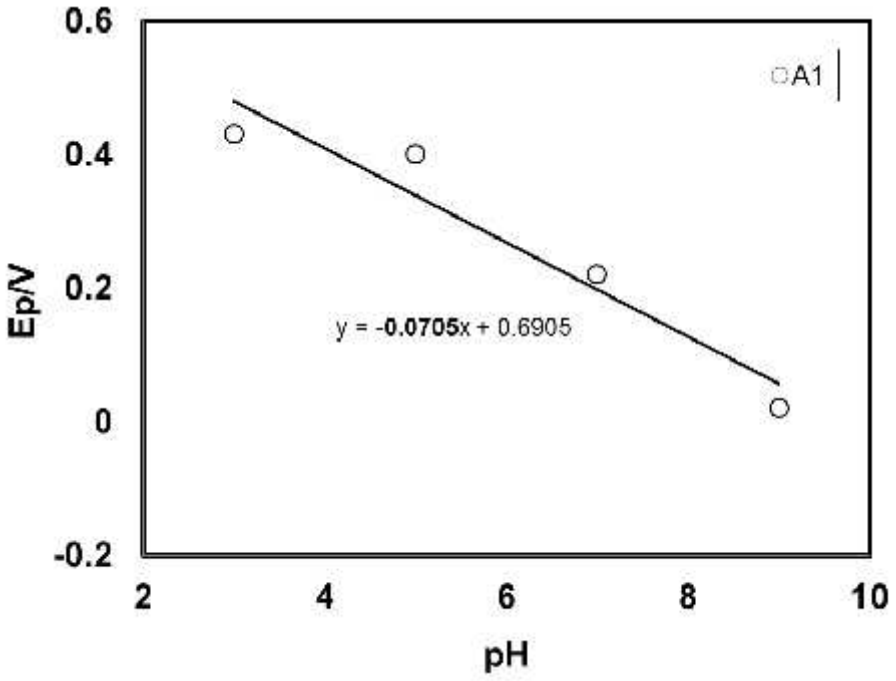

Fig. 4.18: Plots of peak potential (E_p) versus pH (5, 7, 9 and 11) of 2 mM 1,2-dihydroxybenzene with 50 mM L-Alanine of GC electrode at scan rate 0.1 V/s (2^{nd} cycle).

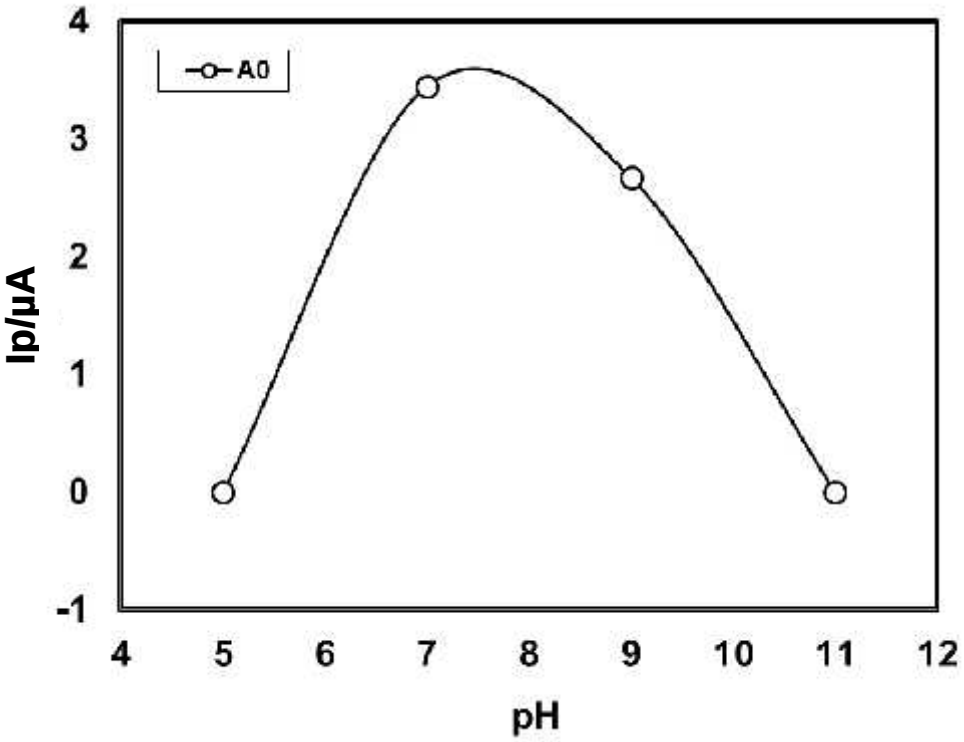

Fig. 4.19: Plot of peak current (I_p) versus pH (5, 7, 9 and 11) of 2 mM 1,2-dihydroxybenzene with 50 mM L-Alanine of GC electrode at scan rate 0.1 V/s (2^{nd} cycle).

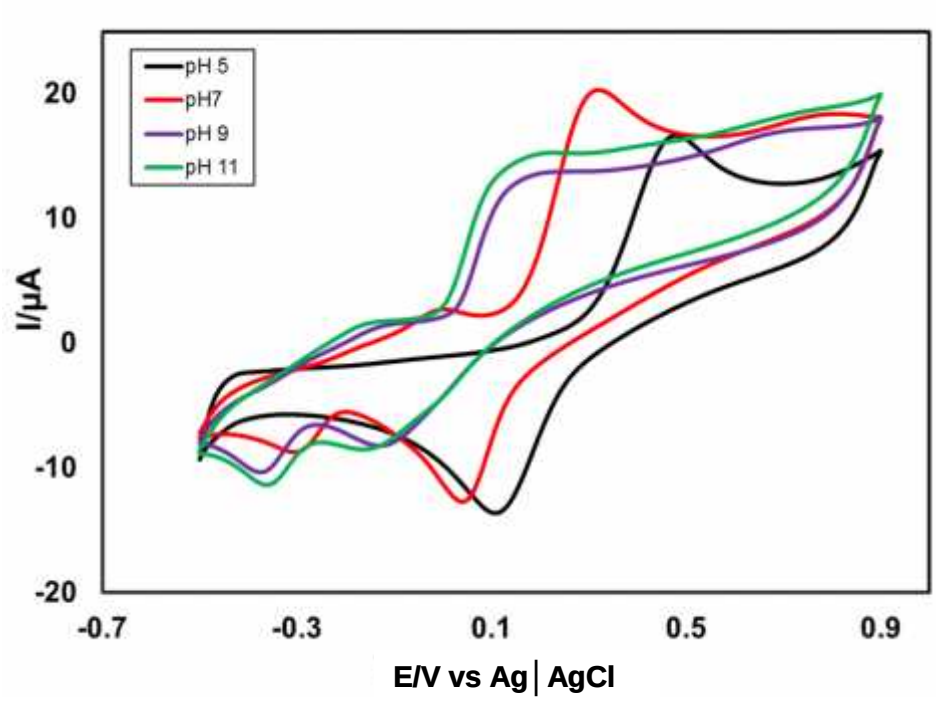

Fig. 4.20: Cyclic voltammogram of 2 mM 1,2-dihydroxybenzene with 50 mM L-Alanine of Pt electrode in different pH (5, 7, 9 and 11) at scan rate 0.1 V/s.

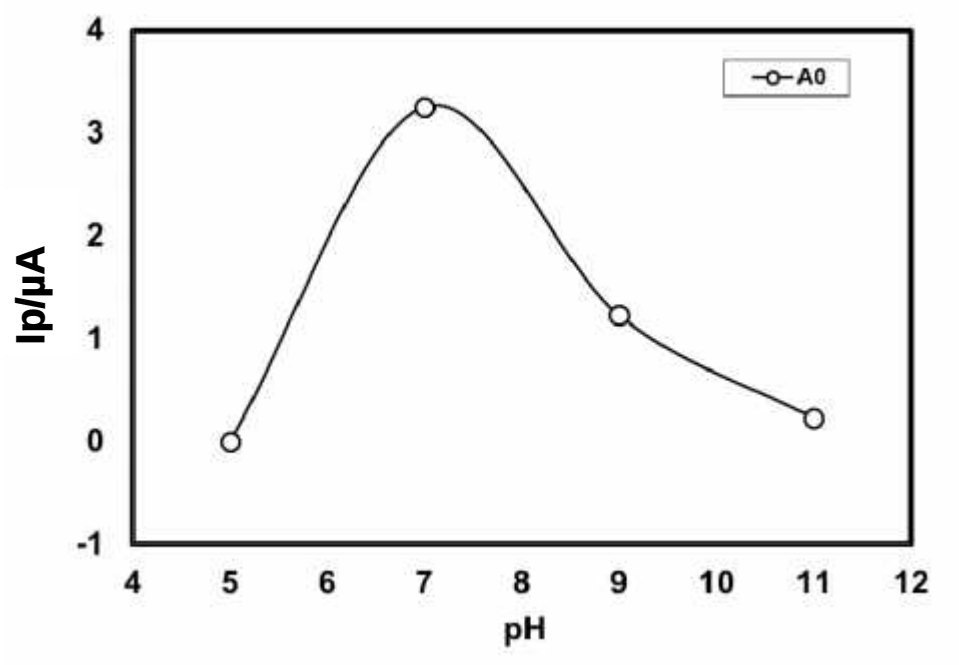

Fig. 4.21: Plots of peak current (I_p) versus pH (5, 7, 9 and 11) of 2 mM 1,2-dihydroxybenzene with 50 mM L-Alanine of Pt electrode at scan rate 0.1 V/s (2nd cycle).

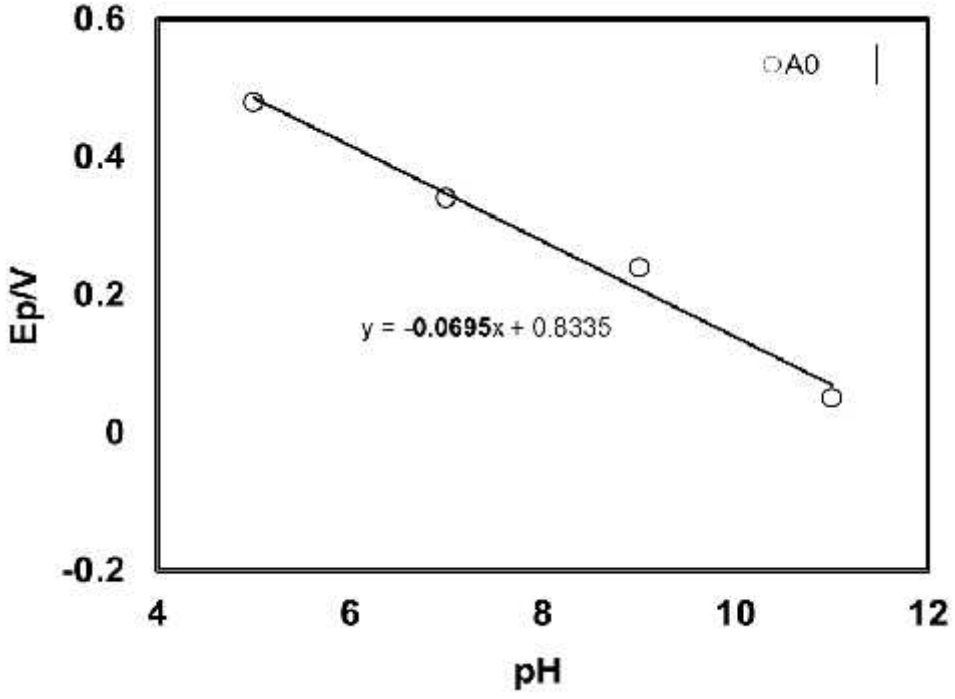

Fig. 4.22: Plot of peak potential (E_p) versus pH (5, 7, 9 and 11) of 2 mM 1,2-dihydroxybenzene with 50 mM L-Alanine of Pt electrode at scan rate 0.1 V/s (2nd cycle).

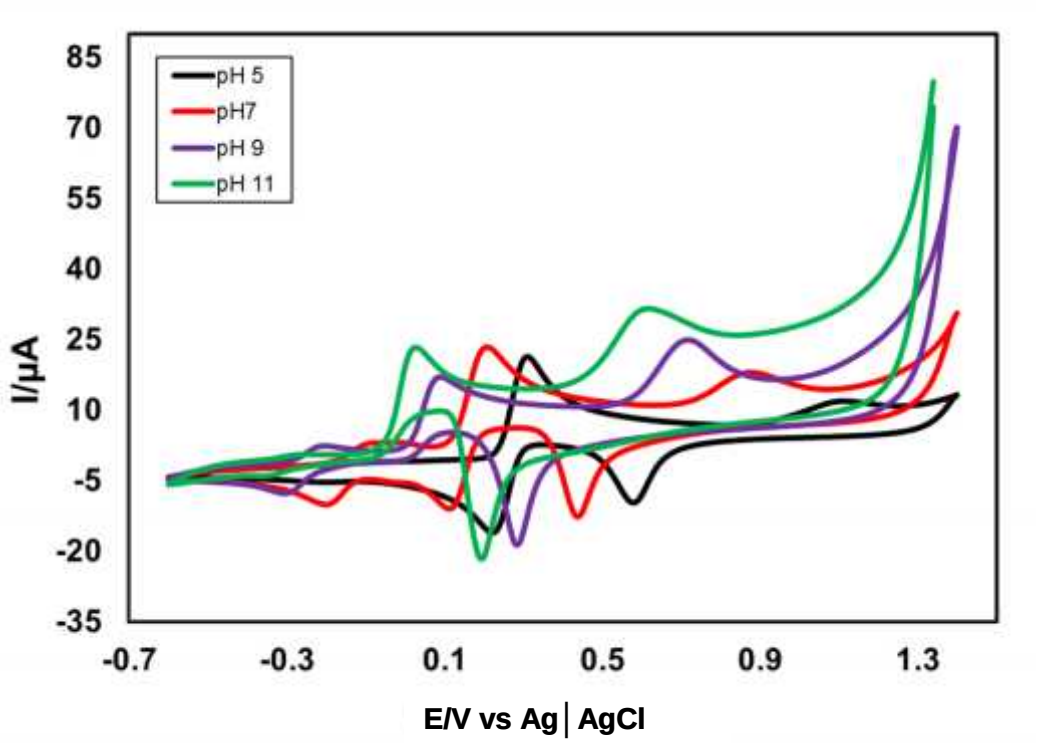

Fig. 4.23: Cyclic voltammogram of 2 mM 1,2-dihydroxybenzene with 50 mM L-Alanine of Au electrode in different pH (5, 7, 9 and 11) at scan rate 0.1 V/s.

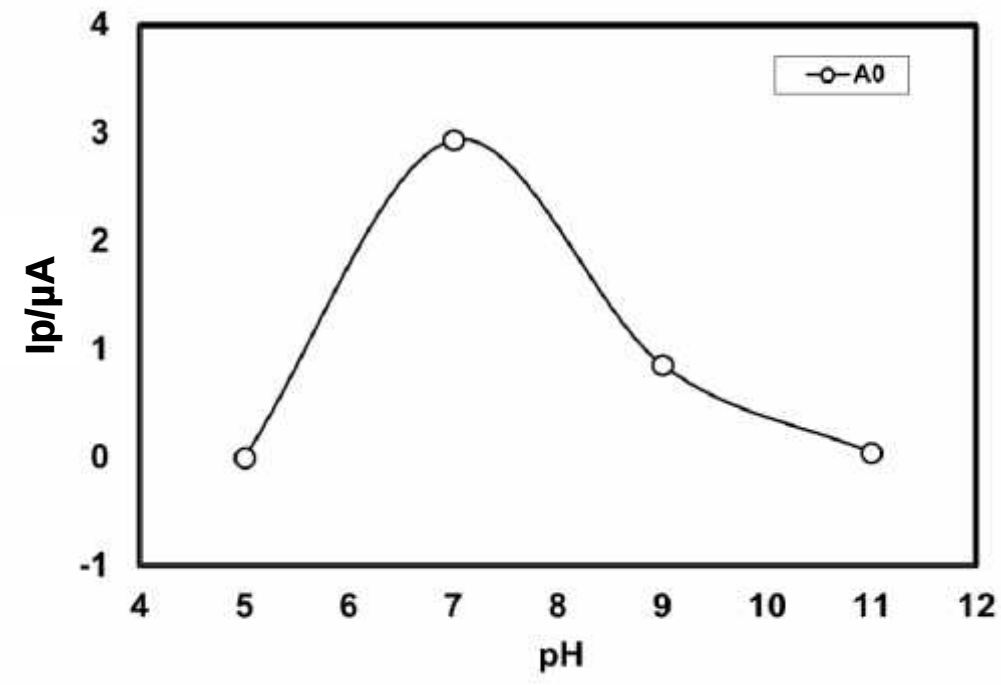

Fig. 4.24: Plots of peak current (I_p) versus pH (5, 7, 9 and 11) of 2 mM 1,2-dihydroxybenzene with 50 mM L-Alanine of Au electrode at scan rate 0.1 V/s (2^{nd} cycle).

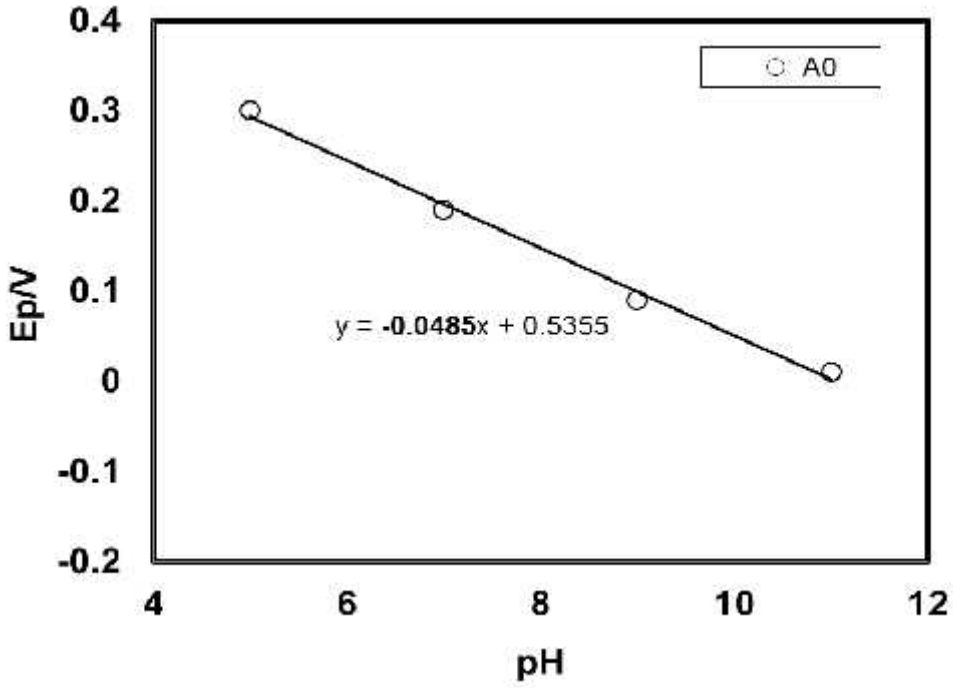

Fig. 4.25: Plot of peak potential (E_p) versus pH (5, 7, 9 and 11) of 2 mM 1,2-dihydroxybenzene with 50 mM L-Alanine of Au electrode at scan rate 0.1 V/s (2nd cycle).

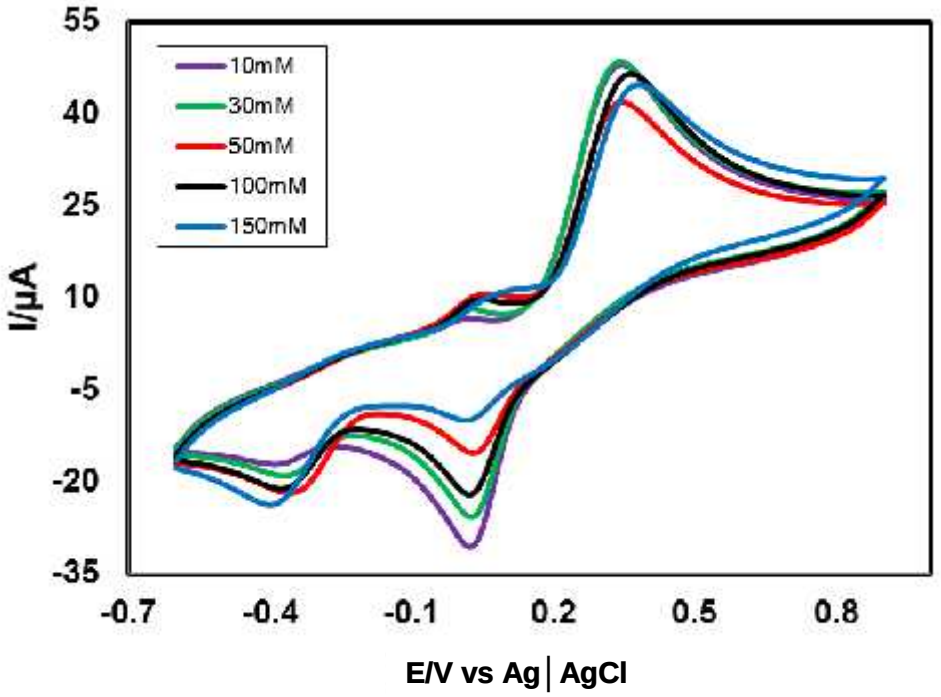

Fig. 4.26: CV of composition changes of L-Alanine (10, 30, 50, 100 and 150 mM) with fixed 2 mM 1,2-dihydroxybenzene of GC electrode at pH 7 and scan rate 0.1 V/s.

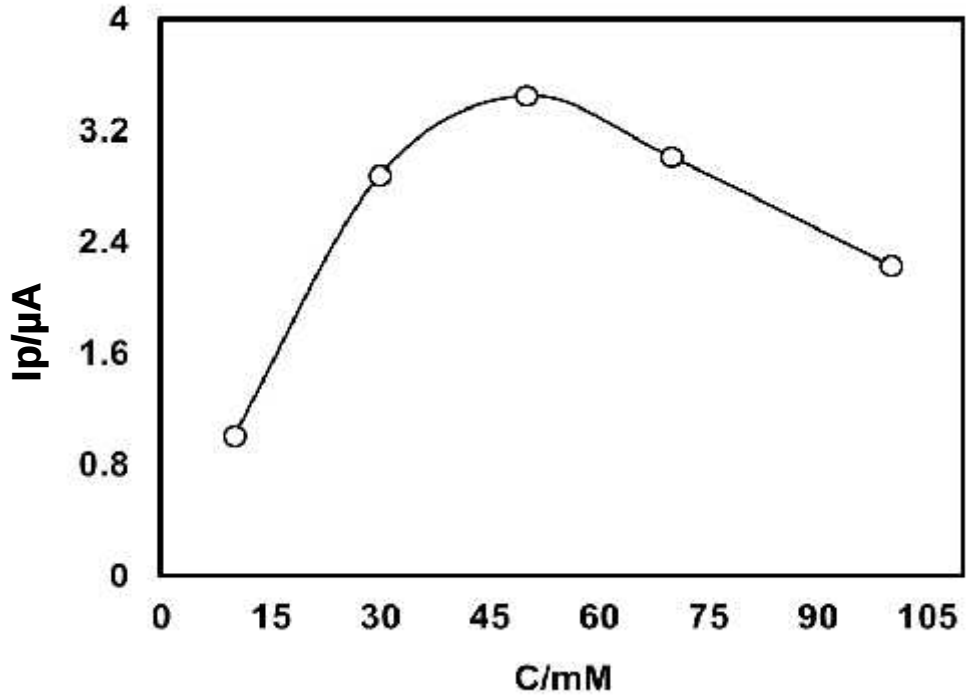

Fig. 4.27: Comparison of cyclic voltammogram of different concentration (10, 30, 50, 100, and 150 mM) of 50 mM L-Alanine with fixed 2 mM 1,2-dihydroxybenzene at GC electrode in buffer solution (pH 7) at scan rate 0.1 V/s (2nd cycle).

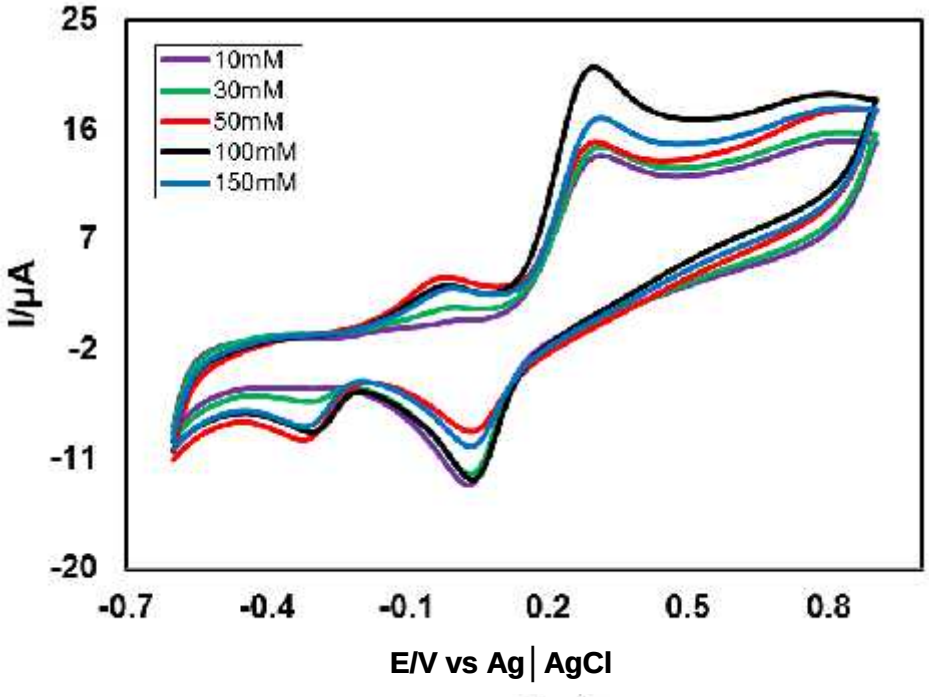

Fig. 4.28: CV of composition changes of L-Alanine (10, 30, 50, 100 and 150 mM) with fixed 2 mM 1,2-dihydroxybenzene of Pt electrode at pH 7 and scan rate 0.1 V/s.

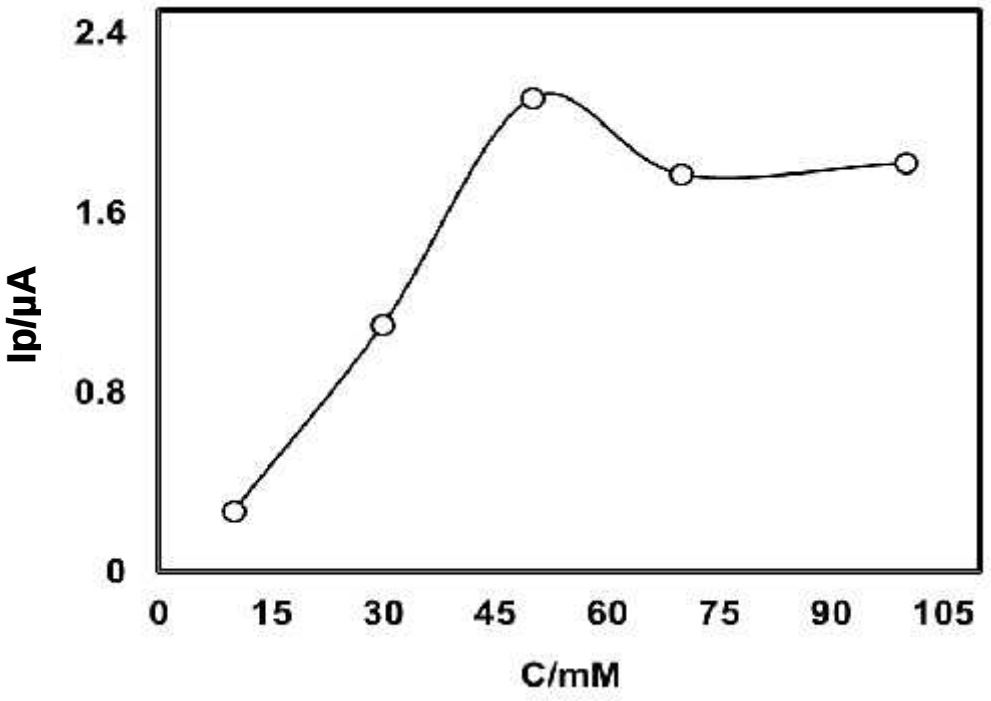

Fig. 4.29: Plots of peak current (I_p) versus concentration (C) of L-Alanine (10, 30, 50, 100 and 150 mM) with fixed 2 mM 1,2-dihydroxybenzene of Pt electrode in buffer solution (pH) at 7 scan rate 0.1 V/s (2^{nd} cycle).

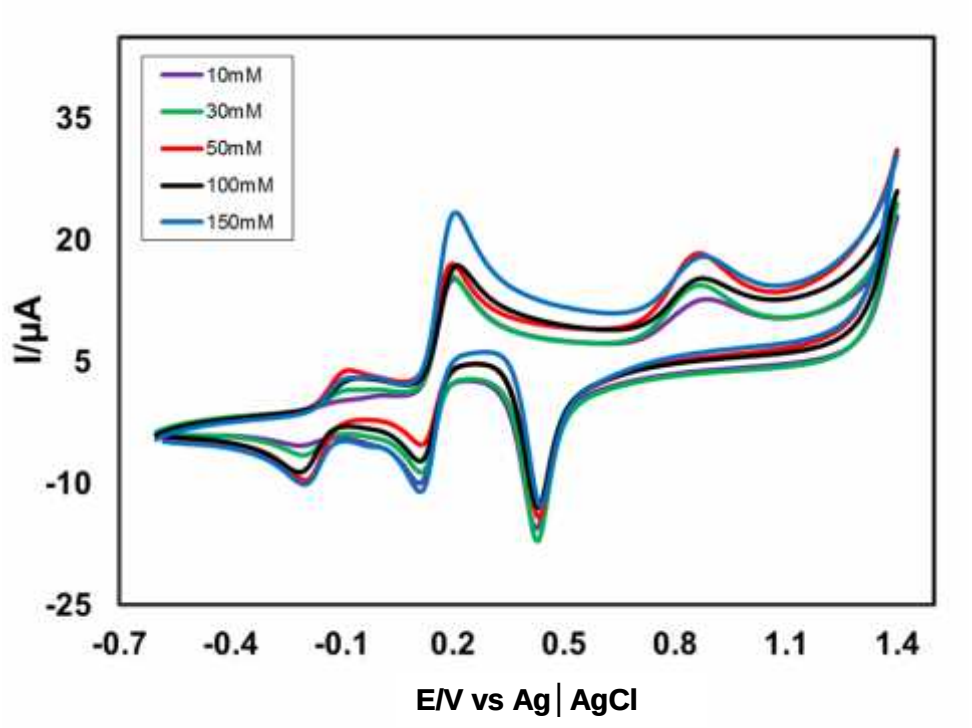

Fig. 4.30: CV of composition changes of L-Alanine (10, 30, 50, 100 and 150 mM) with fixed 2 mM 1,2-dihydroxybenzene of Au electrode at pH 7 and scan rate 0.1 V/s.

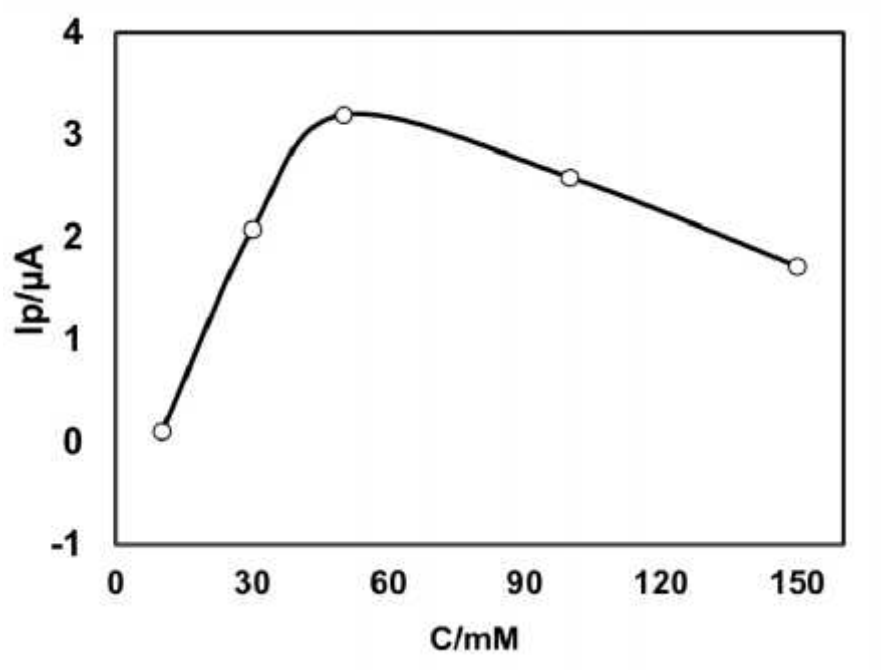

Fig. 4.31: Plots of peak current (I_p) versus concentration (C) of L-Alanine (10, 30, 50, 100 and 150 mM) with fixed 2 mM 1,2-dihydroxybenzene of Au electrode in buffer solution (pH 7) at scan rate 0.1 V/s (2^{nd} cycle).

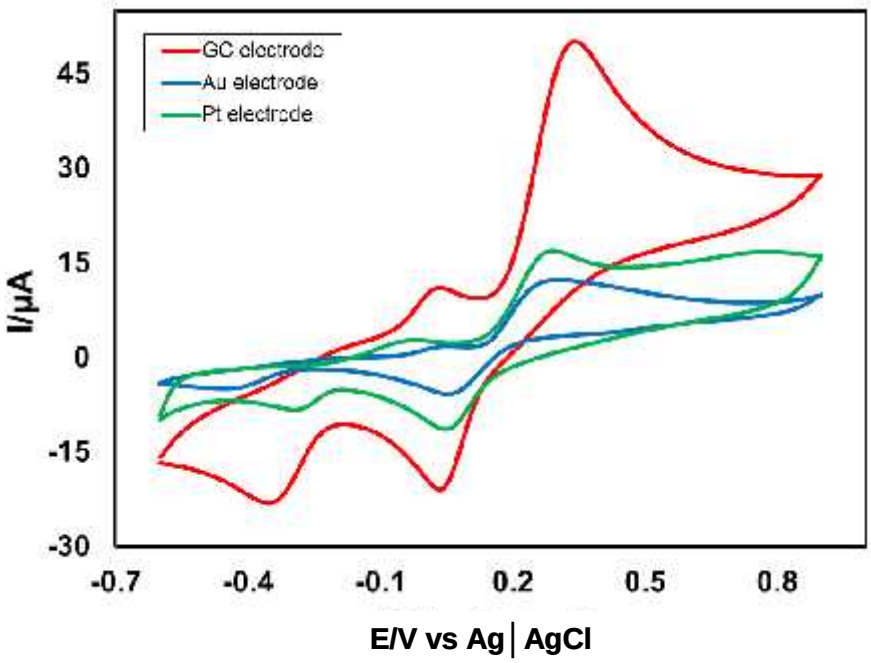

Fig. 4.32: Cyclic voltammogram (CV) of 2 mM 1,2-dihydroxybenzene with 50 mM L-Alanine in GC electrode (3.0mm), Gold electrode (1.6mm) and Platinum electrode (1.6mm) at pH 7 and scan rate 0.1 V/s.

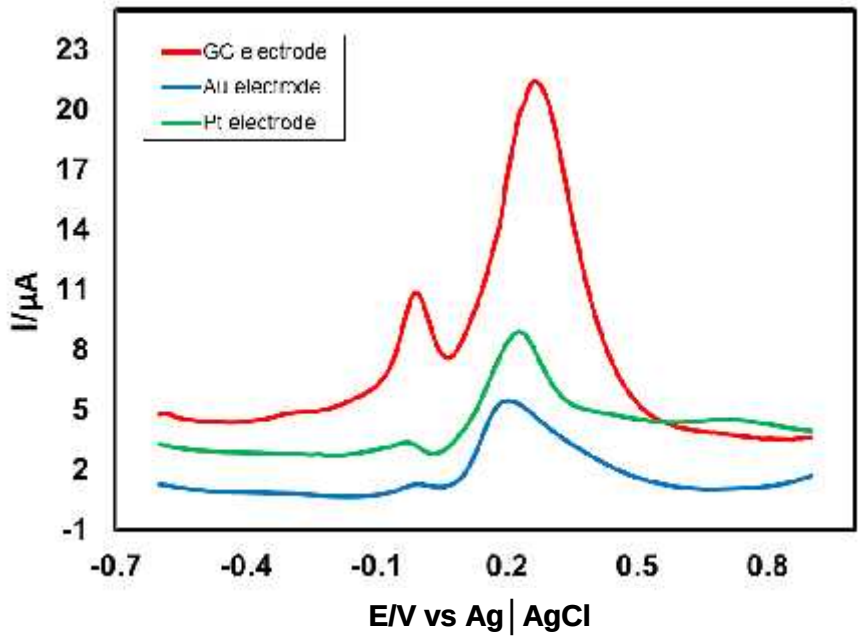

Fig. 4.33: Differential pulse voltammogram (DPV) of 2 mM 1,2-dihydroxybenzene with 50 mM L-Alanine in GC electrode (3.0mm), Gold electrode (1.6mm) and Platinum electrode (1.6mm) at pH 7 and scan rate 0.1 V/s.

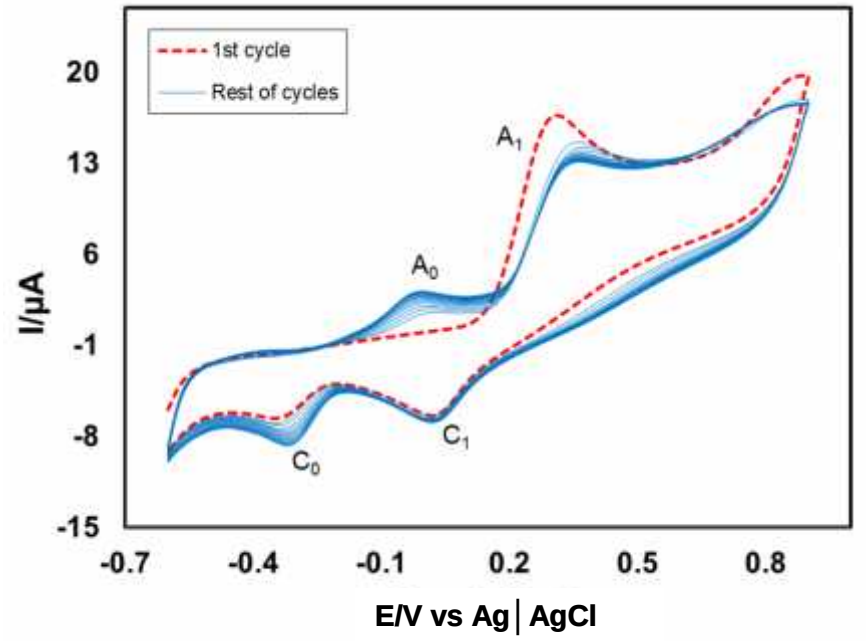

Fig. 4.34: Cyclic voltammogram of 2 mM 1,2-dihydroxybenzene with 50 mM L-Alanine of GC (3mm) electrode in the buffer solution of pH 7 at scan rate 0.1 V/s (15 cycles). The appeared anodic peak current (A_0) and cathodic peak current (C_0) increased with the iteration scan from the first cycle.

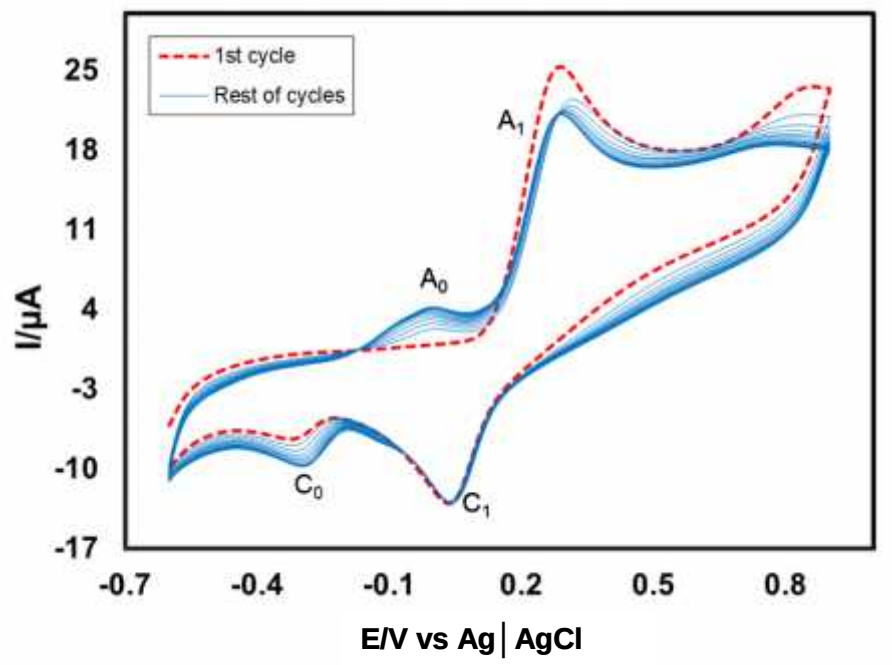

Fig. 4.35: Cyclic voltammogram of 2 mM 1,2-dihydroxybenzene with 50 mM L-Alanine of Pt electrode in the buffer solution of pH 7 at scan rate 0.1 V/s (15 cycles). The appeared anodic peak current (A_0) and cathodic peak current (C_0) increased with the iteration scan from the first cycle.

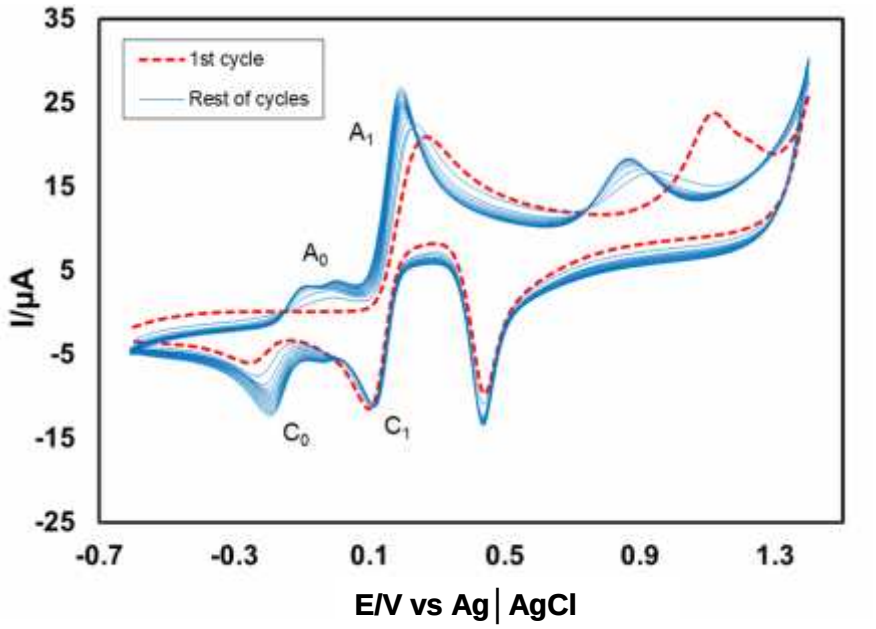

Fig. 4.36: Cyclic voltammogram of 2 mM 1,2-dihydroxybenzene with 50 mM L-Alanine of Au electrode in the buffer solution of pH 7 at scan rate 0.1 V/s (15 cycles). The appeared anodic peak current (A_0) and cathodic peak current (C_0) increased with the iteration scan from the first cycle.

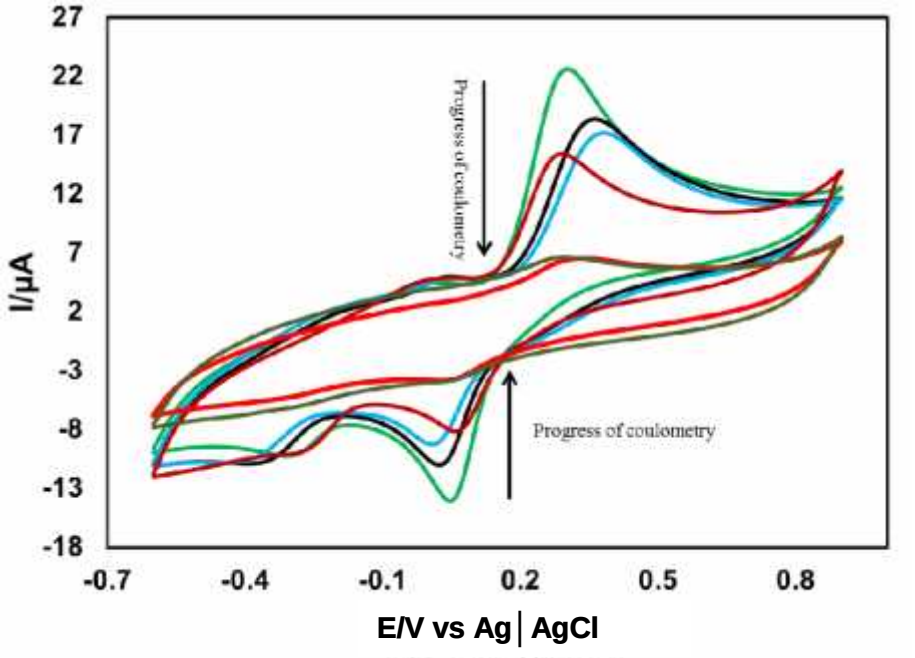

Fig. 4.37: Cyclic voltammogram and (CV) of 1 mM 1,2-dihydroxybenzene in presence of 25 mM L-Alanine of GC electrode during controlled potential coulometry at 0.45 V in pH 7 at scan rate 0.1 V/s.

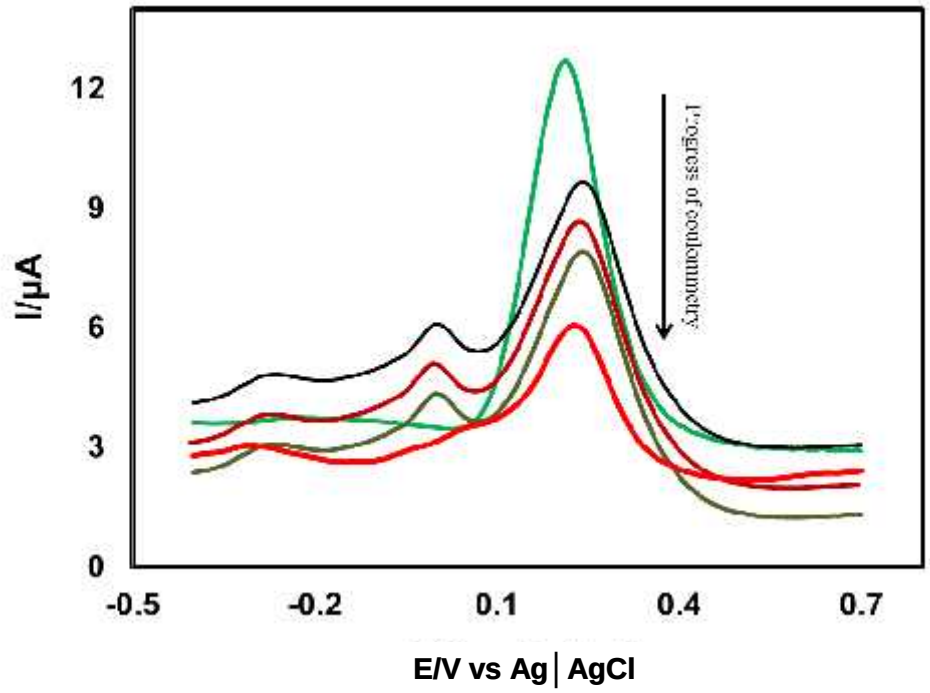

Fig. 4.38: Differential pulse voltammogram (DPV) of 1 mM 1,2-dihydroxybenzene in presence of 25 mM L-Alanine of GC electrode during controlled potential coulometry at 0.45 V in pH 7 at scan rate 0.1 V/s.

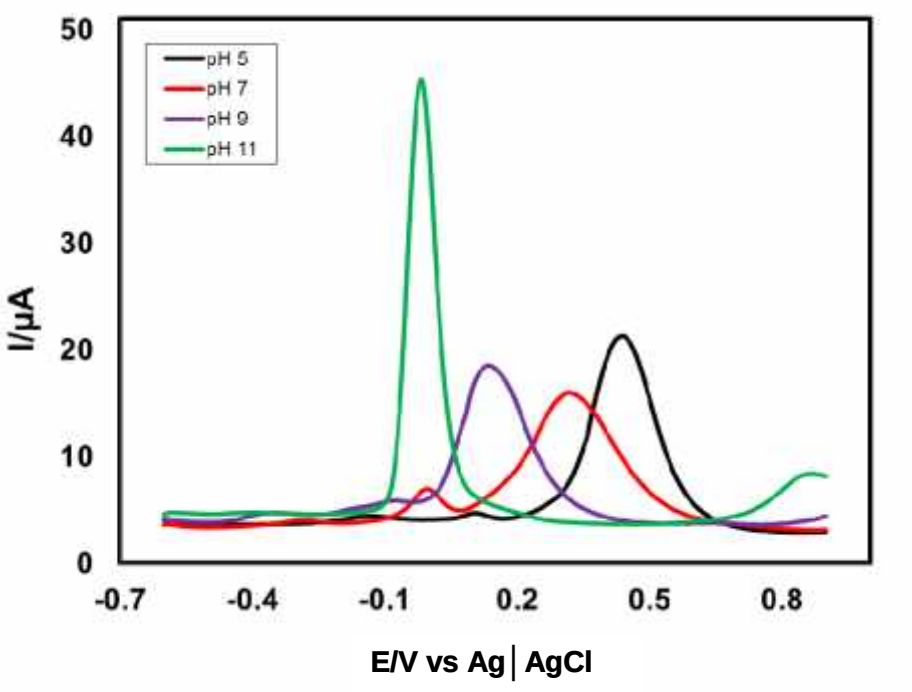

Fig. 4.39: Differential pulse voltammogram (DPV) of 2 mM 1,2-dihydroxybenzene with 50 mM L-Alanine of GC electrode in second scan of different pH (5, 7, 9 and 11) and scan rate 0.1 V/s.

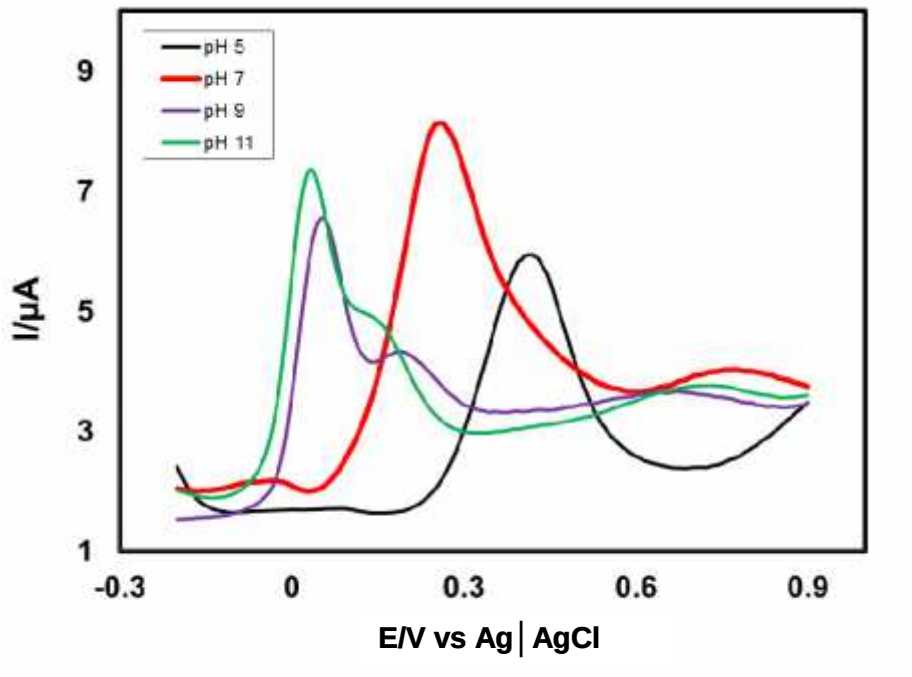

Fig. 4.40: Differential pulse voltammogram (DPV) of 2 mM 1,2-dihydroxybenzene with 50 mM L-Alanine of Pt electrode in second scans of different pH (5, 7, 9 and 11) and scan rate 0.1 V/s.

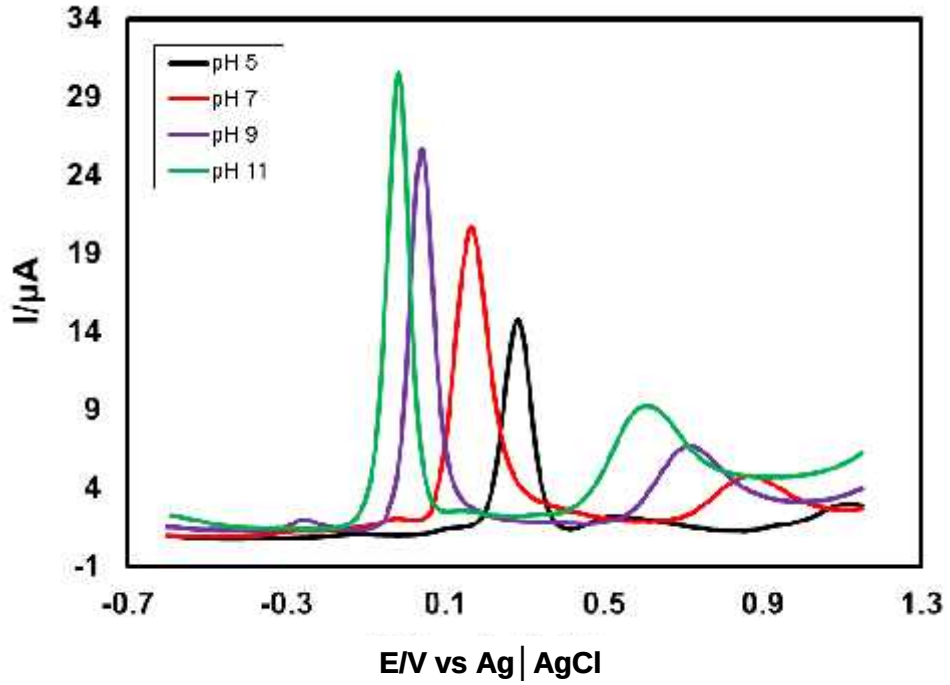

Fig. 4.41: Differential pulse voltammogram (DPV) of 2 mM 1,2-dihydroxybenzene with 50 mM L-Alanine of Au electrode in second scans of different pH (5, 7, 9 and 11) and scan rate 0.1 V/s.

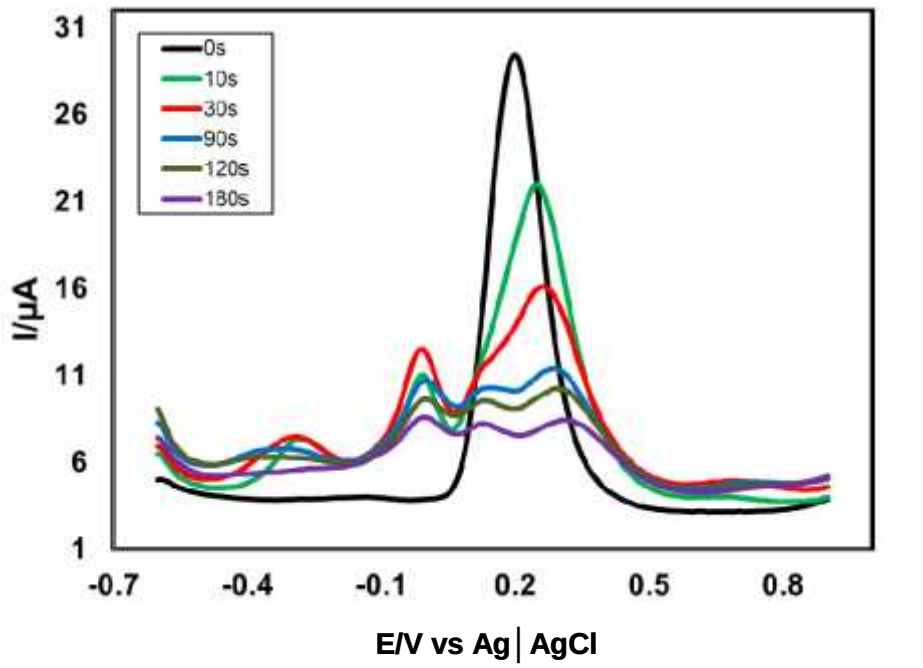

Fig. 4.42: Differential pulse voltammogram (DPV) of deposition time change (0, 10, 30, 60, 90, 120 and 180 s) of 2 mM 1,2-dihydroxybenzene with 50 mM L-Alanine of pH 7 at *E*puls 0.02 V, tpuls 20 ms and scan rate 0.1 Vs^{-1}.

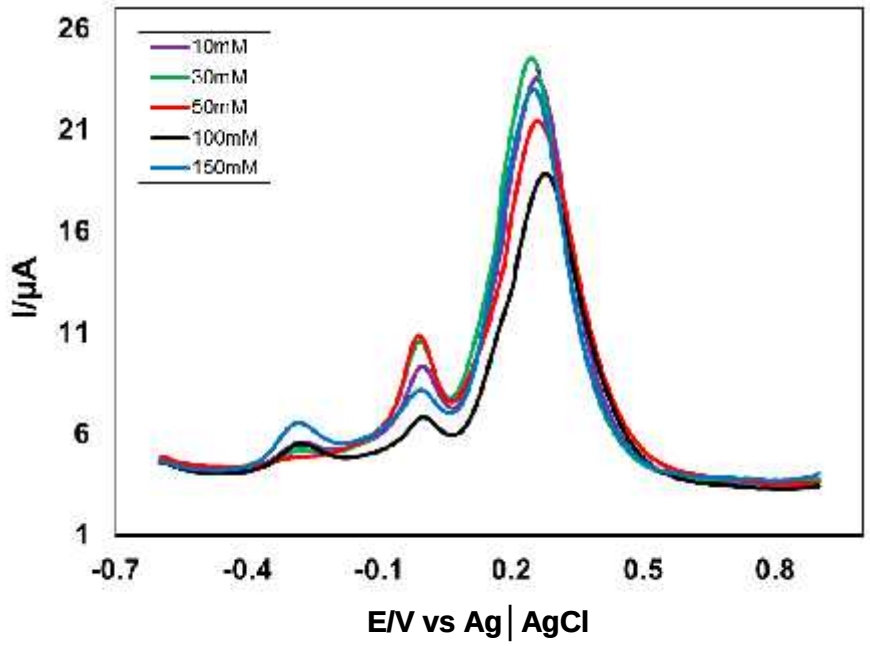

Fig. 4.43: Differential pulse voltammogram (DPV) of composition change of L-Alanine (10, 30, 50, 100 and 150 mM) with the fixed composition of 2 mM 1,2-dihydroxybenzene in second scan of pH 7 at *E*puls 0.02V, tpuls 20ms of GC electrode and scan rate 0.1 Vs^{-1}.

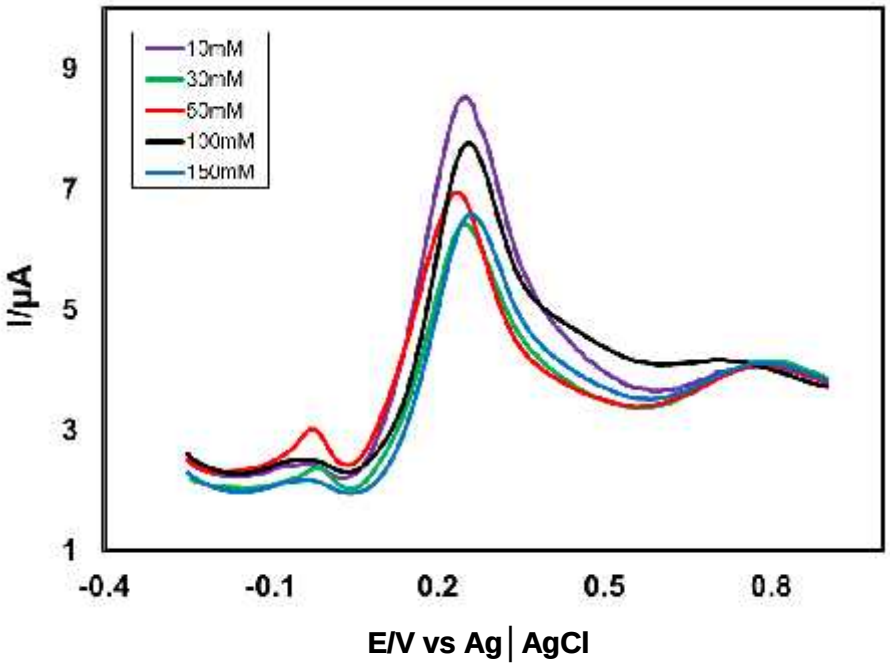

Fig. 4.44: Differential pulse voltammogram (DPV) of composition change of L-Alanine (10, 30, 50, 100 and 150 mM) with the fixed composition of 2 mM 1,2-dihydroxybenzene in second scan of pH 7 at *E*puls 0.02 V, tpuls 20 ms of Pt electrode and scan rate 0.1 Vs^{-1}.

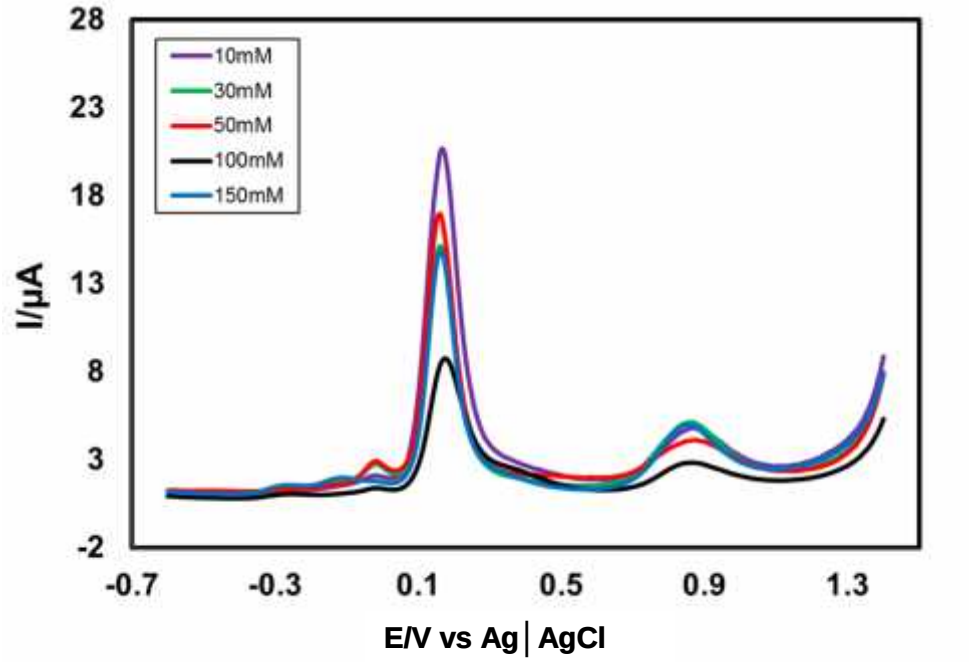

Fig. 4.45: Differential pulse voltammogram (DPV) of composition change of L-Alanine (10, 30, 50, 100 and 150 mM) with the fixed composition of 2 mM 1,2-dihydroxybenzene in second scan of pH 7 at *E*puls 0.02 V, tpuls 20 ms of Au electrode and scan rate 0.1 Vs^{-1}.

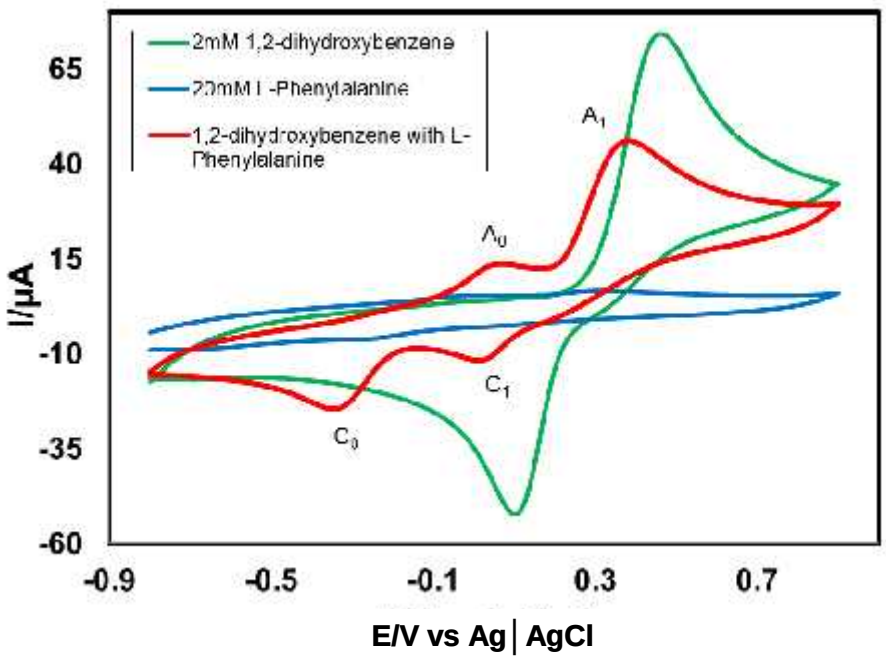

Fig. 4.46: Cyclic voltammogram of 2 mM 1,2-dihydroxybenzene (green line), 20 mM L-Phenylalanine (blue line) and 2 mM 1,2-dihydroxybenzene with 20 mM L-Phenylalanine (red line) of GC electrode in buffer solution (pH 7) at scan rate 0.1 V/s (2nd cycle). A_0 is appeared anodic peak and C_0 is corresponding cathodic peak.

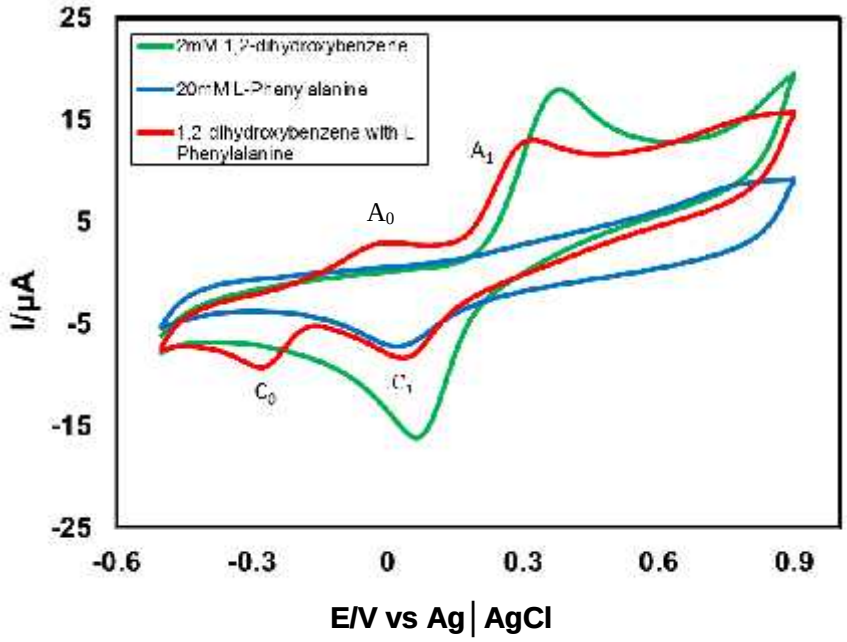

Fig. 4.47: Cyclic voltammogram of 2 mM 1,2-dihydroxybenzene (green line), 20 mM L-Phenylalanine (blue line) and 2 mM 1,2-dihydroxybenzene with 20 mM L-Phenylalanine (red line) of Pt electrode in buffer solution (pH 7) at scan rate 0.1 V/s (2nd cycle). A_0 is appeared anodic peak and C_0 is corresponding cathodic peak.

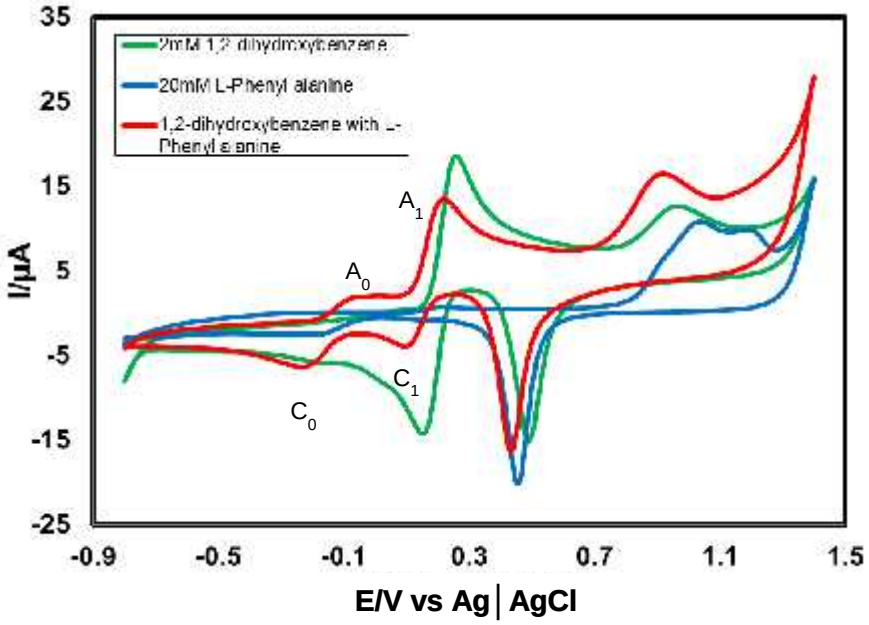

Fig. 4.48: Cyclic voltammogram of 2 mM 1,2-dihydroxybenzene (green line), 20 mM L-Phenylalanine (blue line) and 2 mM 1,2-dihydroxybenzene with 20 mM L-Phenylalanine (red line) of Au electrode in buffer solution (pH 7) at scan rate 0.1 V/s (2nd cycle). A_0 is appeared anodic peak and C_0 is corresponding cathodic peak.

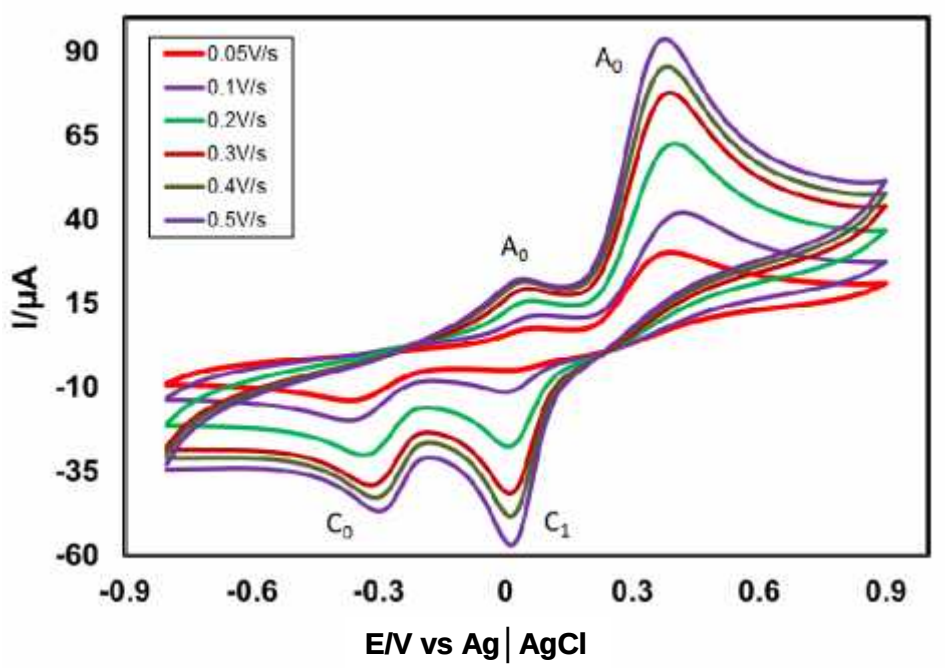

Fig. 4.49: Cyclic voltammogram of 2 mM 1,2-dihydroxybenzene with 20 mM L-Phenylalanine in the second scan of potential at GC electrode in buffer solution (pH 7) at scan rate 0.05 V/s to 0.5 V/s.

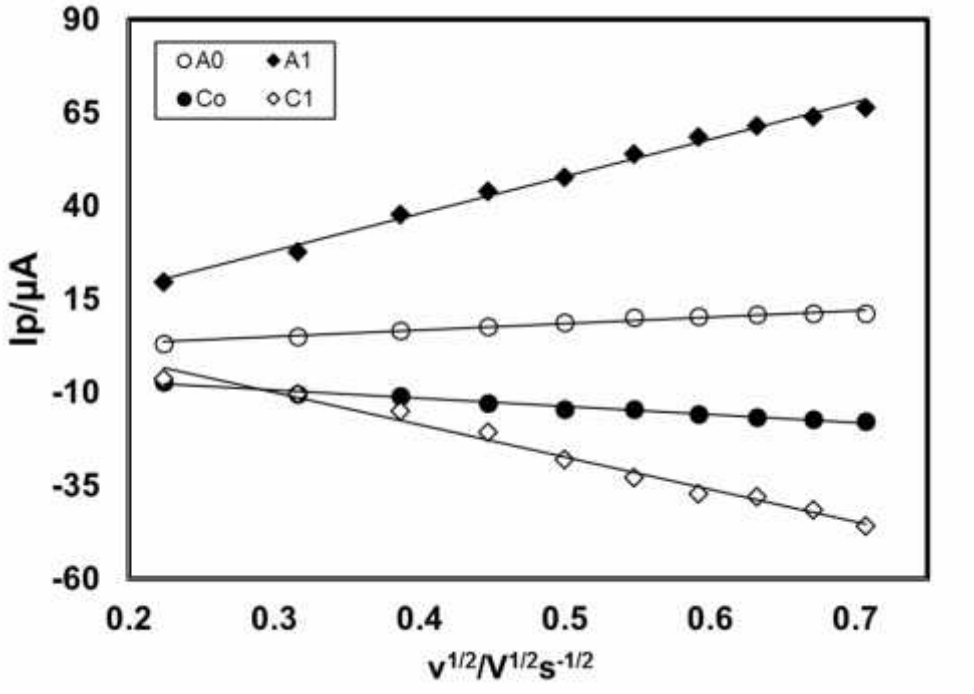

Fig. 4.50: Plots of peak current (I_p) versus square root of scan rate ($v^{1/2}$) of 2 mM 1,2-dihydroxybenzene with 20 mM L-Phenylalanine of GC electrode in buffer solution (pH 7) (2^{nd} cycle).

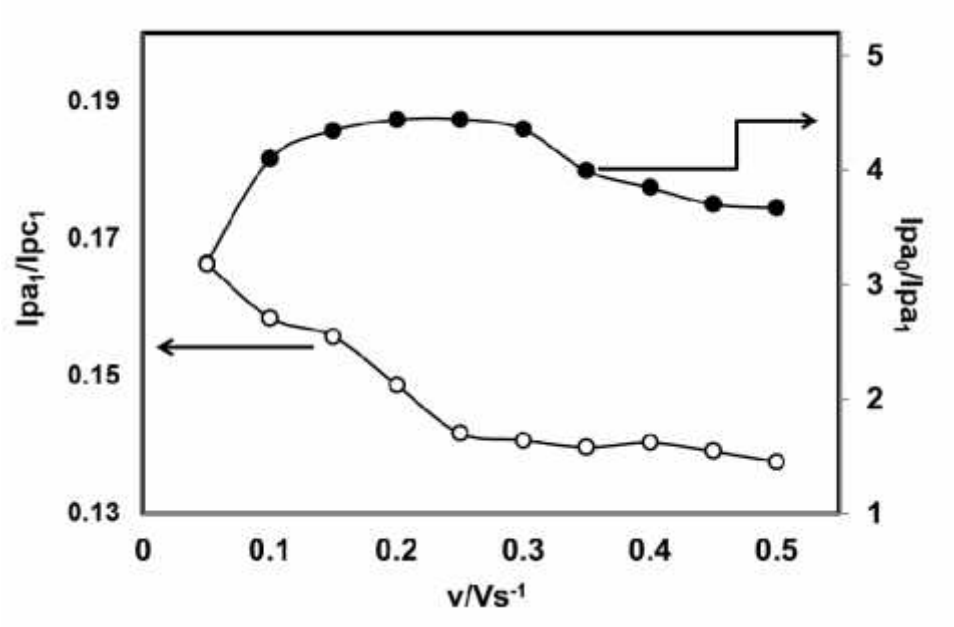

Fig. 4.51: Variation of peak current ratio of corresponding peak (I_{pa1}/I_{pc1}) and anodic peak (I_{pa0}/I_{pa1}) vs scan rate (v) of 2 mM 1,2-dihydroxybenzene with 20 mM L-Phenylalanine of GC electrode in buffer solution (pH 7) at scan rate 0.1 V/s in the second scan of potential.

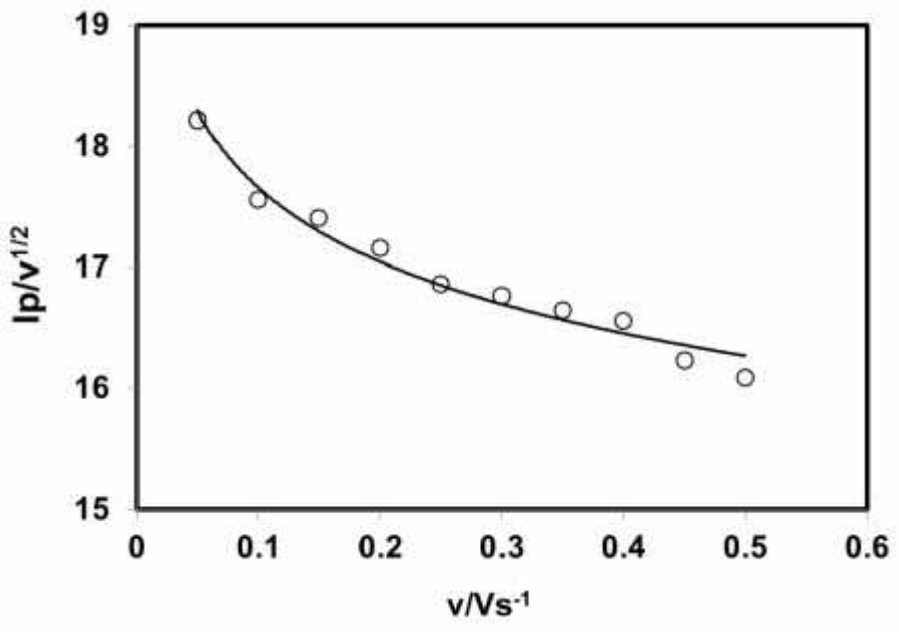

Fig. 4.52: Plot of current function ($I_p/v^{1/2}$) versus scan rate (v) of 2 mM 1,2-dihydroxybenzene with 20 mM L-Phenylalanine of GC electrode in buffer solution (pH 7) of the Appeared anodic peak (A_0).

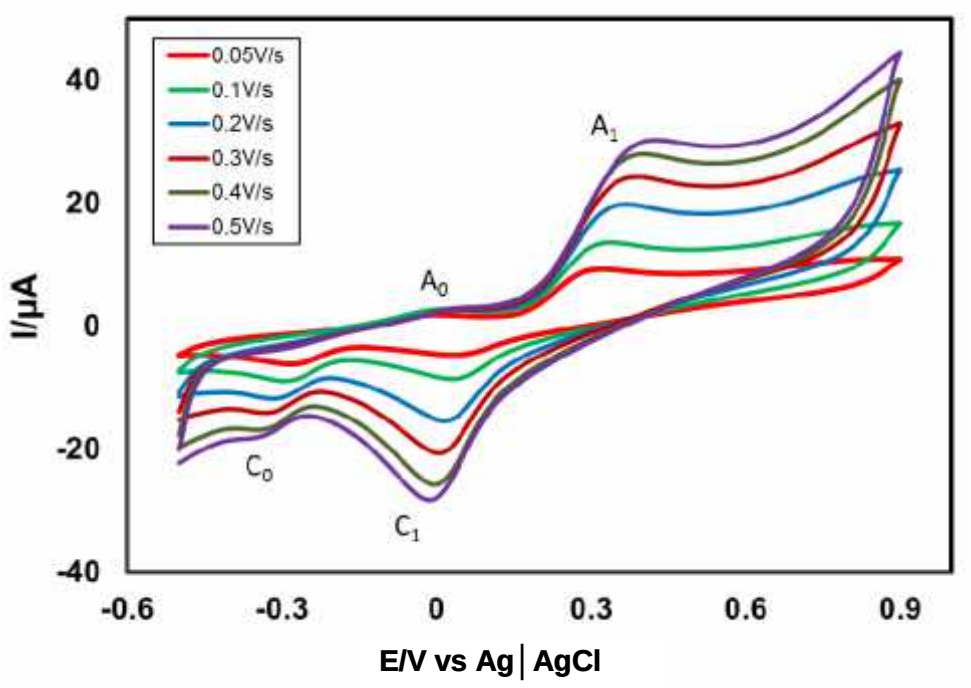

Fig. 4.53: Cyclic voltammogram of 2 mM 1,2-dihydroxybenzene with 20 mM L-Phenylalanine in the second scan of potential at Pt electrode in buffer solution (pH 7) at scan rate 0.05 V/s to 0.5 V/s.

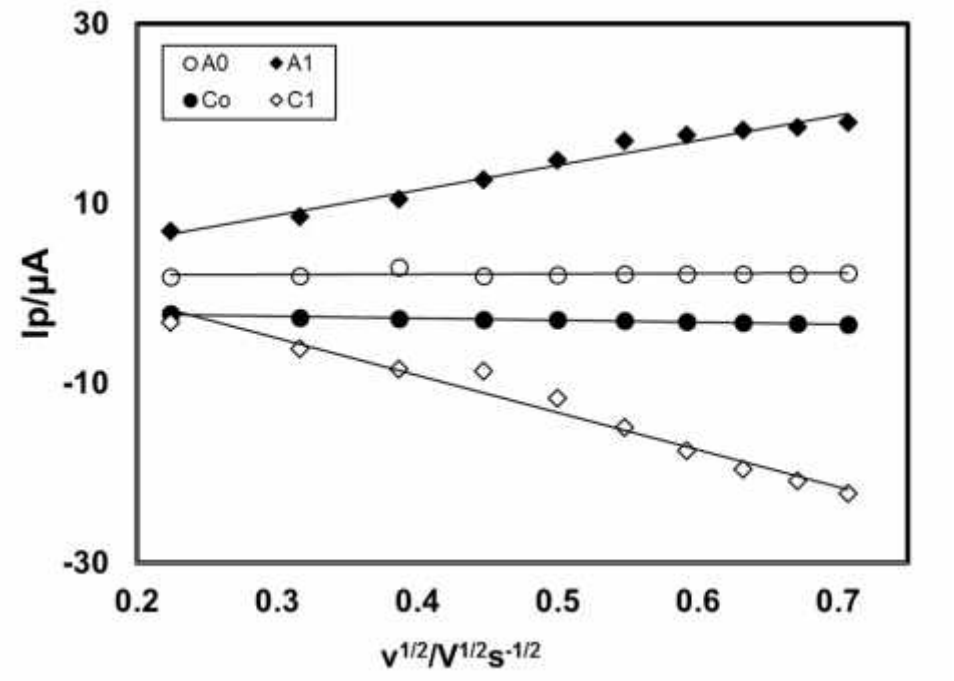

Fig. 4.54: Plots of peak current (I_p) versus square root of scan rate ($v^{1/2}$) of 2 mM 1,2-dihydroxybenzene with 20 mM L-Phenylalanine of Pt electrode in buffer solution (pH 7) (2^{nd} cycle).

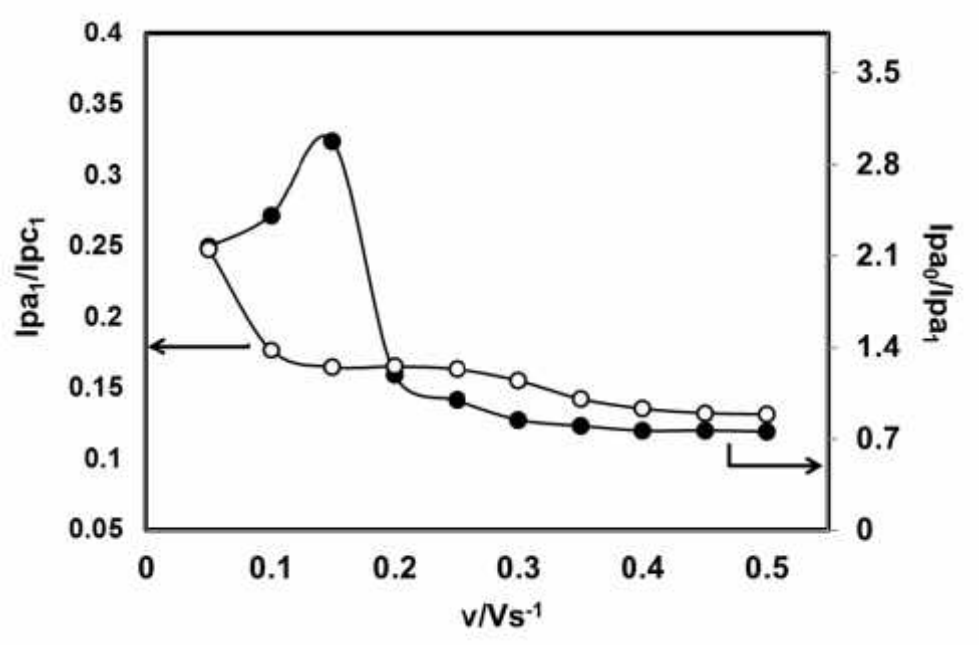

Fig. 4.55: Variation of peak current ratio of corresponding peak (I_{pa1}/I_{pc1}) and anodic peak (I_{pa0}/I_{pa1}) vs scan rate (v) of 2 mM 1,2-dihydroxybenzene with 20 mM L-Phenylalanine of Pt electrode in buffer solution (pH 7) at scan rate 0.1 V/s in the second scan of potential.

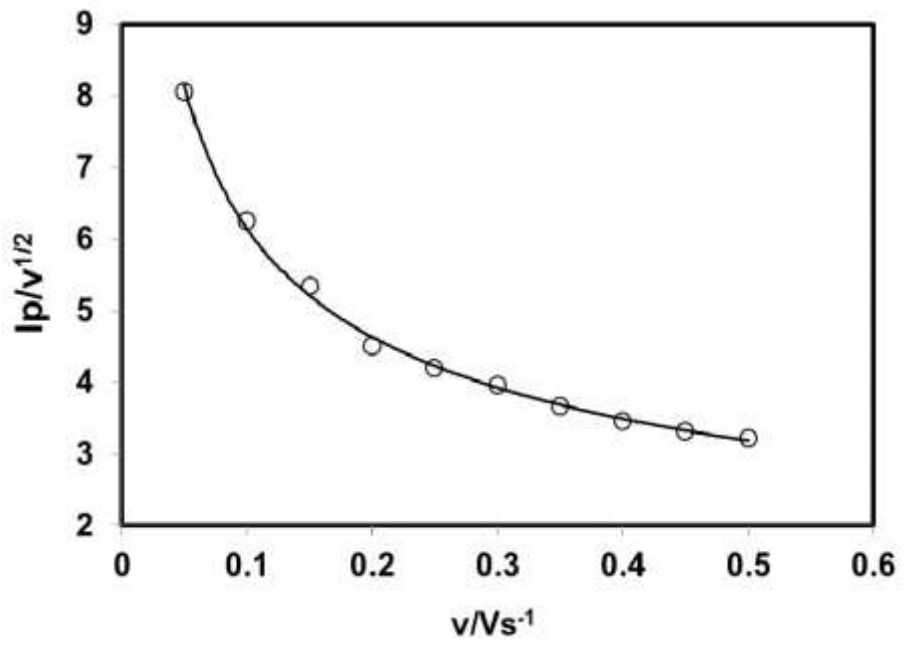

Fig. 4.56: Plots of current function ($I_p/v^{1/2}$) versus scan rate (v) of 2 mM 1,2-dihydroxybenzene with 20 mM L-Phenylalanine of Pt electrode in buffer solution (pH 7) of the Appeared anodic peak (A_0).

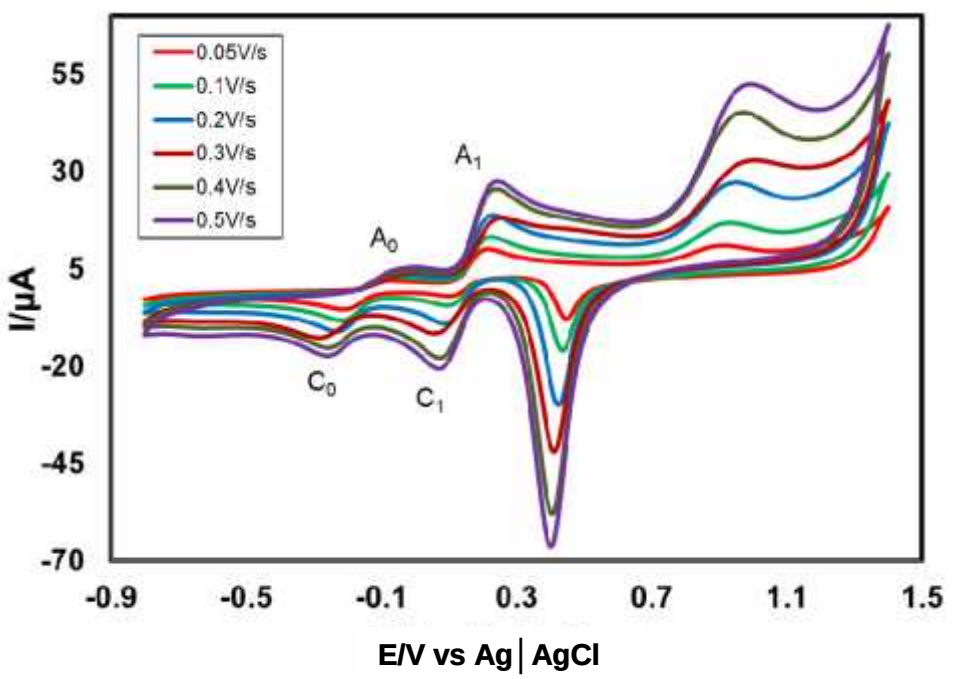

Fig. 4.57: Cyclic voltammogram of 2 mM 1,2-dihydroxybenzene with 20 mM L-Phenylalanine in the second scan of potential at Au electrode in buffer solution (pH 7) at scan rate 0.05 V/s to 0.5 V/s.

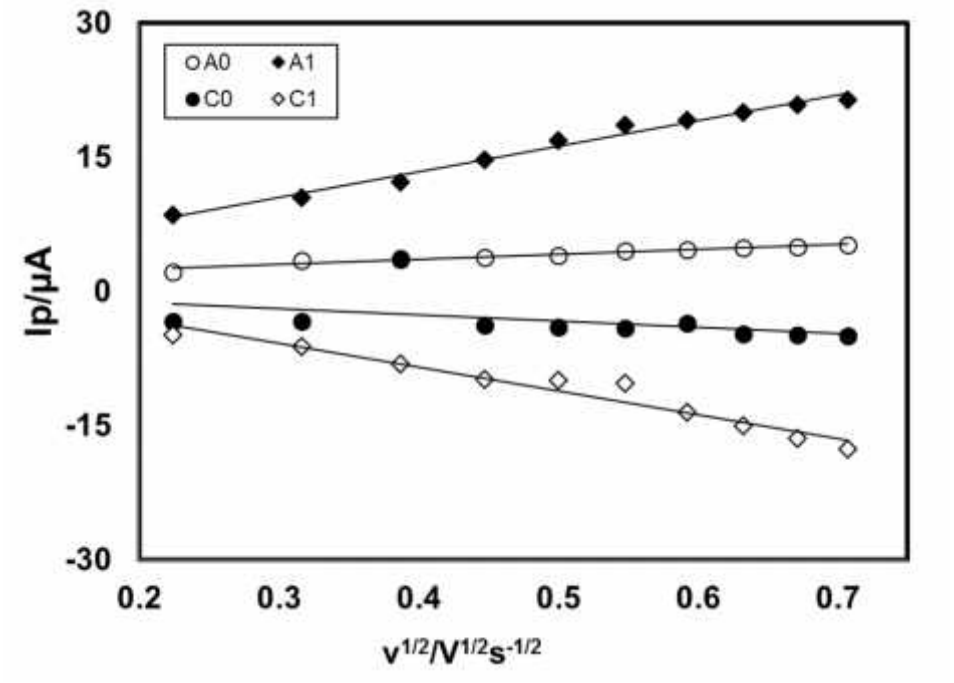

Fig. 4.58: Plots of peak current (I_p) versus square root of scan rate ($v^{1/2}$) of 2 mM 1,2-dihydroxybenzene with 20 mM L-Phenylalanine of Au electrode in buffer solution (pH 7) (2^{nd} cycle).

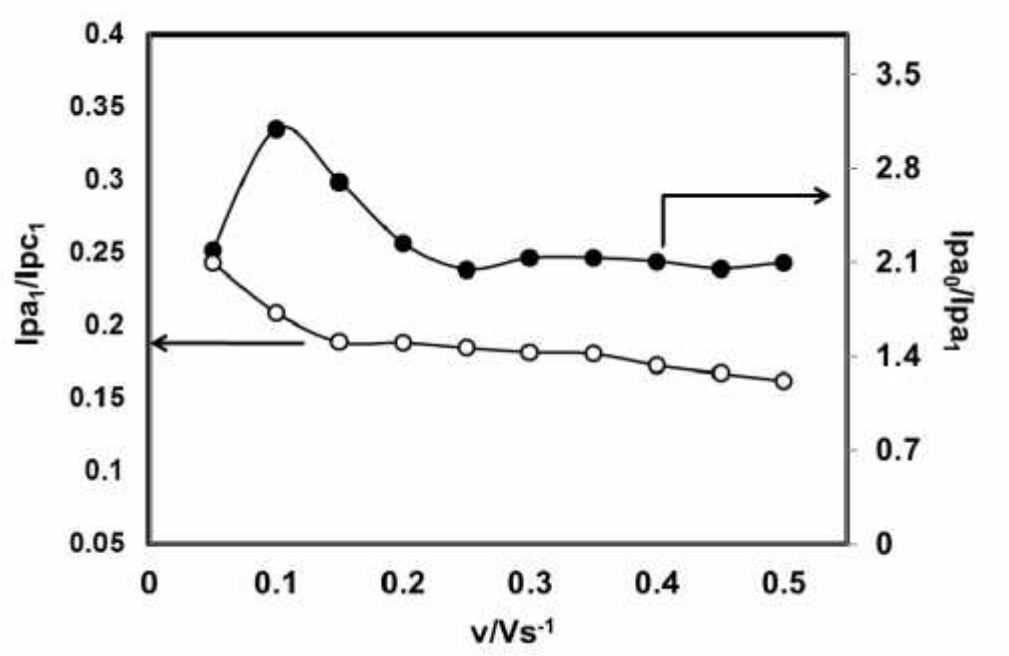

Fig. 4.59: Variation of peak current ratio of corresponding peak (I_{pa1}/I_{pc1}) and anodic peak (I_{pa0}/I_{pa1}) vs scan rate (v) of 2 mM 1,2-dihydroxybenzene with 20 mM L-Phenylalanine of Au electrode in buffer solution (pH 7) at scan rate 0.1 V/s in the second scan of potential.

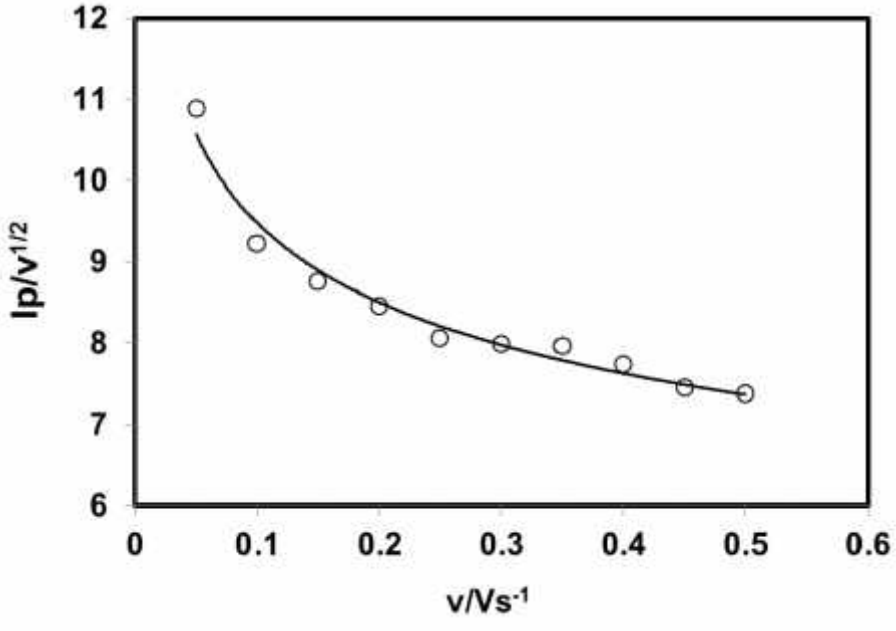

Fig. 4.60: Plots of current function ($I_p/v^{1/2}$) versus scan rate (v) of 2 mM 1,2-dihydroxybenzene with 20 mM L-Phenylalanine of Au electrode in buffer solution (pH 7) of the Appeared anodic peak (A_0).

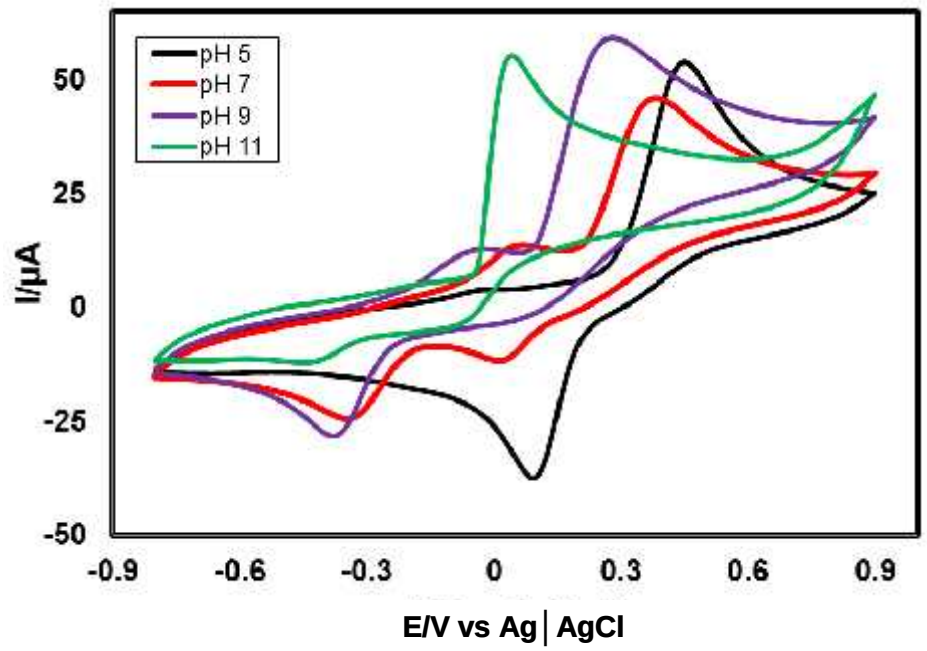

Fig. 4.61: Cyclic voltammogram of 2 mM 1,2-dihydroxybenzene with 20 mM L-Phenylalanine of GC (3mm) electrode in different pH (5, 7, 9 and 11) at scan rate 0.1 V/s.

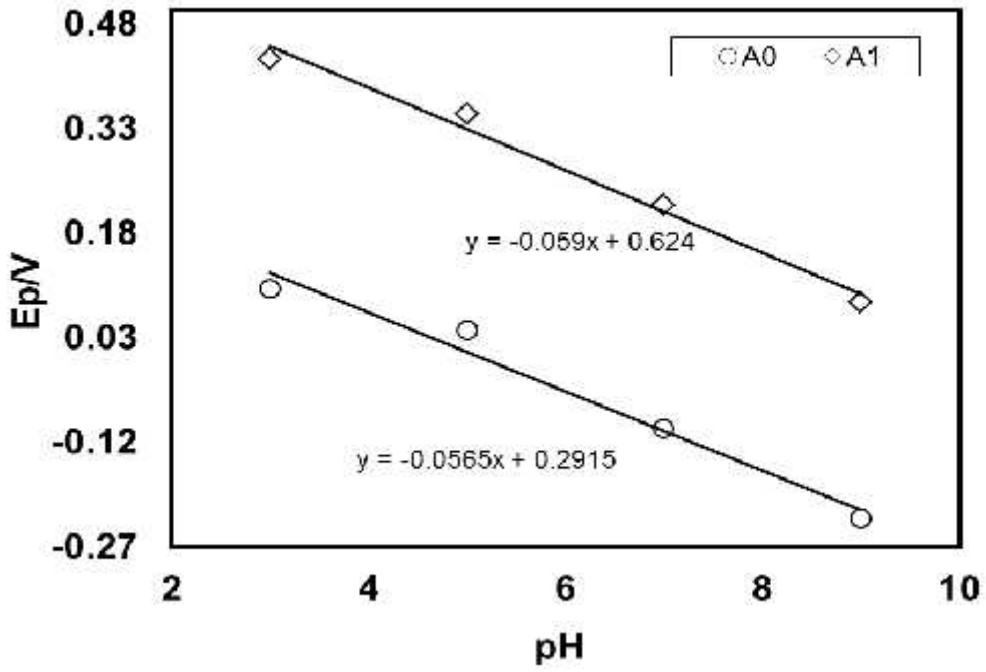

Fig. 4.62: Plots of peak potential (E_p) versus pH (5, 7, 9 and 11) of 2 mM 1,2-dihydroxybenzene with 20 mM L-Phenylalanine of GC electrode at scan rate 0.1 V/s (2^{nd} cycle).

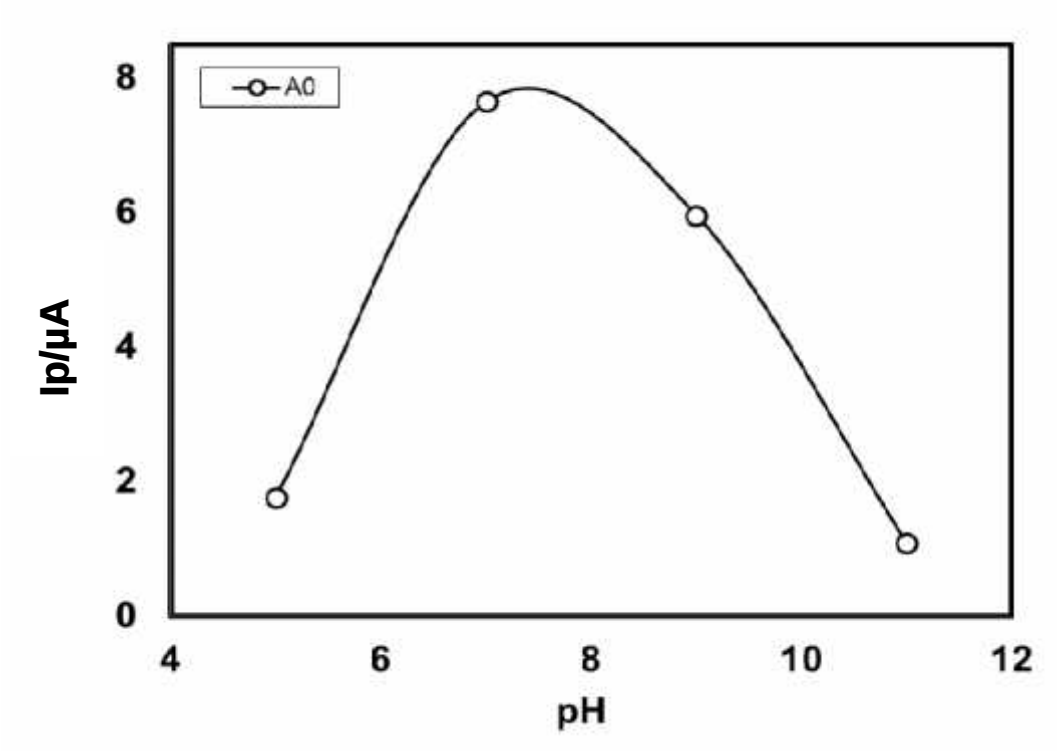

Fig. 4.63: Plot of peak current (I_p) versus pH (5, 7, 9 and 11) of 2 mM 1,2-dihydroxybenzene with 20 mM L-Phenylalanine of GC electrode at scan rate 0.1 V/s (2nd cycle).

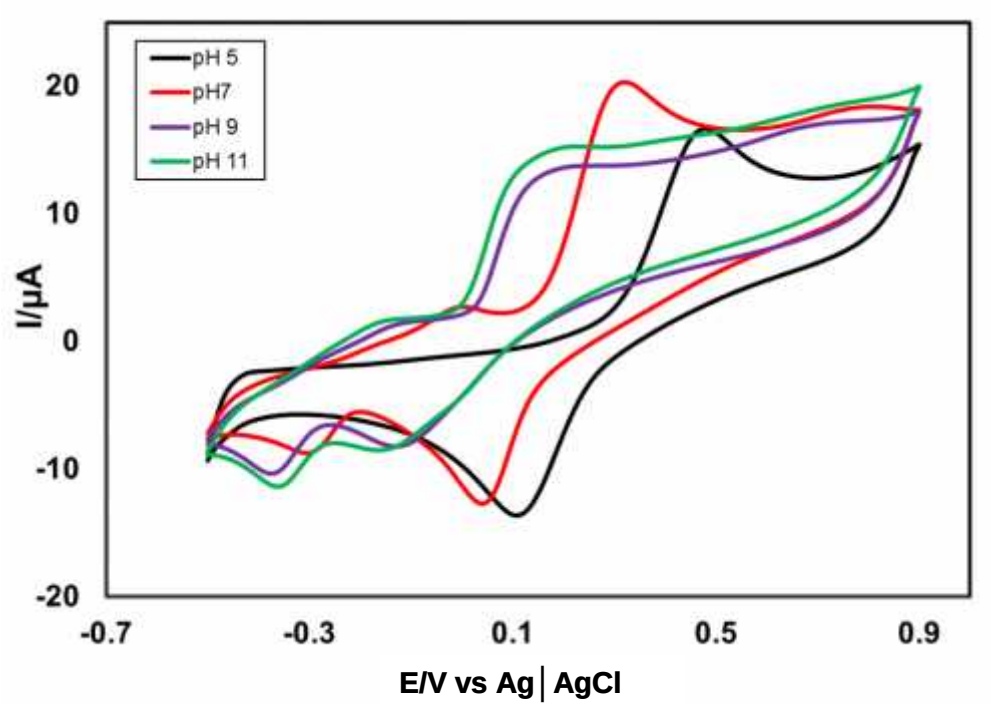

Fig. 4.64: Cyclic voltammogram of 2 mM 1,2-dihydroxybenzene with 20 mM L-Phenylalanine of Pt electrode in different pH (5, 7, 9 and 11) at scan rate 0.1 V/s.

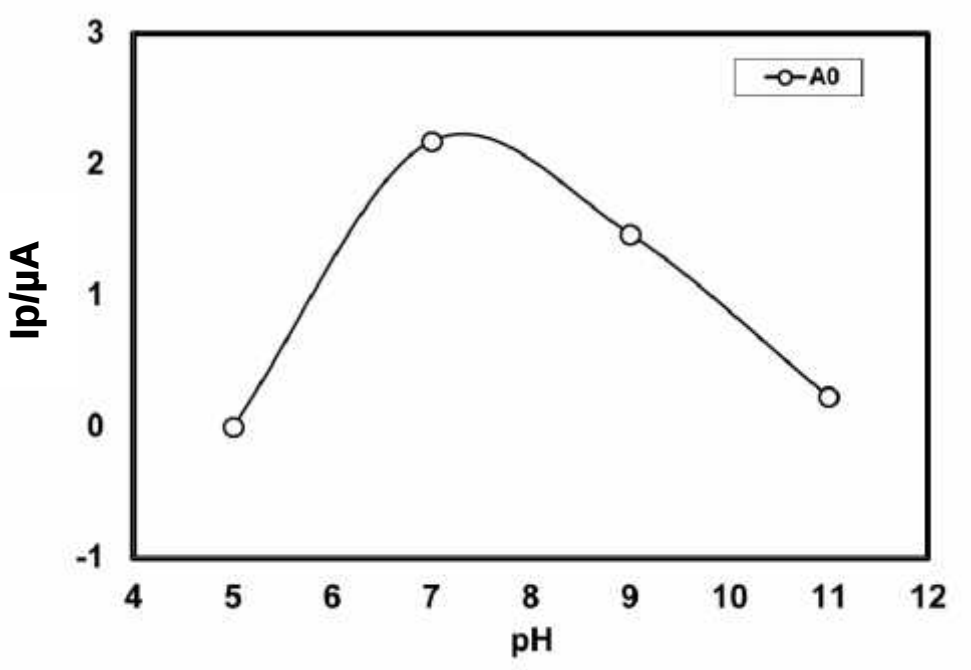

Fig. 4.65: Plots of peak current (I_p) versus pH (5, 7, 9 and 11) of 2 mM 1,2-dihydroxybenzene with 20 mM L-Phenylalanine of Pt electrode at scan rate 0.1 V/s (2nd cycle).

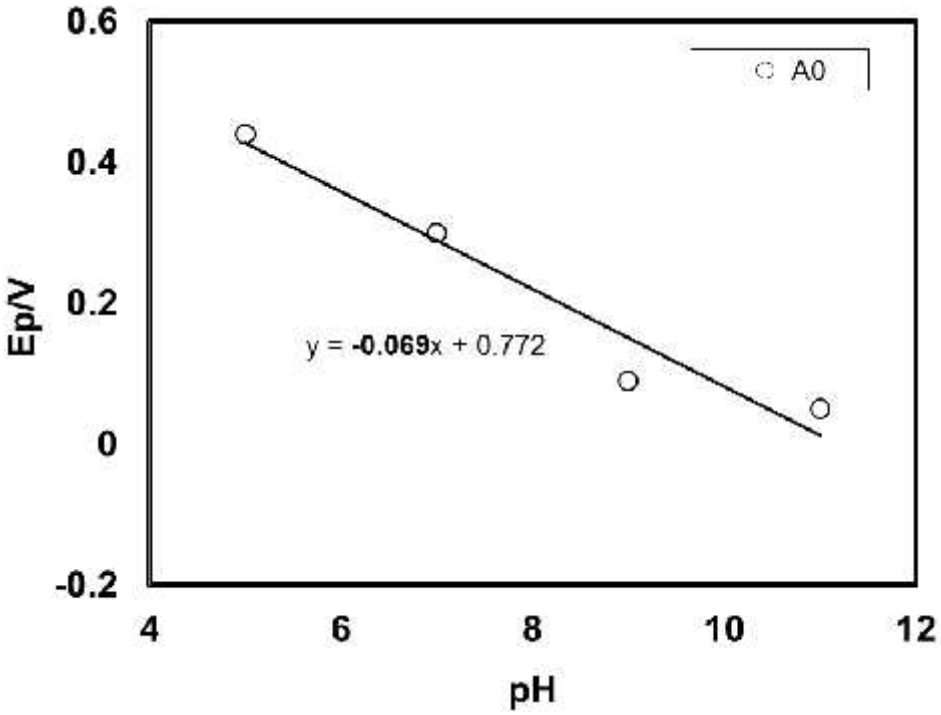

Fig. 4.66: Plot of peak potential (E_p) versus pH (5, 7, 9 and 11) of 2 mM 1,2-dihydroxybenzene with 20 mM L-Phenylalanine of Pt electrode at scan rate 0.1 V/s (2nd cycle).

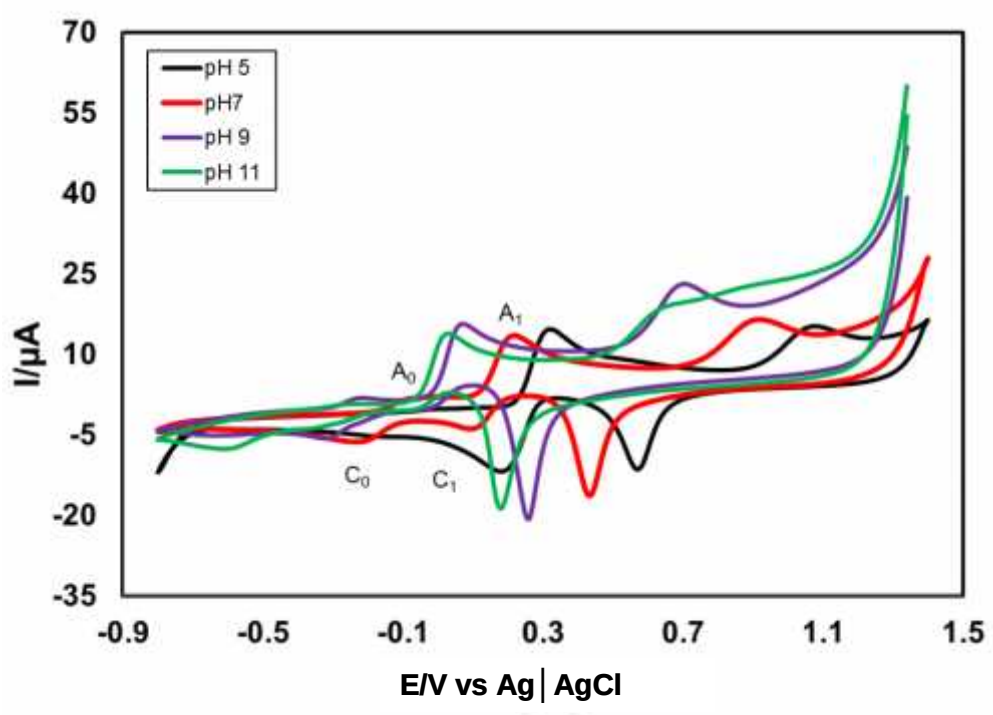

Fig. 4.67: Cyclic voltammogram of 2 mM 1,2-dihydroxybenzene with 20 mM L-Phenylalanine of Au electrode in different pH (5, 7, 9 and 11) at scan rate 0.1 V/s.

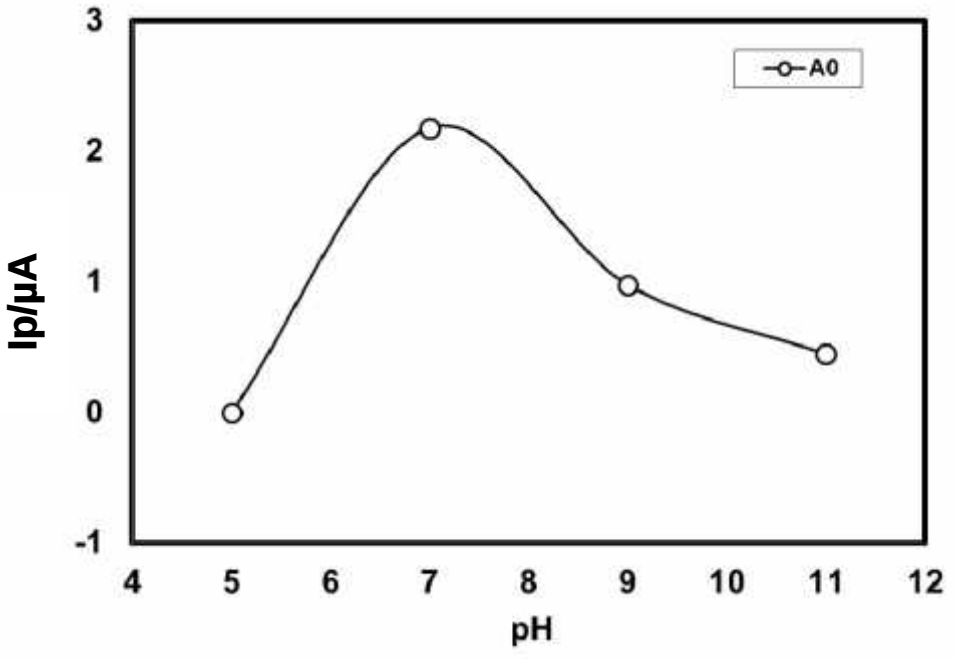

Fig. 4.68: Plots of peak current (I_p) versus pH (5, 7, 9 and 11) of 2 mM 1,2-dihydroxybenzene with 20 mM L-Phenylalanine of Au electrode at scan rate 0.1 V/s (2nd cycle).

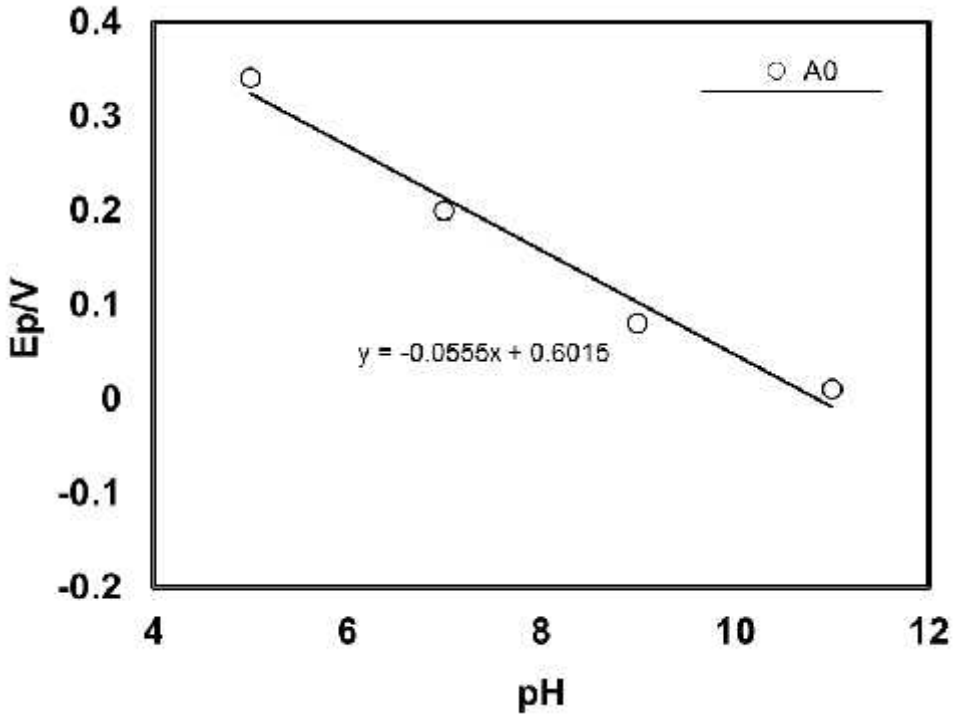

Fig. 4.69: Plot of peak potential (E_p) versus pH (5, 7, 9 and 11) of 2 mM 1,2-dihydroxybenzene with 20 mM L-Phenylalanine of Au electrode at scan rate 0.1 V/s (2nd cycle).

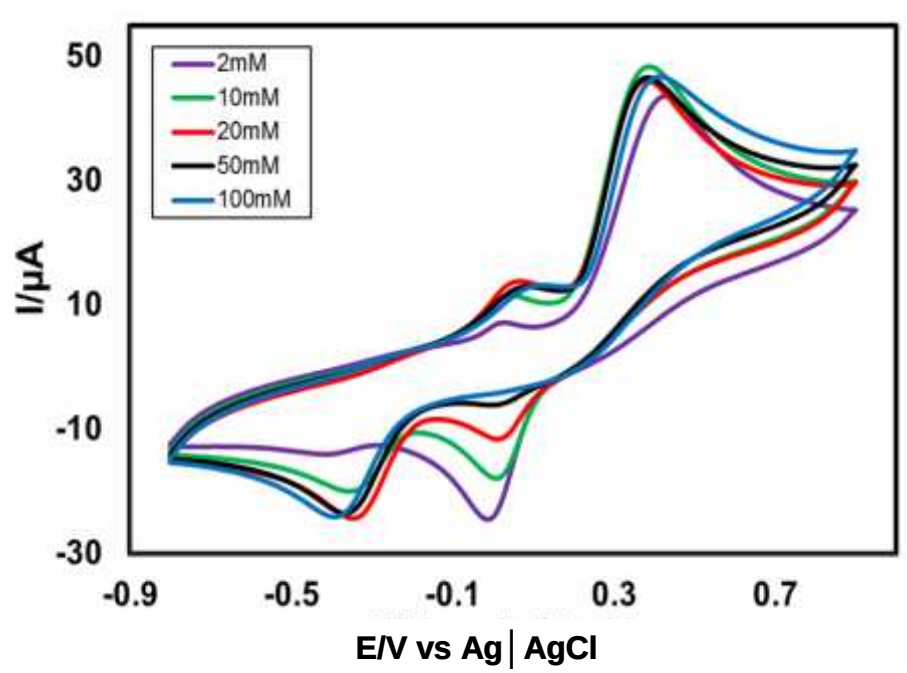

Fig. 4.70: CV of composition changes of L-Phenylalanine (2, 10, 20, 50 and 100 mM) with fixed 2 mM 1,2-dihydroxybenzene of GC electrode at pH 7 and scan rate 0.1 V/s.

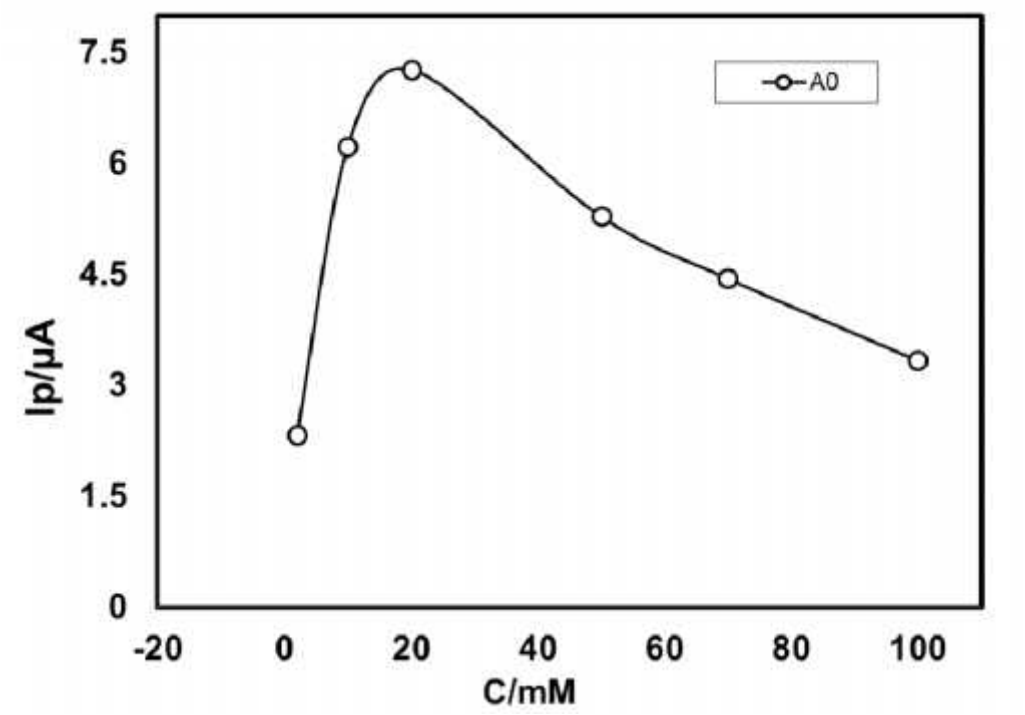

Fig. 4.71: Comparison of cyclic voltammogram of different concentration (2, 10, 20, 50 and 100 mM) of 20 mM L-Phenylalanine with fixed 2 mM 1,2-dihydroxybenzene of GC electrode in buffer solution (pH 7) at scan rate 0.1 V/s (2nd cycle).

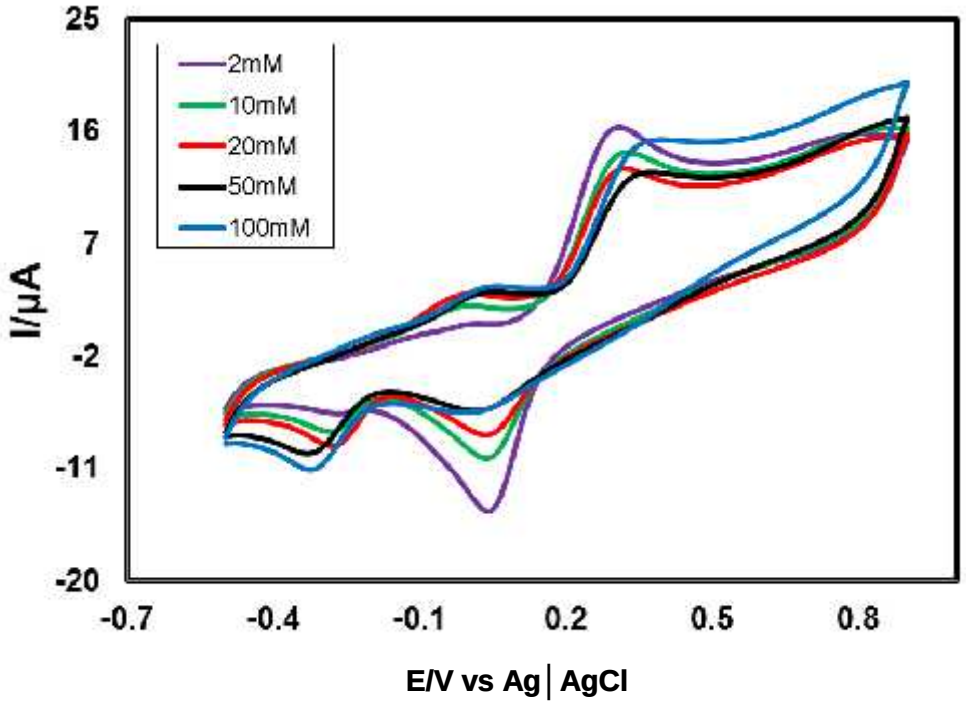

Fig. 4.72: CV of composition changes of L-Phenylalanine (2, 10, 20, 50 and 100 mM) with fixed 2 mM 1,2-dihydroxybenzene of Pt electrode at pH 7 and scan rate 0.1 V/s.

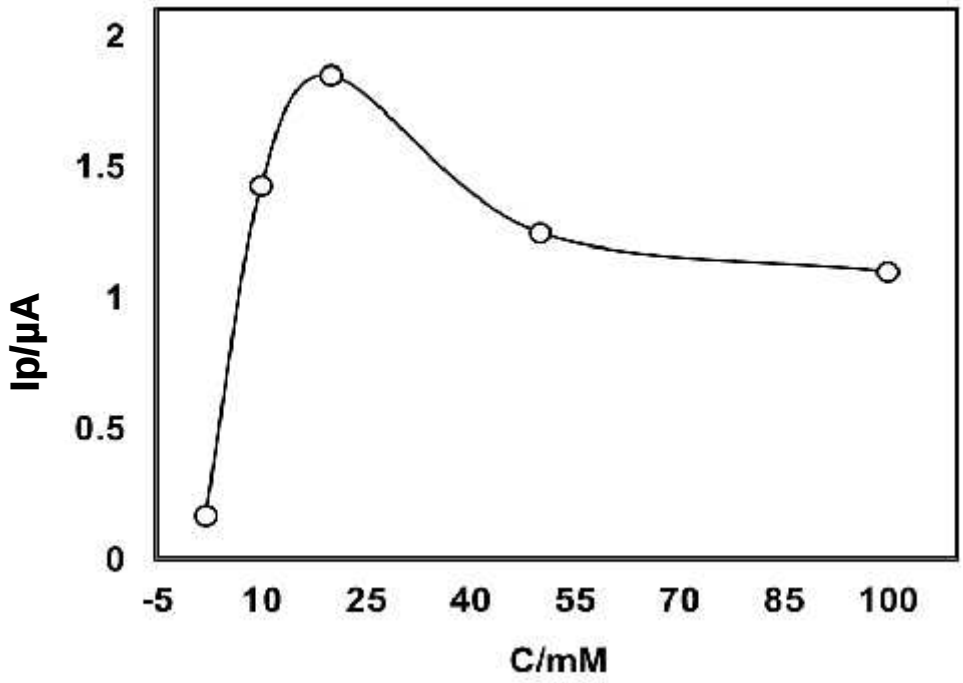

Fig. 4.73: Plots of peak current (I_p) versus concentration (C) of L-Phenylalanine (2, 10, 20, 50 and 100 mM) with fixed 2 mM 1,2-dihydroxybenzene of Pt electrode in buffer solution (pH) at 7 scan rate 0.1 V/s (2^{nd} cycle).

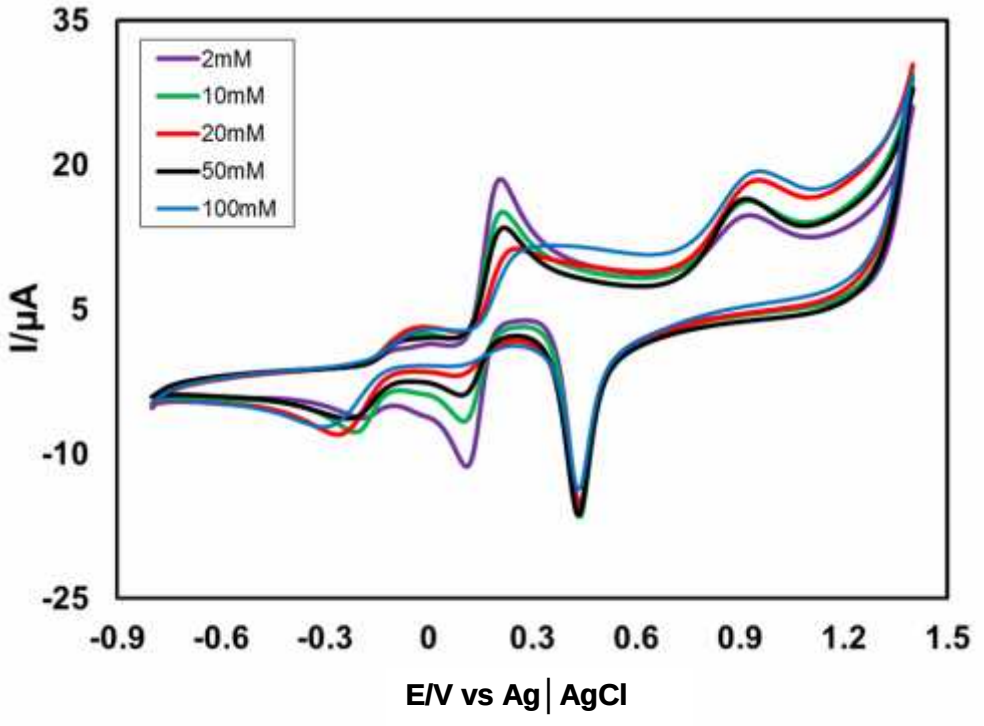

Fig. 4.74: CV of composition changes of L-Phenylalanine (2, 10, 20, 50 and 100 mM) with fixed 2 mM 1,2-dihydroxybenzene of Au electrode at pH 7 and scan rate 0.1 V/s.

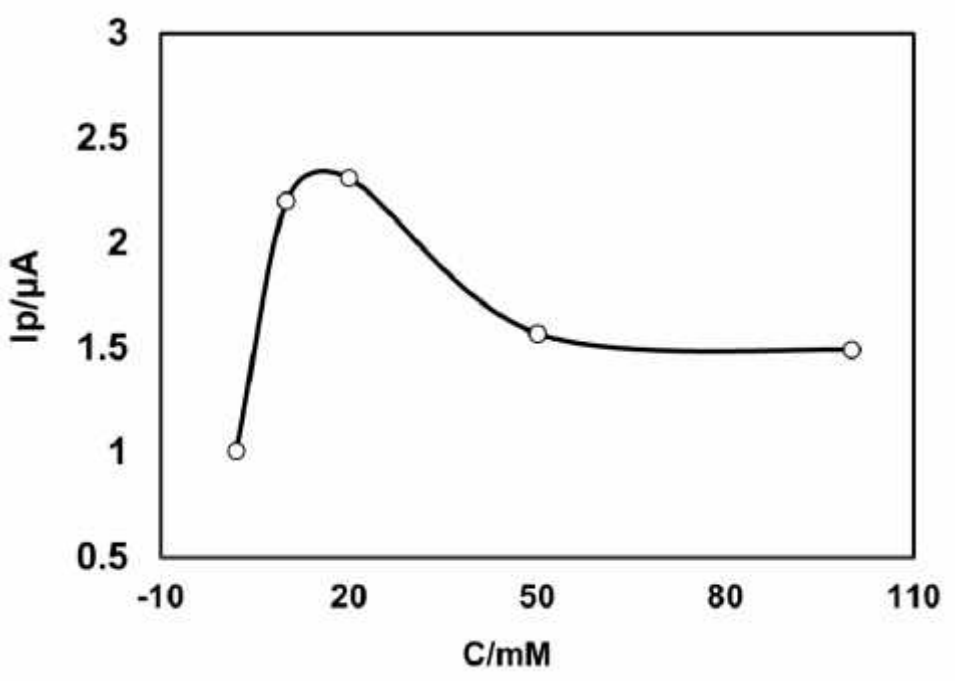

Fig. 4.75: Plots of peak current (I_p) versus concentration (C) of L-Phenylalanine (2, 10, 20, 50 and 100 mM) with fixed 2 mM 1,2-dihydroxybenzene of Au electrode in buffer solution (pH 3) at scan rate 0.1 V/s (2^{nd} cycle).

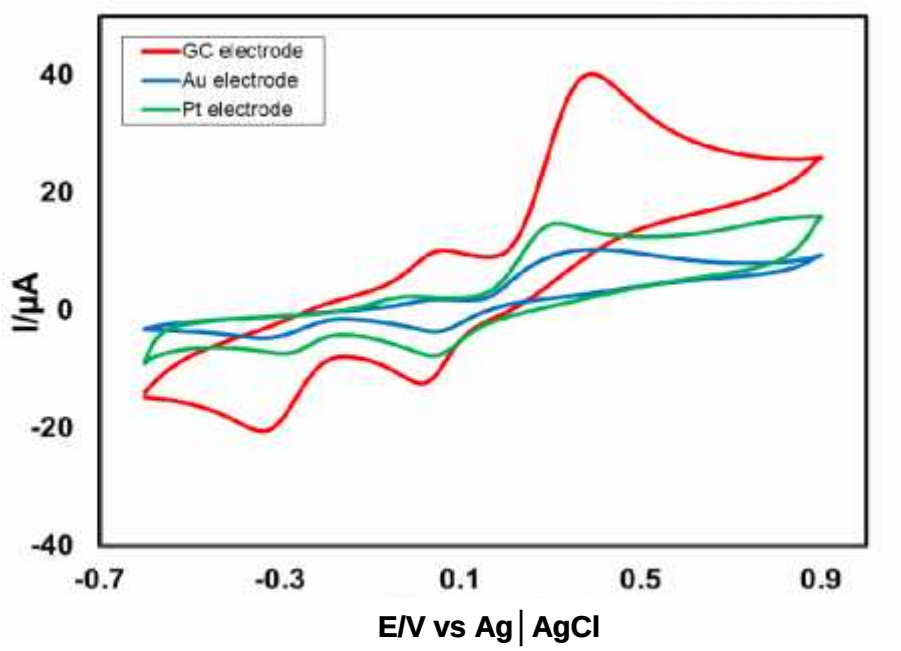

Fig. 4.76: Cyclic voltammogram (CV) of 2 mM 1,2-dihydroxybenzene with 50 mM L-Phenylalanine in GC electrode (3.0mm), Gold electrode (1.6mm) and Platinum electrode (1.6mm) at pH 7 and scan rate 0.1 V/s.

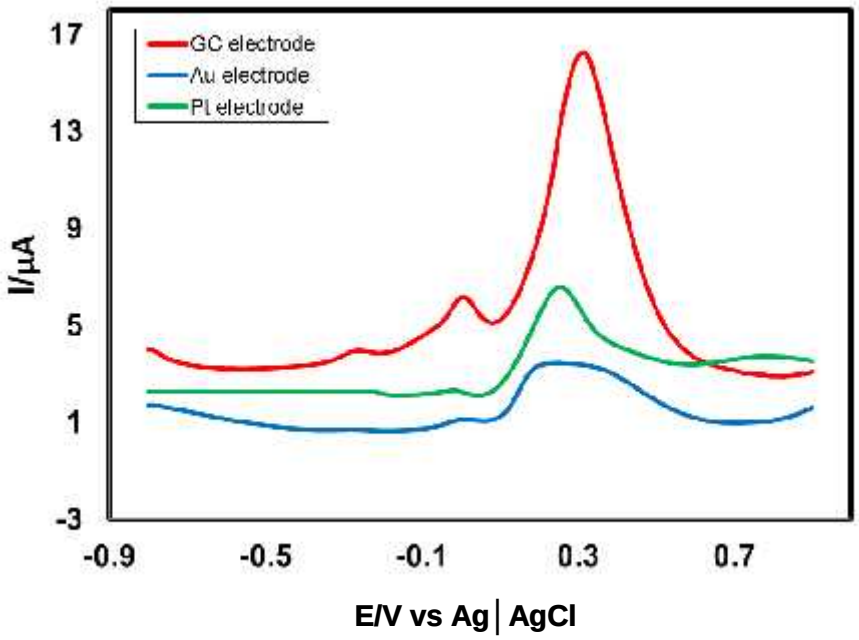

Fig. 4.77: Differential pulse voltammogram (DPV) of 2 mM 1,2-dihydroxybenzene with 20 mM L-Phenylalanine in GC electrode (3.0mm), Gold electrode (1.6mm) and Platinum electrode (1.6mm) at pH 7 and scan rate 0.1 V/s.

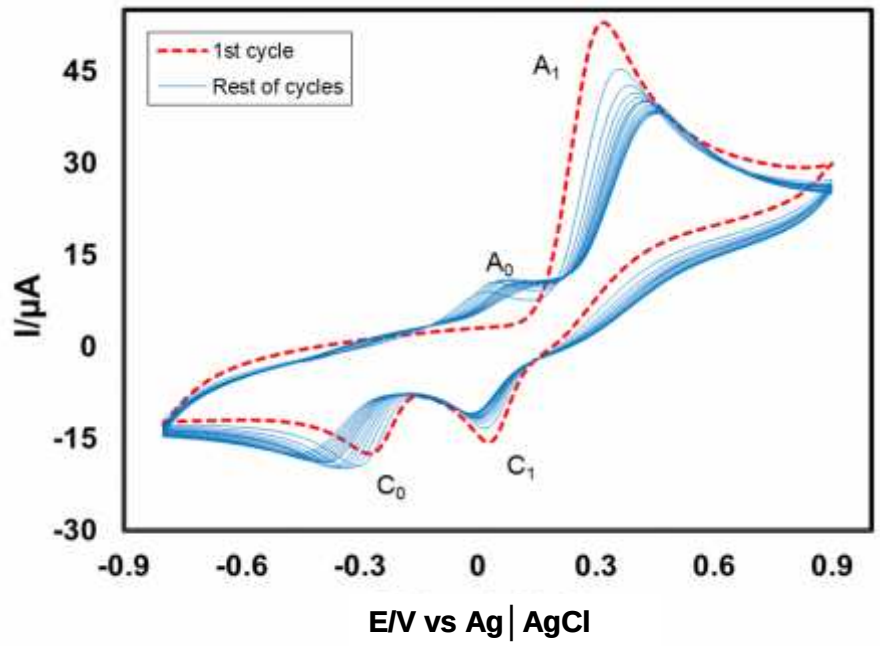

Fig. 4.78: Cyclic voltammogram of 2 mM 1,2-dihydroxybenzene with 20 mM L-Phenylalanine of GC (3mm) electrode in the buffer solution of pH 7 at scan rate 0.1 V/s (15 cycles). The appeared anodic peak current (A_0) and cathodic peak current (C_0) increased with the iteration scan from the first cycle.

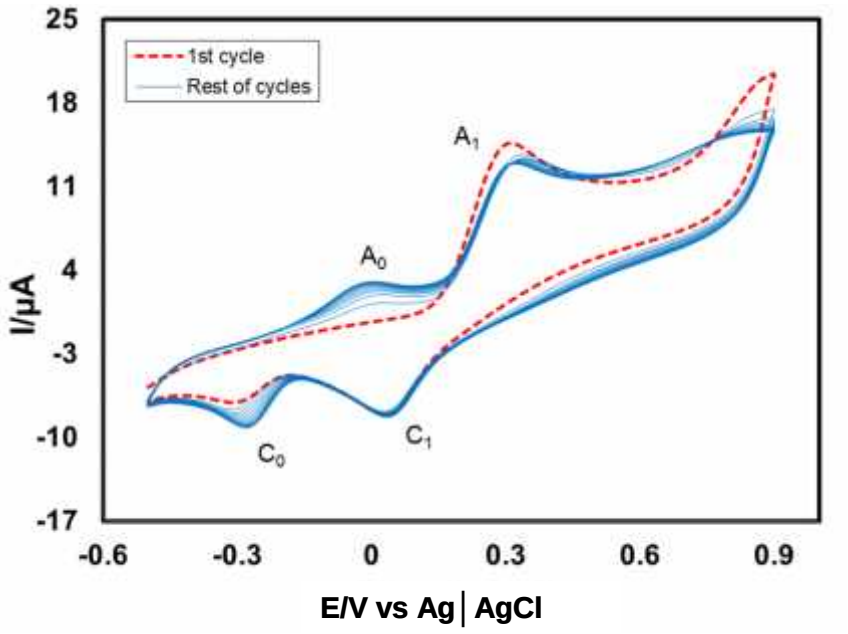

Fig. 4.79: Cyclic voltammogram of 2 mM 1,2-dihydroxybenzene with 20 mM L-Phenylalanine of Pt electrode in the buffer solution of pH 7 at scan rate 0.1 V/s (15 cycles). The appeared anodic peak current (A_0) and cathodic peak current (C_0) increased with the iteration scan from the first cycle.

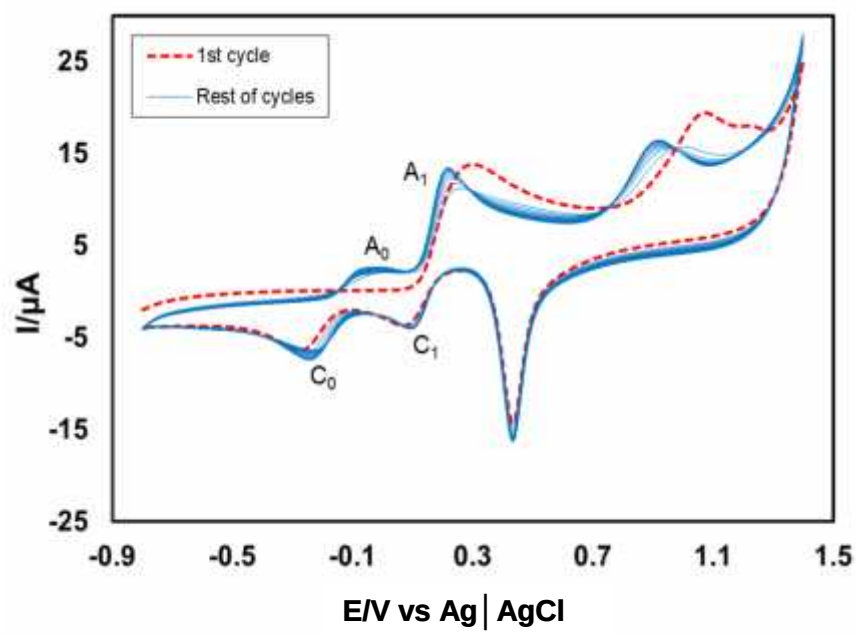

Fig. 4.80: Cyclic voltammogram of 2 mM 1,2-dihydroxybenzene with 20 mM L-Phenylalanine of Au electrode in the buffer solution of pH 7 at scan rate 0.1 V/s (15 cycles). The appeared anodic peak current (A_0) and cathodic peak current (C_0) increased with the iteration scan from the first cycle.

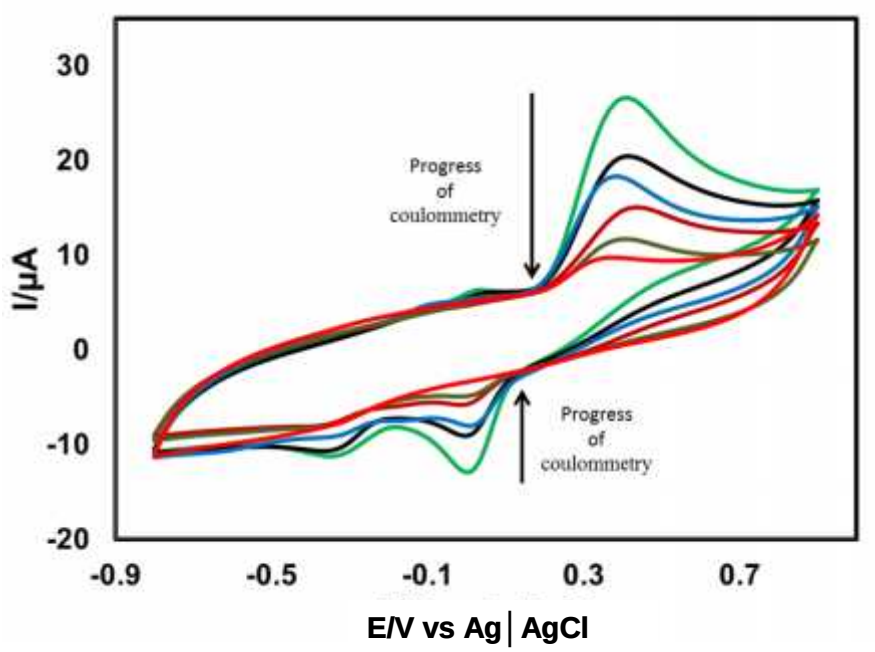

Fig. 4.81: Cyclic voltammogram and (CV) of 1 mM 1,2-dihydroxybenzene in presence of 10 mM L-Phenylalanine of GC electrode during controlled potential coulometry at 0.4 V in pH 7 at scan rate 0.1 V/s.

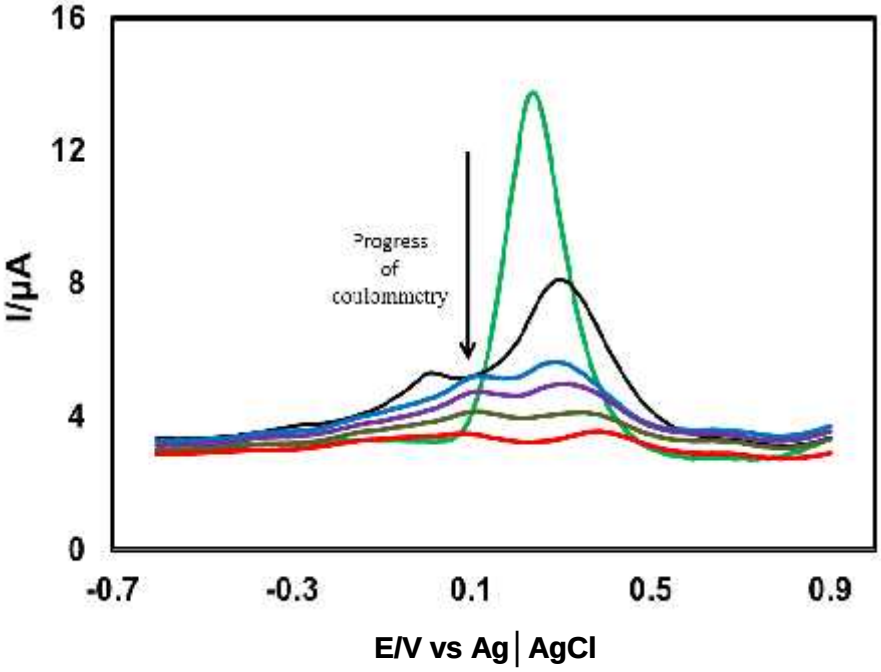

Fig. 4.82: Differential pulse voltammogram (DPV) of 1 mM 1,2-dihydroxybenzene in presence of 10 mM L-Phenylalanine of GC electrode during controlled potential coulometry at 0.4 V in pH 7 at scan rate 0.1 V/s.

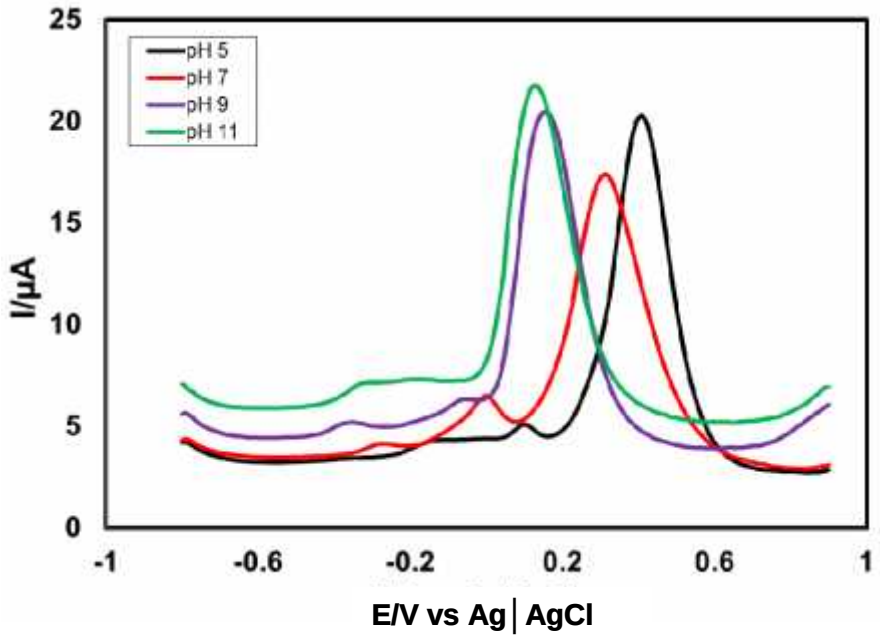

Fig. 4.83: Differential pulse voltammogram (DPV) of 2 mM 1,2-dihydroxybenzene with 20 mM L-Phenylalanine of GC electrode in second scan of different pH (5, 7, 9 and 11) and scan rate 0.1 V/s.

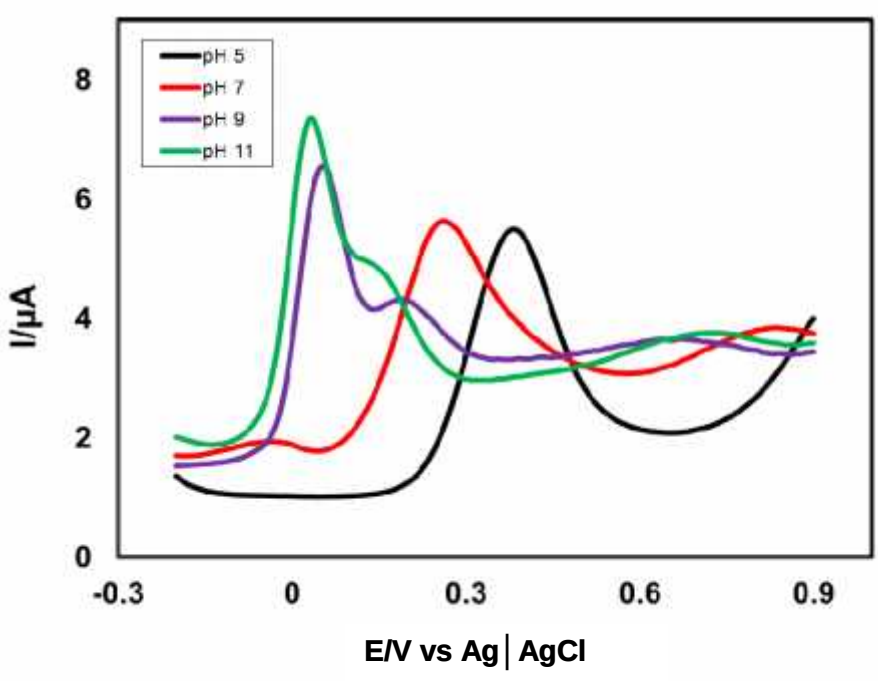

Fig. 4.84: Differential pulse voltammogram (DPV) of 2 mM 1,2-dihydroxybenzene with 20 mM L-Phenylalanine of Pt electrode in second scans of different pH (5, 7, 9 and 11) and scan rate 0.1 V/s.

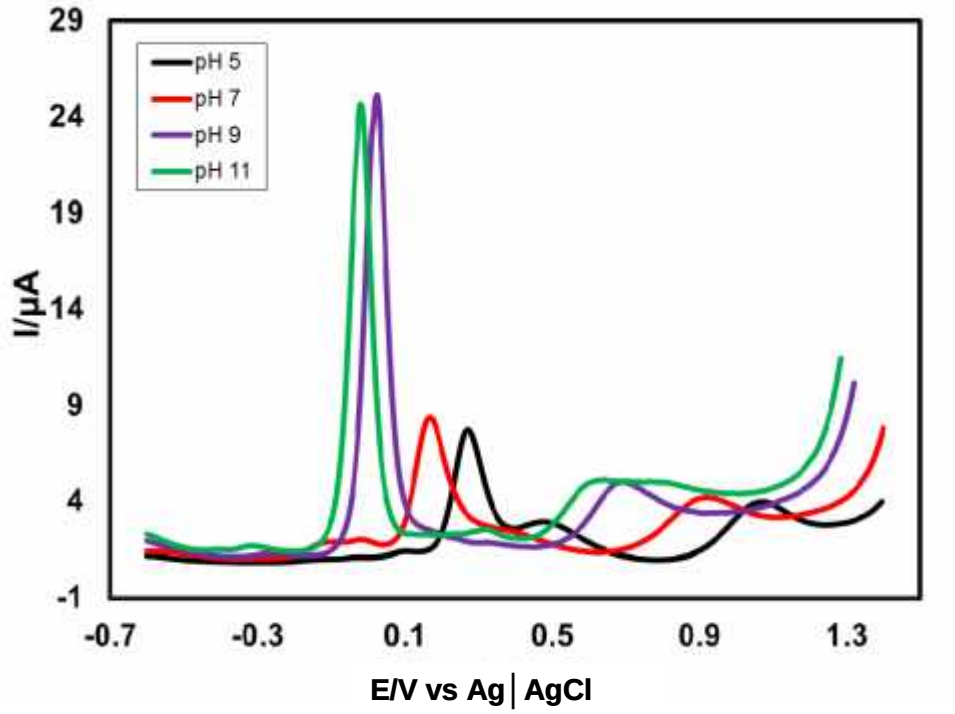

Fig. 4.85: Differential pulse voltammogram (DPV) of 2 mM 1,2-dihydroxybenzene with 20 mM L-Phenylalanine of Au electrode in second scans of different pH (5, 7, 9 and 11) and scan rate 0.1 V/s.

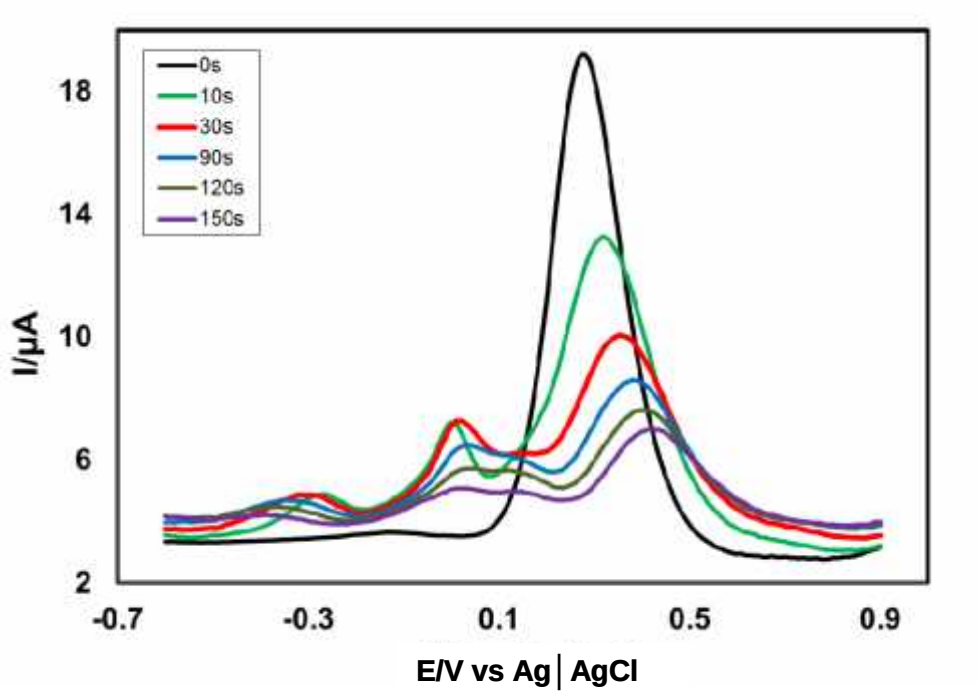

Fig. 4.86: Differential pulse voltammogram (DPV) of deposition time change (0, 10, 30, 60, 90,120 and 150s) of 2 mM 1,2-dihydroxybenzene with 20 mM L-Phenylalanine of pH 7 at *E*puls 0.02 V, tpuls 20 ms and scan rate 0.1 Vs^{-1}.

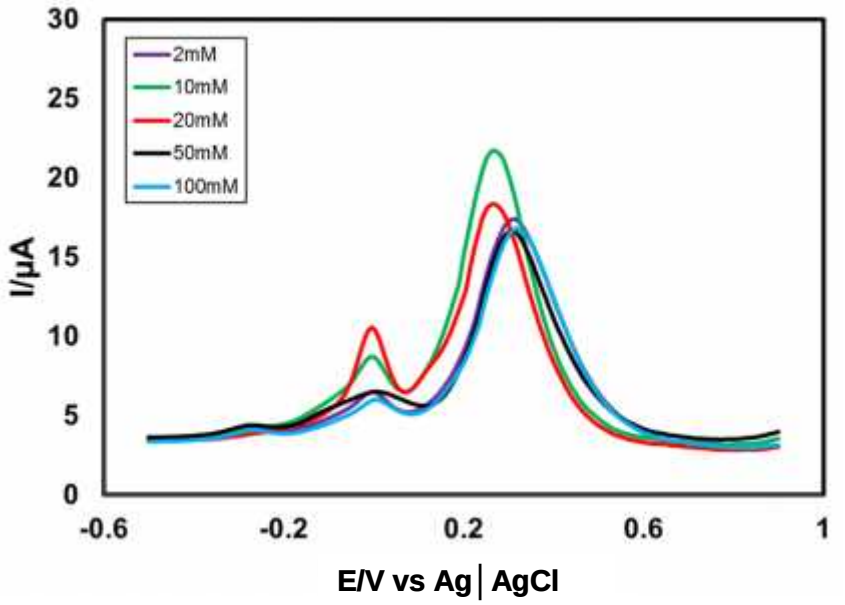

Fig. 4.87: Differential pulse voltammogram (DPV) of composition change of L-Phenylalanine (2, 10, 20, 50 and 100 mM) with the fixed composition of 2 mM 1,2-dihydroxybenzene in second scan of pH 7 at *E*puls 0.02 V, tpuls 20 ms of GC electrode and scan rate 0.1 Vs^{-1}.

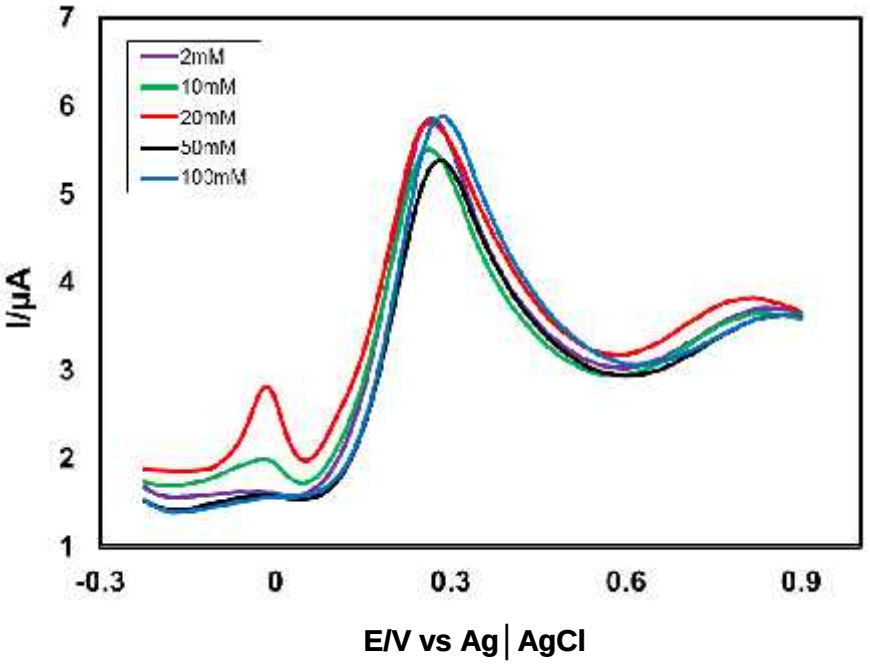

Fig. 4.88: Differential pulse voltammogram (DPV) of composition change of L-Phenylalanine (2, 10, 20, 50 and 100 mM) with the fixed composition of 2 mM 1,2-dihydroxybenzene in second scan of pH 7 at *E*puls 0.02 V, tpuls 20 ms of Pt electrode and scan rate 0.1 Vs^{-1}.

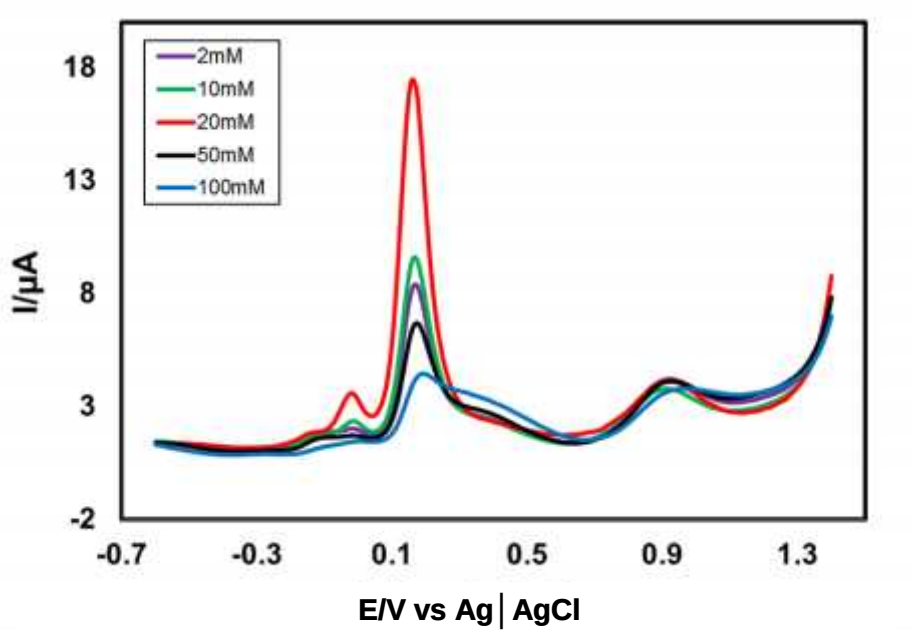

Fig. 4.89: Differential pulse voltammogram (DPV) of composition change of L-Phenylalanine (2, 10, 20, 50 and 100 mM) with the fixed composition of 2 mM 1,2-dihydroxybenzene in second scan of pH 7 at *E*puls 0.02 V, tpuls 20 ms of Au electrode and scan rate 0.1 V/s.

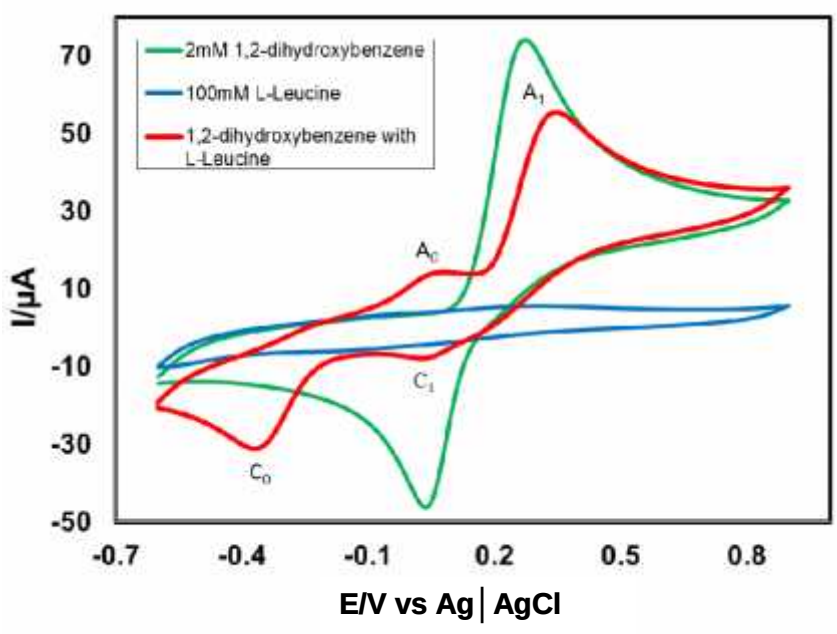

Fig. 4.90: Cyclic voltammogram of 2 mM 1,2-dihydroxybenzene (green line), 100 mM L-Leucine (blue line) and 2 mM 1,2-dihydroxybenzene with 100 mM L-Leucine (red line) of GC electrode in buffer solution (pH 7) at scan rate 0.1 V/s (2nd cycle). A_0 is appeared anodic peak and C_0 is corresponding cathodic peak.

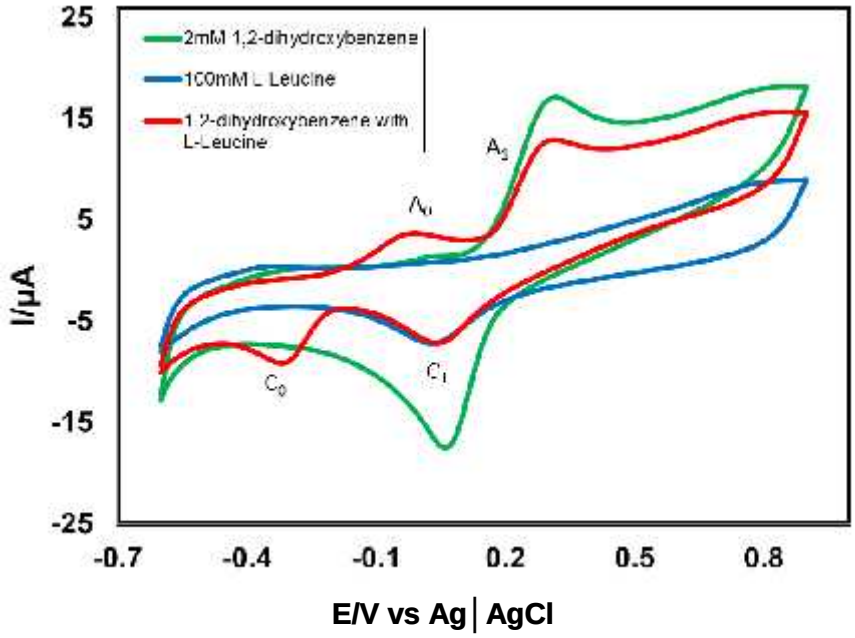

Fig. 4.91: Cyclic voltammogram of 2 mM 1,2-dihydroxybenzene (green line), 100 mM L-Leucine (blue line) and 2 mM 1,2-dihydroxybenzene with 100 mM L-Leucine (red line) of Pt electrode in buffer solution (pH 7) at scan rate 0.1 V/s (2nd cycle). A_0 is appeared anodic peak and C_0 is corresponding cathodic peak.

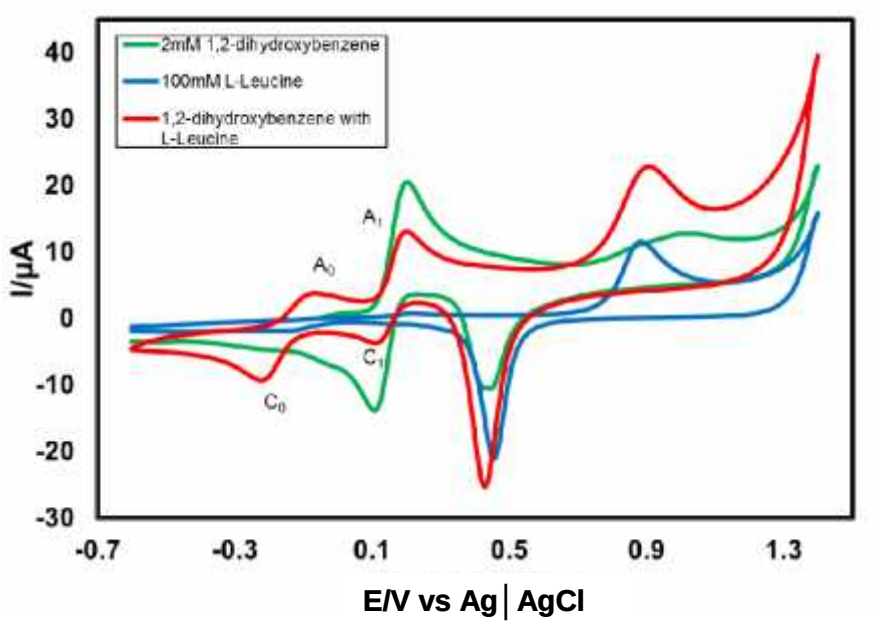

Fig. 4.92: Cyclic voltammogram of 2 mM 1,2-dihydroxybenzene (green line), 100 mM L-Leucine (blue line) and 2 mM 1,2-dihydroxybenzene with 100 mM L-Leucine (red line) of Au electrode in buffer solution (pH 7) at scan rate 0.1 V/s (2nd cycle). A_0 is appeared anodic peak and C_0 is corresponding cathodic peak.

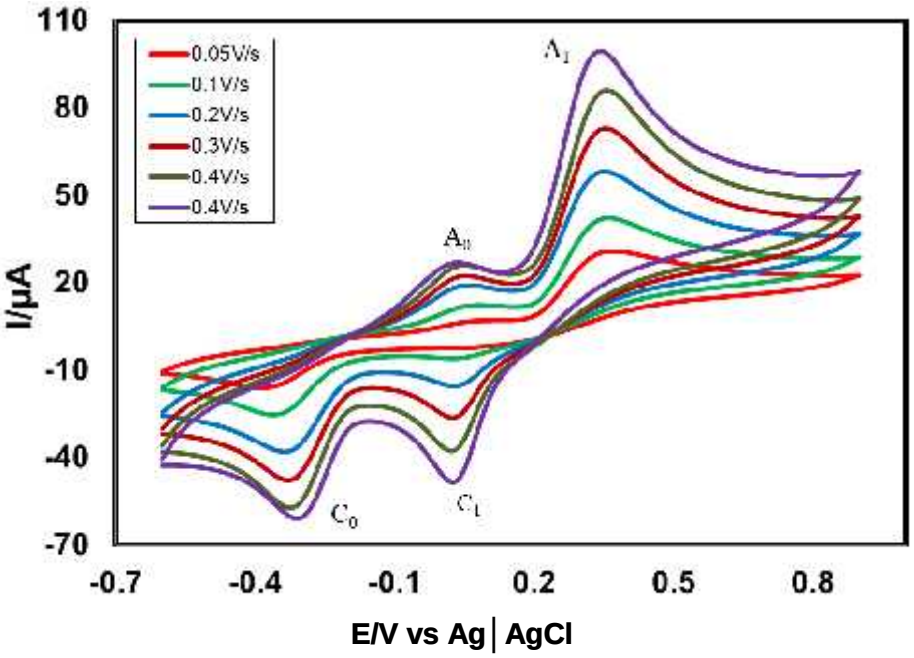

Fig. 4.93: Cyclic voltammogram of 2 mM 1,2-dihydroxybenzene with 100 mM L-Leucine in the second scan of potential at GC electrode in buffer solution (pH 7) at scan rate 0.05 V/s to 0.5 V/s.

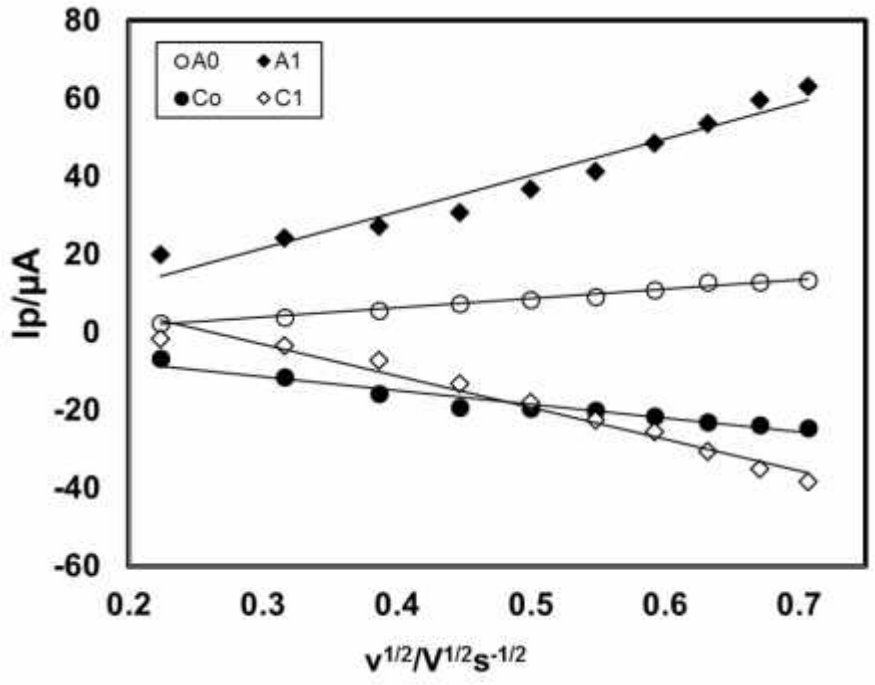

Fig. 4.94: Plots of peak current (I_p) versus square root of scan rate ($v^{1/2}$) of 2 mM 1,2-dihydroxybenzene with 100 mM L-Leucine of GC electrode in buffer solution (pH 7) (2^{nd} cycle).

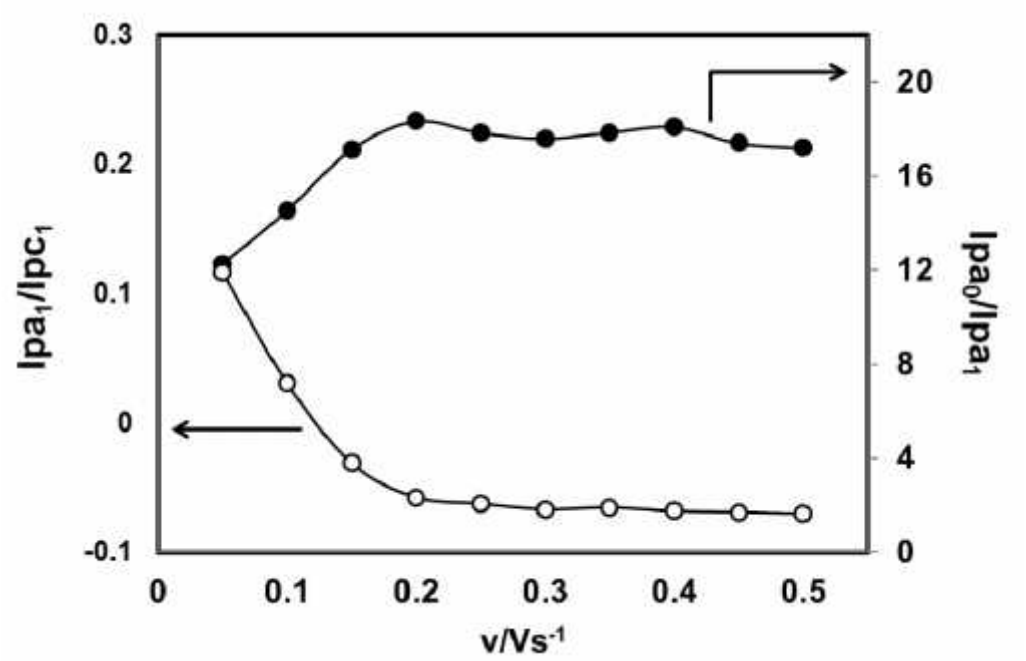

Fig. 4.95: Variation of peak current ratio of corresponding peak (I_{pa1}/I_{pc1}) and anodic peak (I_{pa0}/I_{pa1}) vs scan rate (v) of 2 mM 1,2-dihydroxybenzene with 100 mM L-Leucine of GC electrode in buffer solution (pH 7) at scan rate 0.1 V/s in the second scan of potential.

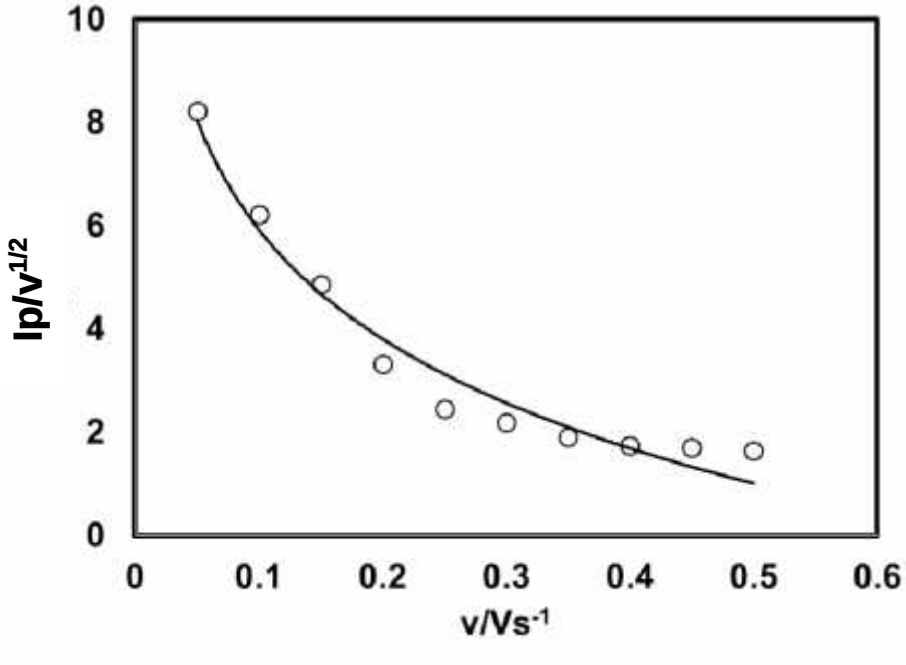

Fig. 4.96: Plot of current function ($I_p/v^{1/2}$) versus scan rate (v) of 2 mM 1,2-dihydroxybenzene with 100 mM L-Leucine of GC electrode in buffer solution (pH 7) of the Appeared anodic peak (A_0).

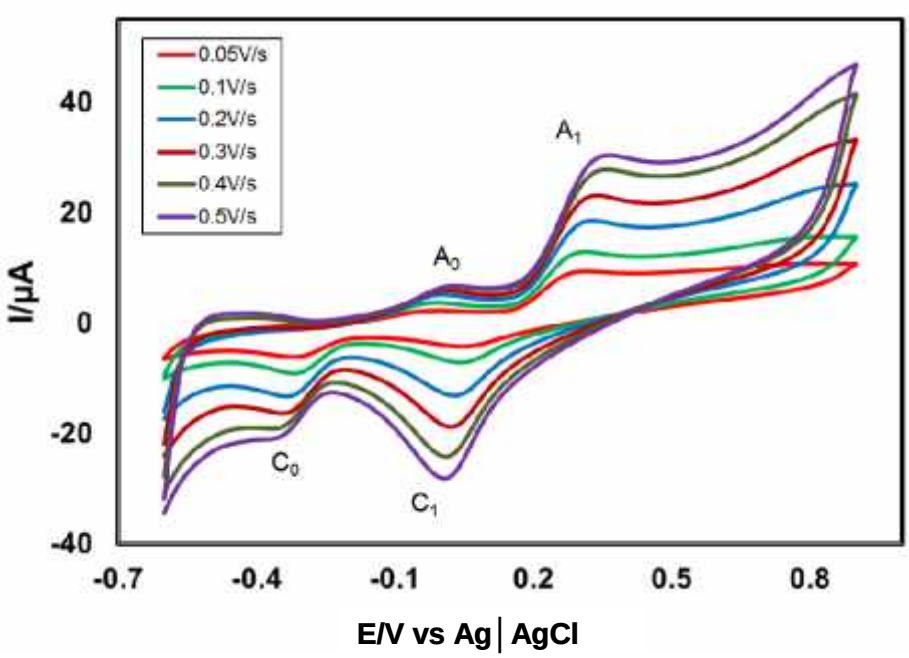

Fig. 4.97: Cyclic voltammogram of 2 mM 1,2-dihydroxybenzene with 100 mM L-Leucine in the second scan of potential at Pt electrode in buffer solution (pH 7) at scan rate 0.05 V/s to 0.5 V/s.

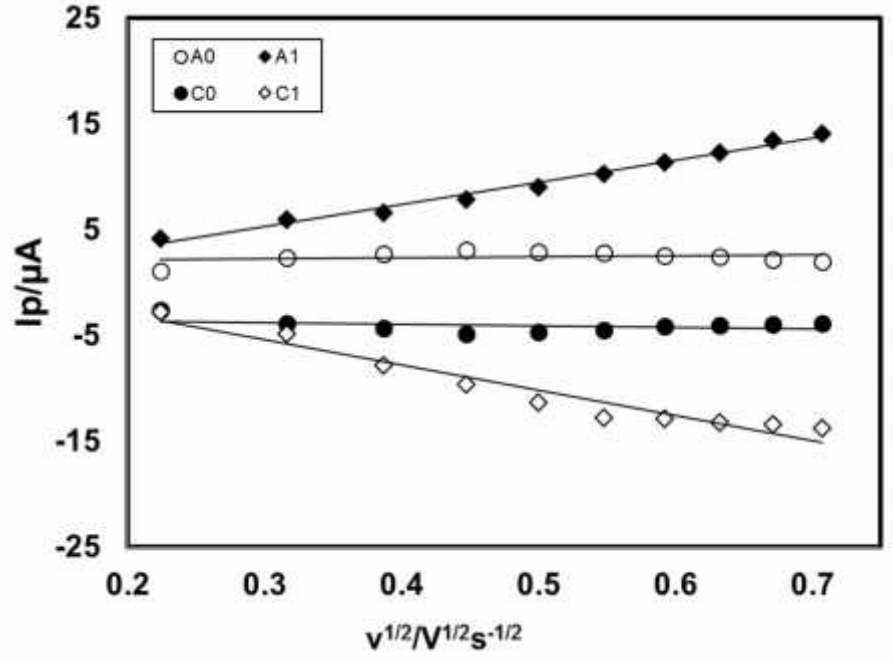

Fig. 4.98: Plots of peak current (I_p) versus square root of scan rate ($v^{1/2}$) of 2 mM 1,2-dihydroxybenzene with 100 mM L-Leucine of Pt electrode in buffer solution (pH 7) (2^{nd} cycle).

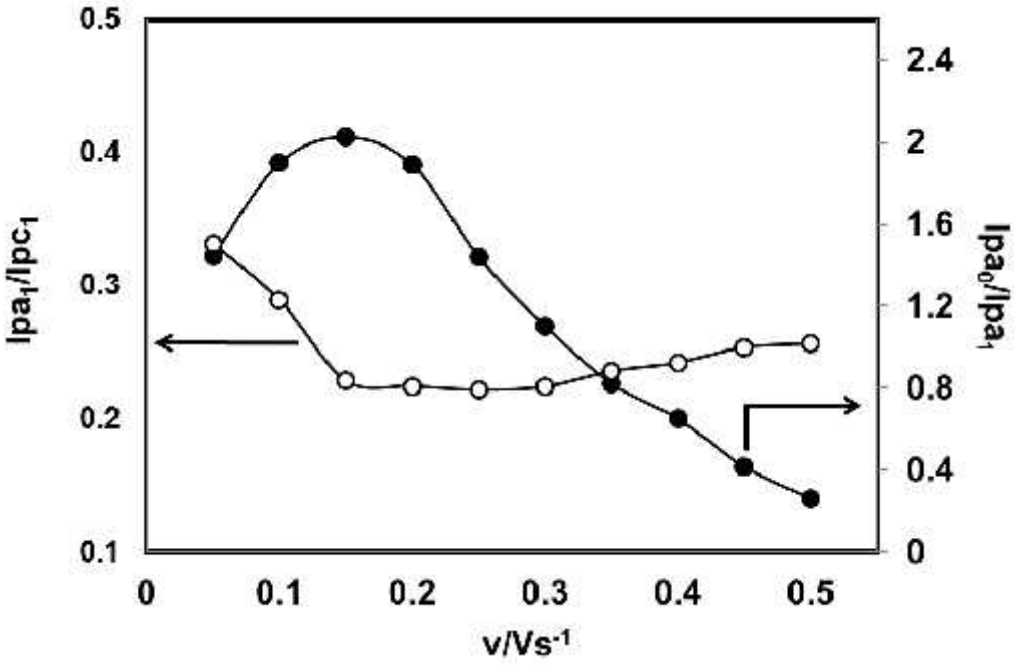

Fig. 4.99: Variation of peak current ratio of corresponding peak (I_{pa1}/I_{pc1}) and anodic peak (I_{pa0}/I_{pa1}) vs scan rate (v) of 2 mM 1,2-dihydroxybenzene with 100 mM L-Leucine of Pt electrode in buffer solution (pH 7) at scan rate 0.1 V/s in the second scan of potential.

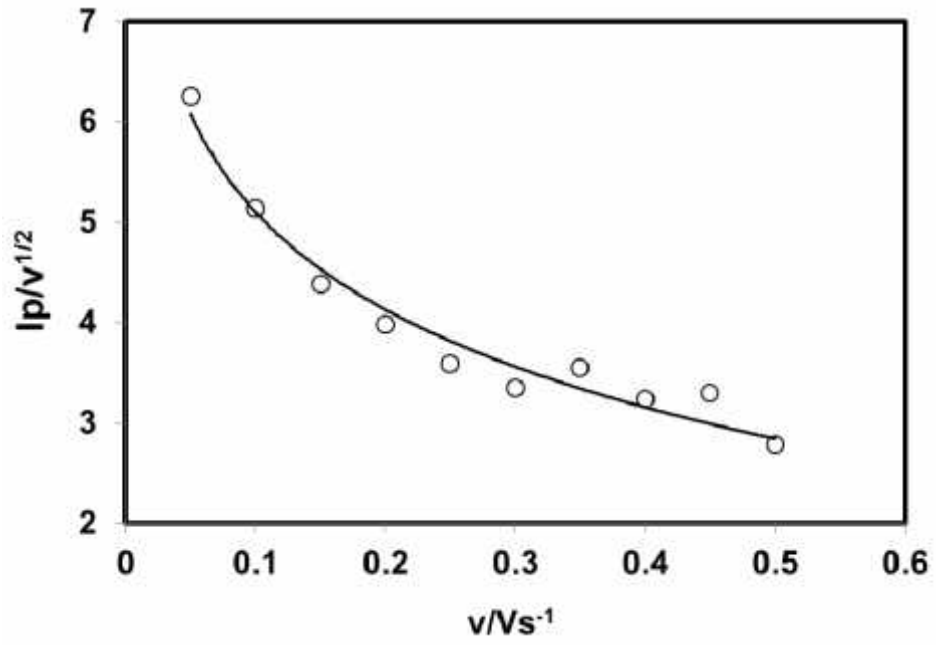

Fig. 4.100: Plots of current function ($I_p/v^{1/2}$) versus scan rate (v) of 2 mM 1,2-dihydroxybenzene with 100 mM L-Leucine of Pt electrode in buffer solution (pH 7) of the Appeared anodic peak (A_0).

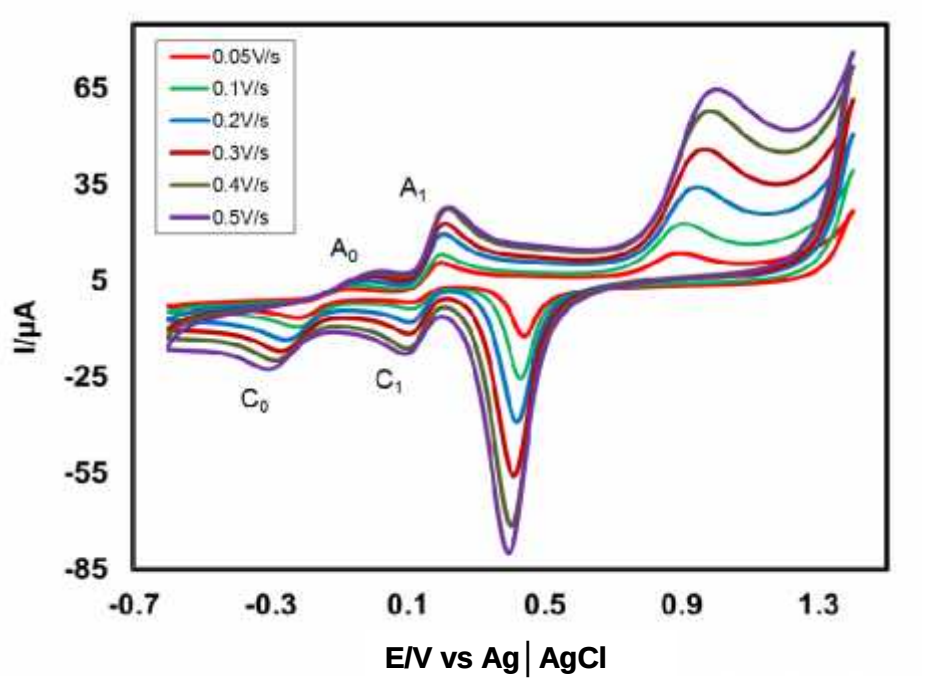

Fig. 4.101: Cyclic voltammogram of 2 mM 1,2-dihydroxybenzene with 100 mM L-Leucine in the second scan of potential at Au electrode in buffer solution (pH 7) at scan rate 0.05 V/s to 0.5 V/s.

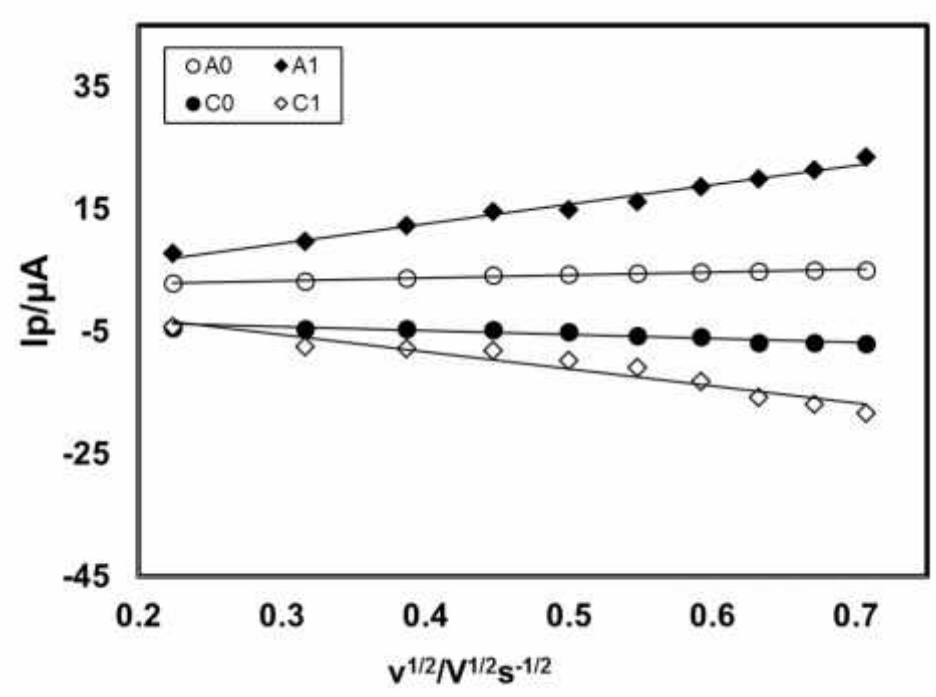

Fig. 4.102: Plots of peak current (I_p) versus square root of scan rate ($v^{1/2}$) of 2 mM 1,2-dihydroxybenzene with 100 mM L-Leucine of Au electrode in buffer solution (pH 7) (2^{nd} cycle).

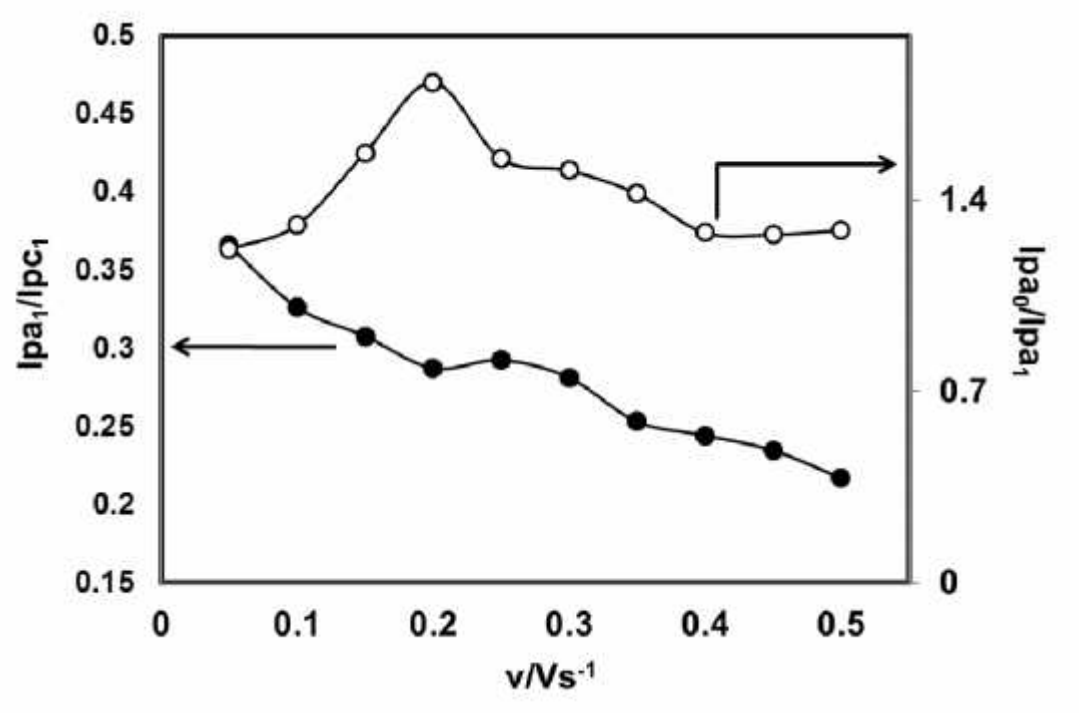

Fig. 4.103: Variation of peak current ratio of corresponding peak (I_{pa1}/I_{pc1}) and anodic peak (I_{pa0}/I_{pa1}) vs scan rate (v) of 2 mM 1,2-dihydroxybenzene with 100 mM L-Leucine of Au electrode in buffer solution (pH 7) at scan rate 0.1 V/s in the second scan of potential.

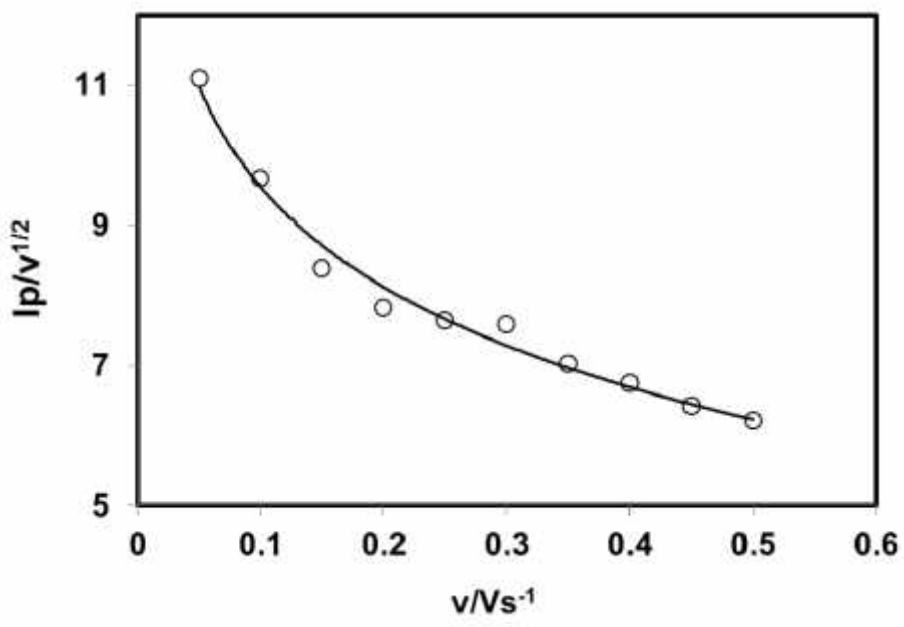

Fig. 4.104: Plots of current function ($I_p/v^{1/2}$) versus scan rate (v) of 2 mM 1,2-dihydroxybenzene with 100 mM L-Leucine of Au electrode in buffer solution (pH 7) of the Appeared anodic peak (A_0).

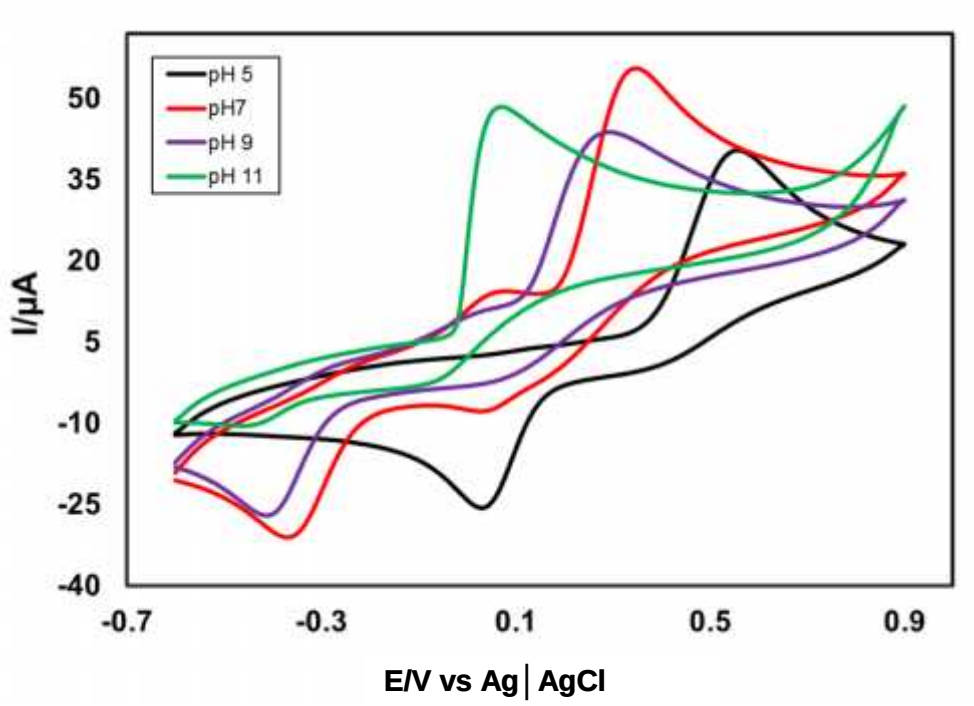

Fig. 4.105: Cyclic voltammogram of 2 mM 1,2-dihydroxybenzene with 100 mM L-Leucine of GC (3 mm) electrode in different pH (5, 7, 9 and 11) at scan rate 0.1 V/s.

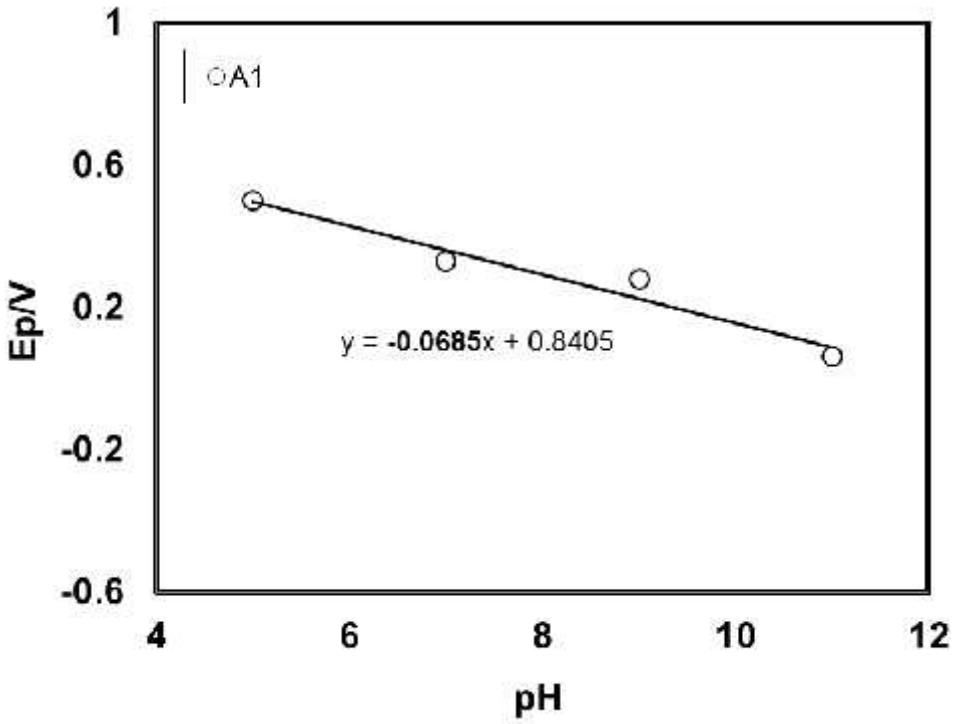

Fig. 4.106: Plots of peak potential (E_p) versus pH (5, 7, 9 and 11) of 2 mM 1,2-dihydroxybenzene with 100 mM L-Leucine of GC electrode at scan rate 0.1 V/s (2^{nd} cycle).

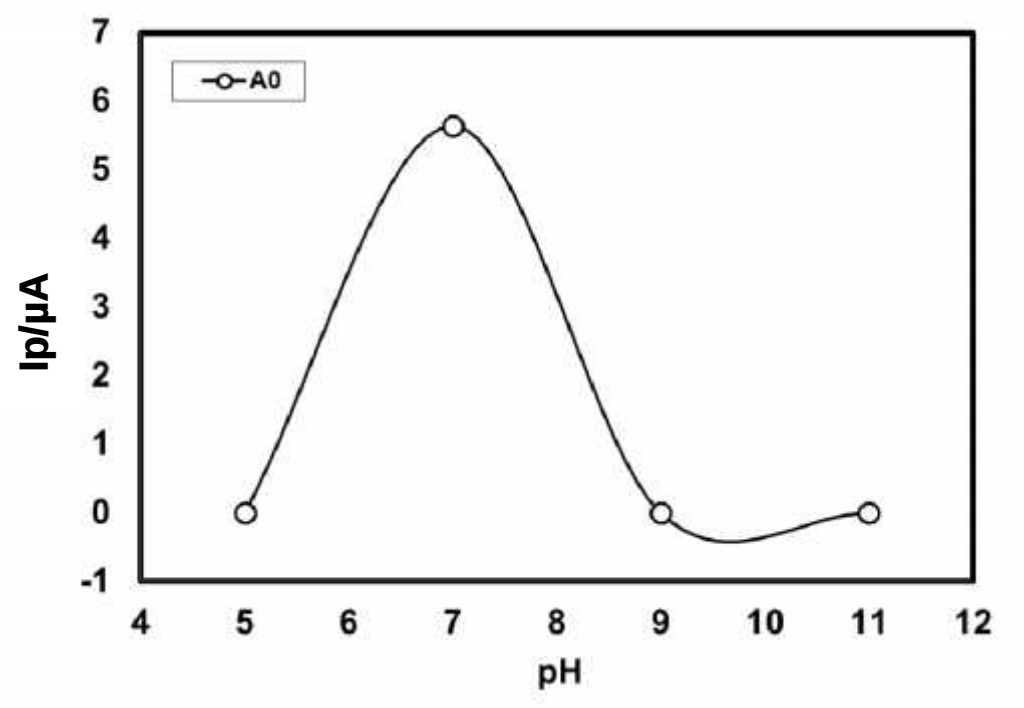

Fig. 4.107: Plot of peak current (I_p) versus pH (5, 7, 9 and 11) of 2 mM 1,2-dihydroxybenzene with 100 mM L-Leucine of GC electrode at scan rate 0.1 V/s (2nd cycle).

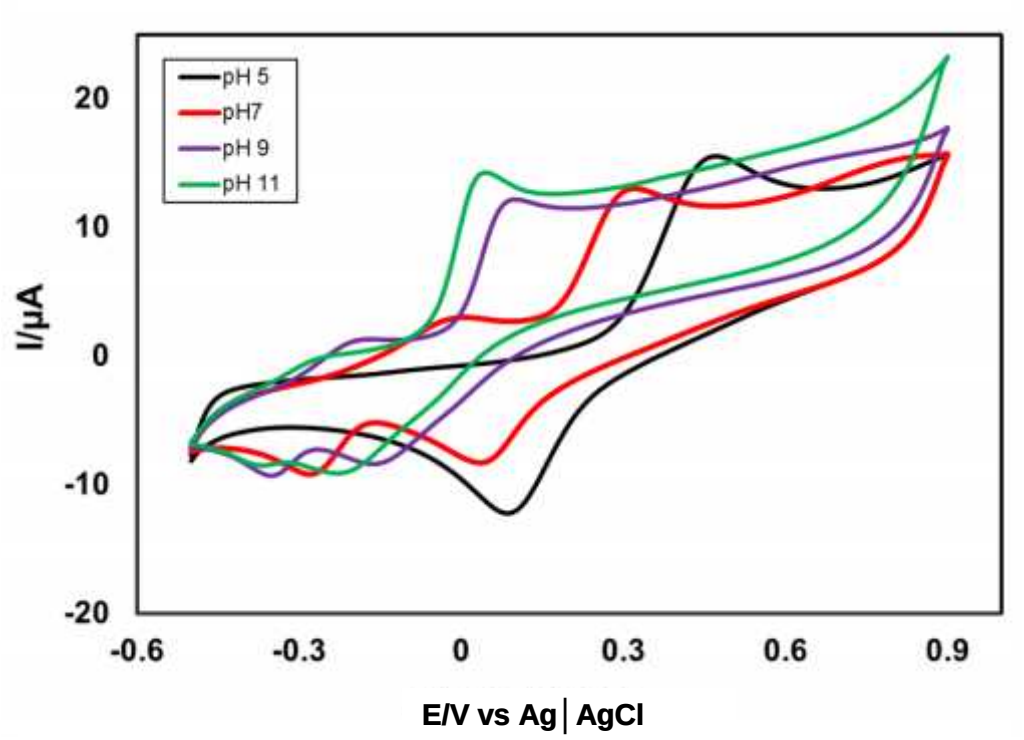

Fig. 4.108: Cyclic voltammogram of 2 mM 1,2-dihydroxybenzene with 100 mM L-Leucine of Pt electrode in different pH (5, 7, 9 and 11) at scan rate 0.1 V/s.

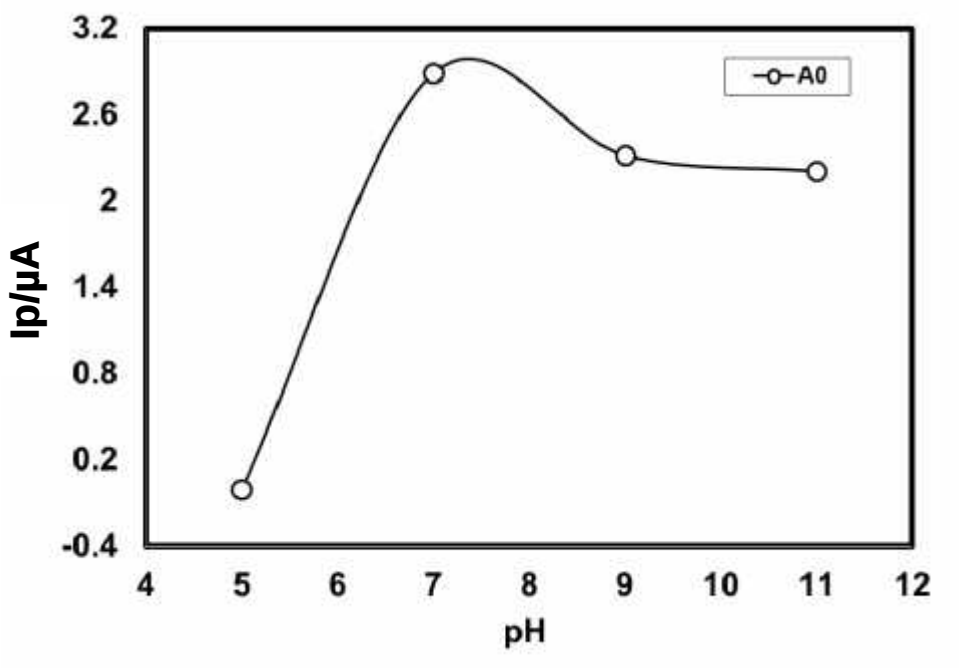

Fig. 4.109: Plots of peak current (I_p) versus pH (5, 7, 9 and 11) of 2 mM 1,2-dihydroxybenzene with 100 mM L-Leucine of Pt electrode at scan rate 0.1 V/s (2nd cycle).

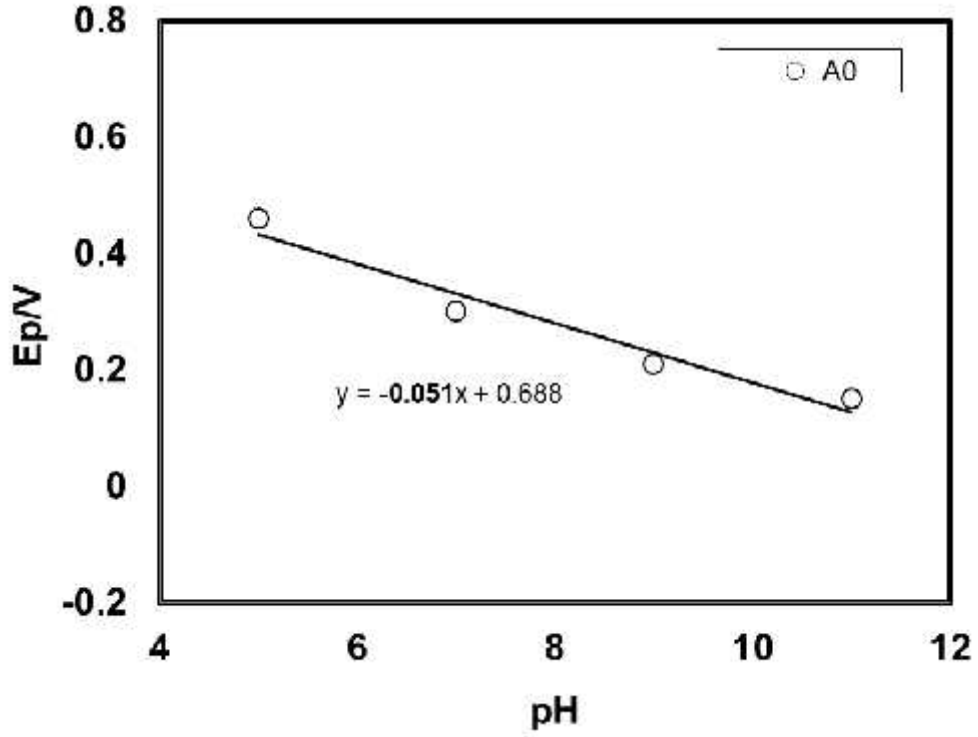

Fig. 4.110: Plot of peak potential (E_p) versus pH (5, 7, 9 and 11) of 2 mM 1,2-dihydroxybenzene with 100 mM L-Leucine of Pt electrode at scan rate 0.1 V/s (2nd cycle).

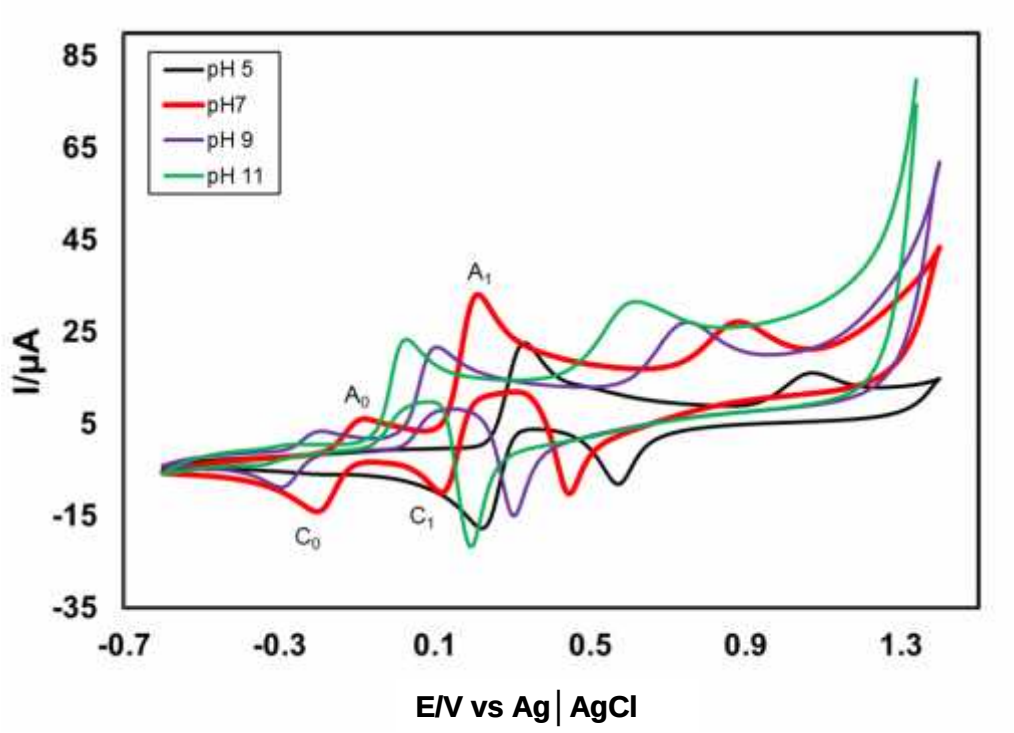

Fig. 4.111: Cyclic voltammogram of 2 mM 1,2-dihydroxybenzene with 100 mM L-Leucine of Au electrode in different pH (5, 7, 9 and 11) at scan rate 0.1 V/s.

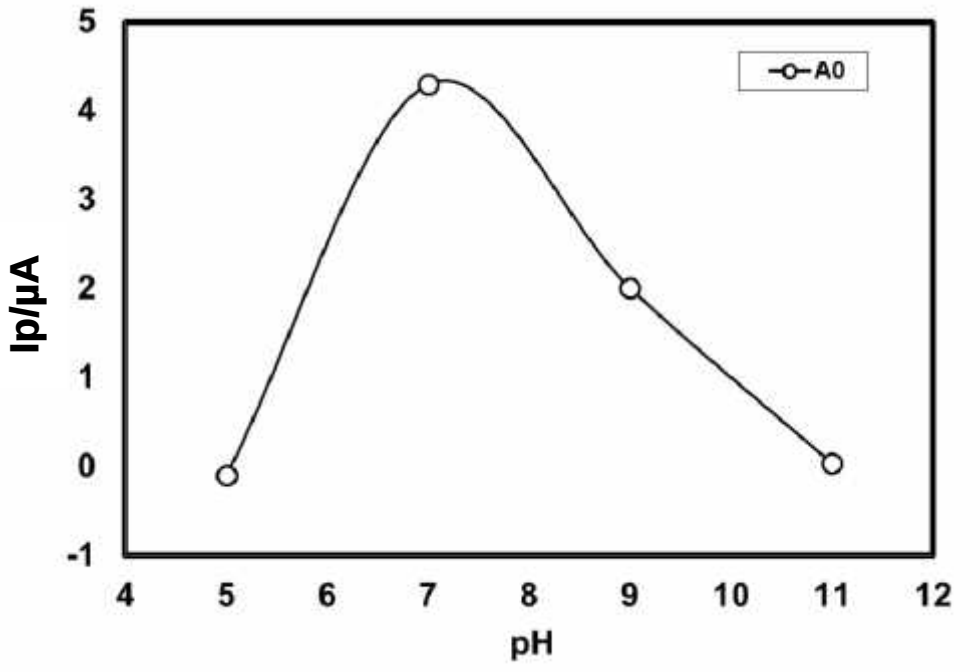

Fig. 4.112: Plots of peak current (I_p) versus pH (5, 7, 9 and 11) of 2 mM 1,2-dihydroxybenzene with 100 mM L-Leucine of Au electrode at scan rate 0.1 V/s (2nd cycle).

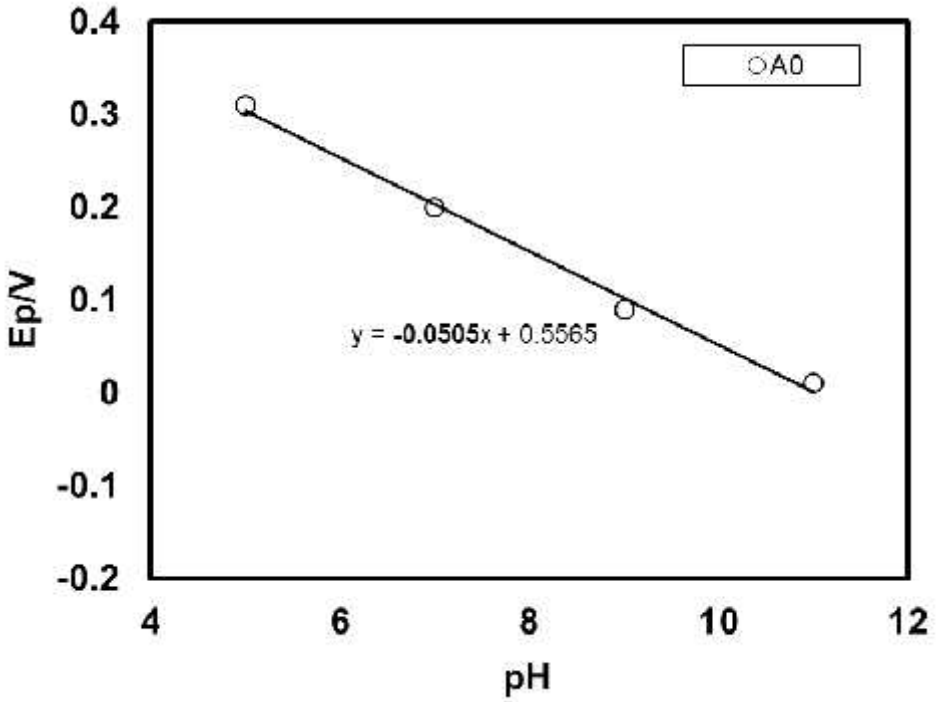

Fig. 4.113: Plot of peak potential (E_p) versus pH (5, 7, 9 and 11) of 2 mM 1,2-dihydroxybenzene with 100 mM L-Leucine of Au electrode at scan rate 0.1 V/s (2nd cycle).

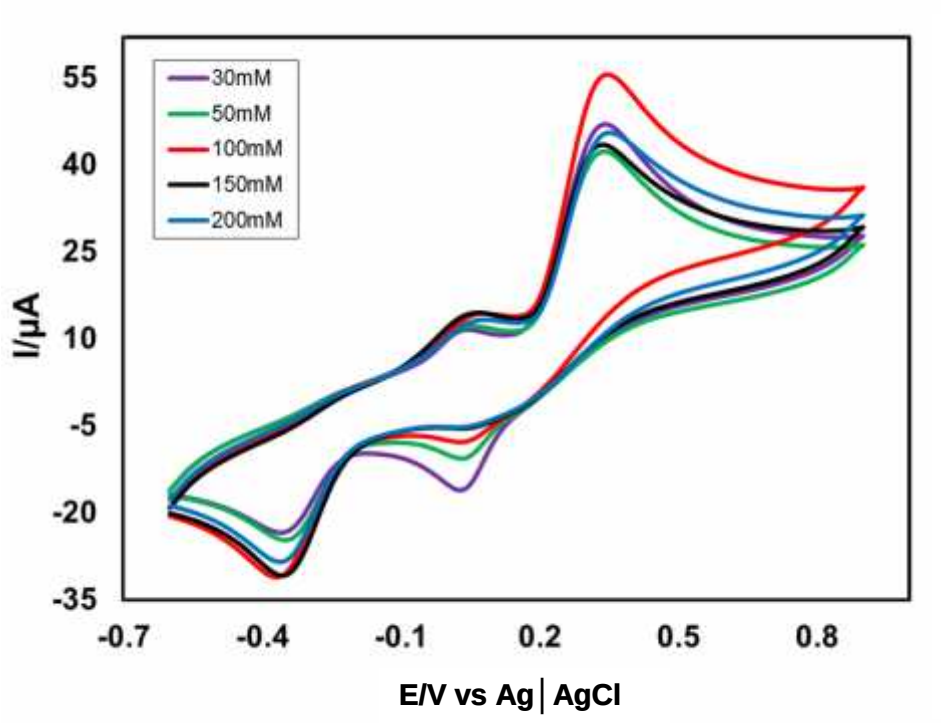

Fig. 4.114: CV of composition changes of L-Leucine (30, 50, 100, 150 and 200 mM) with fixed 2 mM 1,2-dihydroxybenzene of GC electrode at pH 7 and scan rate 0.1 V/s.

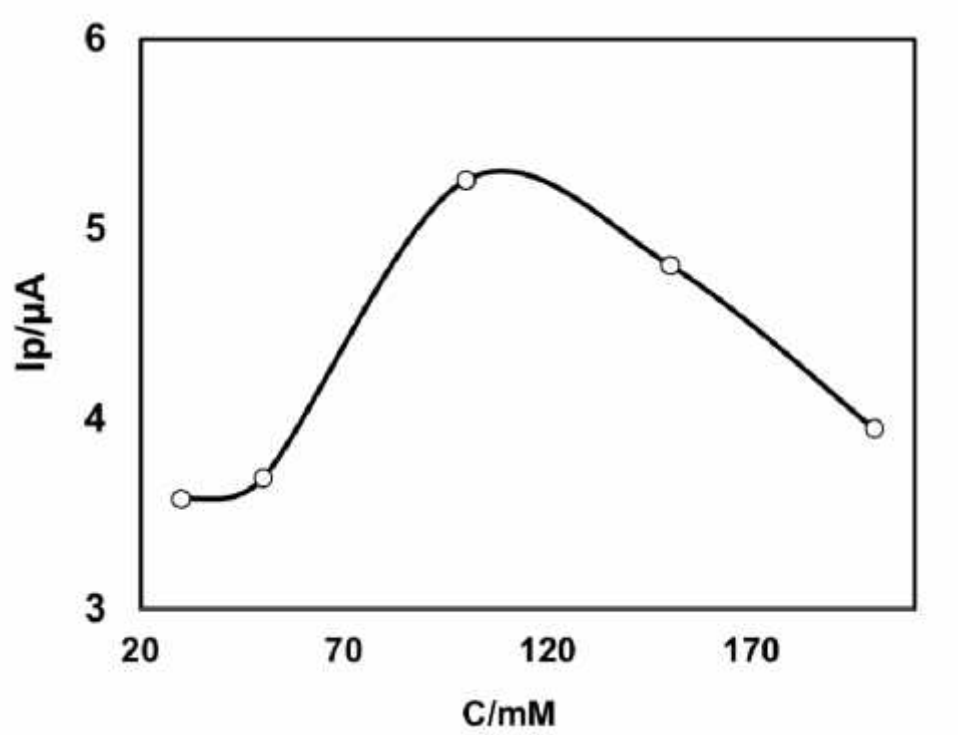

Fig. 4.115: Comparison of cyclic voltammogram of different concentration (30, 50, 100, 150 and 200 mM) of 2 mM 1,2-dihydroxybenzene with 100 mM L-Leucine of GC electrode in buffer solution (pH 7) at scan rate 0.1 V/s (2nd cycle).

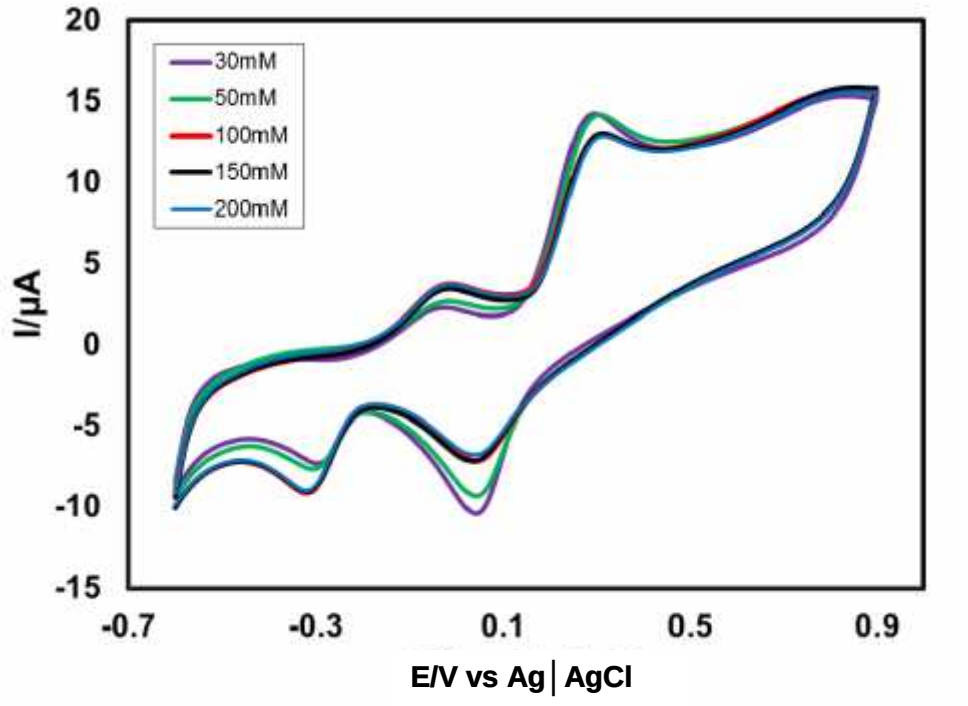

Fig. 4.116: CV of composition changes of L-Leucine (30, 50, 100, 150 and 200 mM) with fixed 2 mM 1,2-dihydroxybenzene of Pt electrode at pH 7 and scan rate 0.1 V/s.

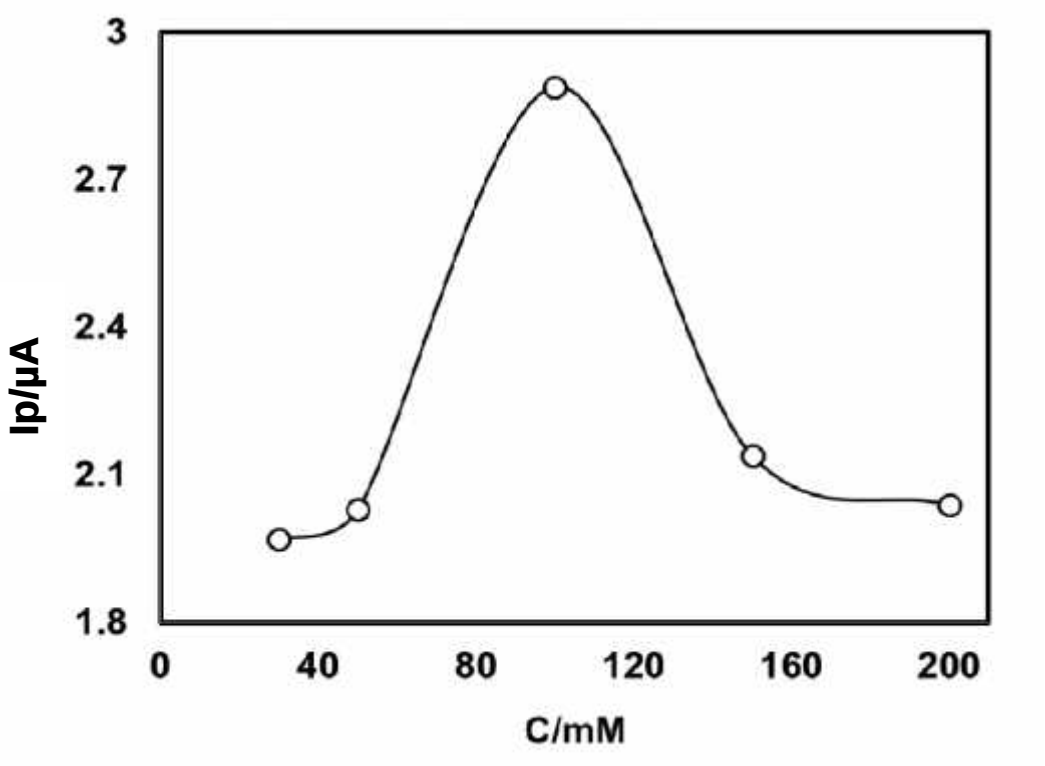

Fig. 4.117: Plots of peak current (I_p) versus concentration (C) of L-Leucine (30, 50, 100, 150 and 200 mM) with fixed 2 mM 1,2-dihydroxybenzene of Pt electrode in buffer solution (pH) at 7 scan rate 0.1 V/s (2^{nd} cycle).

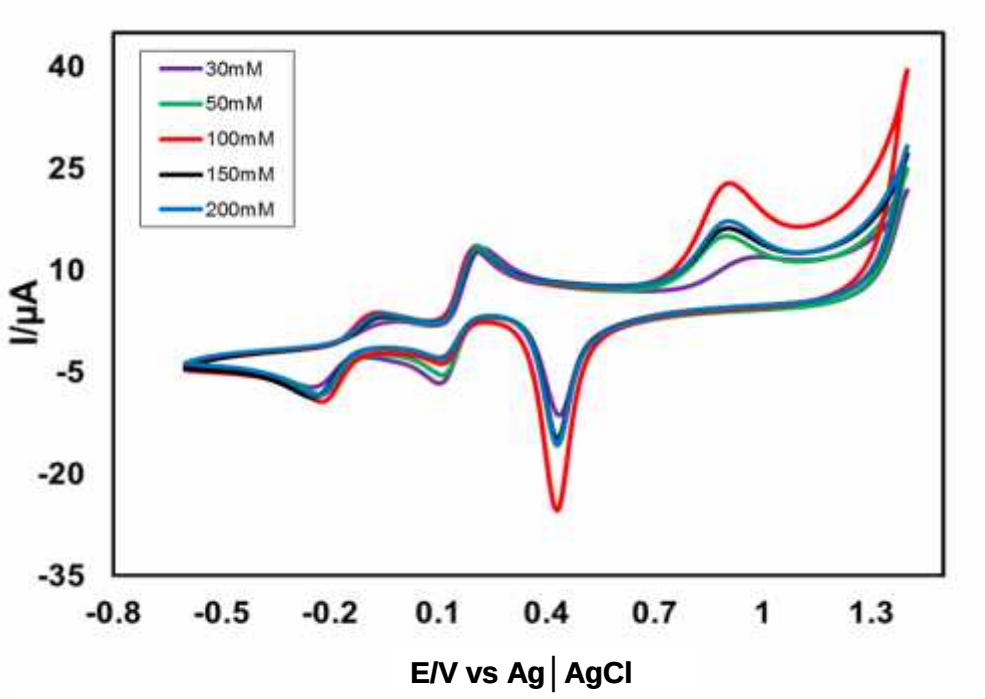

Fig. 4.118: CV of composition changes of L-Leucine (30, 50, 100, 150 and 200 mM) with fixed 2 mM 1,2-dihydroxybenzene of Au electrode at pH 7 and scan rate 0.1 V/s.

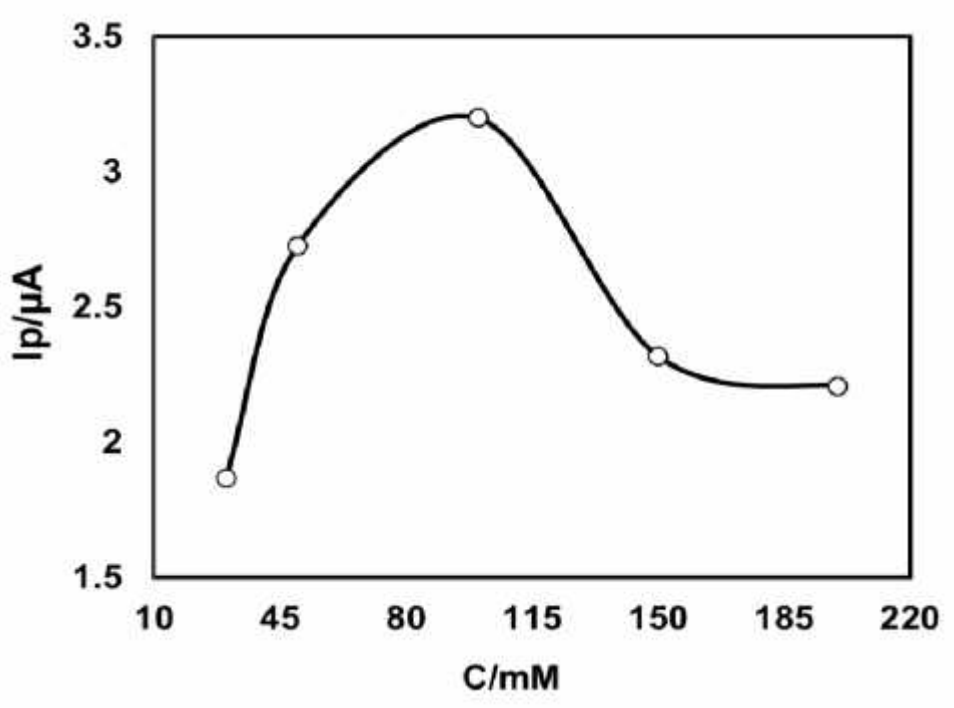

Fig. 4.119: Plots of peak current (I_p) versus concentration (C) of L-Leucine (30, 50, 100, 150 and 200 mM) with fixed 2 mM 1,2-dihydroxybenzene of Au electrode in buffer solution (pH 7) at scan rate 0.1 V/s (2^{nd} cycle).

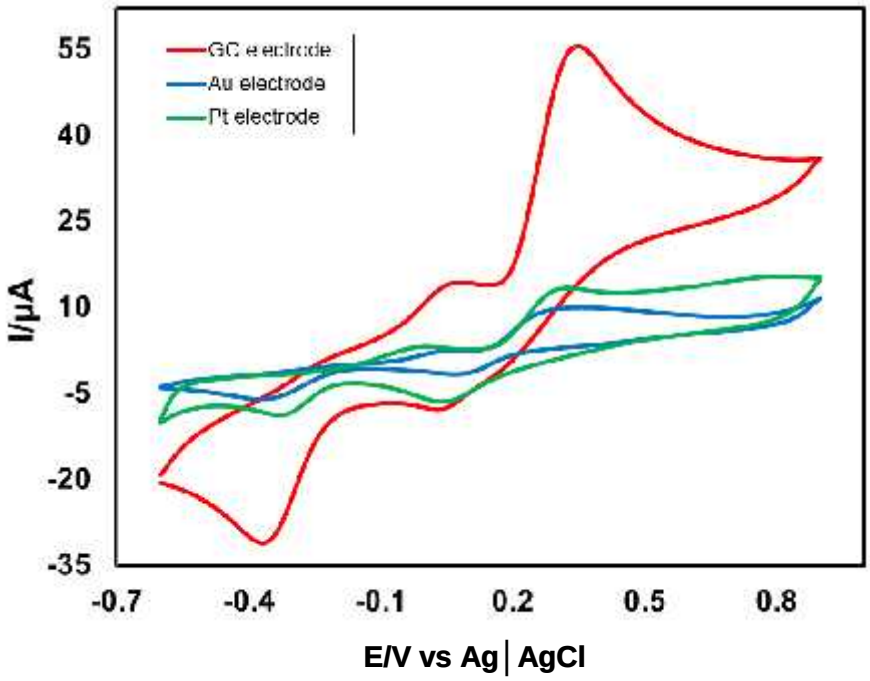

Fig. 4.120: Cyclic voltammogram (CV) of 2 mM 1,2-dihydroxybenzene with 100 mM L-Leucine in GC electrode (3.0 mm), Gold electrode (1.6 mm) and Platinum electrode (1.6 mm) at pH 7 and scan rate 0.1 V/s.

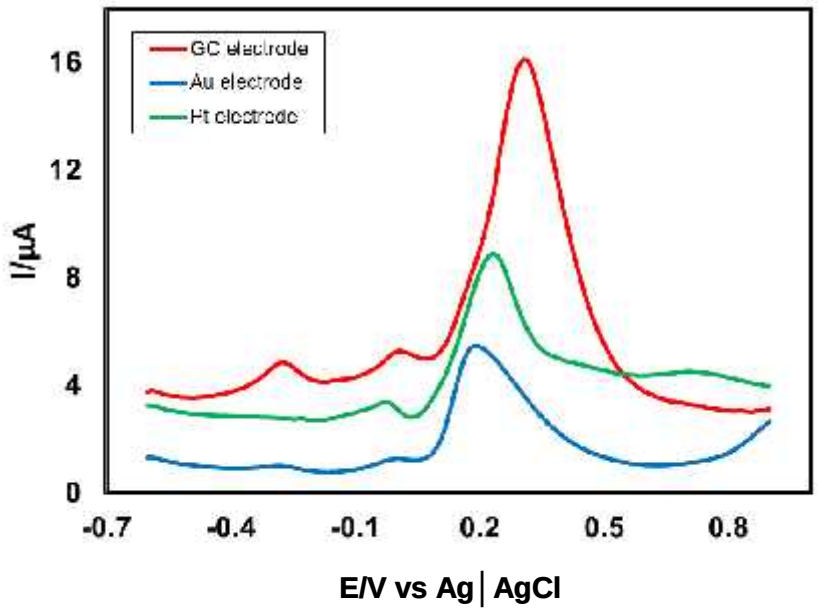

Fig. 4.121: Differential pulse voltammogram (DPV) of 2 mM 1,2-dihydroxybenzene with 100 mM L-Leucine in GC electrode (3.0 mm), Gold electrode (1.6 mm) and Platinum electrode (1.6 mm) at pH 7 and scan rate 0.1 V/s.

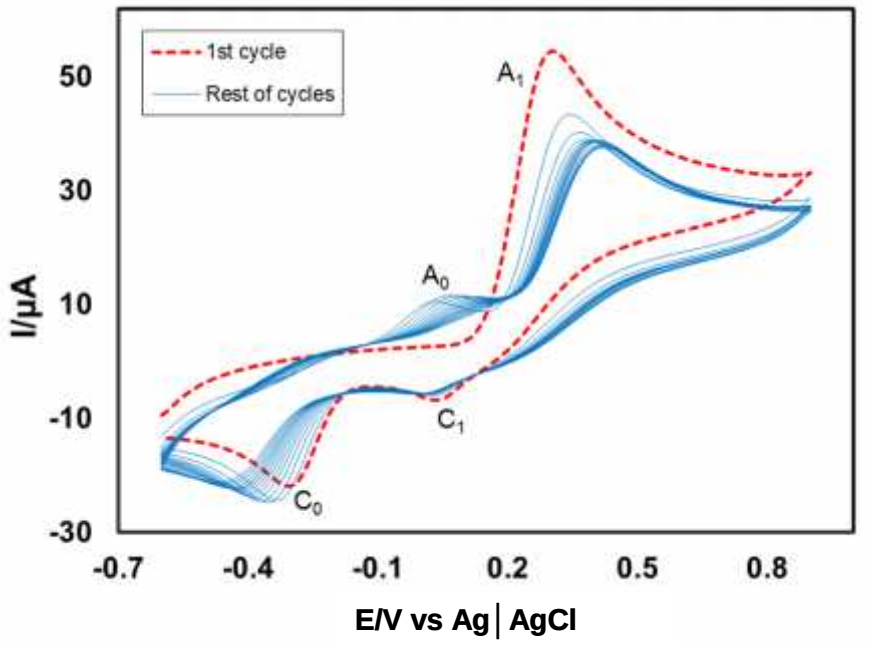

Fig. 4.122: Cyclic voltammogram of 2 mM 1,2-dihydroxybenzene with 100 mM L-Leucine of GC (3 mm) electrode in the buffer solution of pH 7 at scan rate 0.1 V/s (15 cycles). The appeared anodic peak current (A_0) and cathodic peak current (C_0) increased with the iteration scan from the first cycle.

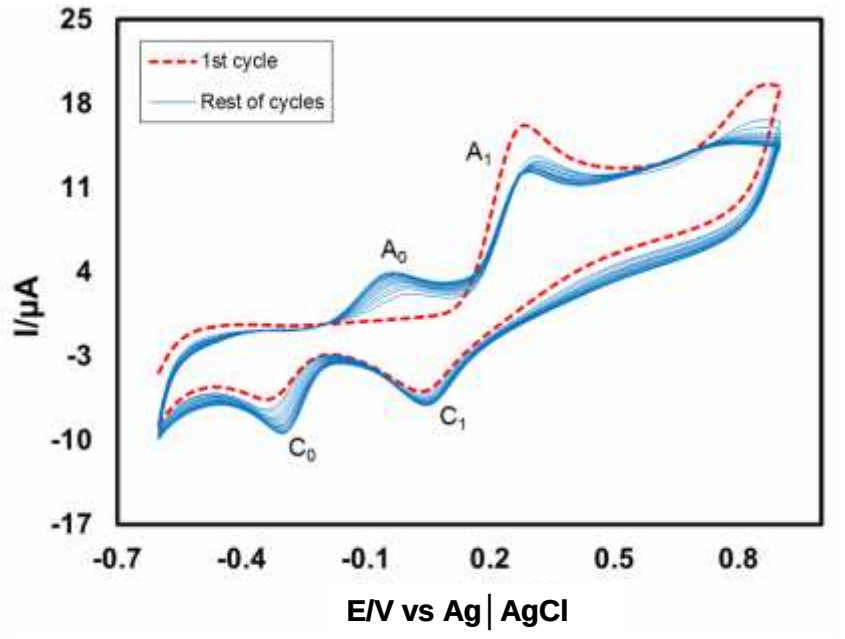

Fig. 4.123: Cyclic voltammogram of 2 mM 1,2-dihydroxybenzene with 100 mM L-Leucine of Pt electrode in the buffer solution of pH 7 at scan rate 0.1 V/s (15 cycles). The appeared anodic peak current (A_0) and cathodic peak current (C_0) increased with the iteration scan from the first cycle.

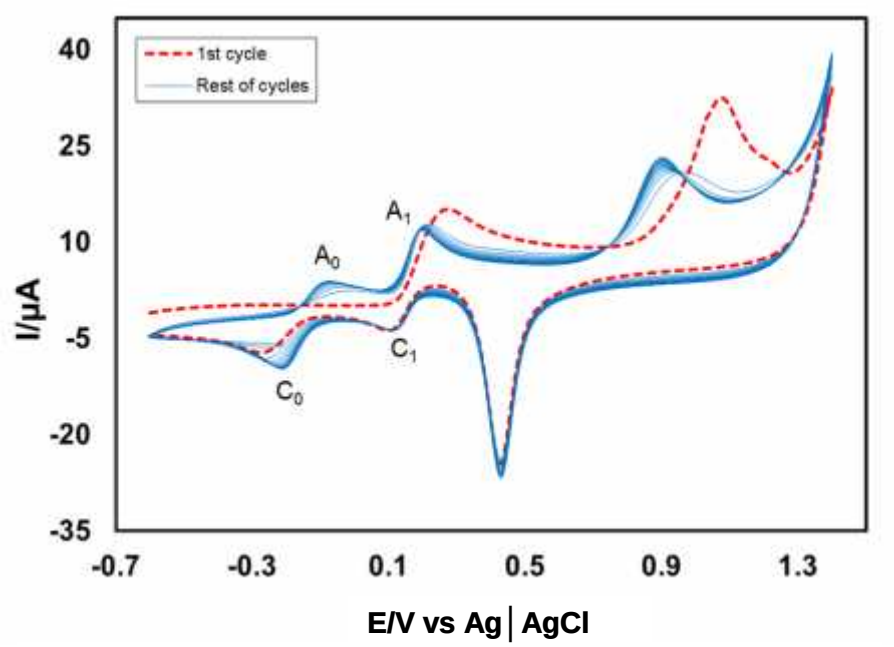

Fig. 4.124: Cyclic voltammogram of 2 mM 1,2-dihydroxybenzene with 100 mM L-Leucine of Au electrode in the buffer solution of pH 7 at scan rate 0.1 V/s (15 cycles). The appeared anodic peak current (A_0) and cathodic peak current (C_0) increased with the iteration scan from the first cycle.

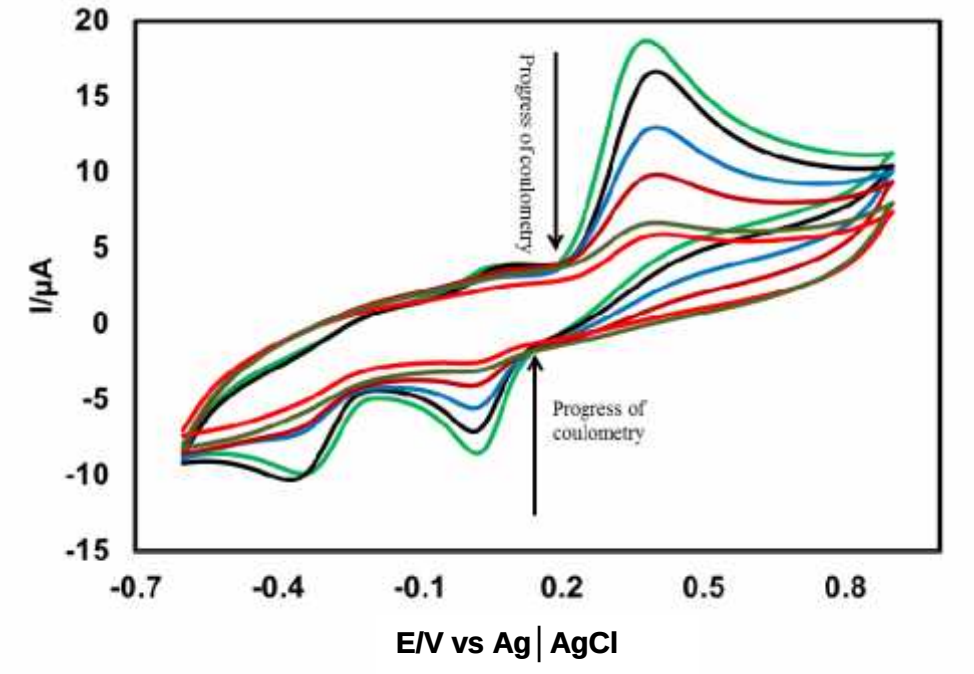

Fig. 4.125: Cyclic voltammogram and (CV) of 1 mM 1,2-dihydroxybenzene in presence of 50 mM L-Leucine of GC electrode during controlled potential coulometry at 0.45 V in pH 7 at scan rate 0.1 V/s.

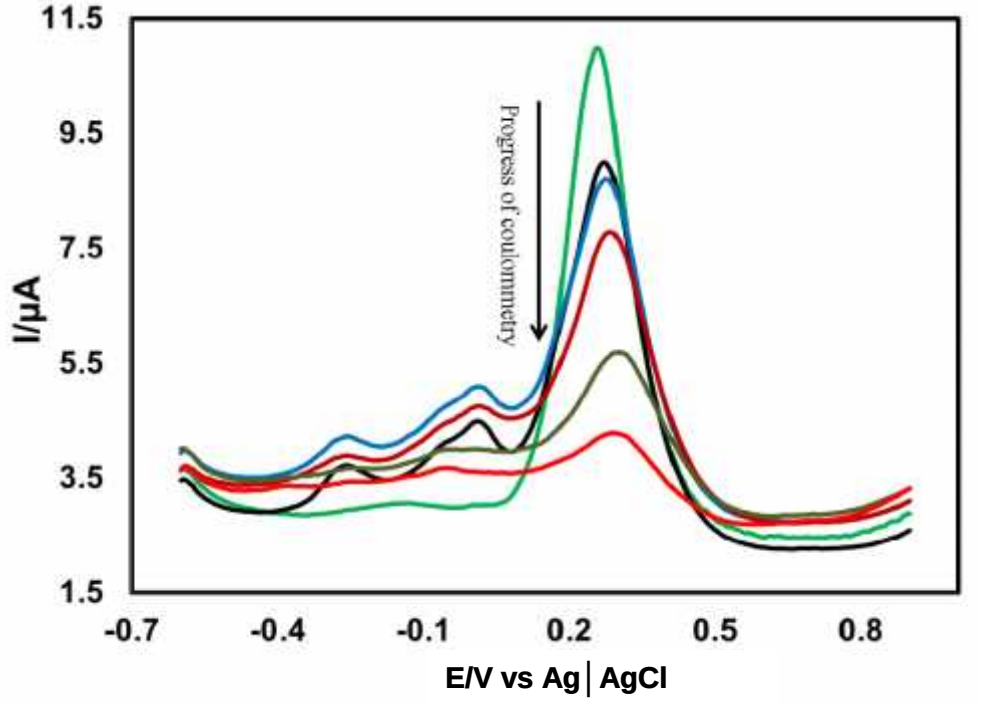

Fig. 4.126: Differential pulse voltammogram (DPV) of 1 mM 1,2-dihydroxybenzene in presence of 50 mM L-Leucine of GC electrode during controlled potential coulometry at 0.45 V in pH 7 at scan rate 0.1 V/s.

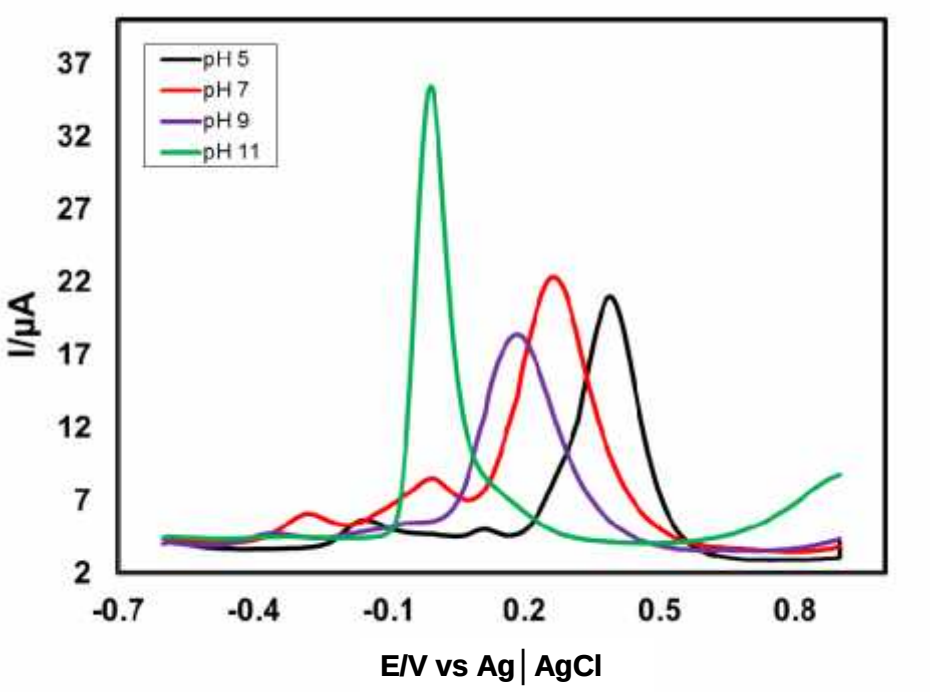

Fig. 4.127: Differential pulse voltammogram (DPV) of 2 mM 1,2-dihydroxybenzene with 100 mM L-Leucine of GC electrode in second scan of different pH (5, 7, 9 and 11) and scan rate 0.1 V/s.

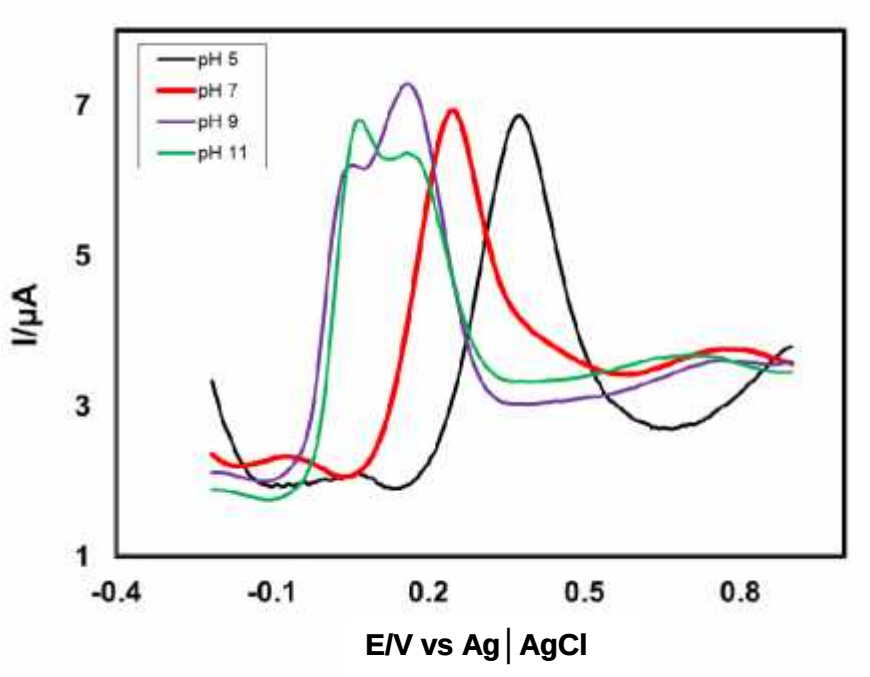

Fig. 4.128: Differential pulse voltammogram (DPV) of 2 mM 1,2-dihydroxybenzene with 100 mM L-Leucine of Pt electrode in second scans of different pH (5, 7, 9 and 11) and scan rate 0.1 V/s.

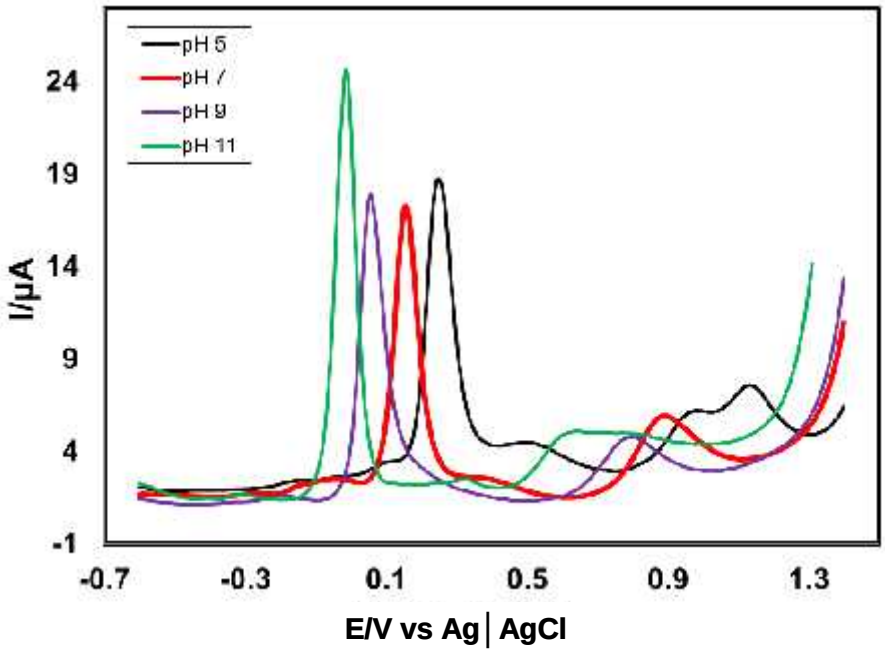

Fig. 4.129: Differential pulse voltammogram (DPV) of 2 mM 1,2-dihydroxybenzene with 100 mM L-Leucine of Au electrode in second scans of different pH (5, 7, 9 and 11) and scan rate 0.1 V/s.

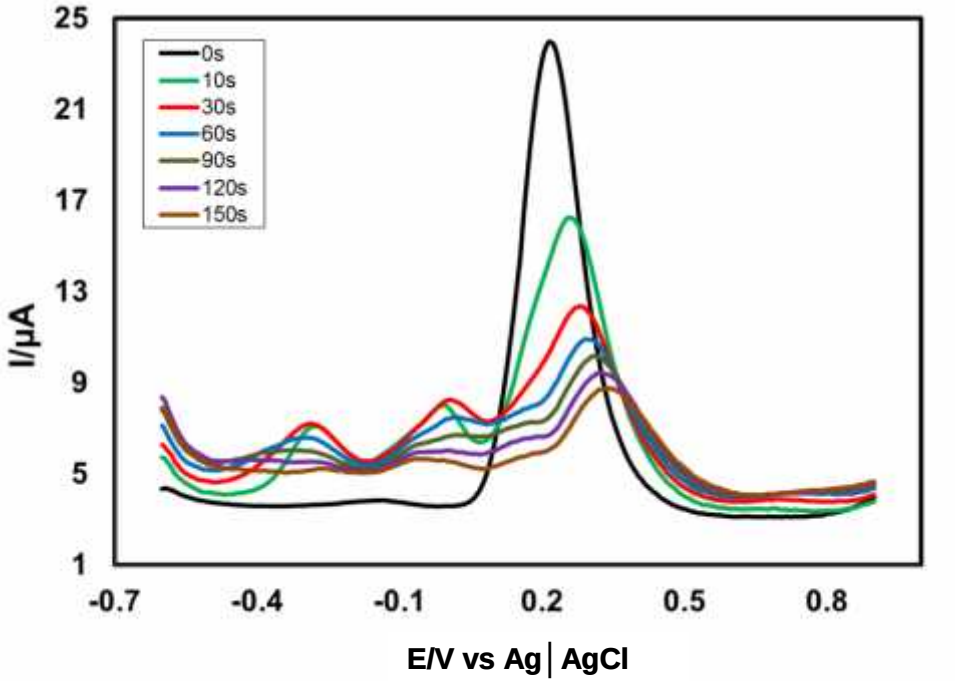

Fig. 4.130: Differential pulse voltammogram (DPV) of deposition time change (0, 10, 30, 60, 90,120 and 150 s) of 2 mM 1,2-dihydroxybenzene with 100 mM L-Leucine of pH 7 at *E*puls 0.02 V, tpuls 20 ms and scan rate 0.1 Vs^{-1}.

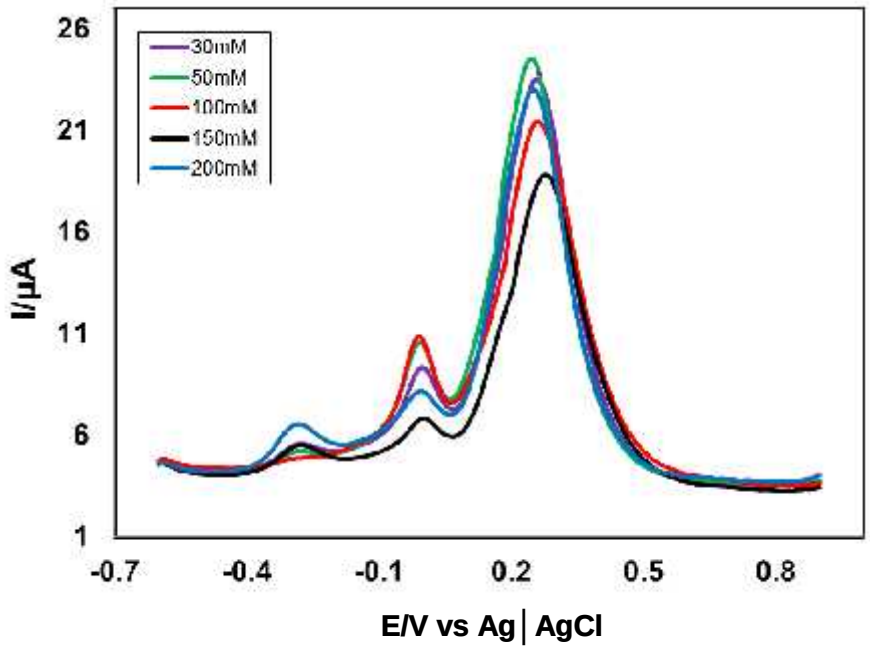

Fig. 4.131: Differential pulse voltammogram (DPV) of composition change of L-Leucine (30, 50, 100, 150 and 200 mM) with the fixed composition of 2 mM 1,2-dihydroxybenzene in second scan of pH 7 at *E*puls 0.02 V, tpuls 20 ms of GC electrode and scan rate 0.1 Vs^{-1}.

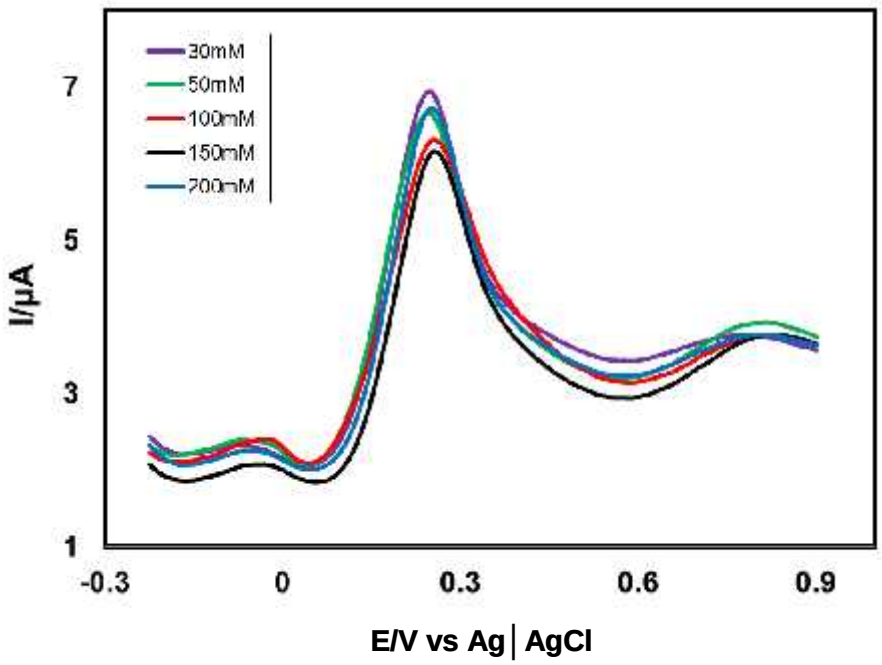

Fig. 4.132: Differential pulse voltammogram (DPV) of composition change of L-Leucine (30, 50, 100, 150 and 200 mM) with the fixed composition of 2 mM 1,2-dihydroxybenzene in second scan of pH 7 at *E*puls 0.02 V, tpuls 20 ms of Pt electrode and scan rate 0.1 Vs^{-1}.

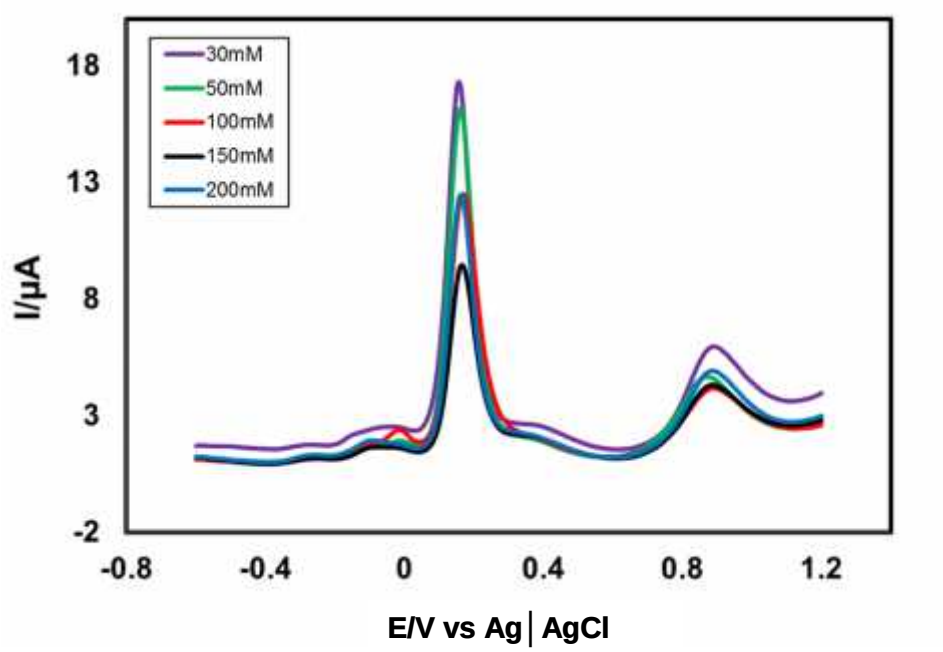

Fig. 4.133: Differential pulse voltammogram (DPV) of composition change of L-Leucine (30, 50, 100, 150 and 200 mM) with the fixed composition of 2 mM 1,2-dihydroxybenzene in second scan of pH7 at *E*puls 0.02 V, tpuls 20 ms of Au electrode and scan rate 0.1 Vs^{-1}.

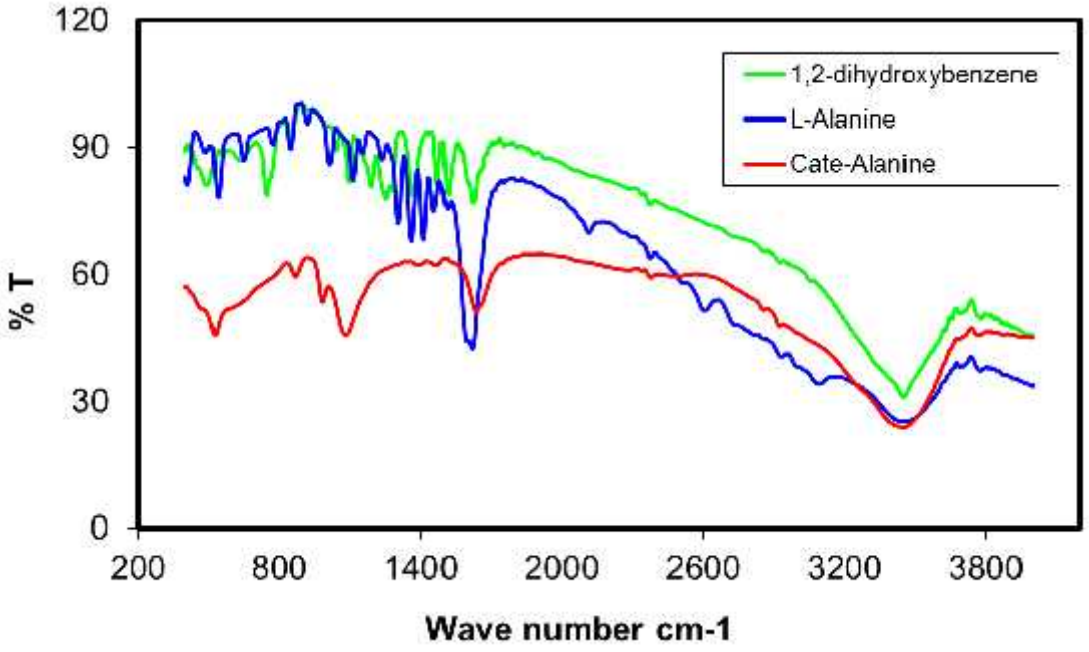

Fig. 4.134: Comparison of FTIR of only 1,2-dihydroxybenzene, only L-Alanine and 1,2-dihydroxybenzene-Alanine adduct.

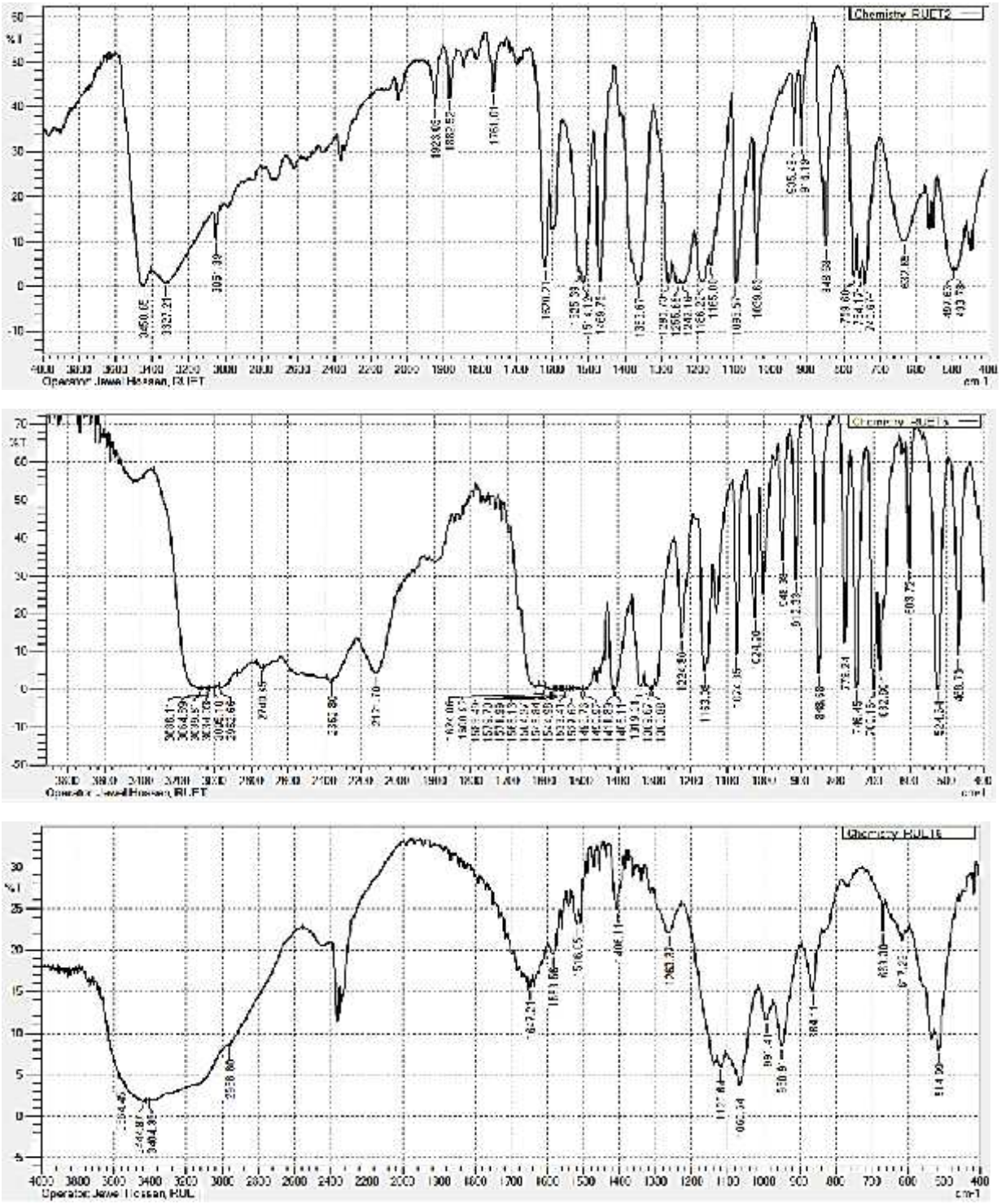

Fig. 4.135: Comparison of FTIR of only 1,2-dihydroxybenzene, only L-phenylalanine and 1,2-dihydroxybenzene-Phenylalanine adduct.

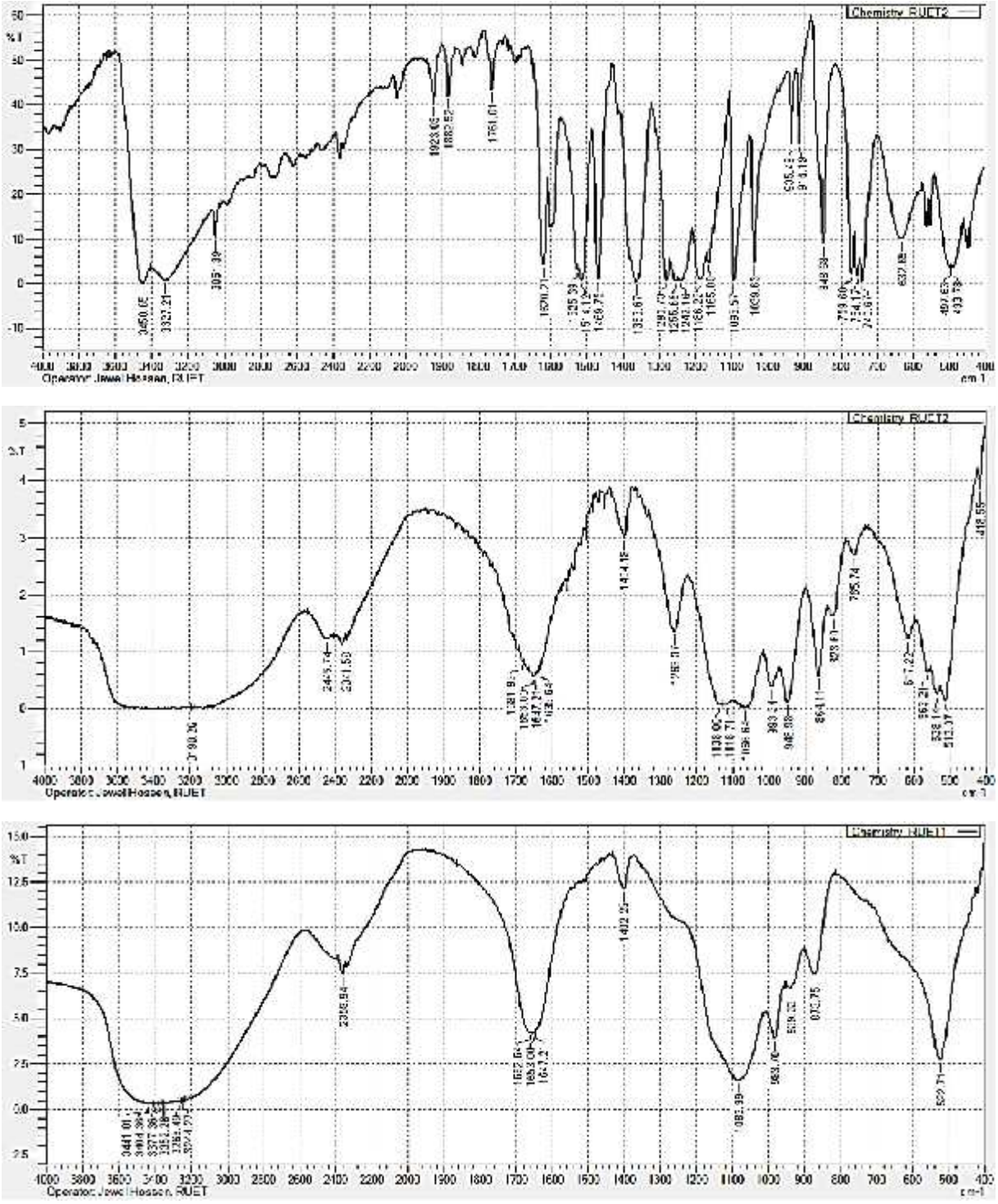

Fig. 4.136: Comparison of FTIR of only 1,2-dihydroxybenzene, only L-Leucine and 1,2-dihydroxybenzene-Leucine adduct.

CHAPTER V

Conclusions

1,2-dihydroxybenzene undergoes electro-oxidation in presence of nucleophiles (L-Alanine, L-Phenylalanine and L-Leucine) to generate *o*-benzoquinone (Michael acceptor) at different pH media (5-11). Pure L-Alanine, L-Phenylalanine and L-Leucine are electro-inactive whereas pure 1,2-dihydroxybenzene is eletro-active. By adding selected nucleophiles in 1,2-dihydroxybenzene solution the products generated from the nucleophilic substitution reaction that undergo electron transfer at more negative potentials than the 1,2-dihydroxybenzene. The substituted products are assumed to be 2-((3,4-dihydroxyphenyl) amino) propanoic acid, 2-((3,4-dihydroxyphenyl)amino)-3-phenyl propanoic acid and 2-((3,4-dihydroxyphenyl)amino)-4-methylpentanoic acid respectively. Voltammetric response of GC electrode is better than Au and Pt electrodes. Electro-oxidation of 1,2-dihydroxybenzene is strongly influenced by the concentration of nucleophiles and mostly favorable in 50 mM of L-Alanine, 20 mM of L-Phenylalanine and 100 mM of L-Leucine respectively. This reaction is also highly pH dependent and the maximum peak current is observed at pH 7 for all studied system. The slope values of first anodic peak (A_1) in Ep vs pH plot are observed (70.5 mV/pH) for 1,2-dihydroxybenzene-Alanine, (59 mV/pH) for 1,2-dihydroxybenzene-Phenylalanine and (68.5 mV/pH) for 1,2-dihydroxybenzene-Leucine respectively. These values are indicative that the electro-oxidation of 1,2-dihydroxybenzene takes place via $1e^{-}/1H^{+}$ transfer process. The current function ($Ip/v^{1/2}$) curve suggests the corresponding nucleophilic addition of 1,2-dihydroxybenzene in presence of L-Alanine, L-Phenylalanine and L-Leucine occur through an ECE mechanism and each redox reaction is controlled by diffusion process with some chemical complications. Noticeable change in fingerprint region of FTIR-spectra also supports the formation of 1,2-dihydroxybenzene-amino acid adducts.

Recommendation

The electrochemical behavior of 1,2-dihydroxybenzene and its derivatives with amino acids such as 1,2-dihydroxybenzene-Alanine, 1,2-dihydroxybenzene-Phenylalanine and 1,2-dihydroxybenzene-Leucine have been studied by means of CV, DPV and CPC techniques throughout in this research. The thermodynamic and anti-microbial properties of 1,2-dihydroxybenzene-amino acid adducts can be further carried out as extension of this research work.

REFERENCES

1. R. H. Thomson, 1987, “Naturally Occurring Quinones”, Chapman and Hall: London, 3rd Ed.
2. K. Hostettmann and I. P. Lea, 1988, “Biologically Active Natural Products”, Oxford University Press, Oxford.
3. Chichirau, A., Flueraru, M., Chepelev, L. L., Wright, J. S., Willmore, W. G., Durst, T., Hussain, H. H. and Charron, M., 2005, Free Radic., Biol. Med., Vol. 38, p. 344.
4. Chen, S. M. and Peng, K. T. J., 2003, Electroanal. Chem., pp. 547, 179.
5. Khalafi, L. and Rafiee, M., 2010, J. Hazardous Materials, p. 801.
6. Md. Nazim Uddin, 2016, “Investigation of the Electrochemical Behavior of Catechol in Presence of Glycine, Aspartic acid and Glutamic acid”, M.Sc. Thesis, KUET.
7. Md. Rabiul Islam, 2016, “Electrochemical Characterization of Some Electroactive Nucleophilic Substitution Reactions”, M.Phil. Thesis, KUET.
8. Md. Alim Uddin, 2015, “Electrochemical Study of Catechol in Presence of Sulfanilic Acid and Diethylamine at Different pH”, M.Sc. Thesis, KUET.
9. A.J. Bard and L. Faulkner, 2001, “Electrochemical Methods”, Wiley, New York.
10. J. Wang, 2006, “Analytical electrochemistry”, John Wiley & Sons.
11. B. Joseph, Jr. Justice, 1987, “voltammetry in the neurosciences: Principles, Methods, and Applications”, The Springer Science and Business Media, New York.
12. Y. Saito, T. Kikuchi, 2014, “voltammetry theory, types and applications”, Nova Science Publishers, Inc. New York.
13. https://en.wikipedia.org/wiki/catechol
14. https://en.wikipedia.org/wiki/alanine
15. https://en.wikipedia.org/wiki/phenylalanine
16. https://en.wikipedia.org/wiki/leucine
17. Nematollahi, D. and Goodarzi, H., 1997, Iran Journal of Science and Technology, Vol. 21, p. 121.

18. Nematollahi, D. and Forooghi, Z., 2002, Tetrahedron Letters, Vol. 58, p. 4949.

19. Shahrokhian, S. and Hamzehloei, A., 2003, Electrochemistry Communications, Vol. 5, p. 706.

20. Grujic, Z., Tabakovic, I. and Trkovnic, M., 1976, Tetrahedron Letters, Vol. 52, p. 4823.

21. Tabakovic, I., Grujic, Z. and Bejtovic, Z., 1983, Journal of Heterocyclic Chemistry, Vol. 20, p. 635.

22. Golabi, S.M, Nourmohammadi, F. and Saadnia, A., 2002, Journal of Electroanalytical Chemistry, Vol. 529, p. 12.

23. Fotouhi, L., Kiani, S.T., Nematollahi, D. and Heravi, M.M., 2007, Journal of Electroanalytical Chemistry, Vol. 10, p. 1002.

24. C.M.A. Brett and A.M.O. Brett, 1993, "Electrochemistry Principles, Methods and Applications", Oxford University Press.

25. M. E. Hossain, 2014, "Electrochemical sensor simultaneous detection and estimation of environmental toxic pollutants", M.Phil Thesis, KUET.

26. D.A. Skoog, F.J. Holler and T.A. Nieman, 2007, "Principles of Instrumental Analysis", Thomson Brooks/ Cole, 6th Ed., pp. 349-351.

27. P.T. Kissinger and W.R. Heineman, 1996, "Laboratory Techniques in Electroanalytical Chemistry", Marcel Dekker, Inc.

28. C.M.A. Brett and A.M.O. Brett, 1998, "Electroanalysis", Oxford University Press.

29. Randles, J.E.B., 1948, Transactions of the Faraday Society, Vol. 44, p. 327.

30. Sevcik, A., 1948, Collection of Czechoslovak Chemical Communications, Vol. 13, p. 349.

31. Bott, A.W., 1994, Curr. Seps., Vol. 13, p. 49.

32. Klinger, R.J. and Kochi, J.K., 1981, Journal of Physical Chemistry, Vol. 85, p. 12.

33. Grujic, Z., Tabakovic, I. and Trkovnic, M., 1976, Tetrahedron Letters, Vol. 52, p. 4823.

34. Tabakovic, I., Grujic, Z. and Bejtovic, Z., 1983, Journal of Heterocyclic Chemistry, Vol. 20, p. 635.

35. Afzal Shah, 2010, "Redox Behavior and DNA Binding Studies of Some Electroactive Compounds", Ph.D Thesis, Department of Chemistry, Quaid-i-Azam University, Islamabad.

36. Nicholson, R.S., 1965, "Analytical Chemistry", Vol. 37, p. 135.

37. Matsuda, H. and Ayabe, Y.Z., 1955, Electrochimica Acta, Vol. 59, p. 494.

38. Andrews, L.J., 1954, Chem. Revs., Vol. 54, p. 713.

39. A.J. Bard and L.R. Faulkner, 1980, "Electrochemical Methods, Fundamentals and Applications", John Wiley, New York.

40. Eyring, H., Glasstone, S. and Laidler, K.J., 1939, The Journal of Chemical Physics, Vol. 7, p. 1053.

41. Reinmuth, W.H., 1962, "Analytical Chemistry", Vol. 34, p. 144.

42. Laviron, E., 1983, J. Electrochim. Interfac. Electrochim., Vol. 1, p. 148.

43. Polcyn, D.S. and Shain, I., 1966, Analytical Chemistry, Vol. 38, p. 370.

44. Aoki, K. and Osteryoung, J., 1981, Journal of Electroanalytical Chemistry, Vol. 122, p. 19.

45. Aoki, K. and Osteryoung, J., 1984, Journal of Electroanalytical Chemistry, Vol. 160, p. 335.

46. Flanagan, J.B. and Marcoux, L., 1973, Journal of Physical Chemistry, Vol. 77, p. 1051.

47. Heinze, J., 1981, Journal of Electroanalytical Chemistry, Vol. 124, p. 73.

48. Shoup, D. and Szabo, A., 1982, Journal of Electroanalytical Chemistry, Vol. 140, p. 237.

49. Gavaghan, D.J. and Rollett, J.S., 1990, Journal of Electroanalytical Chemistry, Vol. 295, p. 1.

50. Qian, W., Jin, B., Diao, G., Zhang, Z. and Shi, H., 1996, Journal of Electroanalytical Chemistry, Vol. 414, p. 1.

51. Ikeuchi, H. and Kanakubo, M., 2000, Journal of Electroanalytical Chemistry, Vol. 493, p. 93.

52. Jr. D.K. Gosser, 1993, "Cyclic Voltammetry (Simulation and analysis of reaction mechanisms)", Wiley-VCH, Inc.

53. F.M. Hawkridgein, P.T. Kissinger and W.R.(Eds.) Heieman, 1996, "Laboratory Techniques in Electroanalytical chemistry", Marcel Dekker Inc., New York. 2nd Ed.

54. J. Wang, 1994, "Analytical Electrochemistry", VCH Publishers Inc., New York.

55. E.R. Brown, R.F. Larg, A. Weissberger and B.(Eds.) Rossiter, 1971, Physical Methods of chemistry, Vol.1-Part IIA, Wiley-Interscience, New York.

56. Armada, P.G, Losada, J. and Perez, S.V., 1996, "Cation analysis scheme by differential pulse polarography", Vol. 73, pp. 544-546.

57. Zhang, J., 1972, Journal of Electroanalytical Chemistry, Vol. 331, p. 945.

58. Nematollahi, D., Afkhami, A., Mosaed, F. and Rafiee, M., 2004, "Research on Chemical Intermediates", Vol. 30, p. 299.

59. Papouchado, L., Petrie, G. and Adams, R. N., 1972, Journal of Electroanalytical Chemistry, Vol. 38, p. 389.

60. Papouchado, L., Petrie, G., Sharp, J.H. and Adams, R.N., 1968, Journal of the American Chemical Society, Vol. 90, p. 5620.

61. Young, T.E., Griswold, J.R. and Hulbert, M.H., 1974, Journal of Organic Chemistry, Vol. 39, p. 1980.

62. Brun, A. and Rosset, R., 1974, Journal of Electroanalytical Chemistry, Vol. 49, p. 287.

63. Stum, D.I. and Suslov, S.N., 1979, Bio. Zika, Vol. 21, p. 40.

64. Rayn, M.D., Yueh, A. and Yu, C.W., 1980, Journal of Electrochemical Society, Vol. 127, p. 1489.

65. Md. Matiar Rahman, 2014, "Electrochemical characterization of biologically important electroactive metal ligand complexes with multi-electron transfer reaction", M.Phil Thesis, KUET.

66. Thibodeau, P.A. and Paquette, B., 1999, Free Radical Biology & Medicine, Vol. 27, p. 1367.

67. Mazzini, S, Monderelli, R, Ragg, E. and Scaglioni, L., 1995, Journal of the Chemical Society, Perkin Transactions, Vol. 2, p. 285.

68. Pasta, M., Mantia, F.L. and Cui, Y., 2010, Electrochimica Acta, Vol. 55, p. 5561.

69. Papouchado, L., Sandford, R.W., Petrie, G. and Adams, R.N., 1975, Journal of Electroanalytical Chemistry, Vol. 65, p. 275.

70. Kiani, A., Raoof, J.B., Nematollahi, D. and Ojania, R., 2005, Electroanalysis, Vol. 17, p.1755.

71. Nematollahi, D. and Golabi S.M., 2000, J. Electroanal. Chem., Vol. 481, p. 208.

72. Shahrokhian, S. and Hamzehloei, A., 2003, Electrochem. Commun., Vol. 5 p. 506.

73. Nematollahi, D. and Golabi, S.M., 2001, Electroanalysis, Vol. 13, p. 1008.

74. Grujic, Z., Tabakovic, I. and Trkovnic, M., 1976, Tetrahedron Lett., Vol. 52, p. 4823.

75. Nematollahi, D. and Goodarzi, H., 2001, J. Electroanal. Chem., Vol. 108, p. 510.

76. Tabakovic, I., Grujic, Z. and Bejtovic, Z., 1983, J. Heterocyclic Chem., Vol. 20, p. 635.

77. Nematollahi, D. and Forooghi, Z., 2002, Tetrahedron, Vol. 58, p. 4949.

78. Golabi, S.M., Nourmohammadi, F. and Saadnia, A., 2002, J. Electroanal. Chem.,Vol. 12, p. 529.

79. Nematollahi, D., Afkhami, A., Mosaed, F. and Rafiee, M., 2004, Research on Chemical Intermediates, Vol. 30 p. 299.

80. Nematollahi, D. and Golabi, S.M., 2000, J. Electroanal. Chem., Vol. 208, p. 481.

81. Mazzini, S., Monderelli, R., Ragg, E. and Scaglioni, L., 1995, J. Chem. Soc. Perkin Trans., Vol. 2, p. 285.

82. Pasta, M., Mantia, F.L. and Cui, Y., 2010, Electrochimica Acta, Vol. 55, p. 5561.

83. Rayn, M.D., Yueh, A. and Yu, C.W., 1980, J. Electrochem. Soc., Vol.127, p. 1489.